ISSN 1913-1844

MODERN APPLIED SCIENCE

Vol. 2, No. 3
May 2008

Canadian Center of Science and Education

CCSE

Modern Applied Science

www.ccsenet.org/journal.html

Vol. 2, No. 3

May 2008

Contents

Modern Applied Science

www.ccsenet.org/journal.html

Vol. 2, No. 3

May 2008

Contents

Modern Applied Science

www.ccsenet.org/journal.html

Vol. 2, No. 3

May 2008

Mixing Effect of Anionic and Nonionic Surfactants on Micellization, Adsorption and Partitioning of Nonionic Surfactant

Mazen Ahmed Muherei (Corresponding author)

Department of Petroleum Engineering, FKKKSA, UTM

81310 Skudai, Johor, Malaysia

Tel: 60-17-768-3487 E-mail: mazen_moherey@yahoo.com

Radzuan Junin

Department of Petroleum Engineering, FKKKSA, UTM

81310 Skudai, Johor, Malaysia

Tel: 60-19-789-9703 E-mail: radzuan@fkkksa.utm.my

Abstract

Nonionic surfactants are always good candidates for surfactant enhanced aquifer remediation (SEAR), enhanced oil recover (EOR) and insitu/ex-situ soil washing. Their wide application is based on their high solubilization capacities and their low bio-toxicity. However, surfactant loss due to adsorption and/or partitioning on adsorbents impairs their effectiveness to solubilize/mobilize and reduce the oil–water interfacial tension (IFT) which renders contaminant remediation process economically unfeasible. In this research anionic (SDS) and nonionic (TX100) surfactants and their mixtures (1:2, 1:1, 2:1; TX100:SDS mass ratios) were evaluated for their ability to reduce surfactant CMCs, partitioning losses to an organic phase and/or adsorption to shale. Result showed that all mixtures behave similarly and have superior properties than both single surfactants. Partitioning and adsorption of TX100 into organic phase (Sarapar147) and shale were decreased by mixing with anionic surfactant (SDS). The data showed a 40% reduction in surfactant losses due to adsorption to shale and around 60% reduction due to both partitioning and adsorption.

Keywords: Surfactant, CMC, Surface tension, Interfacial tension, Adsorption, Partition, Mixed surfactants

1. Introduction

The use of surfactants to decontaminate groundwater aquifers, facilitate/enhance residual oil recovery and in soil-clean up operations is well established, and both anionic and nonionic surfactants have been used to remediate land polluted with oils and hydrocarbons as well as many other organic contaminants. The most important parameter in terms of the ability of a surfactant to mobilize or solubilize hydrophobic contaminants in contaminated soil is the surfactant critical micelle concentration (CMC). In general, concentrations of surfactant in soil-water below the CMC have little or no effect on solubilization of hydrophobic materials. Only when micelles are present does significant desorption of such pollutants from soil surfaces occur (Haigh, 1996).

Nonionic surfactants are often used because of their lower CMCs as compared to ionic surfactants, their higher degree of surface-tension reduction, and their relatively constant properties in the presence of salt, which result in better performance and lower concentration requirements. In particular, the non-ionic ethoxylate surfactants have been suggested for the removal of organic contaminants from soil because of their high solubilization capacity and biodegradability (Kile and Chiou, 1989; Zhou and Rhue, 2000; Paria and Yuet, 2007). However, some concerns with these surfactants are their significant loss to soil and partitioning to organic phase during practical applications (Butler and Hayes, 1998; Zimmerman et al., 1999; Cowell et al., 2000; Zhao et al., 2006; Zhao et al., 2007). Nevertheless, under some conditions, usually at concentration well below CMC, the adsorption of these surfactants to soil can enhance the adsorption of hydrophobic contaminants to soil. This has been attributed to partition of hydrophobic contaminants into surfactant hemi-micelle formed on soil surface (Edwards et al., 1994; Sun et al., 1995; Haigh, 1996).

Anionic surfactant on the other hand, sorb less to soil but they form micelles at higher concentrations in aqueous solutions than nonionic surfactants with an equivalent hydrophobic group (Rosen, 2004) and are more prone to precipitate in presence of multivalent cations (Ca^{++}, Mg^{++}). Substantial loss of surfactant by such mechanisms will definitely reduce their active concentration in aqueous solution, which would greatly reduce the surfactant solubilization and flushing efficiency.

Use of well designed surfactant mixtures may greatly alleviate those problems. A typical feature of ionic (anionic/cationic)-nonionic mixtures is the synergy or anti-synergism (antagonism) at interfaces. For example, the adsorption of one surfactant is either enhanced or retarded by the addition of a small amount of the other surfactant. Furthermore, mixing ionic and nonionic surfactants may raise or lower the CMC from that obtained by ideal mixing.

Generally, several studies had investigated surfactant mixtures of nonionic and anionic surfactants. Most of these studies focused on synergism in critical micelle concentration obtained upon mixing (Janczuk et al., 1995; Owoyomi, 2005; Joshi et al., 2005; Zhang et al., 2005; Mata, 2006; Zhao and Zhu, 2006; Zhao et al., 2006). Other studies deal with solubilization of organic compounds in anionic-nonionic surfactant mixtures (Zhu and Feng, 2003; Zhou and Zhu, 2004; Zhao et al., 2005; Zhou and Zhu, 2005; Zhao and Zhu, 2006; Zhao et al., 2006; Zhao et al., 2007). Several studies deal also with remediation of soil contaminated with specific contaminants (Lee et al., 2004; Zhou and Zhu, 2007; Yu et al., 2007).

Although the adsorption of single surfactants at the solid-liquid interface has been studied intensively, far fewer studies exist for the case of adsorption from mixed surfactant solutions. Adsorption of anionic-nonionic surfactant mixtures on positively and negatively charged surfaces were reported (Wang and Kwak, 1999 [TX100-SDS to positively charged alumina]; Porcel et al., 2001 [TX100-SDS to positively and negatively charged polystyrene latexes]; Yang et al., 2005 [TX100-SDBS to Ca-montmorillonite]; Rao and He, 2006 [SDBS-$A_{12}E_9$ to natural soil]). Accordingly, it is not surprising that only a very few studies have been reported for adsorption of anionic-nonionic surfactant in natural soils and in presence of oil phase.

Generally, researchers found that the CMCs of mixed anionic-nonionic surfactants were lower than those of sole anionic surfactants. Furthermore, with the increase in mole fraction of the nonionic surfactant, the CMCs decrease continuously from the CMC of pure anionic surfactant down to the CMC of pure nonionic surfactant. The experimental CMCs were found lower than the ideal mixing CMCs (Janczuk et al., 1995; Zhu and Feng, 2003; Zhou and Zhu, 2004; Owoyomi, 2005; Zaho et al., 2005; Joshi et al., 2005; Yang et al., 2005; Zhang et al., 2005; Zhao et al., 2006; Zhao et al., 2007).

For the adsorption case of anionic-nonionic surfactant mixtures, which surfactant is adsorbed preferentially depends on the nature and charge of mineral surface. For positively charged surfaces to which anionic surfactants are heavily adsorbed, presence of nonionic surfactant decreases adsorption of anionic surfactant and the adsorption of nonionic surfactant is enhanced where nonionic alone shows trace adsorption (Wang and Kwak, 1999; Paria and Khilar, 2004). On the other hand, for clay minerals that shows affinity to nonionic surfactant, presence of anionic surfactant retard nonionic surfactant adsorption (Paria and Khilar, 2004; Yang et al., 2005).

Recently, mixed nonionic and anionic surfactants were investigated for their abilities to retard non-ionic surfactant sorption and partition to soil and organic phase, respectively. Researchers found mixtures superior to the relevant single ones mainly due to the reduction in nonionic surfactant partition and/or sorption to soil as well as the high solubilization capacity of the mixture. Yang et al. (2005) showed that the amounts of both Triton X100 (TX100) and sodium dodecylbenzene sulfonate (SDBS) sorbed to Ca-montmorillonite are significant. However, the amount of either surfactant sorbed can be decreased and minimized when they are mixed with each other. Furthermore, the extent of the nonionic surfactant (TX100) which partition into the organic phase was found to decrease if the amount of the anionic surfactant (SDBS) increased (Zhao et al., 2006; Zhao et al., 2007). Decreasing loss of surfactant due to partitioning and/or sorption and the greater apparent solubilization of the mixture will reduce surfactants volumes needed and thus the capital expenditure and operation cost (Zhao and Zhu, 2006).

Accordingly, it becomes impressive to investigate the ability of nonionic-anionic surfactants mixtures to reduce CMCs and surfactant losses either by reducing partition to organic phase or adsorption to soil or sediments at different experimental conditions, i.e. different sorbent and different organic phase. This study is intended to investigate the simultaneous losses of sodium dodecyl sulfate (SDS), TX100 and their mixtures by partitioning, adsorption and abstraction. The study will investigate the adsorption of SDS, TX100 and their mixtures to Batu Arang's shale. Surface tensions of surfactants and their mixtures are studied to determine adsorption and micellization properties. Interfacial tensions of surfactants and their mixtures with an oil phase, Sarapar147 are also studied to investigate simultaneous surfactant partitioning, adsorption and micellization.

SDS and TX100 have been selected mainly because they are frequently used by the industry and are then readily available and well priced. Furthermore, both surfactants have been the most extensively studied surfactants from the anionic and nonionic classes, respectively (Mata, 2006). Both surfactants were found successful in the extraction of organic contaminants from soils (Chou et al., 1998; Deshpande et al., 1999; Sanchez-Camazano et al. 2000; Chang et al., 2000; Jada and Hamieh, 2001; Zhang et al., 2001; Chu and Chan, 2003; Sanchez-Camazano et al., 2003; Sanchez-Martin et al., 2003; Rodriguez-Cruz et al., 2004; Saichek and Reddy, 2004; Smith et al., 2004; Urum et al., 2004; Urum and Pekdemir, 2004; Rodriguez-Cruz et al., 2006; Urum et al., 2006).

2. Materials

2.1 Surfactants

Triton X-100 (TX100) extra pure, was purchased from Scharlau Chemie, Spain. Sodium dodecyl sulfate (SDS) was obtained from Merck with a high grade of purity (99%). The oil, Sarapar147, was supplied by Kota Minerals and Chemical Sdn. Bhd. (KMC). Sarapar147 is a colourless mineral oil ranging from C14 to C17 and is derived from petroleum crude oil. All chemicals were used as received without further purification. Selected physicochemical properties of the compounds are presented in Table 1.

2.2 Shale Samples

Samples were collected from an outcrop of a local shale formation (Batu Arang, Selangor, Malaysia). Rock samples were disintegrated into small pieces by a jaw crusher and then ground using rock pulverizer (Fritsch, Germany). Rock samples were air dried for 24hrs followed by oven drying at 105ºC for 24hrs. Density of shale was determined to be 1.94g/cc. Dried rock samples were sieved to obtain particles less than 2mm and larger than 1mm in all experiments.

3. Methods

3.1 Preparation of Surfactant Solutions

The surfactant solutions were prepared in a standard 1000mL volumetric flasks. Surfactants were weighed on mass basis and emptied into the volumetric flask and then double distilled water was used to complete the solution to the final weight (1Kg). After the preparation of the stock solution, it was diluted to obtain desired concentration.

TX100 and SDS solutions were prepared at concentrations ranges from 0.0025wt% to 1wt% corresponding to molar concentrations of 0.039-15.47mM for TX100 and 0.0867-34.68mM for SDS. Mixed surfactant solutions were prepared by mixing SDS and TX100 solutions of the same weight concentrations with different volume ratios (2:1, 1:1, and 1:2 SDS:TX100). This results in a mole fraction of SDS in the total mixtures of 0.82, 0.69 and 0.53, respectively. Mixed surfactant solutions were allowed to equilibrate for at least 5hrs before any measurements were made.

3.2 Surface Tension Measurements

The surface tension technique was applied to determine the CMC in various combinations of shale and/or surfactant systems. The surface tension measurements were carried out with Krüss tensiometer (Krüss GmbH, Hamburg, Instrument Nr, K6) using a platinum-iridium ring at constant temperature (25±1ºC). The tensiometer was calibrated using method described in ASTM Designation: D1331-89. Surface and interfacial tension measurements were undertaken according to the method described in ASTM Designation: D1331-89.

Krüss tensiometer operates on the Du Nouy principle, in which a platinum-iridium ring is suspended from a torsion balance, and the force (in mN/m) necessary to pull the ring free from the surface film is measured. Surface tension value was taken when stable reading was obtained for a given surfactant concentration, as indicated by at least three consecutive measurements having nearly the same value. The average of a series of consistent readings for each sample was then corrected to account for the tensiometer configuration, yielding a corrected surface tension value (Zuidema and Waters, 1941). A correction factor, F, is multiplied by the average dial reading in order to obtain the corrected value for surface/interfacial tension (ST/IFT). Zuidema and Waters (1941) proposed the following empirical correlation to calculate the correction factor:

$$F = 0.725 + \sqrt{\left[\frac{9.075\times10^{-4}(STorIFT)}{\pi^3\Delta\rho g R^3} - \frac{1.679r}{R} + 0.04534\right]}$$

Where F = the correction factor; R =the radius of the ring, cm; r = the radius of the wire of the ring, cm; ST/IFT = the apparent value or dial reading, dyne/cm (mN/m); $\Delta\rho$ = the density difference between the lower and upper phases, g/cc; g = acceleration due to gravity, 980 cm/sec^2. The Equation is applicable only when $0.045 \leq \Delta\rho gR3/(ST \text{ or } IFT) \leq 7.5$

3.3 Interfacial Tension Measurements

Equal volume (15mL) of Sarapar147 and surfactant solution was poured into a glass beaker of 6cm diameter and the resulting mixture used for the interfacial tension studies. The same procedure used for the surface tension measurement was used for the interfacial tension study except that the balance of the tensiometer reading for zero was checked with the platinum-iridium ring completely immersed in the surfactant solution phase and not in the surface or interface of Sarapar147–surfactant. Hence, the platinum ring must be completely immersed in the surfactant phase before the platform is gradually adjusted until a force necessary to detach the platinum ring upward from the surfactant-oil interface is exerted.

3.4 CMC Measurements

The CMC values were obtained through a conventional plot of the surface/interfacial tension versus the surfactant concentration. The CMC concentration corresponds to the point where the surfactant first shows the lowest surface/interfacial tension. The surface/interfacial tension remains relatively constant after this point.

3.5 Adsorption to Shale

Adsorption isotherms were determined by batch equilibrium adsorption procedures. 10g of shale were added to a set of 60mL surfactant solutions (surfactant initial concentrations spans from 0.0025wt% to 1wt%) in a 100mL glass vials (1:6 w/v ratio) and allowed to equilibrate at 25±1 ºC. The surfactant solution-to-soil ratio was designated as 6:1 (v/w) to reach the optimal washing performance (Chu and Chan, 2003; Urum and Pekdemir, 2004). The vials were then agitated on a gyratory shaker at 100rpm (wrist orbital shaker) for 3 hrs and allowed to rest for 16hrs. Surfactant sample aliquots were taken for surfactant concentration determination before and after adsorption. All experiments were conducted with 3 replicates at 25±1ºC. To determine the maximum sorption of surfactants into shale, a surface/interfacial tension method was used. Each adsorption experiment involved 10 batch test samples in 100mL glass vials. The amount of surfactant adsorbed and/or abstracted was computed from the difference of CMC values before and after adsorption, and means of three replicates were used.

4. Results and Discussion

4.1 Surfactant Partition into Sarapar147

Figures 1 and 2 illustrate a typical graph of surface/interfacial tensions against the logarithm of the surfactant dose for fresh solutions. Figure 1 shows surface tensions (STs) while Figure 2 shows interfacial tensions (IFTs). The Figures depict the surface/interfacial tension curves as total surfactant concentration for the mixed SDS-TX100 system in which the molar fractions of SDS are 1, 0.82, 0.69, 0.53 and 0, respectively. Surface tension between water and air was measured as 72.57 mN/m while interfacial tension between water and Sarapar147 was found as 29.64 mN/m. As the surfactant solution is introduced, this value was reduced. As shown in Figures 1 and 2, surface/interfacial tension is concentration dependent. As the surfactant concentration increases, surface/interfacial tension decreases until the surfactant CMC value is reached and remains relatively constant there after wards.

CMC of pure surfactants obtained were compared with those in literature. CMC values of SDS obtained from both surface/interfacial tensions vs. concentration are similar at 0.1wt% (3.468mM/L or 1000mg/L) indicating minor losses of this surfactant to oil phase (Sarapar147). CMC of SDS compares well with those reported in Zhu and Feng (2003), Zhou and Zhu (2004), Zhao et al., (2005) and Zhou and Zhu (2007).

The CMC values of TX100 obtained by surface tension measurements (Figure 1) were much lower than that obtained by interfacial tension measurements (Figure 2). The first value (0.025wt%) was comparable well with values reported in previous published studies (Zhu and Feng, 2003; Zhou and Zhu, 2004; Zhao et al., 2005; Zhou and Zhu, 2007). The second value (0.07wt%), however, was not reported in literature. This is because surface tension technique is often used to determine surfactant CMCs and hence the effect of oil in micellization is ignored. It is rather noteworthy that it is the interfacial tension which is valuable to practical processes and not surface tension. Hence, reporting CMCs using surface tension technique may lead to misleading results. The difference in CMCs (0.045wt% or 0.45g-TX100/L-Sarapar147) may be due to partitioning of TX100 into Sarapar147 which result in loss of some active monomers of TX100.

Zhao et al. (2006 and 2007) reported extensive losses of TX100 due to partitioning into the organic phase, however no SDBS partitioning was found. Losses of TX100 with an initial concentration of 10g/L (1wt%) into Trichloroethene, Chlorobenzene, 1,2-Dichlorobenzene and Tetrachloroethene phases were more than 99%, 97%, 97%, and 15%, respectively when single TX100 was used. They attributed this behavior to the formation of reverse micelles (nonpolar exterior, polar interior) at lower IFTs. The affinity of TX100 to partition increased if the organic phase is polar.

As shown in Figures 1 and 2, the surface/interfacial tensions of mixed surfactants at a given molar ratio decreased with increasing total surfactant concentration. Each surface/interfacial tension curve had a breaking point that was taken as a mixed CMC. The CMCs of the mixtures as determined by surface tension curves are similar and very close to that of pure TX100 determined by surface tension curves (Figure 1). This is generally in agreement with other studies (Zhao et al., 2005; Mata, 2006). The CMCs of surfactants mixtures as determined by interfacial curves (Figure 2) are also nearly similar to pure TX100's CMC determined by surface tension curves, however, they are much lower than that of pure TX100 (0.07wt%) determined by interfacial curves. Therefore, mixtures have eliminated surfactant loss through partitioning. Zhao et al. (2006 and 2007) reported similar findings and found that partitioning of TX100 into nonaqueous phase liquids decreased by mixing with anionic surfactant (SDBS). This trend was attributed to the less affinity of anionic surfactant to partition into the organic phase and the formation of mixed micelles.

4.2 Surfactant Adsorption to Shale

Surfactant adsorption to solid surfaces is a process of transfer of surfactant molecules from bulk solution phase to the surface of the solid surface (Paria and Khilar, 2004). Adsorption can also be considered as a partitioning of the surfactant monomers between the solid surface and the bulk, and can occur if the solid surface is energetically favored by the surfactant in comparison to the bulk solution. Generally, adsorption of surfactants and their mixtures at solid/solution interface is a complex process. The driving force for adsorption is a combination of the electrostatic

interaction, the chemical interaction, the lateral chain–chain associative interaction, the hydrogen bonding and desolvation of the adsorbate species (Zhang and Somasundaran, 2006).

As seen in Figure 3, surface tensions for SDS have not been changed before and after equilibration with shale (SDS=b & SDS=a, respectively). However, surface tensions for TX100 were increased significantly after equilibration with shale (TX=a). Similarly, the CMC of both SDS and TX100 as determined by surface tension technique are different at 0.1wt% and 1.5wt%, respectively. Hence, the CMC of SDS has not been notably changed before and after equilibration with shale. This indicates a minor loss of this surfactant to shale. In contrast, the CMC value of TX100 has been shifted to higher concentrations, i.e., the surfactant was adsorbed heavily to shale. This is a result of less surfactant monomer concentration in surfactant solutions after equilibration with shale. This significant loss of TX100 monomers is attributed to their adsorption to organic matter/clay minerals in shale.

Figure 4 depicts surface tension curves of individual surfactants and their mixtures after equilibration with shale. It is obvious that mixtures at all SDS molar fractions do improve behavior of individual surfactants at air-water interface. All CMCs of SDS-TX100 mixtures are similar to that of pure SDS at 0.1wt% and lower than that of pure TX100 (0.15wt%).

At the CMC values, the concentration of the bulk solutions will be saturated with surfactant monomers. As the fresh surfactant solution start to form micelles at a specific monomer concentration, it is assumed that surfactant/shale supernatant would form micelles at the same monomer concentration indicating the same surface/interfacial tension but at different CMCs. Hence, the amount of surfactant adsorbed to shale can be calculated from difference between CMC obtained after equilibration with shale and/or presence of oil phase and the original CMC. From Figure 3, the difference in pure TX100's CMCs as determined from surface tension curves was found to be 0.125wt% (0.15-0.025wt%). This concentration can be normalized to shale mass by dividing it by sorbent mass and multiplying by solution mass to yield g-TX100 to g-Shale (0.00125×60/10g = 0.0075g-TX100/g-shale or 7.5g-TX100/Kg-shale). Similar values have been reported in literature for natural soil (Zheng and Obbard, 2002; Zhou and Zhu, 2007). Zheng and Obbard (2003) found a maximum loss of 5mmole-TX100/Kg-soil (3.14g-TX100/Kg-soil). Similarly, Zhou and Zhu (2007) reported a maximum loss of about 12mmole-TX100/Kg soil (7.536g-TX100/Kg-soil) to an uncontaminated soil collected from Hangzhou City, China.

Considering the surface tension trends (Figures 1 & 4), CMCs of mixtures were close to TX100 CMC before equilibration with shale and closer to SDS's CMC after equilibration with shale. Hence, the maximum adsorption for mixtures (ΔCMC= 0.1-0.025= 0.075wt%) are lower than that of pure TX100 (ΔCMC= 0.15-0.025= 0.125wt%), i.e. 40% reduction. Accordingly, it can be said that the presence of SDS (at molar ratios used in this work) did reduce sorption of TX100 to shale. This is in agreement with the observation made by other researchers (Zhou and Zhu, 2007; Yu et al., 2007). Zhou and Zhu (2007) found a 45-71% (from 11.6 to 6.41 and 3.33 mM/Kg) decrease in the maximum sorption amount of TX100 while using approximately comparable SDS molar ratios as this study (1:2 and 2:1 SDS:TX100 mass ratio, respectively). Yu et al. (2007) results showed 47-70% (from 15 to 8 and 4.5 mM/Kg) reduction with 1:2 and 2:1 SDS:TX100 mole ratios, respectively.

Generally, the nature of solid surface whether hydrophobic or hydrophilic and the electrical interactions play an important role in the kinetics of adsorption of surfactant at the solid–liquid interface. Electrostatic interactions are most important for anionic SDS surfactant. Most natural surfaces are negatively charged under naturally occurring conditions. As a result, anionic surfactant will experience a repulsive electrostatic interaction with most natural surface; this serves to make them adsorb to a lesser extent than nonionic surfactants for most applications. Adsorption of a nonionic surfactant such as TX-100 has proposed to involve hydrogen bonding. Hydrogen bonding is weaker than electrostatic interactions. It should be noted that for adsorption due to hydrogen bonding to take place, the bond formed between the surfactant functional groups and mineral surfaces should be stronger than that formed between the mineral and interfacial water molecules (Zhang and Somasundaran, 2006). Hydrophobic bonding can also be important for adsorption on solids that possess a fully or partially hydrophobic surface. In this case, surfactant molecules can adsorb flat on the hydrophobic sites on the solid. Such adsorption can also take place on other types of solids that are originally hydrophilic, but that have acquired some hydrophobicity owing to reaction with organic species in solutions (Somasundaran and Huang, 2000).

More importantly, surfactant adsorption is related to the chemical potential of the surfactant molecules (monomers) in solution and the nature of the solid. Under mixed micellization conditions the chemical potential of monomers will be lower than that for the single surfactant system and this in turn can reduce adsorption at the solid-liquid interface. Beyond the CMC, the aqueous monomer concentration will not increase with any further addition of surfactant since the additional surfactant will form micelles. Sorption of TX100 surfactant as well as SDS-TX100 mixtures to shale is limited by their critical micelle concentrations and reaches a plateau at their CMCs. The CMC-limited sorption of surfactants reflects the significant effects in reducing the CMC of surfactant system; in other words, a reduction in their CMCs reduces their sorption to shale.

4.3 Surfactant Losses to Both Shale and Oil

After equilibration with shale and in presence of oil phase, SDS interfacial tension (SDS=a+) has been slightly increased particularly for sub-micellar concentrations (Figure 5). Meanwhile, Interfacial tensions for TX100 were increased significantly (TX=a+). This significant loss of TX100 is attributed to adsorption to organic matter/clay minerals in shale and partitioning into Sarapar147.

CMC of TX100 was attained at 0.25wt% in presence of Sarapar147. This is a perceptible detrimental change in TX100 behavior in presence of both shale and oil. The result shows that both shale and Sarapar147 are responsible for loss of TX100. As shown in Figure 5, the difference in CMCs of pure TX100 as determined from interfacial tension curves was found to be 0.225wt% (0.25-0.025). When normalized to mass of shale and solution a value of 22.5g-TX100/Kg-shale can be estimated. This tremendous loss of TX100 surfactant concentration is due to interaction of TX100 with both shale and Sarapar147.

As shown in Figure 6, surfactant mixtures performed better in presence of both shale and oil. Though the CMCs and interfacial tensions are not lower than those of pure SDS' CMC (0.1wt%), they are however, much lower than that of pure TX100 (2.5wt%). Mixtures result in about 60% reduction in surfactant losses. Hence, it can be said that the presence of SDS significantly reduced adsorption and partitioning of TX100 to shale and Sarapar147, respectively.

It is clear that the addition of SDS has reduced the amount of TX100 adsorbed to shale or partitioned into the oil phase. It is widely accepted among researchers that SDS surfactant is less likely to adsorb to shale and far less likely to partition into an oil phase. However, TX100 surfactant is more liable to sorb onto shale and partition into oil phase (Harusawa et al., 1980; Butler and Hayes, 1998; Zimmerman et al., 1999; Cowell et al., 2000; Zhao et al., 2006; Zhao et al., 2007). Mixing SDS with TX100 may therefore retard the affinity of TX100 to sorb onto shale or partition into oil phase. It is needed to point out that sorption and/or partitioning of any surfactant proceeds through the sorption and/or partitioning of surfactant monomers and micelle formation limits surfactant adsorption and partitioning, i.e., the micelles are not directly sorbed or partitioned (Harusawa et al., 1980; Zhu et al., 2003; Paria and Khilar, 2004). In mixed surfactant solution, the formation of mixed micelles affect the CMC, i.e. mixing will result in a lower CMC. This will reduce the monomer concentration of component surfactant in mixed solution and hence their sorption onto shale and partition to oil phase (Zhou and. Zhu, 2007).

5. Conclusion

The choice of a successful surfactant to enhance remediation must goes beyond selection of surfactant system that efficiently solubilize or mobilizes specific oil contaminants. The surfactant must also be matched to the subsurface soil matrix and salinity conditions. Similarly, surfactant partition tendencies into the specific oil contaminants must be addressed. This may ensure that the surfactant system remains at an active concentration. Surfactants losses to soils and/or oil phase will, through various chemical interactions such as sorption, precipitation and partitioning retard contaminant removal. Surfactant sorption to soil will increase soil/sediment organic carbon content favoring the adsorption of hydrophobic organic compounds, escalate cost of the operation by increasing surfactant doses let alone surfactant pollution to soil/ground water and their effect on contaminant biodegradation.

Attempts made in this work to minimize losses of nonionic surfactant (TX100) to local shale and/or partitioning to oil, Sarapar147, through use of anionic-nonionic (SDS-TX100) surfactant mixture was successful. SDS-TX100 surfactant mixtures were able to maintain their active concentrations in presence of shale and oil while using low initial surfactant concentration as low as 0.1wt%. The experimental data from surface tensions of solutions before equilibration with shale showed that CMCs of mixed surfactants are much lower than that of individual SDS but closer to that of pure TX100. However, data from interfacial tensions showed that CMCs of mixed surfactants are lower than both surfactants. After equilibration with shale the CMCs of mixtures as obtained from surface and interfacial tension data are close to that of pure SDS (0.1wt%) but are much lower than that of pure TX100 (1.5 and 0.25wt%, respectively). Results showed that all mixtures behave similarly and have superior properties than both single surfactants. Partitioning and adsorption of TX100 into organic phase (Sarapar147) and shale were decreased by mixing with anionic surfactant (SDS). The data showed a 40% reduction in surfactant losses due to adsorption to shale and around 60% reduction due to both partitioning and adsorption.

6. References

Butler, E. C., & Hayes, K. F. (1998). Micellar solubilization of nonaqueous phase liquid contaminants by nonionic surfactant mixtures: effects of sorption, partitioning and mixing. *Water Research*, 32, 1345-1354.

Chang, C.-R., Huang, C.-R., & Shu, H.-Y. (2000). Effect of surfactants on extraction of phenanthrene in spiked sand. *Chemosphere*, 41, 1295-1300.

Chou, C. C., Ososkov, V., Zhang, L., & Somasundaran, P. (1998). Removal of nonvolatile hydrophobic compounds from artificially and naturally contaminated soils by column flotation. *Journal of Soil Contamination*, 7, 5, 559-571.

Chu, W., & Chan, K. H. (2003). The mechanism of the surfactant-aided soil washing system for hydrophobic and partially hydrophobic organics. *The Science of the Total Environment*, 307, 83-92.

Cowell, M. A., Kibbey, T. C. G., Zimmerman, J. B., & Hayes, K. F. (2000). Partitioning of ethoxylated nonionic surfactants in water/NAPL systems: effects of surfactants and NAPL properties. *Environ. Sci. Technol.*, 34, 1583-1588.

Deshpande, S., Shiau, B. J., Wade, D., Sabatini, D. A., & Harwell, J. H. (1999). Surfactant selection for enhancing ex situ soil washing. *Water Research*, 33, 351-360.

Edwards, D. A., Adeel, Z., & Luthy, R. G. (1994). Distribution of nonionic surfactant and phenanthrene in a sediment/aqueous system. *Environ. Sci. Technol.*, 28, 1550-1560.

Haigh, S. (1996). A review of the interaction of surfactants with organic contaminants in soil. *The Science of the Total Environment*, 185, 161-170.

Harusawa, F., Taeko, S., Nakajima, H., & Fukushima, S. (1980). Partition isotherms of nonionic surfactants in the water–cyclohexane system and type of emulsion produced. *Journal of Colloid and Interface Science*, 74, 435-440.

Jada, A., & Hamieh, T. (2001). Removal by surfactants of asphalt adsorbed onto clays. *IEEE*, 154-158.

Janczuk, B., Bruque, J. M., Gonzalez-Martin, M. L., & Doradu-Calasanz, C. (1995). The properties of mixtures of ionic and nonionic surfactants in water at the water/air interface. *Colloids and Surfaces A: Physicochemical and Eng. Aspects*, 104, 157-163.

Joshi, T., Mata, J., & Bahadur, P. (2005). Micellization and interaction of anionic and nonionic mixed surfactant systems in water. *Colloids and Surfaces A: Physicochem. Eng. Aspects*, 260, 209-215.

Kile D. E., & Chiou C. T. (1989). Water solubility enhancement of DDT and trichlorobenzene by some surfactants below and above the critical micelle concentration. *Environ. Sci. Technol.*, 23,832–838.

Lee, D. H., Chang, H. W., & Cody, R. D. (2004). Synergism effect of mixed surfactant solutions in remediation of soil contaminated with PCE. *Geosciences Journal*, 8, 3, 319-323.

Mata, J. P. (2006). Hydrodynamic and clouding behavior of Triton X-100 + SDS mixed micellar systems in the presence of sodium chloride. *Journal of Dispersion Science and Technology*, 27, 49-54.

Owoyomi, O., Jide, I., Akanni, M. S., Soriyan, O. O., & Morakinyo, M. K. (2005). Interaction between sodium dodecylsulphate and Triton X-100: molecular properties and kinetics investigations. *Journal of Applied Science*, 5, 4, 729-734.

Paria, S., Manohar, C., & Khilar, K. C. (2003). Experimental studies on adsorption of surfactants onto cellulosic surface and its relevance to detergency. *Journal of the Institution of Engineers, Singapore,* Vol. 43, No. 2, 34-44.

Paria, S., & Yuet, P. K. (2007). Adsorption of nonionic surfactants onto sand and its importance in naphthalene removal. *Ind. Eng. Chem. Res*., 46,108-113.

Porcel, R., Jodar, A. B., Cabrerizo, M. A., Hidalgo-Albarez, R., & Martin-Rodriguez, A. (2001). Sequential adsorption of Triton X-100 and sodium dodecylsulfate onto positively and negatively charged polystyrene latexes. *Journal of Colloid and Interface Science*, 239,568-576.

Rao, P., & He, M. (2006). Adsorption of anionic and nonionic surfactants mixtures from synthetic detergents on soils. *Chemosphere*, 63, 1214-1221.

Rodriguez-Cruz, M. S., Sanchez-Martin, M. J., & Sanchez-Camazano, M. (2004). Enhanced desorption of herbicides sorbed on soils by addition of Triton X-100. *Journal Environ. Qual.*, 33, 920–929.

Rodriguez-Cruz, M. S., Sanchez-Martin, M. J., & Sanchez-Camazano, M. (2006). Surfactant-enhanced desorption of atrazine and linuron residues as affected by aging of herbicides in soil. *Arch. Environ. Contam. Toxicol.*, 50, 128–137.

Rosen, M. J. (2004). *Surfactants and interfacial phenomena*. (4th ed.). New York: Wiley-Interscience.

Saichek, R. E., & Reddy, K. R. (2004). Evaluation of surfactant/cosolvents for desorption/solubilization of phenanthrene in clayey soils. *Intern. Journal Environ. Studies*, Vol. 61, 5, 587-604.

Sanchez-Camazano, M., Rodriguez-Cruz, M. S, & Sanchez-Martin, M. J. (2003). Evaluation of component characteristics of soil-surfactant-herbicide system that affect enhanced desorption of linuron and atrazine preadsorbed by soils. *Environ. Sci. Technol.*, 37, 2758-2766.

Sanchez-Camazano, M., Sanchez-Martin, M. J., & Rodriguez-Cruz, M. S. (2000). Sodium dodecylsulphate-enhanced desorption of atrazine: effect of surfactant concentration and of organic matter content of soils. *Chemosphere*, 41, 1301-1305.

Sanchez-Martin, M. J., Rodriguez-Cruz, M. S., & Sanchez-Camazano, M. (2003). Study of the desorption of linuron from soils to water enhanced by the addition of an anionic surfactant to soil-water system. *Water Research*, 37, 3110–3117.

Smith, E., Smith, J., Naidu, R., & Juhasz, A. L. (2004). Desorption of DDT from a contaminated soil using cosolvent and surfactant washing in batch experiments. *Water, Air, and Soil Pollution*, 151, 71-86.

Somasundaran, P., & Huang, L. (2000). Adsorption aggregation of surfactants and their mixtures at solid-liquid interfaces. *Advances in Colloid and Interface Science*, 88, 179-208.

Sun, S., Inskeep, W. P., & Boyd, S. A. (1995). Sorption of nonionic organic compounds in soil-water systems containing a micelle-forming surfactant. *Environ. Sci. Technol.*, 29, 903–913.

Urum, K., & Pekdemir, T. (2004). Evaluation of biosurfactants for crude oil contaminated soil washing. *Chemosphere*, 57, 1139-1150.

Urum, K., Grigson, S., Pekdemir, T., & McMenamy, S. (2006). A comparison of the efficiency of different surfactants for removal of crude oil from contaminated soils. *Chemosphere*, 62, 1403-1410.

Urum, K., Pekdemir, T., & Copur, M. (2004). Surfactant treatment of crude oil contaminated soils. *Journal of Colloid and Interface Science*, 276, 456-464.

Wang, W., & Kwak. J. C. T. (1999). Adsorption at the alumina-water interface from mixed surfactant solutions. *Colloids and Surfaces A: Physicochemical and Eng. Aspects*, 156, 95-110.

Yang, K., Zhu, L., & Zhao, B. (2005). Minimizing losses of nonionic and anionic surfactants to a montmorillonite saturated with calcium using their mixtures. *Journal of Colloid and Interface Science*, 291, 59-66.

Yu, H., Zhu, L., & Zhou, W. (2007). Enhanced desorption and biodegradation of phenanthrene in soil-water systems with the presence of anionic/nonionic mixed surfactant. *Journal of Hazardous Materials*, 142, 354-361.

Zhang et al. (2005). Interaction of nonionic surfactant AEO9 with ionic surfactants. *Journal Zhejiang Univ.*, SCI 6B, 6, 597-601.

Zhang, L., Somasundaran, P., Ososkov, V., & Chou, C. C. (2001). Flotation of hydrophobic contaminants from soil. *Colloids and Surfaces A: Physicochemical and Eng. Aspects*, 177, 2-3, 235–246.

Zhang, R., & Somasundaran, P. (2006). Advances in adsorption of surfactant and their mixtures at solid/solution interfaces. *Advances in Colloid and Interface Science*, 123-126, 213-229.

Zhao, B., & Zhu, L. (2006). Solubilization of DNAPLs by mixed surfactant: synergism and solubilization capacity. *Journal of Hazardous Materials*, B136, 513-519.

Zhao, B., Chen, X., Zhu, K., & Zhu, L. (2007). Micellar solubilization of TCE and PCE by mixed surfactant: effects of surfactant partitioning and DNAPL mixing. *Colloids and Surfaces A: Physicochemical and Eng. Aspects*, 296, 167-173.

Zhao, B., Zhu, L., & Yang, K. (2006). Solubilization of DNAPLs by mixed surfactant: reduction in partitioning losses of nonionic surfactant. *Chemosphere*, 62, 772-779.

Zhao, B., Zhu, L., Li, W., & Chen, B. (2005). Solubilization and biodegradation of phenanthrene in mixed anionic-nonionic surfactant solutions. *Chemosphere*, 58, 33-40.

Zheng, Z., & Obbard, J. P. (2002). Evaluation of an elevated nonionic surfactant critical micelle concentration in a soil/aqueous system. *Water Research*, 36, 2667–2672.

Zhou, M., & Rhue, R. D. (2000). Screening commercial surfactants suitable for remediation DNAPL source zones by solubilization. *Environ. Sci. Technol.*, 34, 1985-1990.

Zhou, W., & Zhu, L. (2004). Solubilization of pyrene by anionic-nonionic mixed surfactants. *Journal of Hazardous Materials*, B109, 213-220.

Zhou, W., & Zhu, L. (2007). Enhanced desorption of phenanthrene from contaminated soil using anionic/nonionic mixed surfactant. *Environmental Pollution*, 147, 350-357.

Zhou, W., & Zhu, L. (2005). Solubilization of Polycyclic Aromatic Hydrocarbons by Anionic-Nonionic Mixed Surfactants. *Colloids and Surfaces A: Physiochem. Eng. Aspects*, 255, 145-152.

Zhu, L. & Feng, S. (2003). Synergistic solubilization of polycyclic aromatic hydrocarbons by mixed anionic-nonionic surfactants. *Chemosphere*, 53,459-467.

Zimmerman, J. B., Kibbey, T. C. G., Cowell, M. A., & Hayes, K. F. (1999). Partitioning of ethoxylated nonionic surfactant into nonaqueous-phase organic liquids: influence on solubilization behavior. *Environ. Sci. Technol.*, 33,

169–176.

Zuidema, H. H., & Waters, G. W. (1941). A Ring method for determination of interfacial tension. *Industrial and Engineering Chemistry, Analytical Edition*, Vol. 13, 312.

Table 1. Physicochemical properties of chemicals

Chemical	Structure/ Composition	MW[a] g/mol	CMC[b], mg/L (mM/L)	HLB[c]	D[d], g/mL	BP[e], ºC
TX100	$C_{34}H_{62}O_x$(x-11)	646.37	130-200 (0.2-0.31)	13.5[$]	1.070[#]	270[#]
SDS	$C_{12}H_{24}NaSO_4$	288.4	963-2420 (3.32-8.4)	40[$]	0.400[#]	-
Sarapar147	95wt% n-paraffin and 5wt% iso-paraffin	NA	-	-	0.773[#]	258-293[#]

[a] Molecular Weight; [b] Critical micelle Concentration; [c] Hydrophile-lipophile balance; [d] Density; [e] Boiling Point; [$] Zhou and Zhu (2004); [#] Provided by company; NA=Not Available.

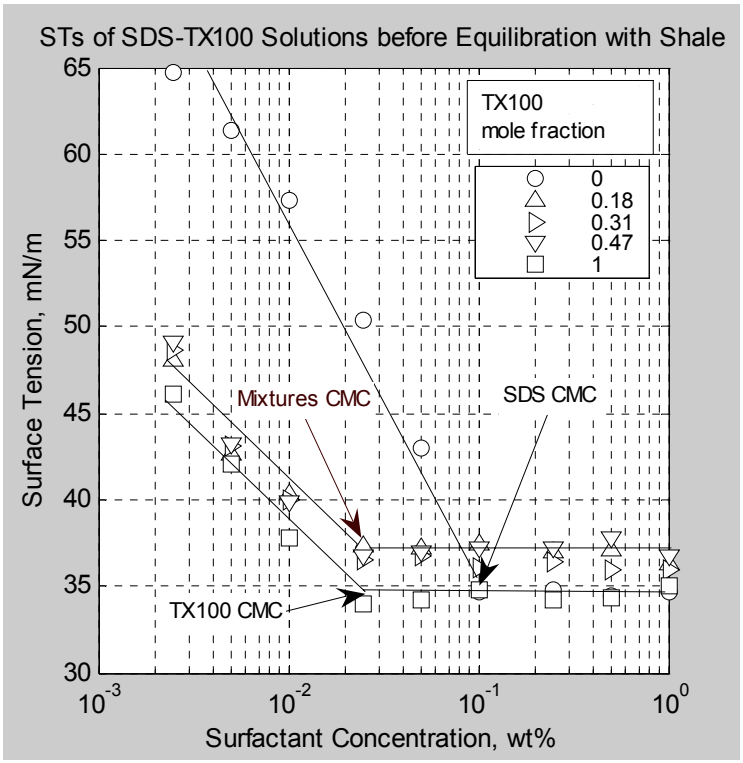

Figure 1. Surface Tension Curves for Pure Surfactants and Mixtures before Equilibration with Shale

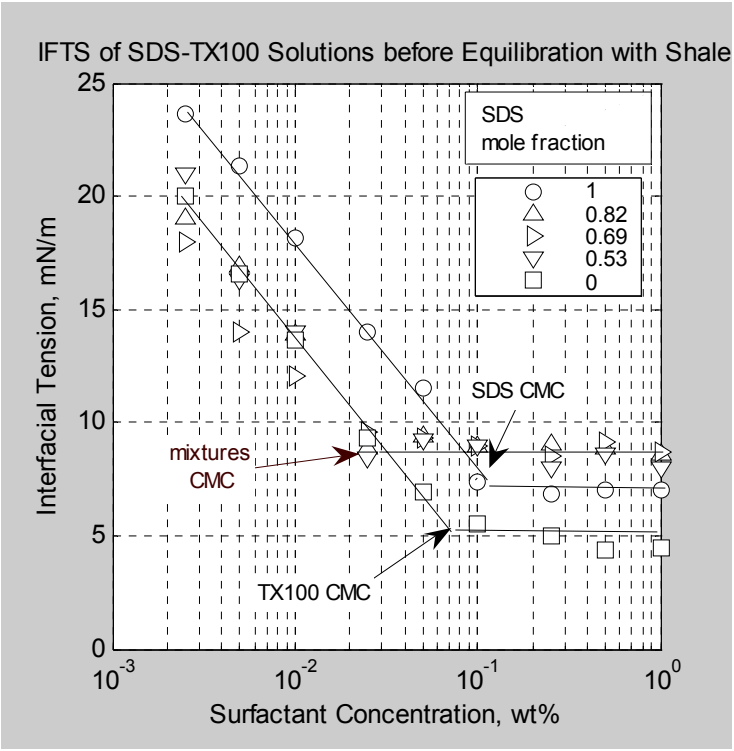

Figure 2. Interfacial Tension Curves for Pure Surfactants and Mixtures before Equilibration with Shale

Modern Applied Science

www.ccsenet.org/journal.html

Vol. 2, No. 3

May 2008

Synthesis of Strong Sweetener Sucralose

Ye Luo, Lei Xu & Xiaofei Sun

College of Pharmacy, Soochow University

Suzhou 215123, China

Tel: 86-512-6588-0413 E-mail: sunxiaofei@suda.edu.cn

Abstract

Synthesize sucralose from sucrose as a starting material by following steps: first synthesis sucrose-6-acetate, and then by chlorination, at last deacetylation. The Synthetic Approach is simple, with high yield and under mild reaction conditions. the ultimate product sucralose was purified and bleaching, and its structure was characterized by the IR, MS, etc.

Keywords: Sucrose-6-acetate, Sucralose, Synthesis

The sucralose is TGS for short, its chemical name is 1 ', 6 ' - dichloro - 1 ', 6 ' -didesoxy - β-D - fructofuranose - 4-chloro - 4- desoxy - α-D - fructofuranose, is one derivative of the halogeno sucrose. It's mild and mellow, with aromatic flavor and stable property, it's low in calories and good for consumers' health; it can be used together with the traditional sweetener, and used independently. it's good in sweet taste and mouth feel (Kang, 2001, pp. 12). However, the sucralose can't rot teeth away, and not cause many diseases as the fructose and maltose, besides its low sugar price is not so high as other nutritional sweeteners(Huang, 2000, pp. 22),moreover, the toxicology and the safety test indicated: sucralose does not have teratogenicity, discontinuity, reproduction toxicity, cancerous as well as nerve toxicity, also does not have any effects on animal's blood sugar level and the insulin secretion (Gao, 2004, pp. 5).Therefore, it could be edible for obese patients, patients with cardiovascular disease and diabetes. It is a strong sweetener prepared by British Professor Hough L in the late 1970s (Yan, 2004, pp 165), it's also artificially developed, and the most competitive, non-nutrition, perfect high-intensity sweetener until now (Tian, 2006, pp. 3).

The demand for sucralose in China is about 50 tons annually, the majority depends on imports, and is only used in some relatively high-grade food at present, it hasn't been widely used in China yet(Shen, 2007,pp. 137).Therefore, if the basic research on the sucralose production technology can be strengthened, that will further improve the technique of production, reduce the cost of product, and extend its application range greatly, and thus give an impetus to the development of food additive industry in China. Nowadays, people have explored many methods of the development about sucralose, such as the tritylation method, the monoesterification, biosynthesis, the hydrolyzing raffinose and the chlorination of sucrose derivative .etc (Chen, 2007, pp. 90). The chemical synthesis method above always take too many steps and the technical process is complex. The fermentation of chemically enzymatic synthesis is complex, and it's difficult to purify the intermediary product, with high cost. The monoesterification only needs three steps in the reaction of synthesis, with high yield and low cost, the intermediary product is easy to separate, so it's an ideal technical process for the synthesis of sucralose (Kang, 2006, pp. 59).

We synthesize sucralose from sucrose as a starting material by following steps: first synthesis sucrose-6-acetate, and then by chlorination, at last deacetylation (just as the following figure shows), and make research on technological process, reaction conditions, etc.

1. Experimental material and equipments

1.1 Chemical materials and reagents

Sucrose, DMF, trimethyl orthoacetate, tert-Butylamine, p-TsOH,1, 1, 2 trichlorethane, thionyl chloride and etc are analytical pure or chemical pure.

1.2 Equipments

RE-2000 Rotary Evaporator (made in Shanghai Yarong Biochemistry Instrument Factory); 85-2A Magnetic Stirrer (made in Jintan Fuhua Instrument Co., Ltd); SHZ-DA Vacuum Pump of Circulating Water(made in Gongyi Yingyu Yuhua Instrument Factory); DZF-6050 Vacuum Drying Oven(made in Shanghai Jinghong Laboratory Instrument Co., Ltd); XT4A Microscopic Melting-point Detector(made in Beijing Keyi Electron Optical Instrument Factory); ProStar LC240 Infrared Spectrophotometer and Saturan2200 mass spectrometer(both made in the US Varian,Inc).

2. Experimental methods and results

2.1 Synthesis of sucrose-6-acetate

Take sucrose (25.0g) to anhydrous DMF (100ml), the reaction mixture is stirred under the room temperature, and trimethyl orthoacetate (10.5ml) is added dropwise slowly, and p-TsOH (0.15g) is added, it's stirred for 2.5 hours, then add distilled water (10ml), keep reaction for 40 minutes again, after that, tert-Butylamine is added, the reaction mixture continues to be stirred for 1.5 hours, when it's finished, concentrate the reactant, add ethyl acetate and methanol, stir the mixture under the heating condition, cool down, at last white powdery crystal (12.8g, 51%.) is separated out. mp 93~95℃, IR (KBr, cm^{-1}): 3416(-OH), 1728 (C=O).

2.2 The chlorination of sucrose - 6- acetate

Take sucrose - 6- acetate (10g) to dissolve in anhydrous DMF (100ml), under the ice-bath condition, add dropwize the mixed solvent of thionyl chloride (23ml) and 1,1,2- trichlorethane (43ml) slowly, when it's finished, maintain the low temperature in 30 minutes; heat up to 115℃ slowly within 2 hours, reflux in 1.5 hours; and then cool off the reaction liquid until the temperature is below 15℃ , add weak aqua ammonia (6mol/L,20ml) dropwise slowly, and keep temperature below 30℃, it is neutralized with the alkaline solution, The organic phase is separated from the aqueous phase, extract the aqueous phase with 1,1,2 trichlorethane(20ml×3),the organic phase is combined, and the solvent was evaporated under the diminished pressure, thick product(5.9g, 59%.) is obtained.

2.3 The preparation of sucralose

Sucrose-6-acetate(5g)dissolves in methanol(28.1ml) which contains sodium methoxide **(**0.11g), under room temperature, diminished pressure condition, the reaction mixture is stirred for 2 hours, the dark-brown crude product is obtained by suction filtration, and then recrystallized with methanol, the product is decolored by active carbon, sucralose(3.6g,70%) is obtained after vacuum drying. mp83~85℃,IR(KBr,cm^{-1}):3452(-OH),1086(C-O),732(C-Cl).MS(m/z):397(MH^+),197(MH^+-$C_6H_9Cl_2O_3$).

3. Discussion

When it comes to the catalytic reaction with p-TsOH, if the quantity of the acid is insufficient, the solution PH value would be high, and the reaction won't be complete, plenty of sucrose have not participated in the reaction, it would affect the yield of sucrose-6-acetate directly. If p-TsOH is excessive, it would make the product break down. if the quantity of tert-Butylamine is insufficient, the PH value of solution is low, the reaction would not be complete.

Since DMF is also used for solvent during the chlorination of sucrose - 6- acetate, after obtaining the sucrose - 6- acetate in the reaction, the solid intermediate may not be obtained directly, it only need provide sucrose - 6- acetate in DMF solution for the chlorination In the process of sucralose's preparation, the chloride reaction is the key to the entire synthesis process. when thionyl chloride is added, the reaction temperature needs to be controlled, because a quantity of heat will be emitted at this time, the product is prone to charring. In order to control the temperature, this ice-bath was used, it could keep the reaction temperature low, be beneficial for the reaction to carry on smoothfully. The mixture of thionyl chloride and 1,1,2- trichloroethane is added dropwise with the dropping funnel, otherwise heat would be emitted too quickly in reaction mixture, the temperature can't be diminished in time, it would have negative effect on the experiment.

We used the method of group protected in our experiment, carried on improvement to the existing preparation method, the product is obtained only through three-step reaction, each step is easy to operate, the raw material is easily obtained, increasing the yield of the product, reducing the production costs greatly and being more helpful for the industrial production.

Acknowledgement

The authors would like to acknowledge College of Pharmacy and The Center of Analysis and Measurement (CAM) at Soochow University for their sponsorship of this work.

References

Kang, W. M**. (**2001). The Characters and Applications of The Sucralose. *Beverage & Fast Frozen Food Industry*, 1(4), pp. 12

Huang, S. M**.,** Zhang, H.G., & Li, S.F. **(**2000). Progress in Research and Application of High-intensity Sweetener Sucralose. *Chemical Industry and engineering Progress*, 19(4), pp. 22

Gao, J. Y**.,** Chen, H. B **(**2004). Application of Sucralose in Sugar Free Chocolate and Chewing Gums. *The food industry*, (6), pp. 5

Yan, R.A**. ,** L,Y. **(**2004). Study on the Synthesis of Sucralose. *Chemical World,* 45 (3), pp. 165

Tian, T. N. **,** Tian, Y. Z. **(** 2006). The Advance of Synthetic Technology Study on the Sweetener Sucralose. *Hebei*

Chemical, 29 (5), pp. 3

Shen, Y. F. **.** Ma, Z. Z. , & Li, H. **(**2007). The Characteristic of Sucralose and Its Application in Food. *China Food Additives*, 29 (4), pp. 137

Chen, J. E. (2007). Development of Super Edulcorant -- Trichlorosaccharose. *Liquor-Making Science & Technology*, (2), pp.90

Kang, W. T. **,** Yang, J. M. , & Chen, Q. etc. **(**2006). The Study of New Kind of Sweetener Sucralose, *China Condiment*, (1), pp. 59

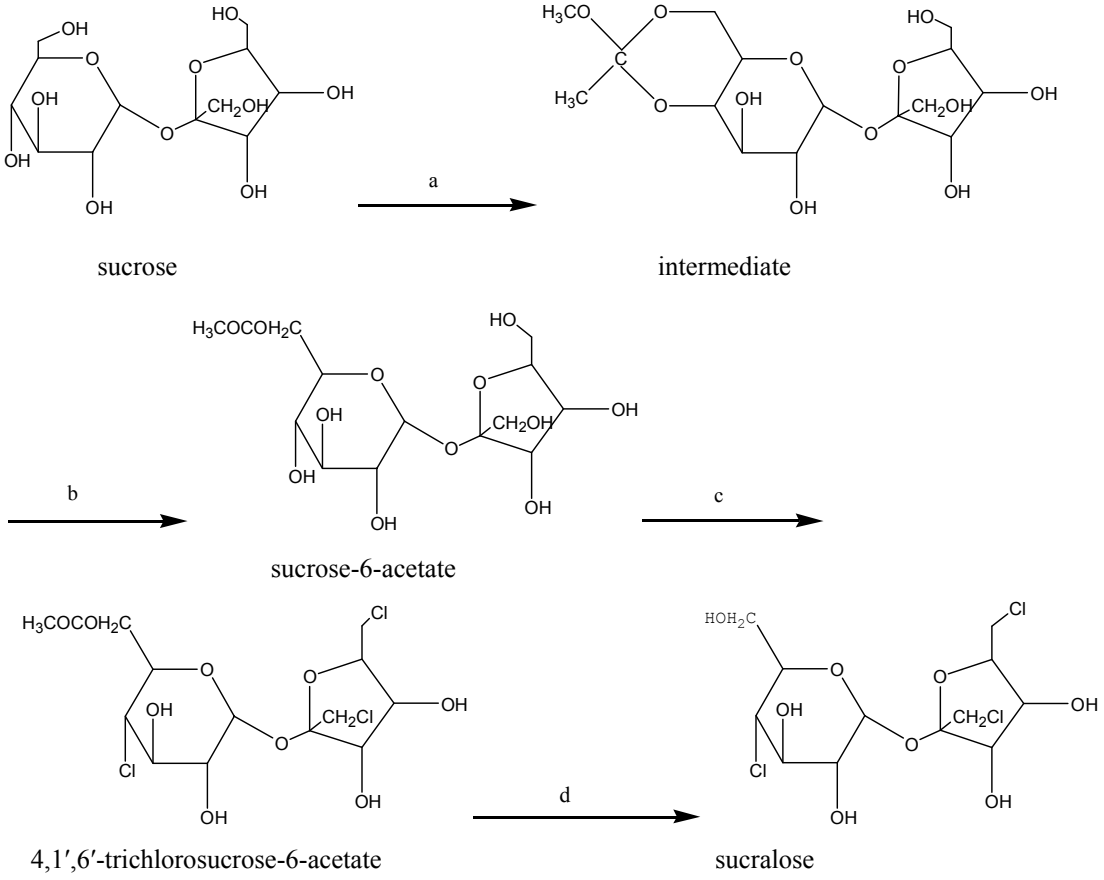

Figure 1. Technical process for synthesizing sucralose: (a)p-TsOH, trimethyl orthoacetate, rt, 2.5h; (b) water, tert-Butylamine, rt 1.5h; (c)1,1,2- trichlorethane, $SOCl_2$ 0℃, 30min; (d) CH_3OH,CH_3ONa, rt, 2h

Modern Applied Science

www.ccsenet.org/journal.html

Vol. 2, No. 3

May 2008

Study of Intermolecular Interactions of Binary Liquid Mixtures by Measuring Intensive Macroscopic Properties at (303.15, 313.15 and 323.15) K and at Ambient Pressure

T.R Kubendran (corresponding author)

Department of Chemical Engineering

Alagappa College of Technology

Anna University, Chennai-600025, India

E-mail: trkubendran@yahoo.co.in

R. Baskaran

Department of chemical engineering

St. Joseph's college of Engineering, Chennai-119, India

E-mail: rbaskaran2000@yahoo.com

Abstract

Measurements of thermodynamic and transport properties have been adequately employed in understanding the nature of molecular systems and physico-chemical behavior in liquid mixtures. These properties are important from practical and theoretical point of view to understand liquid theory. In the present study density (ρ) and viscosity (η), have been measured for a binary liquid mixture of Diacetone alcohol with benzene and chlorobenzene, over the entire composition range at 303.15 K, 313.15 K and 323.15 K and the evaluation of different excess properties. The viscosity values and excess values were fitted to respective models. It was found that in all cases, the data obtained fitted with the values correlated by the corresponding models very well. The molecular interactions existing between the components and comparison of liquid mixtures were also discussed.

Keywords: Binary mixture, Diacetone alcohol, Benzene, Chlorobenzene, Density, Viscosity

1. Introduction

Binary liquid mixtures due to their unusual behavior have attracted considerable attention Ewing et al. (1970). In chemical process industries materials are normally handled in fluid form and as a consequence, the physical, chemical, and transport properties of fluids assume importance. Thus data on some of the properties associated with the liquids and liquid mixtures like Density, and viscosity, find extensive application in solution theory and molecular dynamics Mchaweh et al. (2004). Such results are necessary for interpretation of data obtained from thermo chemical, electrochemical, biochemical and kinetic studies "Kenart, (2000)". Diacetone alcohol is used as coating solvent. Diacetone alcohol + benzene mixture is used in the preparation of tetramethyl oxopiperidine and also acts as pigments. Diacetone alcohol + chlorobenzene mixture is used in the preparation of polymeric photonic crystals which is used for producing switches. In the present paper, we have reported density (ρ) and viscosity (η) of pure diacetone alcohol with benzene and chlorobenzene as well as for the binary system constituted by these chemicals at temperatures of 303.15 K, 313.15 K and 323.15 K. The viscosity values have been fitted to "McAllister, (1960)" model. The deviation values have been fitted to "Redlich-Kister, (1948)" equation. Literature survey showed that no measurements have been previously reported for the mixture studied in this paper.

2. Materials and methods

The chemicals used were of analytical reagent grade obtained from loba chemicals. All were dried over anhydrous calcium chloride and fractionally distilled "Oswal and Patel,(1995)". All the weighing measurements were done with Shimadzu Corporation Japan Type BL 2205 electronic balance accurate to 0.01 g. The possible uncertainty in the mole fraction was estimated to be less than ±0.0001. All the measurements described below were performed at least three times and the results were averaged to give the final values.

2.1 Density

The densities were determined by using bicapillary pycnometer as described by Arun et al.(1995) and calibrated with deionized double distilled water with 0.9960x 10^3 $Kg.m^{-3}$ as its density at temperature 303.15 K. The positions of the liquid level in the two arms were recorded with a help of traveling microscope which could read to 0.01mm. The precision density measurements were within ±0.0003$g.cm^{-3}$. The excess volumes can be computed from experimental density data using the relationship

$$V^E = (x_1M_1 + x_2M_2) / \rho_m - (x_1M_1/ \rho_1 + x_2M_2 / \rho_2) \quad (1)$$

Where x_1 and x_2 refers to the mole fraction of components 1 and 2. $\rho_1$and ρ_2 refers to the density of components 1 and 2. ρ_m is the density of mixture.

2.2 Kinematic viscosity

The Kinematic viscosities were measured as described by Kubendran et al. (2004) at the desired temperature using Ostwald viscometer. The viscometer was calibrated using water. The flow measurements were made with an electronic stopwatch with a precision of 0.01sec. In the calculation of viscosity, two constants a and b of the viscometer in the relation $\nu = (at) - (b/t)$ were obtained by measuring the flow time with high purity benzene at the working temperature. The calculated viscosities were fitted in Eq. (2) and constants were determined. The kinematic viscosity were correlated by means of McAllister model considering three-body interaction, which for a two component mixture gives

$$\ln \nu = x_1^3 \ln \nu_1 + 3 x_1^2 x_2 \ln \nu_{12} + 3 x_1 x_2^2 \ln \nu_{21} + x_2^3 \ln \nu_2 - \ln(x_1 + x_2 M_2 / M_1) + 3x_1^2 x_2 \ln ((2+M_2 / M_1) / 3) + x_2^3 \ln (M_2 / M_1) + 3 x_1 x_2^2 \ln ((1+ 2 M_2 / M_1)/3) \quad (2)$$

Where ν refers to the kinematic viscosity of the mixture of components 1 and 2 having mole fractions x_1 and x_2 respectively. ν_1 and ν_2 refers to the kinematic viscosity of pure liquids 1 and 2 respectively. ν_{12} and ν_{21} represent the interaction parameters obtained by multiple regression analysis. M_1 and M_2 refer to the molecular weight of the two components respectively. The viscosity deviations can be calculated as

$$\Delta \eta = \eta - (x_1 \eta_1 + x_2 \eta_2) \quad (3)$$

where η, η_1, and η_2, are the dynamic viscosities of the mixture and those of the pure components 1 and 2 respectively. The experimentally determined excess volume and viscosity deviation data for the binary system of this investigation have been correlated using Redlich Kister equation by the method of least square.

$$V^E \text{ or } \eta = x_1 x_2 \Sigma a_i (x_1 - x_2)^I \quad (4)$$

3. Results and discussion

"Table 1-3" summarizes experimentally determined densities (ρ) and viscosities (η) of Diacetone alcohol with benzene and chlorobenzene mixtures at 303.15 K, 313.15 K and 323.15 K. "Table 4" represents Redlich-Kister Constants for excess volume, viscosity deviation and McAllister constants for the viscosity of mixtures at 303.15 K, 313.15K, and 323.15 K. Excess volume and viscosity deviation of the mixtures were plotted in Fig.1-4. As seen in Fig.1&2 the excess molar volume values of the mixtures are negative and increases when temperature increases. It can be summarized that excess values may be affected by three factors. The first factor is the specific forces between molecules, such as hydrogen bonds, charge transfer complexes, breaking of hydrogen bonds and complexes bringing negative excess values Changsheng vang et al. (2006). The second factor is the physical intermolecular forces, including electrostatic forces between charged particles and between a permanent dipole and so on induction forces between a permanent dipole and an induced dipole, and forces of attraction (dispersion forces) and repulsion between non polar molecules. Physical intermolecular forces are weak and the sign of excess value may be positive or negative, but the absolute values are small. Third factor is the structural characteristics of the component arising from geometrical fitting of one component in to other structure due to the differences in shape and size of the components and free volume. The negative V^E values in the mixtures under study indicate that interactions between molecules of the mixtures are stronger than interactions between molecules in the pure liquids and that associative force dominate the behavior of the solution Rena et al. (2006). There fore in this system, compression in free volume is considered to occur, making the mixture more compressible than the ideal mixture which ultimately culminates into negative values of V^E. In Fig. 3&4, the deviations in viscosity for the mixtures are positive for all the mole fractions and increases when temperature increases. The viscosity of the mixture strongly depends on the entropy of mixture, which is related with liquid's structure and enthalpy Kauzman et al. (1940), consequently with molecular interactions between the components of the mixture. Therefore the viscosity deviation depends on molecular interactions as well as on the size and shape of the molecules. For negative deviations of Raoult's law and with strong specific interactions, the viscosity deviations are positive.

4. Conclusion

It may be concluded that the interactions resulting in the interstitial accommodation of benzene, and chloro in to diacetone alcohol are the predominant factor over dipole – dipole and dipole induced–dipole interaction. The intermolecular interaction of the mixtures leads to specific type. The excess values of the mixtures show a systematic change with increasing temperature. With an increase in temperature the intermolecular interactions between molecules become weak. At 323.15 K the intermolecular interaction become weak compared with 303.15 K and 313.15 K. It is clear from standard deviation values that McAllister equation can represent the viscosity values, and Redlich Kister equation can represent the excess volume and viscosity deviation values very well. It has been observed that the intermolecular interaction was more with chlorobenzene than with benzene. The algebraic values of excess values fall in the order reflecting an easier flow of the mixture at the direction of decreasing molecular weight of arylhalides.

References

Arun, B. S., Mehdihasan ujjan, B.K., Apoorva, P.H. (1995). Densities, viscosity and ultrasonic velocity studies of binary mixtures of chloroform with pentan-ol, hexanol and heptanol at 303.15 and 313.15K. *J.Chem.Eng.Data,* 40, 845-850.

Changsheng vang, H., Peisheng, Ma. (2006). Density, viscosity and excess volume of binary mixture. *J. Chem. Eng. Data,* 51, 1345-1358.

Ewing, M.B., Levian, B.J., Marsh, K.N. (1970). Excess enthalpies, excess volume and excess Gibbs free energy for mixtures of cyclooctane +cyclopentane at 288.15, 298.15 and 308.15K. *J. chem. Thermdyn.* 2, 689-691.

Kenart, C.M., Kenart, W., (2000).Physico chemical methods used to study internal structures of liquid binary mixtures. *Phys .chem.Liq*. 38, 155-180.

Kauzman, W., Eyring, H.(1940). Viscous flow of larger molecules. *J. Am. Chem. Society,* 62, 3113-3125.

Kubendran,T.R., SenthilRaja,S., (2004).Transport properties of 1,4 Dioxane+Butanol+Carbon tetra chloride. *J. Chem. Eng .Data*, 49,421-425.

McAllister, R.A. (1960).Viscosity of liquid mixtures. *A.I.C.H.E Journal,* 6, 427-431.

Mchaweh, A., Alsaygh, A., Moshfeghian, M. (2004).A simplified method for calculating saturated liquid densities. *Fluid Phase Equilibria*, 224, 157-167.

Oswal, S. L., and Patel, N. B. (1995). Viscosity and excess molar volume of binary mixtures. *J. Chem.Eng.Data*, 40, 845-850.

Redlich, O. Kister, A. T.(1948).Algebraic representation of thermodynamic properties and the classification of solutions. *Ind. Eng. Chem*. 40, 345-348.

Rena, A. C., Ana, C., Gomaz, M., Horacio, N. S. (2006).Density, viscosity, vapor liquid equilibrium, excess molar volume, viscosity deviation and their correlations for the chloroform + 2 butanone binary

system, *J.Chem.Eng.Data*, 51, 1473-1478

Table 1. Diacetone alcohol, benzene and chlorobenzene mixtures at 303.15 K

Diacetone alcohol + benzene			Diacetone alcohol + chlorobenzene		
x_1	ρ/g.cm^{-3}	η/ mpa.s	x_1	ρ/g.cm^{-3}	η/ mpa.s
0.0000	0.8720	0.6905	0.0000	1.1020	0.7705
0.1225	0.8825	0.9699	0.1268	1.0790	1.0555
0.2525	0.8927	1.2658	0.2462	1.0568	1.3221
0.3224	0.8979	1.4200	0.3454	1.0395	1.5440
0.4218	0.9047	1.6482	0.4991	1.0135	1.8770
0.5045	0.9111	1.8400	0.5214	1.0100	1.9331
0.6112	0.9164	2.0800	0.6119	0.9961	2.1331
0.7123	0.9221	2.2828	0.7214	0.9785	2.3441
0.8191	0.9275	2.5151	0.8585	0.9580	2.6221
0.9337	0.9331	2.7600	0.9141	0.9490	2.7224
1.0000	0.9360	2.8900	1.0000	0.9360	2.8900

Molefraction, density and viscosity of diacetone alcohol+ benzene and diacetone alcohol + chlorobenzene mixture at 303.15 K.

Table 2. Diacetone alcohol, benzene and chlorobenzene mixtures at 313.15 K

Diacetone alcohol + benzene			Diacetone alcohol + chlorobenzene		
x_1	ρ/g.cm^{-3}	η/ mpa.s	x_1	ρ/g.cm^{-3}	η/ mpa.s
0.0000	0.8450	0.6780	0.0000	1.0800	0.6914
0.1225	0.8559	0.9378	0.1268	1.0565	0.9771
0.2525	0.8665	1.2250	0.2462	1.0338	1.2210
0.3224	0.8719	1.3710	0.3454	1.0163	1.4661
0.4218	0.8791	1.5810	0.4991	0.9899	1.7994
0.5045	0.8846	1.7700	0.5214	0.9864	1.8551
0.6112	0.8912	2.0000	0.6119	0.9721	2.0661
0.7123	0.8970	2.2130	0.7214	0.9546	2.2662
0.8191	0.9029	2.4210	0.8585	0.9335	2.5444
0.9337	0.9088	2.6600	0.9141	0.9251	2.6331
1.0000	0.9121	2.7910	1.0000	0.9121	2.7910

Molefraction, density and viscosity of diacetone alcohol+ benzene and diacetone alcohol + chlorobenzene mixtures at 313.15 K.

Table 3. Diacetone alcohol, benzene and chlorobenzene mixtures at 323.15 K

Diacetone alcohol + benzene			Diacetone alcohol + chlorobenzene		
x_1	ρ/g.cm^{-3}	η/ mpa.s	x_1	ρ/g.cm^{-3}	η/ mpa.s
0.0000	0.8280	0.6600	0.0000	1.0674	0.5543
0.1225	0.8398	0.9180	0.1268	1.0435	0.8551
0.2525	0.8512	1.2000	0.2462	1.0215	1.1224
0.3224	0.8570	1.3400	0.3454	1.0041	1.3445
0.4218	0.8647	1.5400	0.4991	0.9780	1.6775
0.5045	0.8708	0.8708	0.5214	0.9745	1.7338
0.6112	0.8781	1.9311	0.6119	0.9604	1.9358
0.7123	0.8846	2.1441	0.7214	0.9431	2.1446
0.8191	0.8911	2.3314	0.8585	0.9220	2.4339
0.9337	0.8975	2.5524	0.9141	0.9138	2.5227
1.0000	0.9010	2.6700	1.0000	0.9010	2.6700

Molefraction, density and viscosity of diacetone alcohol+ benzene and diacetone alcohol + chlorobenzene mixture at 323.15 K.

Table 4. Parameters of Redlich and McAllister

Redlich kister constants								McAllister constants		
V^E / cm^3/mole^{-1}				Δη / mpa.s				ν / mpa.s		
A_0	A_1	A_2	S	A_0	A_1	A_2	S	ν_{12}	ν_{21}	S
Diacetone alcohol – benzene										
303.15 K										
- 0.2576	-0.1427	0.3333	0.80	0.0689	0.0235	-0.0549	3.12	2.2082	1.8540	1.40
313.15 K										
-0.1557	-0.0611	0.0261	4.18	0.1316	0.0578	-0.1348	2.15	2.1415	1.7558	1.01
323.15 K										
-0.1280	-0.0226	0.0528	3.12	0.0559	0.1583	-0.1308	1.09	2.1633	1.6717	0.42
Diacetone alcohol – chloro benzene										
303.15 K										
-1.3946	-0.4311	0.9939	0.47	0.1793	0.0582	-0.1343	1.73	2.2738	1.8748	0.70
313.15 K										
-1.2565	-0.2556	0.5894	1.32	0.2402	0.1011	-0.2332	1.02	2.1240	1.7048	2.60
323.15 K										
-1.1253	-0.3754	0.8656	0.45	0.2906	0.1594	-0.3676	0.59	2.0150	1.6312	1.51

Redlich kister and McAllister constants for the diacetone alcohol+ benzene and diacetone alcohol + chlorobenzene mixture at 303.15 K, 313.15 K, 323.15 K.

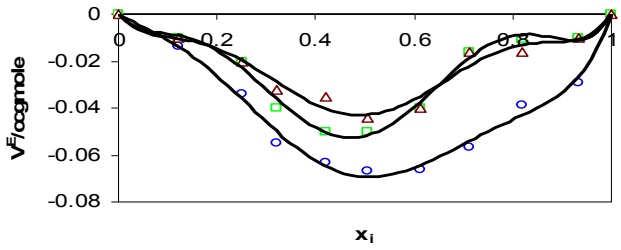

Figure 1. Plot of V^E against x_i of Diacetone alcohol

Diacetone alcohol + benzene at 303.15 K (¤),313.15 K (□) and 323.15 K (Δ)

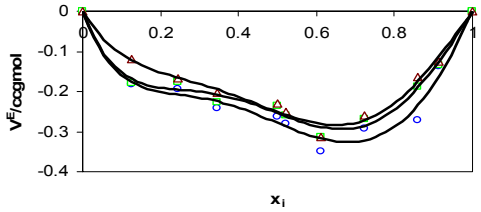

Figure 2. Plot of V^E against x_i of Diacetone alcohol

Diacetone alcohol + chloro benzene at 303.15 K (¤),313.15 K (□) and 323.15 K (Δ)

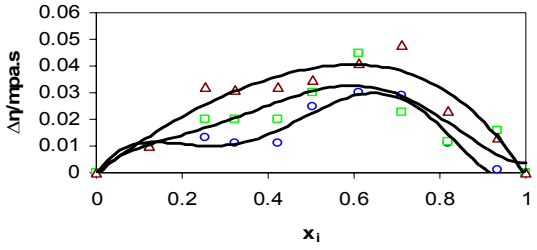

Figure 3. Plot of Δη against x_i of Diacetone alcohol

Diacetone alcohol + benzene at 303.15 K (¤),313.15 K (□) and 323.15 K (Δ)

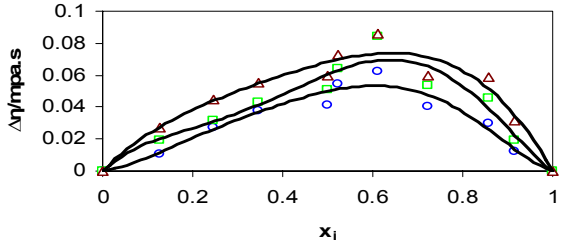

Figure 4. Plot of Δη against x_i of Diacetone alcohol

Diacetone alcohol + chlorobenzene at 303.15 K (¤),313.15 K (□) and 323.15 K (Δ)

Modern Applied Science

www.ccsenet.org/journal.html

Vol. 2, No. 3

May 2008

Enhancement of Enterprise Competitive Predominance Based on Data Mining

Jie Ni

Shandong University of Finance

Jinan 250014, China

E-mail: nj6611@sohu.com

Abstract

Starting from the view of customer relationship management (CRM), this article expatiates on the important and indispensable function and application of data mining in the marketing, and analyzes the principle and flow of data mining in the application of the enterprise.

Keywords: Customer relationship management (CRM), Data base, Data mining, Marketing

1. Meaning of data mining

With the coming of information age and the development of economic integration, challenges that enterprises face increasingly go up. The excessive competition in the market makes the difference among products increasingly reduce, and the high surplus and the diversification of customers' demands make the production management of the enterprise from the product orientation to the customer orientation, and the traditional management method that emphasizes product quality and brand has not ensured that enterprises can win in the competition of modern economy. Just as American Airlines CEO, Donald J. Carty said, free competitive customers had become into the important assets of the enterprise. Through meaningful communications, enterprises can understand and influence customers' behaviors, and realize the intention that enhance customer obtainment, customer retention, customer loyalty and customer profit, which is the customer relationship management (CRM). In fact, the CRM is a sort of management, and it is not the result of technical enhancement, but the technical enhancement offers indispensable technical support of its development. In the past, because of the limitation of technology, the information system of the enterprise is disperse and lacks opening, which induces the integration among trans-systems is difficult to be actualized, and to comprehensively understand customer and grasp customers' character and demand was just a sort of ideal in the past. Under the condition of quick development of network, through the integration of platforms and increasingly mature technologies of data base and data mining, enterprises can effectively grasp customers' behaviors and demands. One research of International Data Corporation showed that the average investment return rate is about 401% after 2~3 years when 62 data bases were installed in North American. In another research by NCR, about 20 data bases realized 300~1000% return rate in less than two years in the retailing. CRM is the most useful tool to obtain maximum possible profit for enterprises, and the data mining is the stable base and wings for this tool.

2. Data mining and its application in the corporate marketing

The so-called data mining is the process picking up concealed, unknown, but potentially useful information and knowledge from large, incomplete, fuzzy and random data. It is the margin science which involves machine learning, mode identification, system theory, artificial intelligence, database management and data visualization. The owner of the Nobel Prize, doctor Penzias though that "the data mining will be more important, because it is so valuable that enterprises will not lose any things about customers any longer. If you don't do something in this domain, you will lose you business" in the review of "computer world". Enterprises have obvious reasons to invest data mining. Through data mining, from large collected and accumulated data, enterprises can respectively aim at problems about management strategy, object orientation, operation efficiency and measurement evaluation, and effectively mine the most important answers concerned by customers, and can direct operators' activities by means of abundant information mined from large of customer data, and make them offer right product and price through the improvement of communication with customers and the right channel at the right time, and accordingly increase business opportunity.

The common application domains of data mining mainly include following aspect.

(1) Direct marketing

Data mining is abroad applied in the direct letter. Through the prediction that which customers are likely to purchase the products of the company, and which sort of product will be purchased will fully reduce the development charge and time of the market.

(2) Objective marketing

As viewed from the objective marketing, when a sort of "new" product or service comes into the market, customers may be attracted to buy, because the "new" product or service is not only associated with the former but ameliorated to fulfill customers' demands of practice and mentality. For example, the bank plans pushing a sort of improved financial product such as new credit card to existing customer group, and the data mining can settle customer data, establish the predictable model and validate it from recent similar business activity or market investigation, and accordingly grasp the total character of the customer group with good reactions to pertinently implement works. When the data mining is applied in the objective marketing, the customer reaction rate can achieve 20-25%, but this number is less than 8% in the past.

(3) Customer retention

Customer retention is a main problem that enterprises face. One research from Harvard University showed that "when the customer consumption reduces 5%, people's confidence to the profitable ability of the enterprise will be fluctuated". Because to looking for new customer demand needs high costs, so the retention of existing customers is the key problem for many enterprises. The customer loss always becomes into the problem that enterprises can not control because it has not any premonition in advance. The customer retention is the similar operation problem with objective marketing, and both can establish the tendency model. Through historical data, this model can validate and find customers with the tendency turning to competitors. Then the business activity will be performed aiming at these customers, and more active marketing strategy will be used to retain customers.

(4) Cross distribution

To add customer value is another key function of marketing. The concept that adds customer occupation rate is important to most enterprises. Two current methods to add customer occupation rate are respectively the product promotion activity based on the customer and the cross distribution. Data mining can help sales personnel know not only which customers are likely to purchase products and which products are likely to be purchased by customers, but also which customers usually purchase what products and which products are usually purchased together, and accordingly make the cross distribution more effective.

(5) Cheating inspection

The data mining can establish the model for the industries which the cheating easily occurs such as insurance counterclaim, mobile telephone call, credit card shopping. Generally, there are several modeling methods. The first one is the method of prediction, which is similar with objective marketing and customer retention. The prediction model can indicate the customer's cheating tendency and compute the customer's cheating probability. For example, the method is applied in the application of credit card, which can predict the probability of cheating. The second one is the method of integration. Here, customers are divided into different groups by the integration arithmetic, and those customers who are unsuitable to any group may be the anti-cheating object because of the deceitful probability, and the Visa Company is benefited from this data mining technology. Many international telecom companies are trying to establish the mobile telephone cheating model, and expect reining the situation through this sort of model.

3. Steps to develop data mining and enhance corporate competitiveness

The data mining model cannot create any values for the enterprise. Only when the enterprise adopts corresponding activities according to the model, it can benefit from the data mining. Therefore, the data mining should be put into a bigger process, and the enterprise should take data mining as the tool of competition, transform the information obtained through data mining to the effective commercial activity, and enhance the competitive predominance of the enterprise to the maximum extent.

The data mining mainly includes following steps.

(1) Confirmation of the topic

The topic must be confirmed by the present market situation and developmental direction, or else, it is useless. For example, for the telecom enterprise, the topic should be how to identify the customer group with values from basic customers of the enterprise, and predict how to retain these customers and implement cross distribution aiming at them. It is the most basic and important topic that data mining faces.

(2) Data collection and database integration

Data collection and database integration are the necessary condition of data mining. At present, the technology and channel of data collection are increasingly broad, for example, the chain supermarket records consumption through code reader and the bank records consumption through credit card. Different market research departments design market investigation or directly purchase data according to different topics to collect large of customer information. In the past, various enterprises and various departments of these enterprises have their own databases which have different setups

and standards, so the integration of these databases is very difficult. The customer oriented data mining can integrate different databases in one enterprise to the uniform customer database, which can well and truly grasp customers' information.

(3) Customer classification and prediction modeling

Through various data analysis methods based on data mining, we can exploringly analyze data, which main intention is to classify different types of customer, understand various types of customer's character, especial those high valuable customers' behavior modes which can bring main profits for the enterprise, and offer effective method to further predict their wills. These models can help enterprises timely find customers' possible premonition to leave, and adopt more attractive products to retain these customers, and they also can find which customers will possess or have possessed the possibility to further develop, and which customers' values will reduce or have reduced. So it can not only exactly grasp intrinsic customer resource, but can incisively find potential customer resource, and pertinently establish marketing strategy and always keep initiative in the market competition.

(4) Scheme establishment

Once those high valuable customers are identified, the enterprise must establish a series of marketing activities and offer products and services with competitiveness for these customers because the objective of the enterprise is to increase these customers' values. Because the products offered to the customers may be multiform, so we can use the method of data mining to confirm which sort of product most suit to these high valuable customers and establish the market scheme pertinently. To establish a pertinent market scheme is a difficult task, and the content of the scheme must base effective information, which can ensure that the scheme can timely follow people's consumption demand and market change. In addition, the special product only is most suitable for the special customer at the special time. For example, high valuable telephone customers are easy to be influenced by higher call charge in the month exceeding planned call charge. And in the special term, other competitors also will adopt effective object promotions aiming at special products of this enterprise. In different terms, single customer's value, loyalty and market orientation also will change with the change of the exterior environment.

(5) Scheme implementation

On the surface, the result of the prediction model is easy to be practiced, but it is a complex thing in fact. The channels between customer and enterprise include the customer service center and interactive WEB site. Enterprises actively communicate with customers, which can make enterprises have chances to obtain the opportunity to strengthen the association with them, and better know their demands. Therefore, first the data mining and the customer communication channel should be integrated. Enterprises can issue new promotion information through the customer service center, and when the high valuable customer calls the center, the promotion object analysis program of the data mining model begins to operate behind the scenes. When the analysis is completed, one or several relative product information fit for this customer will be displayed. At the same time, the customer service center also can collect customer's basic data, understand the feedback information of the promotion and product service, timely adjust the marketing activity to get best effects.

(6) Effect inspection

The obtainment of the data model is not the final objective of the data mining, and the most important objective lies on whether the data model can bring high data assets return rate and whether it can offer actual helps and constructive advices for the market management decision. Which promotion advice should be adopted, which promotion advices should be rejected, why customer will agree to purchase one sort of product but reject to buy another sort of product, all these information should be recorded and used to improve the promotion. Through various recorded indexes, enterprise can exactly measure whether the response of customers to the marketing activity after adopting data mining is enhanced. Much amelioration which is needed in this process can enhance the customer response rate.

4. Principles followed in the data mining process

Data mining is a data analysis process with abundant connotations, and to ensure it is better implemented in the competition among enterprises, following principles should be followed.

First, the process of data mining takes the data as the core. This directional idea should be carried through the CRM all the while. The enterprise CRM system should surround the core content which continually establish and enrich the customer database. Only the enterprise CRM system applying in the customer data analysis and working in advanced software equipments can gradually promote the development of the CRM taking customer data as the core. At present, the customer database establishment work of domestic enterprises is in the beginning stage, the matching research of the CRM software still has some problems, which restricts the space that enterprise applies the data mining technology to some extent, and becomes into the main problem puzzling the study of the data mining theory.

Second, the process of data mining is a dynamic circulation process. As a whole, data mining is a continually embedded

data base process in proper sequence, and only good beginning and precise middle stage can finally gestate scientific data analysis model and decision scheme. Without exact understanding to the problems of the enterprise, there are not specific objective of data collection and the probability of exact understanding for the data meaning. Without customer data and preparative data which can exactly reflect the actuality of the enterprise, the model establishment, scheme establishment, scheme implementation and effect evaluation are useless. Without high quality data, the model will become into the unilateral understanding to the problems of the enterprise. Without the model which can reflect the actuality of the enterprise, the implementation of the scheme based on that only bring unrealistic false decision for the enterprise.

As viewed from the detail, data mining is a repeatable circulatory and spiral ascending data analysis process. Only though continual repetitions and mutual validations among various stages, the feasible data analysis model and decision scheme can be established finally. The obstacle to understand data may come from the fuzzy understanding the problems of the enterprise, and here the repetition of former stage is necessary. The exploring data analysis adopting various analysis methods may require the proper transformation of data format or data type, and here the repetition of former stage is necessary. When revaluating former works through the model, existing oversights and errors are found, and here the repetition of former stage is necessary.

Third, the data mining process is an experience learning process. Though the effect inspection is the final stage of data mining, but its end doesn't mean the terminal of data mining. Every data mining will offer precious practical experience for the next data mining, and every data mining will benefit from last mining process. Therefore, the data mining is a big circulatory process with experiences which are continually accumulated and learned.

Fourth, the successful data mining process is a process continually blending with practice. In the CRM taking data analysis as the core, the mining analysis process of the customer data is closely conjoint with the practical marketing activity. Only the data mining process is blended into the process of the whole management of the enterprise, the data mining can possess wide using space, exert its own potentials and really support the scientific decision for the enterprise.

References

Ronald S. Swift (US), interpreted by Yang, Donglong et al. (2002). *CRM: Accelerating the Enhancement of Profit and Predominance.* Beijing: China Economics Press.

Zhang, Yaoting, Xie, Bangchang & Zhu, Shiwu. (2001). *Introduction and Application of Data Mining: Study Data Mining from Statistical Technology.* Beijing: China Statistics Press.

Zhu, Jianping & Zhang, Runchu. (2002). The Development and Characters of Data Mining. *Statistics and Decision.* No.7.

Modern Applied Science

www.ccsenet.org/journal.html

Vol. 2, No. 3

May 2008

An Introduction to Regression Analysis on Parameters Selection in Beltline Moulding Process

Abdul Talib Bon (Corresponding author)
Department Informatique – Laboratorie L3i, Pole Sciences et Technologie
Universite de La Rochelle
17042 La Rochelle, Cedex 1, France
Tel: 60-12-766-5756 E-mail: talibon@gmail.com

Jean Marc Ogier
Department Informatique – Laboratorie L3i, Pole Sciences et Technologie
Universite de La Rochelle
17042 La Rochelle, Cedex 1, France
Tel: 33-05-4645-8215 E-mail: jean-marc.ogier@univ-lr.fr

Ahmad Mahir Razali
School of Mathematical Sciences, Faculty of Science and Technology
Universiti Kebangsaan Malaysia
86000 Bangi, Malaysia
Tel: 60-17-888-6805 E-mail: mahir@pkrisc.cc.ukm.my

Abstract

The world of manufacturing industries is forced to meet the demand of the end users in many different aspects especially to reduce the number of defects and production cost. Since then, the manufacturers have many introduced techniques and strategies in order to achieve zero defects for end products. Therefore, this research is an early attempt to introduce a proper method for manufacturers to achieve their goal starting from parameters selection and then optimization to control the belt line moulding production process. We apply regression analysis to make parameters selection and then used the best variables selected to optimize or in this case to minimize defects in belt line moulding process. The findings from this study we found from the correlation model only three parameters have strong correlation of fourteen parameters were studied. The results are very useful evidence and applicability to beltline moulding manufacturer for implementation.

Keywords: Belt line moulding, Regression analysis, Parameters selection, Process

1. Introduction

The manufacturing industries in Malaysia nowadays go toward in the competition scenario from light industries to heavy industries. The competitions not only based on quantity of sales or products but they are looking on how the product precise can be meet from industry to satisfy what the end user needs. Therefore, all manufacturing industries must be capable to produce services or product took initiatives to customer's needs and desire at the best quality product and minimum cost. In this research the authors study more specific area in beltline moulding in automotive manufacturing. Beltline moulding is a process with many variations in raw materials, machinery conditions and ambient conditions. It also has a temporal aspect where line conditions change during operation, affecting the end product. Typical process control procedures include statistical analysis of periodic batch samples, control charts of sample mean or range, and trial and error. Beltline moulding companies are concerned with automating information flow and the use of intelligent computer controls can play an important role

2. Significance and Benefits of Proposed Research

The application of quantitative technique in improving a product process thus far is still a recent phenomenon. There is an urgent need for more objectives, realistic and accurate model for future planning and policy evaluation. This is quite obvious as the automotive manufacturing sector (beltline part of car body) undergoes structural changes and is becoming more complex due to technological advances, manufacturing management, product demand and competition from other manufacturer.

3. The Objective of the Study

In view of the importance of having such tools, the study aims to achieve the following objectives:

i. To select the best parameter settings from the four factors.

ii. To apply Correlation Modelling approach for parameter selection.

4. The Scope of the Research

The key issue that to some extent would limit the reliability and validity of the analysis is the availability of data that are relevant to scope of the study. Moulding manufacturing is known to be affected by many factors like material, machine, measurement, human etc. The detail list of the dependent and independent variables used in this research are suggested by many researchers in manufacturing and one of the known as Yazici (1990). The data used in this study are cited from daily data from beltline moulding manufacturer for Malaysia's national car. The area of this study will be determined later depend on the availability of the data set. At this stage, the authors are preparing memorandum of understanding (MoU) in research collaboration between moulding Manufacturer Company and the authors.

5. Literature Review

5.1 Belt Line Moulding Process

5.1.1 Extrusion Process

The very important part in roll forming process is extrusion process. Basically many definitions authors found about extrusion which is ampef.com defined extrusion is process by which polymer is propelled continuously along a screw through regions of high temperature and pressure where it is melted and compacted, and finally forced through a die (slit) to form a thin film.

Meanwhile, Ampef. (2002) defined extrusion as a forming technique whereby a material is forced, by compression, through a die orifice, and Jason, Leadbitter, (2004) defined it is a method of processing plastics where the material is pushed through a die under pressure to form a continuous strip of a particular shape. Additionally, extrusion is a fabrication process in which a heat-softened polymer is forced continually by a screw through a die Seymour and Carraher, (1993). The extrusion can be further defined as the process of manufacturing and/or shaping a material by forcing it through a die (RoofHelp.com, 2006).

5.1.2 Roll Forming Process

In the manufacture of automobile mouldings, especially the belt line mouldings that border the interface between a car door panel and the bottom outside edge of the door windows, it has become aesthetically fashionable to provide a strip of stiff decorative or ornamental plastic material on the outer or inner side of the arch or channel shaped moulding in combination with the coil look of an exposed portion of the core material. In addition to these aesthetic functions, the inner portion of the moulding comprises a flocked elastomeric lip adapted to bear against the window, sealing the door from the elements, and providing a guide for reciprocating movement of the window.

6. Research Methodology

The research purpose of modelling in manufacturing industry is to apply parameters selection analysis using regression and correlation analysis. Regression analysis is used to reduce a set of large number of variables to a smaller number of variables. The regression model used is as shown below:

$$Y = \beta_0 + \beta_1 X_1 + \beta_2 X_2 + \ldots + \beta_m X_m + \varepsilon$$

where Y = Response variable (dependent)

$\beta_0 \ldots. \beta_m$ = Parameters

$X_1 \ldots. X_m$ = Predictor variables (independent)

and ε is a random error term.

The technique of least squares is used to estimate the parameters $\beta_0, \beta_1, \ldots\ldots, \beta_m$. In this technique, we minimizing the sum of the squared differences of the actual Y values and the values of Y predicted by the regression equation. The computation can be shown easily in matrix notation. Suppose $\boldsymbol{Y}$ is a vector of observed values of Y, the $\boldsymbol{X}$ matrix is a matrix for the independent variables, and the ε as an error vector such that;

$$\boldsymbol{Y}=\begin{bmatrix} y_1 \\ . \\ . \\ y_n \end{bmatrix}, \boldsymbol{X}=\begin{bmatrix} 1 & x_{11} & . & . & x_{1m} \\ . & . & . & . & . \\ . & . & . & . & . \\ 1 & x_{n1} & . & . & x_{nm} \end{bmatrix}, \boldsymbol{\varepsilon}=\begin{bmatrix} \varepsilon_1 \\ . \\ . \\ \varepsilon_n \end{bmatrix}$$

Then the regression model can be represented in the matrix notation as

$$\boldsymbol{Y}=\boldsymbol{X}\boldsymbol{\beta}+\boldsymbol{\varepsilon}$$

Where is $\boldsymbol{\beta}'=(\beta_0,\beta_1,...,\beta_m)$ is the vector of parameters. By solving the set of normal equations given by

$$\boldsymbol{X}'\boldsymbol{X}\boldsymbol{\beta}=\boldsymbol{X}'\boldsymbol{Y}$$

and assuming the matrix $\boldsymbol{X}'\boldsymbol{X}$ is non-singular, a unique solution will be found which is given by

$$\hat{\boldsymbol{\beta}}=(\boldsymbol{X}'\boldsymbol{X})^{-1}\boldsymbol{X}'\boldsymbol{Y}$$

Correlation analysis is a technique for investigating the relationship between two quantitative or continuous variables. The correlation coefficient, r is a measure of the strength of the association between the two sets of variables. The most common correlation coefficient is the Pearson's correlation coefficient which is defined as

$$r=\frac{\sum_{i=1}^{n}(x_i-\bar{x})(y_i-\bar{y})}{\sqrt{\left[\sum_{i=1}^{n}(x_i-\bar{x})^2\right]\left[\sum_{i=1}^{n}(y_i-\bar{y})^2\right]}}$$

where (x_i,y_i) are pairs of sample points $\bar{x}$ and $\bar{y}$ are the means of measurements on the variables. Generally, the correlation coefficient varies from -1 to +1.

7. Results and Discussions

In this research, we shall discuss the analysis of the relationship between two quantitative outcomes using scatter plot. A scatter plot is simply a cloud of points of the two variables under investigation. From the scatter plot, we can see very clearly whether there is a linear association between the two variables and guess accurately the value of the correlation coefficient. After looking a scatter plot, we then go ahead and confirm the association by conducting a correlation analysis. We use the correlation coefficient, *r* to describe the degree of linear relationship between the two variables.

Table 1 gives a guideline on the strength of the linear relationship corresponding to the correlation coefficient value. Values near 0 means no (linear) correlation values near $\pm$ 1 means very strong correlation. The negative sign means that the two variables are inversely related, that is, as one variable increases the other variable decreases.

The scatter plots of sets of data with varying degrees of linear association, we found the closer to zero the correlation coefficient is, the less the points fall on a straight line (hence the term "linear" correlation coefficient). For the cylinder factor, where are have six parameters been involved in this analysis. Where are cylinder 1 (CY1), cylinder 2 (CY2), cylinder 3 (CY3), cylinder 4 (CY4), adapter (ADPT) and die. From the correlation analysis we found CY1 and CY2 have strong correlation coefficients with 0.927 and between CY2 and CY3 with 0.839. While, strong correlation also between CY1 and CY4 with Pearson's r = 0.873. All of the very strong correlations in this factor fall the positive correlation. From the correlation we can summary result base on very strong correlations. The parameters involved are CY1, CY2 and CY4 as shown as Table 2. From the Table 2, we can illustrate to 3-Dimension graphic as Figure 1 shown very strong relationship between CY1, CY2 and CY4 in the cylinder factor.

Factors score covariance matrix shown as Table 3 that although theoretically the factor scores should be entirely uncorrelated the covariance is not zero, which is a consequence of the scores being estimated rather than calculated exactly.

The scatter plot for heater factor, we found not have any strong correlation between parameters where heater no. 1 (current unit), H1_C; heater no. 1 (temperature unit), H1_T; heater no. 2 (current unit), H1_C; and heater no. 2 (temperature unit), H1_T. That means no any correlation between four parameters. The plot indicates a lack of a relationship between the all variables with Pearson correlation coefficient between -0.015 to 0.332 with p-value is 0.05 levels (2-tailed).

The scatter plot for power panel with four parameters are looper, roller, pulling and cutter, most of the correlation coefficient is to negative one, the more the points will fall along a line stretching from the upper left to the lower right. However, looper and roller have strong correlation with 0.790, with a 2-sided 1%. Table 4 from the output listing shown gives the actual value of the correlation coefficient along with its p-value. The correlation coefficient is 0.790 and the p-value is 0.01. From these values, it can be concluded that the correlation coefficient is significant beyond the 1 percent level. In other words, looper had moderately strong correlation with roller. From the coil factor all the parameters which is coil thickness, width and burr where no any correlation to each others

have. That shown very weak correlation in this factor. A relationship between all parameters is not apparent from the plot, Pearson correlation coefficient less than 0.3 ($p<0.05$).

Besides that the scatter plot for raw material composition factor shows some degree of association between tensile strength and elongation break which the Pearson correlation coefficient, r is about +0.789 ($p<0.01$). The Table 5 from the output listing are shown below. Notice that the Pearson correlation coefficients are exactly 0.789 and significant beyond the 1 percent level. The association between the two parameters is significant indicating that the two parameters the 98 data in a similar way.

The closer the correlation coefficient is to one, the more the points will fall along a line stretching from the lower left to the upper right. The scatter plot for ambient conditions factor clearly shows a linear association between the two variables air velocity and air exchange rate coefficient of correlation which r is +1. Data lie on a perfect straight line with a positive slope. This indicates as the air velocity score get higher, so will the air exchange rate in higher. Meanwhile, the others correlation between air velocity with temperature and relative humidity, temperature with relative humidity, and relative humidity with air exchange rate do not show any degree of linear association at all, r less than 0.4.

8. Conclusion

We can conclude from the Correlation modelling analysis for six factors not all factors gave the strong correlation between parameters. We found that model for selected parameters involved in beltline moulding process factor as shown in Table 6 as a conclusion. We select correlation coefficient value at least 0.8 which shown very strong in strength of linear relatively.

References

Ampef. (2002). When the world thinks of plastic films, it thinks of PET: Glossary Terms. [Online] Available: http://www.ampef.com/gloss.html

H. Yazici. (1990). Implementation of SPC techniques in the PVC pipe industry. *Engineering Management Journal*, 2(3), 59-64.

Jason, Leadbitter, (2004), NZ Newsletter Issue 13. [Online] Available: http://www.hydropolymers.com/en/ media_room/glossary (January 2004)

M. Pagano & K Gauvreau. (2000). *Principles of Biostatistics*. (2nd ed.). Duxbury: Pacific Grove, CA.

RoofHelp.com, (2006), What's Inside: Glossary [Online] Available: http://www.roofhelp.com/Glossary/ glossary_e.htm

R. J. Freund & R. C. Little. (2000). *SAS® System for Regression*. (3rd ed.). Cary, NC: SAS Institute Inc.

Seymour & Carraher, (1993), Polymer Chemistry Dekker [Online] Available: http://www.matse1. mse.uiuc.edu/~tw/ polymers/glos.html

Y. H. Chan. (2003). Biostatistics 104: Correlational Analysis. *Singapore Medical Journal*, 44(12), 614-619.

Table 1. Strength of Linear Relationship

Correlation Coefficient value	Strength of linear relationship
At least 0.8	Very strong
0.6 up to 0.8	Moderately strong
0.3 to 0.5	Fair
Less than 0.3	Poor

Source: Y H Chan (2003)

Table 2. Correlation Coefficients between CY1, CY2 and CY4

	CY2	CY4
CY1	0.927	0.873
CY2	1	0.839

Table 3. Factor Score Covariance Matrix

Factor	CY2	CY4
CY2	17.246	9.817
CY4	9.817	7.938

Table 4. Correlation between Looper and Roller Correlations

		Looper	Roller
Looper	Pearson Correlation	1.000	.790**
	Sig. (2-tailed)	.	.000
	N	43	43
Roller	Pearson Correlation	.790**	1.000
	Sig. (2-tailed)	.000	.
	N	43	43

** Correlation is significant at the 0.01 level (2-tailed)

Table 5. Correlation between Tensile Strength and Elongation Break Correlations

		Tensile Strength	Elongation Break
Tensile Strength	Pearson Correlation	1.000	.789**
	Sig. (2-tailed)	.	.000
	N	98	98
Elongation Break	Pearson Correlation	.789**	1.000
	Sig. (2-tailed)	.000	.
	N	98	98

** Correlation is significant at the 0.01 level (2-tailed)

Table 6. Model for Strong Correlation for Selected Parameters

	CY1	CY4	Air velocity
CY2	0.93	0.839	-
CY4	0.87	1.0	-
Air Exchange Rate	-	-	1.0

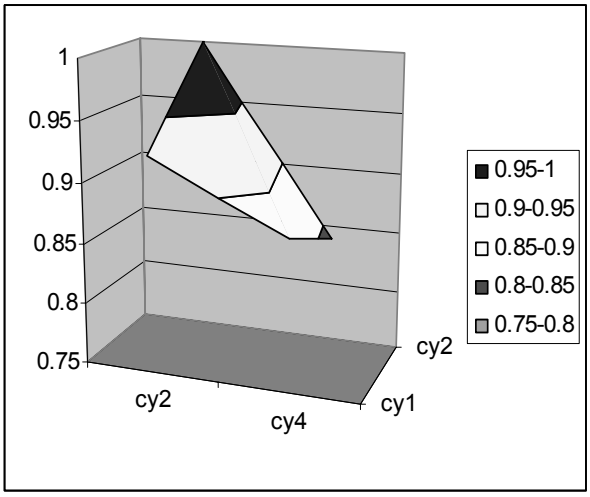

Figure 1. Correlation Graph between CY1, CY2 and CY4

Modern Applied Science

www.ccsenet.org/journal.html

Vol. 2, No. 3

May 2008

Influence of Twisting Ratio and Loop Length on Loop Deflection of Flat Fabrics

Jiaxuan Zhang

College of Art and Appareluages, Tianjin Polytechnic University

Tianjin 300160, China

E-mail: dianzizhufu@tom.com

Jin Li

School of Textiles, Tianjin Polytechnic University

Tianjin 300160, China

E-mail: jinylee@163.com

Abstract

Twisting ratio and loop length are the main factors to make the loop of plain-knitted fabric deflective. Through taking the wool/acrylic blended knitted fabrics as the experimental material and knitting single plain-knitted fabric on the computer-controlled flat knitting machine, in this article, we validate and compare influences of twisting ratio and loop length on the deflection angle of wale. Through the experiment, conclusions include that the linear relationship is presented between the wale deflection angle and the twist of the bunched line (when the twist of the single yarn is certain), and the loop deflection of the fabric with long length loop will change more obvious with the change of twist, and the rinse can strengthen the tendency of the deflection of wale loop.

Keywords: Flat plain-knitted fabric, Loop deflection, Twisting ratio, Loop length

The optimal conformation of fabric is that the vertical loop wale and the horizontal loop course are arranged at a right-angle, but in fact, the deflection tendency always occurs in both for single jersey (Wu, 2004, p.69-70). The deflection and distortion of fabrics puzzle many enterprises all along, because these phenomena not only influence the attractive suit form, but also influence the comfort and increase the difficulty of fabric in its late manufacture.

In early 1980s, through large numbers of experiments, G.W. Smith demonstrated that the loop deflection of fabric was decided by the yarn twist liveliness, the fabric tensity and the number of the knitted machine, and the yarn twist liveliness was the main reason. But the loop deflection direction of fabric is mainly decided by the twist direction of the yarn, and when the Z yarn is used to knit, the loop of the fabric inclines rightward, and when the S yarn is used to knit, the loop of the fabric inclines leftward (Chen, 2006, p.13-15).

1. Experimental material and parameter enactment

1.1 Experimental material

Because the bunched lines with reverse twist has good mightiness, good handle and blare, stable twist circle, small twist shrinking, small single yarn deflection and small elongation, so in this experiment, we adopt 48 pieces of wool/acrylic (30/70) single yarn with Z twist as the raw material to twist up 48^2 pieces of bunched lines through double reverse. The twist is completed on the thin yarn sample machine made by Tianjin Polytechnic University, and the twist of the single yarn in the experiment is 556.9tpm, and the twist coefficient of the single yarn is 80.38, and the twist is measured on the Y331 twist testing machine.

1.2 Confirmation of the twisting ratio

Various characters of the bunched line are decided by the mutual relationship between the stress distribution and structure of the fibers in the bunched line to large extents. The twist breadth denotes the deflection degree between the fiber and the axes, and approximatively represents the fiber distortion and stress degree, and the blare and the handle of the bunched line are decided by the deflection degree of the fiber on the surface of the bunched line (M.D. de Araujo & G.W. Smith, 1989, p.350-356).

(1) If the twist breadth of the bunched line equals to the twist breadth of the single yarn, so the upper fiber is parallel with the axes direction, and the twist breadth is zero, and the surface of the bunched line can acquire optimal blare, soft handle and good lengthways wearable capability. Here, the twist coefficient of the bunched line α_1 and the twist

coefficient of the single yarn α_0 have the relationship.

$$\alpha_1=\frac{\sqrt{2}}{2}\alpha_0$$

(2) If the twist breadth of the bunched line is double to the twist breadth of the single yarn, so the twist breadths on the inner layer and the outside layer are consistent, and the stress distribution on the inner layer and the outside layer is even, and the mightiness of the bunched line is optimal. Here, $\alpha_1=\sqrt{2}\ \alpha_0$.

According to the relationship between the twist breadth of the bunched line and the twist breadth of the single yarn, three twisting ratios in common use are respectively confirmed as 0.414, 0.707 and 1. From experimental data, we can see that when the twisting ratios are 0.717 and 1, for the bunched line through adding twist, its self twist direction is the direction Z, and when the twisting ratio is 0.414, for the bunched line through adding twist, its self twist direction is the direction S. Because we need to find out the critical point that the self twist direction changes in the experiment, so we select a relative smaller twist coefficient 0.2, here, the self twist direction is the direction S, which can make the data on the both sides are close to balance at the critical point. The parameters of the bunch adding twist are seen in Table 1.

Because of the uncontrolled factors in the machine and the yarn, differences will occur in the actual twist of the bunched line measured after twist combination and the nominal twist of the bunched line through computation, both represent linear relationship, which is seen in Figure 1 (For convenient for computation, all twists of the bunched line in the following text are nominal twists).

1.3 Confirmation of knitted parameter

We take the above bunched line knit to single plain-knitted fabric on the computer-controlled flat knitting machine STOLL CMS 320 TC which machine number is 12 needles/ 25.4mm. We use the curving yarn depth of the machine in the experiment to control the loop length of the fabric, and according to the branch quantity, twist and flat knitting machine capability, we can choose the curving yarn fabrics with loop depths including 5.6mm, 6.1mm, 6.6mm and 7.2mm.

2. Measurement of the loop deflection angle of the fabric

Next, we implement the dry looseness disposal and the wet looseness disposal for the fabrics.

2.1 Measurement of the loop deflection angle under the dry looseness situation

After 24 hours' balance under standard atmosphere, we measure the course deflection angle of the fabric. Measure 5 data in different places on every fabric and take the average value. The course deflection degree is measured by the course deflection angle θ, which is seen in Figure 2, and θ= arctan (a/b). The deflection angles of various fabrics after balance are seen in Table 2 (Chen, 2006, p.13-15).

2.2 Measurement of the loop deflection angle under the wet looseness situation

To every fabric, we implement five-time disposal of "rinse- drying in the shade" and respectively record the loop course deflection angle at a time.

3. Analysis of experimental results

Through experimental data, we can see that the loop deflection angle is relative to the twist of the bunched line. The values of the loop deflection angle reduce with the increase of the twist of the bunched line. When the loop deflection direction is right, the angle of the loop deflection reduces with the increase of the twist, and when the loop deflection gradually reduces to 0°, the direction of the loop deflection begin to turn left and the twist continually increases and the angle of the loop deflection also increases.

The loop deflection angle and the twist of the bunched line basically present linear relationship. To the fabric with loop length of 6.6mm, the linear expression between loop deflection angle and the twist of the bunched line is $y=-0.1105x+28.35$, and the correlation degree R^2 is 0.9929, so according to that, we can predict that when the twist of the bunched line is 256.6tpm, the loop deflection is 0°.

The loop deflection angle is relative to the loop length, and when the twist of the bunched line is certain, the deflection degree of the fabric with long loop length is bigger than the fabric with short loop length, i.e. the loop deflection of the fabric with long loop length has a more obvious change with the change of twist. The relationships between the twist of the bunched line and the loop deflection angle are seen in Figure 3 and Figure 4.

The rinse has certain influences to the loop deflection angle and it can strengthen the deflection tendency that the loop turns right. With the increase of the rinse time (when the rinse exceeds four time), the further deflection tendency of the loop begins to gradually reduce. The relationship between the twist of the bunched line and the loop deflection angle of the fabric is seen in Figure 5.

4. Experimental conclusions

Through the experiment, we can see that the course deflection of the fabric is induced by the inner stress of the yarn adding twist, and the deflection angle and the twist of the bunched line present linear relationship (when the twist of the single yarn is certain), and the loop deflection of the fabric with long loop length changes more obvious with the change of the twist, and the rinse can strengthen the course loop deflection tendency of the fabric.

Comparing the relationship between the loop deflection angle and the twist before the rinse with that after rinse, we find that the twist of the bunched line when the loop deflection is 0° after rinse is bigger than that before rinse. Therefore, aiming at different rinse frequencies for different fabric in daily life, we can reasonably choose a relationship between rinse times and loop deflection angle and exactly and effectively confirm an optimal twist of the bunched line to make the loop deflection of the fabric achieve minimum.

References

Chenyan & Shenwei. (2006). Study of the Wale Deflection of Single Weft Plain Fabric. *Knitting Industries*. No.1. p.13-15.

Di, Jianfeng. (1997). Influence of Yarn Twisting Back Moment on Loop Deflection of Fabrics. *Journal of Textile Research*. No.8.

M.D. de Araujo & G.W. Smith. (1989). Spirality of Knitted Fabrics, Part I: The Nature of Spirality. *Textile Research Journal.* Vol.59. p.247-256.

M.D. de Araujo & G.W. Smith. (1989). Spirality of Knitted Fabrics, Part II: The Effect of Yarn Spinning Technology. *Textile Research Journal.* Vol.59. p.350-356.

Ozkan Celik, Nuray Ucar & Seniz Ertugrul. (2005). Determination of Spirality in Knitted Fabrics by Image Analyses. *Fibres & Textiles in Eastern Europe.*Vol.13. No.3(51).

Peng, Liyun, Cheng, Yukun & Guo, Xiuping. (2005). Control of Distorted Deformation of Plain Knitted Cotton Garments. *Knitting Industries*. No.4(4). p.20-22.

P.K. Banerjee & T.S. Alaiban. (1988). Geometry and Dimensional Properties of Plain Loops Made of Rotor Spun Cotton Yarns, Part II: Spirality of the Wale. *Textile Research Journal.* Vol.58. p.287-290.

Wu, Honglie. (2004). Methods for Mending Lengthwise Distortion of Single Jersey. *Wool textile Journal*. No.2. p.69-70.

Yang, Suoting. (2004). *Spinning Technology.* Beijing: China Textile & Apparel Press. May, 2004.

Yu, Xufen. (2004). *Experimental Technology of Spinning Material.* Beijing: China Textile & Apparel Press. March, 2004.

Zhang, Yiping. (2005). An Analysis of the Skewing and Twisting of Knitted Face Fabric. *Shanghai Textile Science & Technology*. No.10. 33(10).

Table 1. Parameter table of the bunch adding twist

Twist parameter of the single yarn	Twisting ratio	Twist parameter of the bunched line	Nominal twist of the bunched line	Actual twist of the bunched line	Self twisting direction of the bunched line
80.38	0.2	16.08	79	74.8	S
80.38	0.414	33.28	163	14.9	S
80.38	0.707	56.83	278	258.8	Z
80.38	1	80.38	394	359.6	Z

Table 2. Table of fabric deflection angles (Right deflection is plus, left deflection is negative, and the unit is °.)

Loop length (mm) / Twist of the bunched line (tpm)	5.6	6.1	6.6	7.2
79	14.6	17.0	18.4	23.5
163	9.5	10.5	12.1	13.7
278	-1.0	-1.9	-2.6	-3.3
394	-10.9	-11.8	-15.5	-19.8

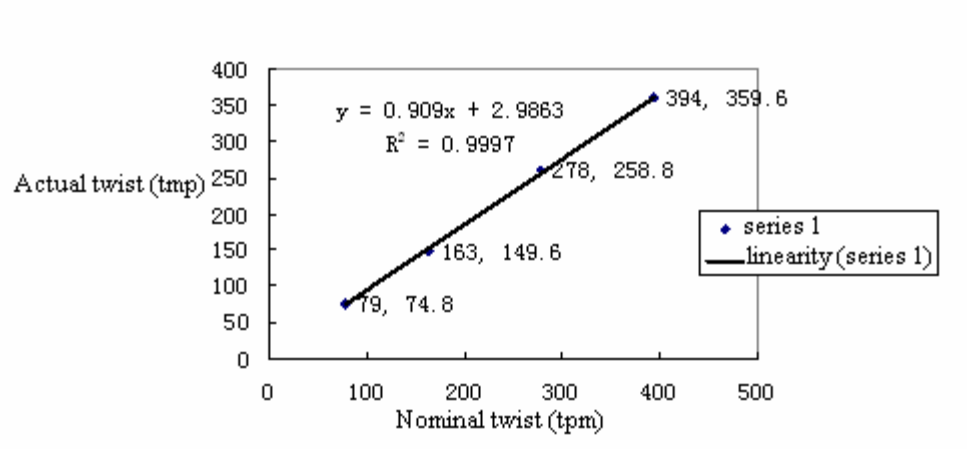

Figure 1. Relationship between the Nominal Twist and the Actual Twist of the Bunched Line

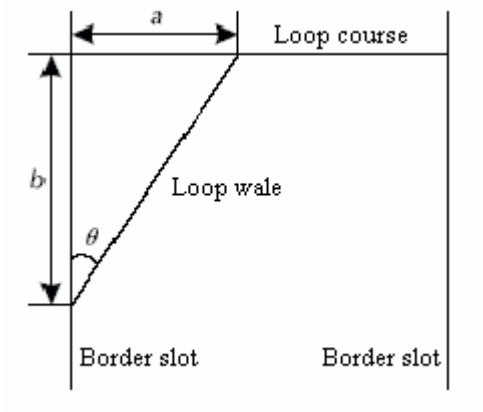

Figure 2. Z Twisting Yarn Wale Deflection

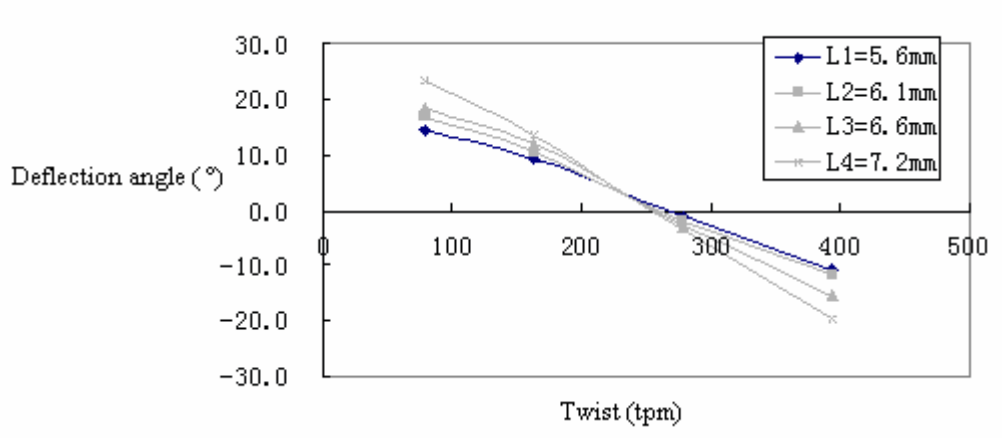

Figure 3. Relationship between Loop Deflection Angle and Twist

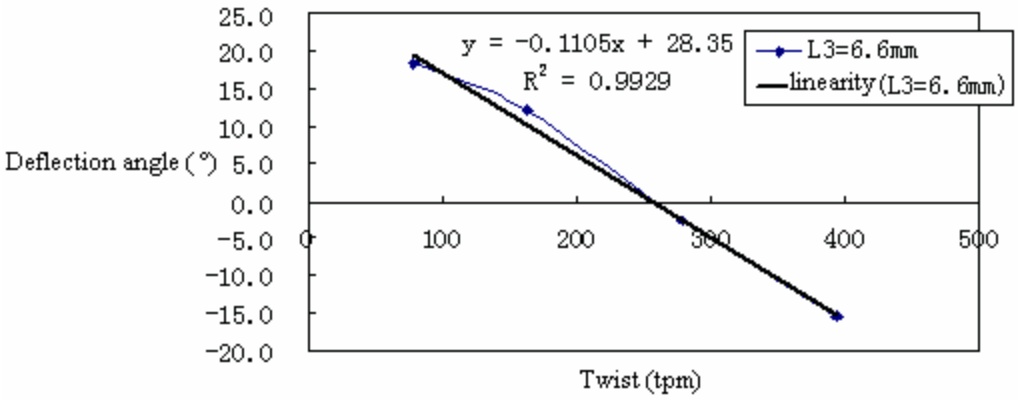

Figure 4. Relationship between Loop Deflection Angle and Twist When the Loop Length is 6.6mm

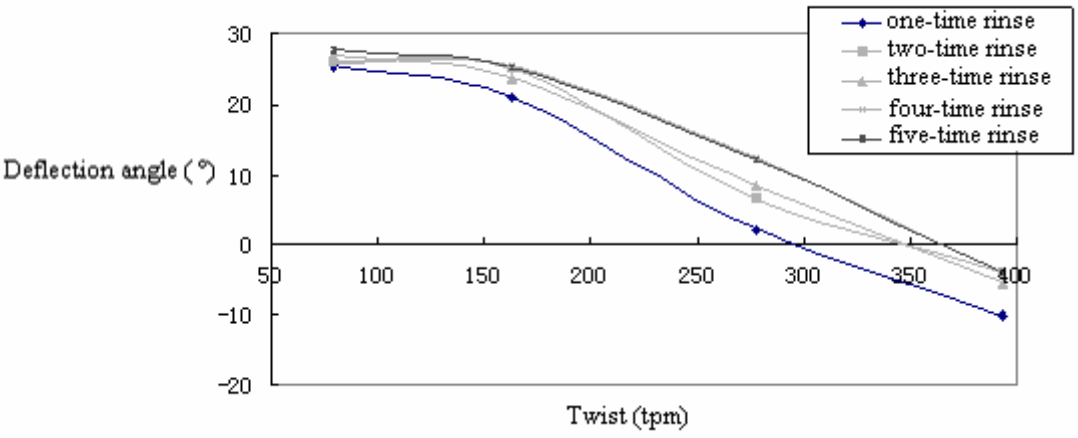

Figure 5. Relationship between Loop Deflection Angle and Twist after Rinse

Modern Applied Science

www.ccsenet.org/journal.html

Vol. 2, No. 3

May 2008

Analysis of Unbonded Prestressed Concrete T-type Beam's Dynamic Characteristics

Yingge Wang

Department of Civil Engineering, Jiaying University

Meizhou 514015, Guangdong, China

E-mail: summerc29@126.com

Abstract

Prestressed force's impacts on simple T-type beam's vibration such as vertical bending, horizontal bending, torsioning, etc., were researched in this paper. It also separately sets up beam element model basing on prestressed concrete equivalent load principle and solid element model taking slippage between prestressed reinforcing steel bar and concrete into account, and developed simulation analysis on two linear steel bar lay-outs & two curving ones. The computed results of different models & different steel bar lay-outs were analyzed and contrasted with each other, as produced simple T-type beam's frequency influencing factors.

Keywords: Prestressed beam, Unbonded, Equivalent load, Dynamic characteristics

1. Introduction

Unbonded prestressed T-type beam is widely applied in engineering structure for research on its dynamic characteristics is of great engineering significance. Domestic and overseas scholars' understandings of prestressed force's effect on concrete beam's dynamic characteristics are different. The early theory thought that frequency increases along with prestressed force's reduction, and prestressed force is sensitive to lower frequency. Saiidi M, Douglas B, Feng S carried on indoor model experiment on simple rectangular solid sectioned beam with prestressed force group disposed at its centre. Their conclusion was that beam's bending basic frequency increases along with prestressed force's increase while prestressed force's influence on frequency is relatively small. Through theoretical analysis A.Dall, Asta and Dezi thought that prestressed force's influence on frequency is small, and could be overlooked. Abraham, etc. thought that prestressed force's influence on beam's vibration modality is quite small.

Numerous researches indicate that besides prestressed force's strength, prestressed beam's mode is more influenced by shape of section, boundary conditions, lay-out of prestressed steel bars, elasticity coefficient, section's moment of inertia, crack size, distribution and so on.

The present analysis mainly concentrates on vertical vibration. Because of T-type beam's particularity, its vibration characteristics like horizontal bending, torsioning and so on are necessary to be taken into account. This article separately sets up beam element model and solid plus link element model of simple T-type prestressed beam utilizing equivalent load method & initial stress method. Furthermore, different lay-outs of reinforcing bars are computed & analyzed.

2. Prestressed equivalent load

The prestressed force in concrete's section of post-tensioning prestressed components comes from extrusion between prestressed steel bars & concrete and polar anchor's collected load. So function of prestressed force could be equivalent to a group of load acting on the concrete structure, as is equivalent load usually called. To separate prestressed force from concrete components and to analyze separately when computing exact equivalent load could derive the equivalent load according to equilibrium conditions. As to computation formula of equivalent load caused by simple beam's prestressed force: component of polar collected force N_p produced by prestressed steel bars at axial direction is $N_p \cos\theta$; prestressed beam's striding height is usually large; angle θ of prestressed steel bars' tangent and axis is small; $N_p \cos\theta \approx N_p$, polar axial force N_p^* is equivalent to N_p. When polar force simplified to direction of axis, it produces equivalent eccentric torque $M_P^* = N_p \cos\theta \cdot e \approx N_p e$. As to inter-segment, extrusion between prestressed steel bars and concrete produces equivalent distributing force. According to the equilibrium condition, $q(x) = N_P d^2 y / dx^2$ could be obtained. As to straight pole of constant section, the prestressed equivalent load is related with prestressed steel bars'

effective tension, polar eccentric distance and prestressed steel bars equation's second differential, and irrelated with structural form.

As to straight line reinforcing bars, the prestressed steel bars equation's second differential is zero; the equivalent inter-segment load is zero, viz. the straight line prestressed steel bars produce no extrusion on concrete at the vertical direction.

The parabola reinforcing bars whose rise is f : the prestressed steel bars equation $y = ax^2 + bx + c$. According to geometric relations: $a = 4f/L^2$. It's obvious that when prestressed steel bars are dual parabola reinforcing bars, the equivalent inter-segment load is a constant.

Fig. 1 is concrete simple beam's equivalent load of straight line reinforcing bars and dual parabola reinforcing bars. The prestressed steel bars' effective tension N_P, the eccentric distance is e_p, f is the parabola's rise.

3. Dynamic characteristics computation and analysis

3.1 Model's construction

Model's parameters: Simple beam's length 24m; size of the section is shown in Fig. 3 & Fig. 4. The concrete's elastic coefficient is 3.8×104 MPa, the density is 2600 kg/m3, steel bar 210 GPa, the density is 7800 kg/m3. The two straight line steel bars' lay-outs and two curve steel bars' lay-outs are considered separately. The situations in which effective prestressed forces exerted are 0, 1000 kN, 2000 kN and 3000 kN.

The available element forms equivalent load method may adopt are mainly the BEAM series, the SHELL series and the SOLID series. Taking this method's characteristics into account, the structural components adopt space beam element BEAM188 to construct the model. The BEAM188 element is good to analyze beam structure from thin-tall to medium thick & length. The element bases on the first-phased cut & distortion theory and Timoshenko Beam Structural Theory, taking effect of cut & distortion into account. Merits of equivalent load method are simpler model construction, direct model construction irrespective of specific position of steel bars, easier grid division and ease of obtaining structure's overall effect under function of prestressed force. But it's unable to take distribution & direction of steel bars' function to concrete into account.

In the initial stress method, unbonded prestressed concrete components' unbonded steel bars' slippage from concrete shouldn't be neglected; components are divided into two parts of reinforced concrete and prestressed steel bars when constructing the model; the prestressed steel bars are simulated by LINK8 element, and the concrete is simulated by SOLID95 element. SOLID95 is higher element form of SOLID45 (3-dimensional 8 nodes), defining 20 nodes with each one having 3 planar motion degrees-of-freedom. This element permits irregular form, reducing no accuracy. So it especially suits models whose boundaries are curve. Furthermore, its displaced form's compatibility is good. Exertion of the prestressed steel bars' prestressed force adopts initial stress method. Connection of two parts is realized through degree-of-freedom's coupling. The nodes of LINK8 and SOLID95 are all only having planar motion degree-of-freedom along directions of three coordinate axes; when simulating the unbonded form, the prestressed steel bars' longitudinal planar motion degree-of-freedom is released; the other two directions' nodes' degrees-of-freedom need to be coupled to guarantee same value of the corresponding ones. As to situation of curved prestressed steel bars, sufficient elements should be defined to guarantee prestressed steel bars' proper radians. Moreover, cushions need to be arranged to solid elements when exerting restriction or to partially strengthen them to avoid stress concentration brought by local distortion.

Fig. 5 shows frequencies by two model construction methods with no prestressed force exerted. In the figure, V, H, T & L are respectively vertical bending, horizontal bending, torsioning and axial expansion. The computed frequencies and lineups by two methods are consistent too each other. The lower self-vibration frequencies of horizontal bending & axial expansion on the beam plane surface especially fit well.

3.2 Frequency's variation under function of prestressed force

Table 1. shows the computed frequency's variation along with prestressed force's alteration basing on equivalent load method and utilizing beam element model construction. It could be seen that form of reinforcing bars influences little to the result. Equivalent load method only takes prestressed force as exterior load to exert on the structure, and is unable to take distribution and direction of steel bars' action to concrete into account. Different lay-outs of steel bars only cause the exerted load's change while this kind of change's influence on the prestressed beam's frequency is slight.

The result also reveals that the beam's every phase's frequencies take on a linear trend of decreasing along with the prestressed force's increase, and the lower frequencies obviously vary more greatly than the higher frequencies. This is consistent with traditional computational theory. The Eluer-Bernoulli beam theory could be referred to support: Supposing prestressed beam is isotropic simple beam under axial force's action, the beam's curving differential equation

is

$$p(x,t)=\frac{\partial^2}{\partial x^2}\cdot\frac{EI\partial y^2}{\partial x^2}+\frac{N\partial y^2}{\partial x^2}+\frac{m\partial y^2}{\partial t^2} \quad (1)$$

To solve it,

$$\omega_n=\frac{n^2\pi^2}{l^2}\cdot\left(1-\frac{Nl^2}{n^2\pi^2E_cI_c}\right)^{1/2}\cdot\left(\frac{E_cI_c}{m}\right)^{1/2} \quad (2)$$

In the formula, N is the effective tensioning force; EI is the beam's flexural rigidity; ω_n is the beam's n-phased frequency; l is the beam's span; m is the unit length mass. From the formula it could be seen that prestressed simple beam's frequencies reduce along with the axial force's increase.

Table.2 is the result computed by initial stress method. It indicates that lay-out of steel bars affects beam's frequency greatly. As to situation of reinforcing bars' disposed at straight line's centroid, the frequencies increases along with prestressed force's decrease. But to eccentric straight line reinforcing bars and curve reinforcing bars, when prestressed force increases, variation of different phases' frequencies is not the same. Vertical vibration, torsioning and axial expansion's basic frequencies decrease along with prestressed force's increase; horizontal vibration's basic frequencies take on tendency of increase. Some higher frequencies also increase along with prestressed force's increase. But in brief, the computed frequencies obtained through prestressed force method using model of solid steel bars receive less influence from prestressed force; especially the basic frequencies at different directions, they all change below 0.12%. Only change of torsioning's higher frequency is relatively greater, but the utmost is no less than 2%.

4. Conclusion

Model of prestressed simple beam constructed according to equivalent load mechanism cannot take distribution and direction of steel bars' action to concrete into account. So different lay-outs of steel bars' influence on the prestressed beam's frequencies is slight. And because the model adopts beam element, the beam's frequencies appear consistent with traditional computational theory: Increase along with prestressed force's decrease, and the lower frequencies obviously alter more greatly than the higher frequencies.

As to solid, isotropic and non-dehiscenced element, the computed result demonstrates that prestressed force's influence on beam's dynamic characteristics is weak and mainly decided by lay-out of prestressed steel bars. If prestressed steel bars are eccentric straight linear or parabolic disposed, the frequencies possibly increase along with prestressed force's increase, but the alteration scope is small. The conclusion drawn from model of solid steel bars tallies with presently existing tentative data, and is still coincident with actual ones.

References

Saiidi, M, Douglas, B & Feng, S. (1994). Prestress force effect on vibration frequency of concrete bridges. *Journal of Structural Engineering*. 120. 2233-2241.

A Dall Asta, L. Dezi St. (1996). Discussion about Prestress force effect on vibration frequency of concrete bridges. *Journal of Structural Engineering*. 122, 458-460.

ABRAHAM M A, PARK S Y, STUBS N. (1995).Loss of prestress prediction on nondestructive damage location algorithms. *SPIE Structures and materials*. 2446, 60-67.

Xia, Zhanghua & Zong, Zhouhong. (2007). Analysis of prestressed force's impact on concrete beam's dynamic characteristics. *Journal of Vibration and Shock*. 26. 129-134. (in Chinese).

Yang, Haixu, Liu, Wancheng, Wang, Haibiao & Yang, Donghui. (2005) Characteristics & application of unbonded prestressed steel bars' equivalent load. *Journal of Harbin Institute of Technology*. 37, 1087-1089. (in Chinese).

Table 1. Frequency varying proportion by equivalent load method

	modality	V1	H1	V2	T1	T2	V3	H2	T3	L1	H3
	prestress	Frequency variation (%)									
	1000kN	-0.976	-0.342	-0.250	-0.055	-0.188	-0.118	-0.120	-0.057	0.000	-0.094
Linear pattern 1	2000kN	-1.963	-0.684	-0.506	-0.117	-0.375	-0.235	-0.243	-0.113	-0.003	-0.187
	3000kN	-2.957	-1.029	-0.756	-0.178	-0.563	-0.353	-0.362	-0.173	-0.005	-0.283
	1000kN	-0.976	-0.422	-0.250	0.018	-0.270	-0.118	-0.194	0.015	0.000	-0.148
Linear pattern2	2000kN	-1.963	-0.847	-0.506	0.037	-0.541	-0.235	-0.387	0.033	-0.003	-0.295
	3000kN	-2.957	-1.275	-0.756	0.055	-0.806	-0.353	-0.581	0.048	-0.005	-0.443
	1000kN	-0.976	-0.342	-0.250	-0.055	-0.188	-0.118	-0.120	-0.057	0.000	-0.094
Curve pattern 1	2000kN	-1.963	-0.684	-0.506	-0.117	-0.375	-0.235	-0.243	-0.113	-0.003	-0.187
	3000kN	-2.957	-1.029	-0.756	-0.178	-0.563	-0.353	-0.362	-0.173	-0.005	-0.283
	1000kN	-0.976	-0.342	-0.250	-0.055	-0.188	-0.118	-0.120	-0.057	0.000	-0.094
Curve pattern 2	2000kN	-1.963	-0.684	-0.506	-0.117	-0.375	-0.235	-0.243	-0.113	-0.003	-0.187
	3000kN	-2.957	-1.029	-0.756	-0.178	-0.563	-0.353	-0.362	-0.173	-0.005	-0.283

Table 2. Frequency varying proportion by initial stress method

	modality	V1	H1	V2	T1	T2	V3	H2	T3	L1	H3
	prestress	Frequency variation (%)									
	1000kN	-0.005	-0.017	-0.041	-0.014	-0.267	-0.066	-0.009	-0.258	-0.005	-0.105
Linear pattern 1	2000kN	-0.011	-0.032	-0.089	-0.020	-0.533	-0.131	-0.022	-0.516	-0.013	-0.209
	3000kN	-0.016	-0.047	-0.137	-0.027	-0.800	-0.200	-0.031	-0.777	-0.020	-0.316
	1000kN	-0.029	0.006	0.014	-0.027	0.101	0.021	-0.025	0.099	-0.013	0.037
Linear pattern2	2000kN	-0.047	0.019	0.041	-0.047	0.208	0.055	-0.040	0.203	-0.018	0.085
	3000kN	-0.068	0.032	0.062	-0.068	0.314	0.090	-0.059	0.305	-0.025	0.133
	1000kN	-0.019	0.011	0.021	-0.014	0.231	-0.017	-0.012	0.015	-0.008	-0.039
Curve pattern 1	2000kN	-0.040	0.019	0.034	-0.027	0.456	-0.035	-0.022	0.026	-0.013	-0.081
	3000kN	-0.058	0.028	0.048	-0.047	0.670	-0.055	-0.034	0.035	-0.018	-0.122
	1000kN	-0.034	0.024	0.062	-0.020	0.664	0.024	-0.012	0.250	-0.005	0.004
Curve pattern 2	2000kN	-0.071	0.045	0.116	-0.047	1.311	0.045	-0.028	0.491	-0.010	0.009
	3000kN	-0.111	0.068	0.171	-0.067	1.939	0.066	-0.040	0.726	-0.018	0.011

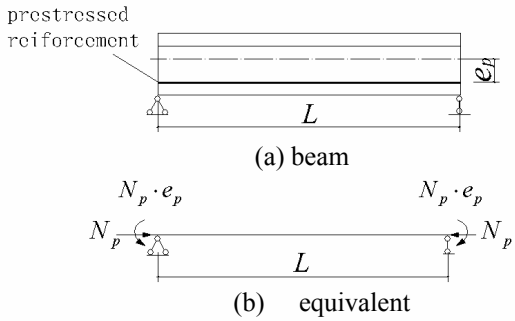

Figure 1. Straight line steel bar's equivalent prestressed force

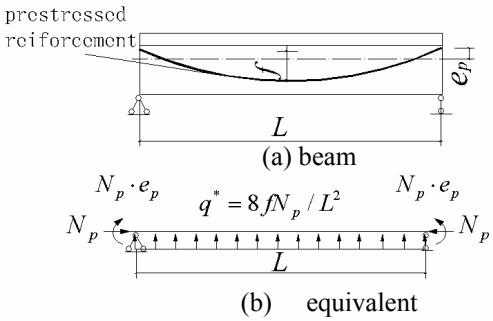

Figure 2. Parabolic steel bar's equivalent prestressed force

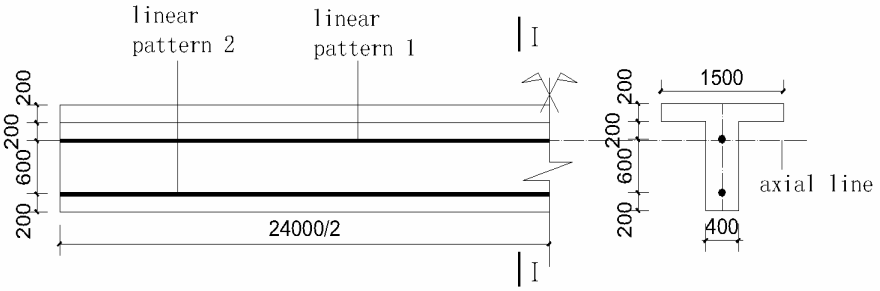

Figure 3. Straight line pre-stressed steel bars' lay-out (mm)

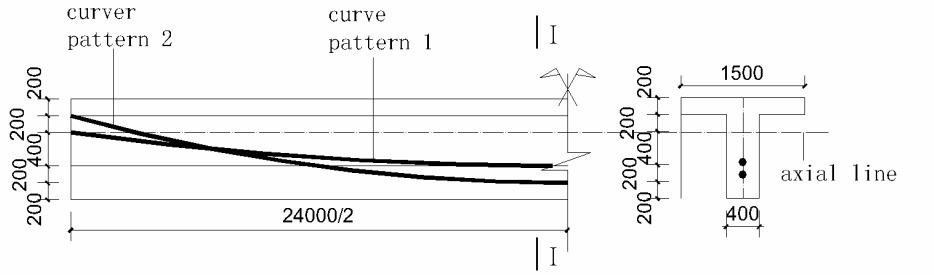

Figure 4. Parabolic pre-stressed steel bars' lay-out (mm)

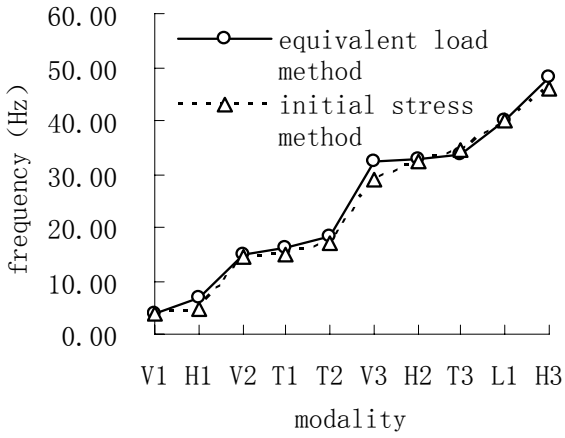

Figure 5. Frequency calculated by two methods

Modern Applied Science

www.ccsenet.org/journal.html

Vol. 2, No. 3

May 2008

First Row Transition Metal Oxide Based Catalysts for the In-situ Reactions of Methanation and Desulfurization in the Removal of Sour Gases from Simulated Natural Gas

Wan Azelee Wan Abu Bakar, Mohd. Yusuf bin Othman, Ching Kuan Yong & Junaidi Mohd. Nasir

Department of Chemistry, Faculty of Science

Universiti Teknologi Malaysia

81310 UTM Skudai, Johor, Malaysia

Tel: 60-13-746-6213 E-mail: wanazelee@yahoo.com

The research is financed by Universiti Teknologi Malaysia and Ministry of Science, Technology and Innovation, Malaysia through IRPA Vot 74248.

Abstract

The objective of this novel catalyst development is to achieve both low temperature and high conversion of sour gases of H_2S and CO_2 present in the natural gas. The results showed that the conversion of H_2S to elemental sulfur on all of the potential catalysts was achieved 100 %. However, methanation of CO_2 in the presence of H_2S yielded 0.7 % CH_4 over Fe/ Zn/ Cu/ Ti-Al_2O_3 catalyst, 1.1 % CH_4 over Fe/ Zn/ Cu-Al_2O_3 catalyst and the highest is 6.1 % CH_4 over Pr/ Co/ Ni-Al_2O_3 catalyst at maximum studied temperature of 300 ^oC. The catalysts were further characterized by X-rays Photoelectron Spectroscopy and Nitrogen Adsorption analysis. XPS results revealed Ni^{2+} ion in the NiO and Ni^{3+} in Ni_2O_3 species, spinel compound of Co_3O_4 on the Pr/ Co/ Ni-Al_2O_3 catalyst. N_2 adsorption-desorption analysis illustrated 7.9 % increment of surface area over the spent Pr/ Co/ Ni-Al_2O_3 catalyst, which assumed to be responsible for the dramatical increased of the methanation activity of this catalyst at the reaction temperature of 300 ^oC.

Keywords: Titanium, Copper, Nickel, Methanation, Desulfurization, Natural gas

1. Introduction

Crude natural gas is categorized as a sour gas due to the contamination of carbon dioxide (CO_2) and hydrogen sulfide (H_2S). These corrosive elements may deteriorate the pipeline systems and become a safety hazard and also contribute to the environmental issue. Recently, the removal of these sour gases via chemical conversion techniques becomes the most promising technique. The catalysts for the CO_2 methanation have been extensively studied because of their application in the conversion of CO_2 gas to produce methane, which is the major component in natural gas. However, the presence of H_2S in the natural gas and certain industrial processes is known to cause poisoning of the metal surface with both sulfur and hydrogen.

The essential requirement for the correct selection of the oxide system is its ability to accept and to activate CO_2 and H_2S. The acid nature of CO_2 and H_2S necessitates the employment of a catalytic system with basic properties. Such requirements are met with some transition metal oxides and apparently some Lanthanide oxides. Their acid and redox properties may be changed by adding other oxides (Krylov *et al.*, 1998). Investigation done by Wang *et al.* (2007) found that the adsorption strength of CO_2 is controlled by the Lewis basicity of a catalyst, *d*-band center of the metal surface, charge transfer from the metal surfaces to the chemisorbed CO_2. The major reason for the much slower of the catalyst science of mixed metal oxide is its significantly complexity compared with metal based catalyst, e.g. possible presence of multiple oxidation states, variable local coordination, coexisting bulk and surface phases as well as different surface termination functionalities such as M-OH, M=O or M-O-M (Wachs, 2005). Metal oxides are less active than metals, but they are stable in catalytic conditions.

Praseodymium oxide has been investigated as the most effective rare earth metal oxide when it was dopped onto NiO based catalyst for CO_2 methanation reaction at 400 ^oC. Later, cobalt oxide was found as the most suitable dopant towards the Pr/ Ni catalyst (Wan Abu Bakar, 2005). Kulshreshtha *et al.* (1990) have been reported that Fe-Ti-Sn intermetallics are capable of CO methanation and almost completely converted CO to methane at 323 ^oC. This investigation concluded that the catalytic activity of the intermetallics is significantly improved by Sn substitution. Later, Pineda *et al.* (1997) found

out when zinc oxide and zinc ferrite catalysts were dopped with Cu and Ti, their catalytic performance on H_2S desulfurization process could be increased. The addition of Ti may increase the stability of ZnO towards reducing agent such as H_2. However, the addition of Cu do not affect the stability of catalyst but improve the catalyst performance by changing the surface of the catalyst during calcination and activation process. It has been found that CO_2 strongly chemisorbs on the Fe (110) surface with the strongest binding energy, whereas CO_2 has moderate strength on the (111) surface of Co, Ni, Rh, Pd with slightly positive binding energies (Wang *et al.*, 2007). The selection of support is considered as important since it may influence both the activity and selectivity of the reaction. It has been discovered that the addition of alumina may increase the methanation activity although there is a presence of low concentration of H_2S (Happel & Hnatow, 1981). Therefore, Al_2O_3 is selected as the support for all of the studied catalysts in this research.

Efforts to search for efficient catalyst and to explore new technology in order to meet the demands of the economical feasibility of in-situ reactions of methanation and desulfurization for the purification of natural gas have not been extensively studied. The objective of this novel catalyst development is to achieve both low temperature and high conversion of sour gases. At low temperature, application of the novel catalyst in gas industry is more likely. However, problem arises because exothermic reaction of conversion of CO_2 to CH_4 is unfavorable at low temperature due to its low energy content.

2. Experimental

2.1 Preparation of catalysts

The catalysts were prepared by impregnation method, namely, impregnating appropriate amount of metal nitrate salts on Al_2O_3 beads support for 15 minutes and dried at 80^oC for 24 hours. It was then calcined in air at 400^oC for 5 hours. Ti^{4+} sol for the Ti based catalyst was prepared by dissolving 6 g of polyethylene glycol (PEG) with 600 mL ethanol. Then, 31.8 g diethanolamine (DEA) followed by 85.2 g titanium (IV) isopropoxide ($Ti(iso)_4$) was added when PEG completely dissolved. After that, 5.4 mL of distilled water was added and stirred for 10 minutes to get a homogeneous solution. Al_2O_3 beads were dipped into the Ti^{4+} sol and then dried in the oven at 80^oC for 30 minutes. The following metal oxides were impregnated onto the Al_2O_3 according to the above said method.

2.2 Catalytic activity measurements

In-situ reactions of methanation and desulfurization was performed from room temperature up to 300 ^oC with temperature rate of 5 ^oC/ min. CO_2 and H_2 gases were introduced into the reactor system in a stoichiometric ratio of 1: 4. About 2.5 mL/ min H_2S gas was introduced into the gas stream. This composition is similar to the content of sour gases in Malaysian natural gas, which is 5 % of H_2S and 20 % of CO_2. Screening on the produced gas stream was done by using FTIR analysis. Percentage conversion of CO_2 and H_2S was obtained by calculating the peak area of their respective stretching band. Off line Gas Chromatography analysis was done on the product gas to determine the selectivity and yield of CH_4 gas due to the low sensitivity of FTIR towards stretching band of CH_4.

2.3 Characterization of catalysts

2.3.1 X-rays Photoelectron Spectroscopy

The potential catalysts were characterized by using Kratos instrument XSAM HS surface analysis spectrometer with Mg Kα X-rays source (1253.6 eV). Sample was introduced into the spectrometer in flowing argon atmosphere, and evaporated at least 6×10^9 Torr before spectrum was recorded. The spectrum was taken at 10 mA and 14 kV energy source at 2 sweeps.

2.3.2 Nitrogen Adsorption Analysis

The N_2 adsorption-desorption isotherms for the catalysts were measured by Micromeritics ASAP 2010. All samples were evacuated at 120 ^oC prior to the measurement. The specific surface area was calculated using the BET method. The total pore volume was determined at a relative pressure of $P/ P_o = 0.99$.

3. Results and Discussion

3.1 In-situ reactions of CO_2 methanation and H_2S desulfurization

Figure 1 shows the details trend on the percentage conversion of CO_2 and H_2S over the potential Pr/ Co/ Ni (5: 35: 60)-Al_2O_3, Fe/ Zn/ Cu (4: 16: 80)-Al_2O_3 and Fe/ Zn/ Cu/ Ti (5: 5: 40: 50)-Al_2O_3. Table 1 shows the yield of CH_4 which indicated the methanation activity of the studied catalysts.

Fe/ Zn/ Cu/ Ti (5: 5: 40: 50)-Al_2O_3 catalyst showed a relatively higher H_2S conversion activity than the other two catalysts at temperature lower than 200 ^oC. It could be assigned as the best H_2S desulfurization catalyst among the studied catalysts due to its ability to convert higher percentage of H_2S at light off temperature. Pineda *et al.* (1997) have reported the presence of Ti may increase the H_2S desulfurization process at lower temperature. It had been proven that TiO_2 could influence the dissociation of H_2S to H^+ and HS^- at the early stage due to its weak electron interaction in the *d* orbital (Blesa *et al.*, 1993). The graph in Figure 1 shows a decrease on the conversion of H_2S over Fe/ Zn/ Cu-Al_2O_3 and Fe/ Zn/ Cu/

Ti-Al_2O_3 catalysts from room temperature to 40 ^oC. This phenomenon was assigned to the adsorption of H_2S by the catalysts at lower temperature. Both the catalysts, completely removed H_2S at reaction temperature of 100 ^oC. At temperature higher than 200 ^oC, the H_2S desulfurization activity decreased in a great order over Fe/ Zn/ Cu-Al_2O_3 and Fe/ Zn/ Cu/ Ti-Al_2O_3 catalysts. This may due to the uptake of H_2 by sulfur deposited on the surface of the catalysts to form H_2S. Therefore, H_2S desulfurization reaction at temperature higher than 200 ^oC is unfavored over these two catalysts. On the other hand, Pr/ Co/ Ni-Al_2O_3 catalyst showed a totally different trend in the conversion of H_2S compared to the copper and titanium oxide based catalysts. The conversion of H_2S over this catalyst gradually increased by the increasing of temperature until 100 % conversion of H_2S was achieved at reaction temperature of 280 ^oC.

During CO_2 methanation in the presence of H_2S, all the three catalysts showed a gradual increase until maximum studied temperature of 300 ^oC. Pr/ Co/ Ni-Al_2O_3 and Fe/ Zn/ Cu-Al_2O_3 catalysts yielded the same amount of CH_4 at reaction temperature of 200 ^oC (0.7 %), but Pr/ Co/ Ni-Al_2O_3 catalyst performed dramatically high CO_2 methanation and H_2S desulfurization activities at 300 ^oC. Pr/ Co/ Ni-Al_2O_3 gave the highest conversion of CO_2 where it converted 19.2 % of CO_2 and yielded 6.1 % of CH_4 at 300 ^oC. It is believed that Pr was able to generate active sites for the in-situ reactions of CO_2 and H_2S conversion at higher temperature. Rare earth metal oxides may increase the stability of catalyst at high temperature and avoid the sintering of nickel (Miao *et al.*, 1997). At 300 ^oC, Fe/ Zn/ Cu-Al_2O_3 catalyst converted 12.7 % of CO_2 and yielded 1.1 % of CH_4. Fe/ Zn/ Cu/ Ti-Al_2O_3 catalyst yielded no CH_4 at 100 ^oC and gave only 0.7 % of CH_4 at 300 ^oC. The CO_2 methanation activity over this catalyst is considered very low. Basu *et al.* (2004) have proven that the addition of TiO at a high concentration may increase the surface oxygen storage. However, this property did not assist the adsorption of CO_2 on the catalyst surface. Besides that, the interaction between Ti and H_2 is weak because H_2 prefer to adsorb on the defect TiO lattice. Thus prevent the adsorption of H_2 during CO_2 methanation (Henrich & Cox, 1994). It has also been reported by Fournier (1986) that CH_4 formation from C is easier on Co (100) than Fe (110). The presence of subsurface C tends to increase the activation energy required for the hydrogenation steps and hence CH_4 formation becomes more difficult in the presence of Fe-carbides. Miao *et al.* (1997) also suggested that the interaction between transition metal and Al_2O_3 support is one of the most important factors that determined the redox ability. Nickel oxide based catalyst is the most suitable for the in-situ reactions of CO_2 methanation and H_2S desulfurization according to the results obtained in Figure 1 and Table 1.

3.2 Characterization of Catalysts

3.2.1 X-rays Photoelectron Spectroscopy (XPS)

The surface active components on the fresh and after catalytic testing (spent) catalysts of Pr/ Co/ Ni (5: 35: 60)-Al_2O_3, Fe/ Zn/ Cu (4: 6: 80)-Al_2O_3 and Fe/ Zn/ Cu/ Ti (5: 5: 40: 50)-Al_2O_3 were accomplished through XPS. All data was corrected by using the binding energy, E_b, of C 1*s* at 284.5 eV as standard.

The E_b resulted from deconvolution peaks of Ni (2*p*) and Co (2*p*) from Pr/ Co/ Ni-Al_2O_3 was depicted in Table 2. The E_b of each species observed in Ni (2*p*) region for the fresh Pr/ Co/ Ni-Al_2O_3 catalyst are characteristic of the Ni^{2+} ion from the NiO at the E_b of 854.2 eV ($2p_{3/2}$) and 871.8 eV ($2p_{1/2}$), similar assignment to the data obtained made by Nefedov *et al.* (1975) who investigated on some coordination compounds; and Lorenz *et al*. (1979) who studied ESCA on NiO/ SiO_2 and NiO-Al_2O_3/ SiO_2 catalysts. The existence of Ni (2*p*) peak at 856.8 eV ($2p_{3/2}$) and 874.3 eV ($2p_{1/2}$) was attributed to the presence of Ni^{3+} in Ni_2O_3. Ni^{3+} shows a higher binding energy because the E_b of the metal increases when the covalency decreases (Vederine *et al.*, 1978). As the ionic radius of Ni^{2+}> Ni^{3+} and furthermore the covalency of Ni^{3+} decreases compare to Ni^{2+}. It is known that Ni^{3+} is more reactive than Ni^{2+}. It could be suggested that Ni_2O_3 is responsible to be the active site for this catalyst. The lower percentage H_2S desulfurization over Pr/ Co/ Ni (5: 35: 60)-Al_2O_3 at reaction temperature below 200 ^oC may be resulted from the lack of Ni_2O_3 present, which is an oxygen rich compound. XPS data also revealed the presence of spinel compound, Co_3O_4 on the surface of the catalyst, which is in accord with those reported by Kim (1975), Zeng *et al.* (1995), and Riedel & Schaub (2003) who worked with the CoO, CoO-ZrO_2 and Co Fischer-Tropsch catalyst, respectively. The existence of the spinel compound in the catalyst was assigned to be good for the catalytic efficiency as it provides more active sites for the reaction and also it can easily change forms according to the environment, whether it is more to Co^{2+} or Co^{3+}.

After the exposure to the in-situ reactions of CO_2 methanation and H_2S desulfurization environment, NiO was disappeared in the spent catalyst. Similar phenomenon also reported by Djaidja *et al.* (2000). NiO phase was disappeared in their used Ni/ Sm_2O_3 and Ni/ La_2O_3 catalysts. Ni_2O_3 was detected in both of their fresh and used catalysts and they suggested that Ni_2O_3 phase is needed in the oxidative transformation of methane reaction course. The absence of NiO was presumably contributed to the increasing of the catalytic performance over this catalyst at maximum study temperature of 300 ^oC. The Co (2p) peaks shifted to a lower E_b of 778.7 eV ($2p_{3/2}$) and 782.8 eV ($2p_{1/2}$) indicating no changes in the Co oxidation state on the surface.

According to the XPS analysis, 0.7 % of Pr was available on the fresh Pr/ Co/ Ni-Al_2O_3 catalyst, while only 0.2 % of Pr was available on the spent catalyst. This reduction may due to the agglomeration of other elements that forced the Pr element to move into the bulk of the catalyst.

Even though the EDX analysis revealed the weight percentage of Zn as 0.2 % in the Fe/ Zn/ Cu-Al_2O_3 catalyst, no peak assigned to Zn was detected from the deconvolution peak of Zn. This may due to the agglomeration of the other elements, which thus pushed Zn into the lattice structure of the catalyst or poisoning from carbon compound during XPS analysis. The lower loading of Zn that is insensitive to the XPS analysis is also a factor. The E_b resulted from deconvolution peaks of Cu (2*p*) and Fe (2*p*) from Fe/ Zn/ Cu-Al_2O_3 catalyst was tabulated in Table 3. The fresh Fe/ Zn/ Cu-Al_2O_3 catalyst contained normal spinel compound of $CuFe_2O_4$. This spinel compound turned to inverse spinel structure after the catalytic testing. A normal spinel compound is the active site for this catalyst. Fe^{3+} made up the octahedral site while Cu^{2+} made up the tetrahedral site (Ando *et al.*, 1998a; 1998b) as illustrated in Figure 2. Peaks referred to normal spinel compounds of $CuFe_2O_4$ or Fe_3O_4 appeared at E_b of 710.1 eV ($2p_{3/2}$) and 723.7 eV ($2p_{1/2}$). $CuFe_2O_4$ and Fe_3O_4 were assumed to act as active species on the surface. Fe_3O_4 is considered as the more dominant structure compared to $CuFe_2O_4$ and it is also the active site for H_2S desulfurization. Peak area of these peaks is high enough, which indicated the formation of surface Fe in a large amount. This also proved that Fe_3O_4 is a more dominant structure compared to $CuFe_2O_4$. The spent Fe/ Zn/ Cu-Al_2O_3 catalyst showed deconvolution peaks of $CuFe_2O_4$ or Fe_3O_4 at E_b of 710.1 eV ($2p_{3/2}$) and 723.7 eV ($2p_{1/2}$) but with 85.3 % reduction of peak area. This may due to the inverse spinel structure that contributed to the presence of larger amount of surface copper.

Normal spinel compound of $CuFe_2O_4$ was revealed from the deconvoution peak of Cu (2p) for the fresh and spent Fe/ Zn/ Cu/ Ti-Al_2O_3 catalysts (Table 4). Peaks referred to normal spinel compounds of $CuFe_2O_4$ or Fe_3O_4 appeared at E_b of 709.7 eV ($2p_{3/2}$) and 723.2 eV ($2p_{1/2}$) on the fresh Fe/ Zn/ Cu/ Ti-Al_2O_3 catalyst. There are another peaks at E_b of 712.4 eV ($2p_{3/2}$) and 726.1 eV ($2p_{1/2}$) assigned to the Fe^{3+} bound to hydroxyl group ($^-$OH) in agreement with Shah *et al.* (2002). The higher binding energy of these peaks is due to the high electronegativity of hydroxyl group. $^-$OH ligand is more electronegative than oxygen. The presence of hydroxyl ligand could increase the oxidation reaction over Fe/ Zn/ Cu/ Ti-Al_2O_3 catalyst due to its high electron density nature. Morrison (1998) also proved that TiO_2 in Fe/ Zn/ Cu/ Ti-Al_2O_3 catalyst contributed to the presence of Fe^{3+}-OH and thus active site for the H_2S desulfurization. The adsorption process of H_2S at low temperature that may inhibit H_2S desulfurization could be avoided. On the other hand, the spent Fe/ Zn/ Cu/ Ti-Al_2O_3 catalyst also showed a lower peak area for deconvolution peaks of $CuFe_2O_4$/ Fe_3O_4 at 710.5 eV ($2p_{3/2}$) and 724.1 eV ($2p_{1/2}$). This may resulted from carbon coking on the surface of the catalyst during XPS analysis or the formation of CuO obstructed the distribution of Fe on the catalyst surface. Similar with Fe/ Zn/ Cu-Al_2O_3 catalyst, no peak assigned to Zn was detected even though 0.1% of Zn was revealed by EDX analysis. In addition, the presence of Ti in the Fe/ Zn/ Cu/ Ti-Al_2O_3 catalyst also could not be detected due to the narrow diameter of Ti compared to Cu and Fe. It is believed that Ti was left inside the lattice structure of the catalyst. The interaction of electron from Ti is weak due to the distance of Ti inside the catalyst structure is comparably farer than those species on the surface.

3.2.2 Nitrogen Adsorption Analysis

One of the most characteristic properties of the surface of a solid is its ability to adsorb gases and vapours. Table 5 summarized the BET surface area and BJH desorption average pore diameter of the fresh supported catalysts and after in-situ reactions testing catalysts (spent catalysts). The fresh catalysts showed relatively narrower pore size compared to the spent catalysts. It is believed that some of the pores collapsed during the in-situ reactions of CO_2 methanation and H_2S desulfurization leading to the enlargement of the pores. From the BET surface area analysis, the surface area of the spent Pr/ Co/ Ni-Al_2O_3 catalyst is higher than the fresh catalyst. This could explain the dramatical increased of the methanation activity of this catalyst at the reaction temperature of 300 ^oC. It is assumed that the increasing of the surface area with respect to temperature finally increase the catalytic activity of the Pr/ Co/ Ni-Al_2O_3 catalyst at higher temperature. By referring to the XPS analysis, Co ions were detected as spinel compound of Co_3O_4 on the surface. It is believed that Co_3O_4 contributed to the increment of surface area over this catalyst. Besides that, NiO might play a role too. NiO is present in the fresh Pr/ Co/ Ni-Al_2O_3 catalyst but absent in the spent Pr/ Co/ Ni-Al_2O_3 catalyst. It was observed that Fe/ Zn/ Cu/ Ti-Al_2O_3 catalyst posseses the highest surface area and narrowest pore size. This was supported by Yamasaki *et al.* (1999) that the addition of TiO_2 in the catalyst may increase the surface area and decrease the particle size. These features increased the H_2S desulfurization activity but not the CO_2 methanation activity. However, the catalytic activity of a particular catalyst not only depends on the BET surafce area and pore size, but also included other factors such as type of pores, shape of pores and the degree of porosity (Wan Abu Bakar, 2000). The Fe/ Zn/ Cu -Al_2O_3 catalyst showed reduction of 34 % and Fe/ Zn/ Cu/ Ti-Al_2O_3 catalyst showed reduction of 17 % in surface area after undergoing catalytic testing. This reduction is possibly due to the sulfur poisoning on the surface of the catalysts during H_2S desulfurization, or collapsed of the pores during prolongs catalytic reaction. This was also proven by the Energy Dispersive X-rays Analysis, which indicated the appearance of sulfur element. However, the isotherm plot of the fresh and spent catalysts did not show significant difference. All the catalysts showed Type IV isotherm plot and H3 type hysteresis loop.

4. Conclusion

Nickel oxide based catalyst is the most potential for the in-situ reactions of CO_2 methanation and H_2S desulfurization compared to the copper oxide and titanium oxide based catalysts. It is capable of 100 % conversion of H_2S to elemental sulfur and yielded 6.1 % of CH_4 at reaction temperature of 300 ^oC. The aim to obtain high H_2S desulfurization rate at low temperature was achieved. However, improvement is needed for the CO_2 methanation reaction. Therefore, further efforts are needed in the future work in the attempt to obtain catalysts that may increase the conversion rate of CO_2 and H_2S simultaneously at much lower temperature.

References

Ando, H., Fujiwara, M., Matsumura, Y., Miyamura, H., Tanaka, H. & Souma, Y. (1998a). Methanation of Carbon Dioxide over $LaNi_4$ X-Type Intermetallic Compounds as Catalyst Presursor. *Journal of Alloys and Compounds*, 223, 139-141.

Ando, H., Qiang, X., Fujiwara, M., Matsumura, Y., Tanaka, H. & Souma, Y. (1998b). Hydrocarbon Synthesis from CO_2 over Fe-Cu Catalysts. *Catalysis Today*, 45, 229-234.

Basu. B., Vleugels, J. & Der Biest, O.V. (2004). Transformation Behaviour of Tetragonal Zirconia: Role of Dopant Content and Distribution. *Materials Science and Engineering A*, 366, 338-347.

Blesa, M.A., Morando, P.J. & Regazzoni, A.E. (1993). Chemical Dissolution of Metal Oxides. Florida, United States of America: CRC Press, Inc., 269-272.

Djaidja, A., Barama, A. & Bettahar, M.M. (2000). Oxidative transformation of methane over nickel catalysts supported on rare-earth metal oxides. *Catalysis Today,* 61, 303-307.

Fournier, J. A. (1986). *Characterization of some iron catalysts for the reduction of carbon monoxide and the effect of residence time and temperature on the nature of carbon monoxide reduction products.* PhD Thesis. Brown University, United States of America.

Happel, J. & Hnatow, M. A. (1981). U.S. Patent 4, 260, 553. Washington DC: U.S. Patent and Trademark Office.

Henrich, V.E. & Cox, P.A. (1994). The Surface Science of Metal Oxides. Cambridge University Press, Great Britain, 128-138.

Kim, K.S. (1975). X-ray Photoelectron Spectroscopics studies of the electronic structure of CoO. *Physical Review B,* 11 (6), 2177-2187.

Krylov, O.V., Mamedov, A.Kh. & Mirzabekova, S.R. (1998). Interaction of carbon dioxide with methane on oxide catalysts. *Catalysis Today,* 42, 211-215.

Kulshreshtha, S. K., Sasikala, R., Gupta, N. M. & Iyer, R. M. (1990). Carbon monoxide methanation over $FeTi_{1-x}Sn_x$ intermetallics: Role of second phase. *Catalysis Letter,* 4 (2), 129-138.

Lorenz, P., Finster, J., Wendt, G., Salyn, J.V., Žumadilov, E.K. & Nefedov, V.I. (1979). ESCA investigations of some NiO/ SiO_2 and NiO-Al_2O_3/ SiO_2 catalysts. *Journal of Electron Spectroscopy and Related Phenomena,* 16, 267-276.

Miao, O., Xiong, G.X., Sheng, S.S., Cui, W., Xu, L., & Guo, X.X. (1997). Partial oxidation of methane to syngas over nickel-based catalysts modified by alkali metal oxide and rare earth metal oxide. *Applied Catalysis A: General,* 154, 17-27.

Morrison, S.R. (1998), Chemisorption on Nonmetallic Surface. In: Anderson, J.R. and Boudart, M. (eds). *Catalytic Science and Technology*, 3, 199-229.

Nefedov, V.I., Gati, D., Dzhurinskii, B.F., Sergushin, N.P. & Salyn, Ya.V. (1975). Simple and coordination compounds. *Russian Journal of Inorganic Chemistry,* 20, 2307-2314.

Pineda, M., Fierro, J. L. G., Palacios, J. M., Cilleruelo, E. G. & Ibarra, J. V. (1997). Characterization of Zinc Oxide and Zinc Ferrite Doped with Ti and Cu as Sorbents for Hot Gas Desulfurization. *Applied Surface Science*, 119, 1-10.

Riedel, T. & Schaub, G. (2003). Low-temperature Fisher-Tropsch synthesis on cobalt catalyst-effects of CO_2. *Topics in Catalysis,* 26 (1-4), 145-155.

Shah, P., Shoma, M., Kawaguchi, K. & Yamaguchi, I. (2002). Growth Conditions, Structural and Magnetic Properties of M/Fe_3O_4/I (M = Al, Ag and I = Al_2O_3 and MgO) Multilayers. *Journal of Magnetism and Magnetic Materials*, 214, 1-5.

Vederine, J.C., Hollinger, G. & Minh, O.T. (1978). Investigations of Antigorite and Nickel Supported Catalysts by X-ray Photoelectron Spectroscopy. *The Journal of Physical Chemistry,* 82, 1515.

Wan Abu Bakar, W.A. (2000). *Personnel Communications.* Universiti Teknologi Malaysia, Malaysia.

Wan Abu Bakar, W.A. (2005). *Personnel Communications.* Universiti Teknologi Malaysia, Malaysia.

Wachs, I.E. (2005). Recent conceptual advances in the catalysis science of mixed metal oxide catalytic materials. *Catalysis Today*, 100, 79-94.

Wang, S.G., Liao, X.Y., Cao, D.B., Huo, C.F., Li, Y.W., Wang, J.G. & Jiao, H.J. (2007). Factors controlling the interaction of CO_2 with transition metal surfaces. *Journal of Physical Chemistry C,* 111, 16934-16940.

Yamasaki, M., Komori, M. Akiyama, E., Habazaki, H., Kawashima, A., Asami, K. & Hashimoto, K. (1999). CO_2 Methanation Catalysts prepared from Amorphous Ni-Zr-Sm and Ni-Zr Misch Metal Alloy Precursors. *Material Science and Engineering A*, 267, 220-226.

Zeng, H.C., Lim, J. & Tan, K.L. (1995). Memory effect of ZrO_2 matrix on surface Co_3O_4-CO position. *Journal of Material Research,* 10, 3096-3105.

Table 1. Yields from in-situ reactions of CO_2 methanation and H_2S desulfurization over Al_2O_3 supported Pr/ Co/ Ni (5: 35: 60), Fe/ Zn/ Cu (4: 16: 80) and Fe/ Zn/ Cu/ Ti (5: 5: 40: 50) catalysts

Catalyst	**Temperature (^oC)**	**Converted CO_2 (%)**		**Unreacted CO_2 (%)**
		CH_4	**$CO + H_2O$**	
Pr/ Co/ Ni (5: 35: 60)-Al_2O_3	100	0.4	10.7	88.9
	200	0.7	14.1	85.2
	300	6.1	13.1	80.8
Fe/ Zn/ Cu (4: 16: 80)-Al_2O_3	100	0.6	5.9	93.5
	200	0.7	11.3	88.0
	300	1.1	11.6	87.3
Fe/ Zn/ Cu/ Ti (5: 5: 40: 50)-Al_2O_3	100	0.0	0.7	99.3
	200	0.4	6.2	93.4
	300	0.7	7.3	92.0

Table 2. XPS data of Ni (2*p*) and Co (2*p*) for fresh and spent Pr/ Co/ Ni (5: 35: 60)-Al_2O_3 catalysts

Catalyst	**Weight (%)**	**Binding Energy (eV)[a]**		**ΔE_{SO}[b] (eV)**	**Peak Area[c] ($2p_{3/2}$)**	**Peak Assignment**
		$2p_{3/2}$	**$2p_{1/2}$**			
Pr/ Co/ Ni (5:35:60)-Al_2O_3 (fresh)	5.1	854.2	871.7	17.5	167.9	Ni^{2+} in NiO
		856.8	874.3	17.5	115.6	Ni^{3+} in Ni_2O_3
	1.6	779.8	794.0	14.2	127.6	Co_3O_4
Pr/ Co/ Ni (5:35:60)-Al_2O_3 (spent)	7.6	856.8	874.3	17.5	233.3	Ni^{3+} in Ni_2O_3
	1.6	781.7	796.1	14.4	92.9	Co_3O_4

[a] Binding energy, E_b corrected by specific operation charge effect (284.5 eV)

[b] ΔE_{SO} (difference of 2 spin orbit) = $E_b(2p_{1/2})$ - $E_b(2p_{3/2})$

[c] Peak Area = Peak Intensity × FWHM (Full Width Half Maximum)

Table 3. XPS data of Cu (2*p*) and Fe (2*p*) for fresh and spent Fe/ Zn/ Cu (4: 16: 80)-Al_2O_3 catalysts

Catalyst	**Weight (%)**	**Binding Energy (eV)[a]**		**ΔE_{SO}[b] (eV)**	**Peak Area[c] ($2p_{3/2}$)**	**Peak Assignment**
		$2p_{3/2}$	**$2p_{1/2}$**			
Fe/ Zn/ Cu (4:16:80)-Al_2O_3 (fresh)	1.8	933.7	953.6	19.9	21.6	$CuFe_2O_4$ (normal spinel)
	3.6	710.1	723.7	13.6	66.7	$CuFe_2O_4$/ Fe_3O_4 (normal spinel)
Fe/ Zn/ Cu (4:16:80)-Al_2O_3 (spent)	4.2	935.1	954.9	19.8	23.9	$CuFe_2O_4$ (inverse spinel)
	3.4	710.1	723.7	13.6	9.8	$CuFe_2O_4$/ Fe_3O_4 (normal spinel)

[a] Binding energy, E_b corrected by specific operation charge effect (284.5 eV)

[b] ΔE_{SO} (difference of 2 spin orbit) = $E_b(2p_{1/2})$ - $E_b(2p_{3/2})$

[c] Peak Area = Peak Intensity × FWHM (Full Width Half Maximum)

Table 4. XPS data of Cu (2*p*) and Fe (2*p*) for fresh and spent Fe/ Zn/ Cu/ Ti (5: 5: 40: 50)-Al_2O_3 catalysts

Catalyst	**Weight (%)**	**Binding Energy (eV)[a]**		**ΔE_{SO}[b] (eV)**	**Peak Area[c] ($2p_{3/2}$)**	**Peak Assignment**
		$2p_{3/2}$	$2p_{1/2}$			
Fe/ Zn/ Cu/ Ti (5:5:40:50)-Al_2O_3 (fresh)	3.6	933.6	953.5	19.9	247.6	$CuFe_2O_4$ (normal spinel)
	3.8	709.7	723.2	13.5	12.5	$CuFe_2O_4$/ Fe_3O_4 (normal spinel)
		712.4	726.1	13.7	6.4	Fe^{3+}-OH
Fe/ Zn/ Cu/ Ti (5:5:40:50)-Al_2O_3 (spent)	3.7	933.7	953.5	19.9	59.9	$CuFe_2O_4$ (normal spinel)
	2.8	710.5	724.1	13.6	10.0	$CuFe_2O_4$/ Fe_3O_4 (normal spinel)

[a] Binding energy, E_b corrected by specific operation charge effect (284.5 eV)

[b] ΔE_{SO} (difference of 2 spin orbit) = $E_b(2p_{1/2})$ - $E_b(2p_{3/2})$

[c] Peak Area = Peak Intensity × FWHM (Full Width Half Maximum)

Table 5. BET surface area and BJH desorption average pore diameter of the fresh and after in-situ reactions testing catalysts

Al_2O_3 Supported Catalyst	Condition	S_{BET} [a] ($m^2 g^{-1}$)	d [b] (nm)
Pr/ Co/ Ni = 5: 35: 60	Fresh	166.2	5.6
Pr/ Co/ Ni = 5: 35: 60	Spent	180.4	5.9
Fe/ Zn/ Cu = 4: 16: 80	Fresh	184.8	5.1
Fe/ Zn/ Cu = 4: 16: 80	Spent	121.6	7.1
Fe/ Zn/ Cu/ Ti = 5: 5: 40: 50	Fresh	259.2	2.6
Fe/ Zn/ Cu/ Ti = 5: 5: 40: 50	Spent	215.6	3.2

[a] BET surface area

[b] BJH desorption average pore diameter

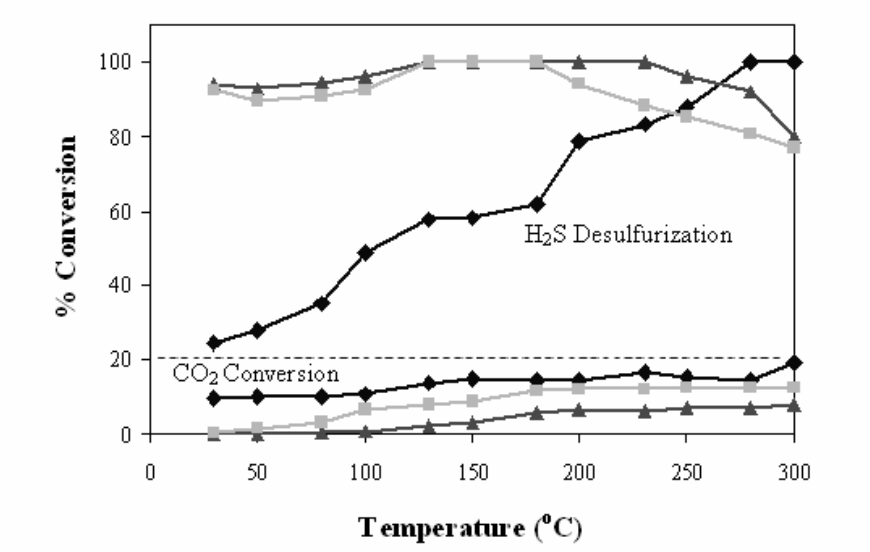

Figure 1. Percentage conversion of CO_2 and H_2S versus reaction temperature under in-situ reactions of CO_2 methanation and H_2S desulfurization over (♦) Pr/ Co/ Ni (5: 35: 60)-Al_2O_3; (■) Fe/ Zn/ Cu (4: 16: 80)-Al_2O_3; (▲) Fe/ Zn/ Cu/ Ti (5: 5: 40: 50)-Al_2O_3 catalysts.

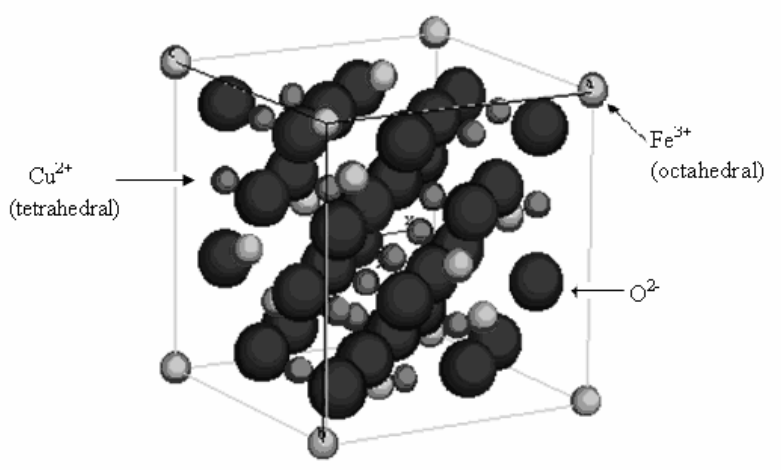

Figure 2. An illustration diagram of normal spinel compound of $CuFe_2O_4$.

Modern Applied Science

www.ccsenet.org/journal.html

Vol. 2, No. 3

May 2008

A Study on the Relationship between RPE and Bogy Enginery Evaluation Index

Wen Du

Physical Education Teaching Section, Inner Mongolia Medical College, Huhhot 010059, China

E-mail: du_wen2007@126.com

Abstract

The "rating of perceived exertion (RPE)" is a simple and effective index to evaluate sports intensity between physiology and psychology, which is being studied and applied in many European and American countries at present. The deep research of this index has great significance promoting competitive sports and nationwide body-building.

Keywords: Rating of perceived exertion (RPE), Cardiovascular, Incretion, Blood lactic acid

1. RPE and its meanings

RPE is a sort of simple and effective medical supervision method to evaluate sports intensity, which is researched and applied in many European and American countries at present. RPE is the index between physiology and psychology. In 1962, Borg firstly put forward the 21 points table measuring the perceived exertion (Borg, G., 1962, p.1-63), and in 1970, he further introduced the 15 points table to open out the change of sports function about body sports intensity. For example, the table was used to measure the RPE of healthy adults and trainers, and the result showed that on which degree the physiological index had pertinence with the psychological index. Afterward, that result was abroad applied in those swimming and running patients (Borg, G., 1970, p.4548-57 & 1970, p.92-8 & 1970, p.17-26). In fact, the appearance of RPE is psychological, but it reflects the change of physiological enginery. That is the reason why European and American physiologists simultaneously measured and comprehensively analyze the RPE index and the change of physiological index. The basic concept of RPE rating comes from human feeling of subjective physical force, because human possess the strong ability to perceive energy consumption, i.e. perceiving exertion. This sort of perceiving exertion offers a sort of basic information to human, i.e. the human endurance degree to certain sports intensity or the pain degree human subjectively feels. In actual living or sports practice, proper physiological intensity stimulation will be a sort of active feeling if it is a sort of amused experience though sometimes the intensity is little large. Therefore, psychologist, sports psychologist and medical staff have so many enthusiasms to study the relation between enginery perceiving degree and intensity load, and the enginery level of athlete or diseased symptom. Based on above cognitions, many people thought this sort of subjective feeling should be changed to the index with actual meanings, and it was very important to adopt a sort of method to quantize it, and this method could be used by most people and without influences of sex, age and race. Based on this concept, Borg firstly put forward "RPE".

The modern sports training theory thinks that the sport is the comprehensive representation of bogy ability and psychological ability, which is completely different with the view that thought the body sport is irrespective with psychological factor early. At present, people thought the body sport is not the physical sport all along, because the stress status when the body exercises contains psychological factors. It can induce enthusiasms and competitive consciousness to mobilize body potential to adapt present stress under the special condition when certain motivation starts. At that time, various physiological and psychological indexes in the body will change with the change of the intensity. So according to the concept of RPE put forward by Borg, we can find out the quantitive relation between RPE and concrete physiological and psychological indexes (Kurokawa, 1992, p.277-88).

2. Borg's RPE grade table and its meanings

The intention that Borg established RPE is to take the value of RPE as a sort of simple tool to evaluate and regulate sports intensity in human physical exercise. The measurement division of RPE includes all perceived exertion range from the lightest exertion to the most intense exertion and organically combines the physiological index. The Borg's RPE intensity includes that 6 represents easy at all, 7-8 represents extremely easy, 9 represents very easy, 10-12 represents easy, 12-14 represents little difficult, 15-16 represents difficulty, 17-18 represents very difficult, 19 represents extremely difficult and 20 achieves the maximum of the body. The measurement of 6-20 accords with the intensity of 60-200 times per minute heart rate. He thought that the verbal RPE value in certain intensity sport must linearly

increase with the power of the power bicycle, and this linear relation must not mean the simple process between heart rate and perceived exertion. However, it made the value of RPE possess special actual meanings.

The perceived exertion generally refers to the feeling of a collectivity or complete sports degree. It is a sort of complex feeling which involves various different signals. In these signals, the changes of muscle, joint sport and breath circulation system going with the pains to the sport will make perceived exertion change to the comprehensive physiological and psychological feelings. In sport, we sometimes require the tester try to differentiate the local feeling from working organ with the discomfort in the chest.

Before the RPE index is confirmed, it is very important to understand age differences and individual differences. The sports sort is selected according to these characters. At present, adopted sports sorts include lab power bicycle and electric running platform, and the sport mainly aim at the training, competition and nationwide body-building. When the power bicycle is used, it begins from small intensity such as 10w, 30w or 50w and sustains certain time such as 5 minutes. Then, the power bicycle increases with same w value such as 30w or 50w, and the tester does the sport in another 5 minutes under this intensity, and in this way, until the maximum sports level is achieved, which is equal to 160-180 times per minute (youth and wrinkly) or 130-150 times per minute (the elderly). The sports sorts can change with the testers' differences, the intention of the research or possible clinic symptom. If the sports time is enough long, the increase of heart rate will be stopped, but the tester's perceived exertion will continually increase. Under large intensity sport, the relation between above heart rate with RPE is stable, and generally the proper oxygen sport intensity is approximately in "13" (some persons may feel difficult or hard), and its range is generally in "13-15". To some persons who want to complete several groups of interval training plan or more training intensity, "17" or "19" can be adopted in the training. But it only aims at athletes, and the person who has heart blood vessel disease absolutely adopts this intensity.

3. RPE and the change of body incretion

After training, whether trainer or non-trainer, their body incretion levels will change to different extents. In the periodic sport, the changes of cortisal (C), free testosterone (FT)/cortisal, and total testosterone (TT)/cortisal may be influenced by the sports quantity or sports intensity. For the tester who continually increases sports intensity in short time, whose TT and FT levels reduce obviously and the creatine kenase (CK) ascends obviously. The change of above indexes will follow the decrease of sports ability and the increase of RPE grade. Even once the sport reduces, the TT and FT levels will increase and the CK level will reduce at the same time. Therefore, the indexes of TT, FT and CK may be the useful indexes to regulate excessive training (Hackney, 1989, p.117-27 & Hackney, 1988, p.60-5). Skrinar et al reported the large intensity endurance training which 15 female athletes took part in from 6 weeks to 8 weeks (Skrinar, 1983, p.1239-50). They respectively measured the RPE values before the training, in the training and after the training in the standard running platform experiment. The endurance training could make the center RPE and total RPE reduce, but it had no influences to the local RPE. The research result indicated that the blood lactic acid had pertinence with the local RPE, but the blood catecholamine had pertinence with the central RPE.

4. RPE and the change of blood lactic acid

The changes of the maximum ventilation exchange (VE), the ventilation gas exchange rate (VGER), the convalescence lactate concentration (La) and the RPE level are related with the sports sort. The research result thought that in healthy female group, the age factor would not be the factor which induces the decrease of body sports ability when using corresponding small muscle group to exercise before 60 years old. The reason inducing the decrease of sports ability mainly rests with the surroundings but not the nerve centre (Aminoff, 1996, p.180-5 & Aminoff, 1998, p.109-20). Kang et al observed 7 testers' functions of carbohydrate to RPE when they rode the bicycle from middle intensity to the exhausted intensity, discussed the relation between the hypo-margin intensity sport and RPE in 2 hours. The testers implemented sport in 70% of maximum corresponding oxygen absorption until up to the exhausted intensity. The testers took orally 6% dextrose/saccharose liguor 0. 6kg-1.hr^{-1} per kg avoirdupois, or took orally the artificial complex as the comfort medicine per 20 minutes. In the whole sports process, they measured lag RPE, chest RPE and total RPE per 20 minutes, and measured the oxygen absorption, ventilation exchange, dextrose oxygenation rate, blood dextrose concentration, glycerol and blood lactic acid (Mielke, 2008, p.293-302). The result also indicted that the decrease of blood carbohydrate induced by 70%VO_2max sustainable sport strengthened lag RPE and total RPE, and except for possible useful index such as carbohydrate, other indexes might function to the exhausted perceived exertion. The lag RPE and total RPE after 2 hours middle intensity sport possessed certain value to predict endurance sports ability of hypo-margin intensity. As we know, the training can produce different function to the body sport and emotion status. Though the training levels of trainer and non-trainer are completely different, but under most situations, testers' heart rates and RPE ascend linearly and the change of blood lactic acid accumulation level after training is very obvious. When the change of the heart rate is contrary to the change of RPE, the non-trainer's individual RPE grade is 15, and his heart rate of bicycle sport and running actually achieves 15-20 times per minute. On certain RPE level, the athlete's changes of above indexes have no obvious difference with runners. That indicated the special training can not only

enhance the body sports ability, but enhance athlete's psychological reactive ability.

References

Aminoff, T., Smolander, J. & Korhonen, O. et al. (1996). Physical Work Capacity in Dynamic Exercise with Differing Muscle Masses in Healthy Young and Older Men. *Eur J Appl Physiol Occup Physiol.* No.73(1-2). p.180-5.

Aminoff ,T., Smolander, J. & Korhonen, O., et al. (1998). Prediction of Acceptable Physical Work Loads Based on Responses to Prolonged Arm and Leg Exercise. *Ergonomics.* No.41(1). p.109-20.

Borg, G. & Linderholm H. (1970). Exercise Performance and Perceived Exertion in Patients with Coronary Insufficiency, Arterial Hypertension and Vasoregulatory Asthenia. *Acta Med Scand.* No.187(1-2). p.17-26.

Borg, G. (1970). Perceived Exertion as an Indicator of Somatic Stress. *Scand J Rehabil Med.* No.2(2). p.92-8.

Borg, G. (1962). Physical Performance and Perceived Exert ion. *Lund: Gleerup.* p.1-63.

Borg, G. (1970). Physical Training 3: Perceived Exertion in Physical Work. *Lakartidningen.* No.67(40).p.45, 48-57.

Hackney, AC. (1989). Endurance Training and Testosterone Levels. *Sports Med.* No.8(2). p.117-27.

Hackney, AC., Sinning, WE., & Bruot, BC. (1988). Reproductive Hormonal Profiles of Endurance-trained and Untrained Males. *Med Sci Sports Exerc.* No.20(1). p.60-5.

Kang, J., Robertson, RJ. & Goss, FL., et al. (1996). Effect of Carbohydrate Substrate Availability on Ratings of Perceived Exertion During Prolonged Exercise of Moderate Intensity. *Percept Mot Skills.* No.82(2). p.495-506.

Kurokawa, T. and Ueda, T. (1992). Validity of Ratings of Perceived Exertion as an Index of Exercise Intensity in Swimming Training. *Ann Physiol Anthropol.* No.11(3). p.277-88.

Mielke, M., Housh, TJ. & Malek, MH., et al. (2008). The Development of Rating of Perceived Exertion-based Tests of Physical Working Capacity. *J Strength Cond Res.* No.22(1). p.293-302.

Skrinar, GS., Ingram, SP. & Pandolf, KB. (1983). Effect of Endurance Training on Perceived Exertion and Stress Hormones in Women. *Percept Mot Skills.* No.57(3 Pt 2). p.1239-50.

Modern Applied Science

www.ccsenet.org/journal.html

Vol. 2, No. 3

May 2008

A Repeated Convex Fuzzy Cooperative Game

Zuofeng Gao

Department of Science, Yanshan university

Qin Huangdao 066004, China

Yongbo Yu (Corresponding author)

Department of Science, Yanshan University

Qinhuangdao 066004, China

E-mail: yongbo12345@163.com

Hongxin Bai

Department of Science, Yanshan University

Qinhuangdao 066004, China

Chunyan Han

Department of Science, Yanshan university

Qin Huangdao 066004, China

Supported by the Foundation for the natural science of Hebei province of China (A2005000301)

Abstract

This paper introduces repeated theory on the base of fuzzy cooperative game by Aubin etal in 1974 and then constructs repeated fuzzy games theory. It gives the conception of repeated convex fuzzy cooperative games and studies the property of repeated convex fuzzy games.

Keywords: Fuzzy game, Convex, Repeated cooperative game

1. Introduction

The theory of fuzzy cooperative game had been studying widely and deeply since it was introduced by Aubin(1974, 1981), and Jorge ovido (1999) studied the theory of a repeated cooperative games. In this paper, we combine the two theory and construct a repeated fuzzy cooperative game.

The purpose of this paper is on one hand to present a detailed characterization of repeated convex fuzzy games and on the other hand to study the property of repeated convex fuzzy games.

2. Fuzzy cooperative games and convex fuzzy cooperative games

Let $N=\{1,2\cdots\cdots n\}$ be a nonempty set of players considering possibilities of cooperation. A fuzzy coalition is a vector $S\in[0,1]^N$. The ith coordinate S_i of S is called the participation level of player i in fuzzy coalitions S. For each crisp coalition S, its characteristic vector is e^S, with $(e^S)_i=1$ if $i\in S$; $(e^S)_i=0,$ if $i\in N/S.$

A fuzzy game with player set N is a map $v:\ F^N\to R$ with the property $v(0)=0$,The map V assigns to each fuzzy coalition can achieve in cooperation. The set of fuzzy games with player set N will be denoted by FG^N.

Definition 1: Let $v\in FG^N$.Then v is called a convex fuzzy game if function $v:[0,1]^N\to R$ is a supermodular and coordinate-wise convex function on $[0,1]^N$. (see reference R.Branzei (2003))

3. Repeated fuzzy cooperative games

We repeat m times (m may be ∞) this fuzzy cooperative games, we denote by $([0,1]^N, v_t, t)$ the stage fuzzy cooperative games (N, v) that agents play in period t. The characteristic function of the game $([0,1]^N, v_t, t)$ is defined for all $S \in [0,1]^N$ by $V_t(S) = (1-\delta)\delta^t V(S)$.

We define the repeated fuzzy cooperative game, so that it has the same structure as the fuzzy cooperative game.

Definition 2 Let $S^t \subseteq [0,1]^N$ denote a coalition formed at time t .Let $\theta = (S^0, S^1, \cdots S^t)$ $= (S^t)_0^m \in H$ be a fuzzy coalition sequence, we define the repeated fuzzy characteristic function w as

$$W(\theta) = (1-\delta)\sum_{t=0}^{m} \delta^t V(S^t) \qquad (1)$$

we denote by H the set of all coalition sequences.

Definition3: A tuple(H,w) is repeated fuzzy cooperative games, where H is a fuzzy coalition sequence, w is the repeated fuzzy characteristic function defined by (1) The set of repeated fuzzy games with player set N will be denoted by $(FG_t^N)_{t=0}^m$.

4. Main result

Let $\theta = (S^t)_{t=0}^m \in H$, $\psi = (T^t)_{t=0}^m \in H$ be two coalition sequences such that for all $0 \le t \le m$, $S^t \cap T^t = \phi$, $\theta \cup \psi = (S^t \cup T^t)_{t=0}^m$, $\theta \cap \psi = (S^t \cap T^t)_{t=0}^m$, then

Theorem 1: If $v \in FG^N$ is convex game ,then the repeated fuzzy cooperative w is convex game with satisfies

(i) Supermodular property $w(\theta \cup \psi) + w((\theta \cap \psi) = w(\theta) + w(\psi)$ (2)

(ii) Coordinate-wise function Let $w(S^{-i}\|z) = f_{s^{-i}}(z)$ for each $i \in N$ .The t-stage game function

$f_{s^{-i}}^t : [0,1]^N \to R$ with $f_{s^{-i}}^t(z) = v(s^{-i}t\|z)$ be a convex function and continue in $[0,1]$. (3)

Proof: See reference Gao Zuo-feng (2006).

The next lemma for repeated convex fuzzy game is related with the increasing marginal contribution property for players. It states that a level increase of a player in a repeated fuzzy coalition sequence has more beneficial effect in a larger coalition than in a small coalition sequences. For $\theta = (S^t)_{t=0}^m \in H$, $\psi = (T^t)_{t=0}^m \in H$, we use the notation $S^t \le T^t$ *iff* $S_i^t \le T_i^t$ for each $i \in N$.

Lemma: Let $w \in (FG_t^N)_{t=0}^m$ be a repeated convex fuzzy cooperative games. Let $i \in N$ $\theta, \psi \in H$ with $\theta \le \psi$ and let $\varepsilon^t \in R_+$, $t = 0,1 \cdots m$ with $0 \le \varepsilon^t \le 1 - T^t$ Then

$$w(\theta + X_{t=0}^m \varepsilon^t e^i) - w(\theta) \le w(\psi + X_{t=0}^m \varepsilon^t e^i) - w(\psi) \qquad (4)$$

Proof: Suppose $N = \{1,2 \cdots n\}$, Define the fuzzy coalition sequence of t-stage games $P_0^t, P_1^t, \cdots P_n^t$ by $P_0^t = S^t$ and $P_k^t = P_{k-1}^t + (S_k^t - T_k^t)e^k$ for $k = \{1,2, \cdots n\}$.Then $P_n^t = T^t$ .To prove (4) it is sufficient to show that for each $k = \{1,2, \cdots n\}$ the inequality (I^k) holds

$$v(P_k^t + X_{t=0}^m \varepsilon^t e^i) - v(P_k^t) \ge v(P_{k-1}^t + X_{t=0}^m \varepsilon^t e^i) - v(P_{k-1}^t) \qquad (I^k)$$

Note that (I^k) follows from coordinate-wise convexity of w and (I^k) for $(k \ne i)$,from the supermodularity property with $P_{k-1}^t + \varepsilon^t e^t$ in the role of S^t and P_k^t in the role of T^t ,Then $S^t \cup T^t = P_k^t + \varepsilon^t e^i$, $S^t \cap T^t = P_{k-1}^t$,

$$w(\theta + X_{t=0}^m \varepsilon^t e^i) - w(\theta)) = (1-\delta)\sum_{t=0}^{m} \delta^t \left[v(S^t + \varepsilon^t e^i) - v(S^t)\right] = (1-\delta)\sum_{t=0}^{m} \delta^t \left[v(P_0^t + \varepsilon^t e^i) - v(P_0^t)\right]$$

$$\le (1-\delta)\sum_{t=0}^{m} \delta^t \left[v(P_1^t + \varepsilon^t e^i) - v(P_1^t)\right] \le \cdots \le (1-\delta)\sum_{t=0}^{m} \delta^t \left[v(P_n^t + \varepsilon^t e^i) - v(P_n^t)\right]$$

$$= (1-\delta)\sum_{t=0}^{m} \delta^t \left[v(T^t + \varepsilon^t e^i) - v(T^t)\right]$$

$$= w(\psi + X_{t=0}^m \varepsilon^t e^i) - w(\psi) \quad .$$

The next theory introduces a characterizing property for repeated convex fuzzy games. Similar to fuzzy game, we also call the increasing average marginal return property (IAMR-Property).

Theorem 2: Let $w \in (FG_t^N)_{t=0}^m$ be a repeated convex fuzzy game, let $i \in N, \theta, \psi \in H,$ with $\theta \le \psi$ and let

$S_i^t + \varepsilon_1^t \le T_i^t + \varepsilon_2^t \le 1$ then

$$\frac{1}{\sum_{t=0}^{m} \varepsilon_1^t}\left[w(\theta + X_{t=0}^{m}\varepsilon_1^t e^i) - w(\theta)\right] \le \frac{1}{\sum_{t=0}^{m} \varepsilon_2^t}\left[w(\psi + X_{t=0}^{m}\varepsilon_2^t e^i) - w(\psi)\right]$$

Proof: From Lemma (with S^t, $T^t + (S_i^t - T_i^t)e^i$ and ε_1^t in the roles of S^t T^t *and* ε respectively) It follows that

$$\frac{1}{\sum_{t=0}^{m} \varepsilon_1^t}\left[w(\psi + X_{t=0}^{m}(S_i^t - T_i^t + \varepsilon_1^t)e^i - w(\psi + X_{t=0}^{m}(S_i^t - T_i^t)e^i\right] \ge \frac{1}{\sum_{t=0}^{m} \varepsilon_1^t}\left[w(\theta + X_{t=0}^{m}\varepsilon_1^t e^i) - w(\theta)\right]$$

Further, from the coordinate-wise convexity (by noting $T_i^t + (S_i^t - T_i^t + \varepsilon_1^t) \le T_i^t + \varepsilon_2^t$ $T_i^t + (S_i^t - T_i^t) \le T_i^t$) it follows that

$$\frac{1}{\sum_{t=0}^{m} \varepsilon_2^t}\left[w(\psi + X_{t=0}^{m}\varepsilon_2^t e^i) - w(\psi)\right] \ge \frac{1}{\sum_{t=0}^{m} \varepsilon_1^t}\left[w(\psi + X_{t=0}^{m}(S_i^t - T_i^t + \varepsilon_1^t)e^i - w(\psi + X_{t=0}^{m}(S_i^t - T_i^t)e^i\right]$$

$$\ge \frac{1}{\sum_{t=0}^{m} \varepsilon_1^t}(w(\theta + X_{t=0}^{m}\varepsilon_1^t e^i) - w(\theta))$$,resulting in the desired inequality.

Theorem 3： If $w \in (FG_t^{N})_{t=0}^{m}$. Then the following assertions are equivalent:

(i) w is a convex games

(ii) w satisfies the increasing average marginal return property of repeated fuzzy cooperative games.

Proof: We know from theorem that convex game satisfies IAMR-property. On the other hand, it is clear that IAMR-property implies the coordinate-wise convexity property. Hence, we only have to prove that the IAMR-property implies the supermodularity property. So given $\theta = (S^t)_{t=0}^{m} \in H$ $\psi = (T^t)_{t=0}^{m} \in H$,we only prove the supermodularity inequality (2) holds.

Let $P^t = \left\{i \in N \middle| T_i^t < S_i^t\right\}$. If $P^t = \phi,$ then (2) follows from the fact that $S^t \cup T^t = T^t,$ $S^t \cap T^t = S^t$. For $P^t \ne \phi,$ arrange the elements of P^t in t-stage as a sequence $\sigma_t(1), \sigma_t(2), \cdots,$ $\sigma_t(P^t),$ where $P^t = \left|P^t\right|$,and put $\varepsilon_{\sigma_t(k)}^t = S_{\sigma_t(k)}^t - T_{\sigma_t(k)}^t > 0$ for $k \in \left\{1,2\cdots P^t\right\}$. Note that in this case $S^t = S^t \cap T^t + \sum_{k=1}^{P^t} \varepsilon_{\sigma_t(k)}^t e^{\sigma_t(k)}$, $S^t \cup T^t = T^t + \sum_{k=1}^{P^t} \varepsilon_{\sigma_t(k)}^t e^{\sigma_t(k)}$

Hence,

$$w(\theta) - w(\theta \cap \psi) = \sum_{r=1}^{P^t}\left[w(\theta \cap \psi + \sum_{k=1}^{r} X_{t=0}^{m}\varepsilon_{\sigma_t(k)}^t e^{\sigma_t(k)}) - w(\theta \cap \psi + \sum_{k=1}^{r-1} X_{t=0}^{m}\varepsilon_{\sigma_t(k)}^t e^{\sigma_t(k)})\right]$$

$$w(\theta \cup \psi) - w(\psi) = \sum_{r=1}^{P^t}\left[w(\psi + \sum_{k=1}^{r} X_{t=0}^{m}\varepsilon_{\sigma_t(k)}^t e^{\sigma_t(k)}) - w(\psi + \sum_{k=1}^{r-1} X_{t=0}^{m}\varepsilon_{\sigma_t(k)}^t e^{\sigma_t(k)})\right]$$

From these equalities the supermodularity inequality (2) follows because the IAMR-property implies for each $r \in \left\{1,2\cdots P^t\right\}$:

$$w(\theta \cap \psi + \sum_{k=1}^{r} X_{t=0}^{m}\varepsilon_{\sigma_t(k)}^t e^{\sigma_t(k)}) - w(\theta \cap \psi + \sum_{k=1}^{r-1} X_{t=0}^{m}\varepsilon_{\sigma_t(k)}^t e^{\sigma_t(k)}) \le w(\psi + \sum_{k=1}^{r} X_{t=0}^{m}\varepsilon_{\sigma_t(k)}^t e^{\sigma_t(k)}) - w(\psi + \sum_{k=1}^{r-1} X_{t=0}^{m}\varepsilon_{\sigma_t(k)}^t e^{\sigma_t(k)}).$$

References

Gao, Zuo feng. et al. (2006). The cores and the stable for repeated fuzzy cooperative game. *Operations and research and management science*. 2006, 15(4); 68-72.

J. P. Aubin. (1981). Cooperative fuzzy games. *Mathematics of Operations Research*.1981, (6): 1-13.

Jorge Oviedo. (2000). The core of a repeated n-person cooperative game, *European Journal of Operational Research* 127, 2000, 519-524.

R.Branzei, D. Dimitrov, S. Tijs. (2003). Convex fuzzy games and participation monotonic allocation. schemes Center DP2002-13. Tilburg University. The Netherlands. 2002, *Fuzzy Sets and Systems* 139(2003) 267-281.

Xie, Z. (2004). *Game Theory*. ChangSha: National University of Defense Technology Press.

Modern Applied Science

www.ccsenet.org/journal.html

Vol. 2, No. 3

May 2008

Logic Learning in Hopfield Networks

Saratha Sathasivam

School of Mathematical Sciences, University of Science Malaysia

Penang, Malaysia

E-mail: saratha@cs.usm.my

Wan Ahmad Tajuddin Wan Abdullah

Department of Physics, Universiti Malaya

50603 Kuala Lumpur, Malaysia

E-mail: wat@um.edu.my

The research is partly financed by an FRGS grant from the Ministry of Higher Education, Malaysia.

Abstract

Synaptic weights for neurons in logic programming can be calculated either by using Hebbian learning or by Wan Abdullah's method. In other words, Hebbian learning for governing events corresponding to some respective program clauses is equivalent with learning using Wan Abdullah's method for the same respective program clauses. In this paper we will evaluate experimentally the equivalence between these two types of learning through computer simulations.

Keywords: Logic programming, Hebbian learning, Wan Abdullah's method, Program clauses

1. Introduction

Recurrent neural networks are essentially dynamical systems that feed back signals to themselves. Popularized by John Hopfield, these models possess a rich class of dynamics characterized by the existence of several stable states each with its own basin of attraction. The (Little-)Hopfield neural network [Little (1974), Hopfield (1982)] minimizes a Lyapunov function, also known as the energy function due to obvious similarities with a physical spin network. Thus, it is useful as a content addressable memory or an analog computer for solving combinatorial-type optimization problems because it always evolves in the direction that leads to lower network energy. This implies that if a combinatorial optimization problem can be formulated as minimizing the network energy, then the network can be used to find optimal (or suboptimal) solutions by letting the network evolve freely.

Wan Abdullah (1991,1992) and Pinkas (1991) independantly defined bi-directional mappings between propositional logic formulas and energy functions of symmetric neural networks. Both methods are applicable in finding whether the solutions obtained are models for a corresponding logic program.

Subsequently Wan Abdullah (1991, 1993) has shown on see how Hebbian learning in an environment with some underlying logical rules governing events is equivalent to hardwiring the network with these rules. In this paper, we will experimentally carry out computer simulations to support this.

This paper is organized as follows. In section 2, we give an outline of doing logic programming on a Hopfield network and in section 3, Hebbian learning of logical clauses is described. In section 4, we describe the proposed approach for comparing connection strengths obtained by Wan Abdullah's method and Hebbian learning. Section 5 contains discussions regarding the results obtained from computer simulations. Finally concluding remarks regarding this work occupy the last section.

2. Logic Programming on a Hopfield network

In order to keep this paper self-contained we briefly review the Hopfield model (extensive treatments can be found elsewhere [Geszti (1990), Haykin (1994)]), and how logic programming can be carried out on such architecture. The Hopfield model is a standard model for associative memory. The Hopfield dynamics is asynchronous, with each neuron updating its state deterministically. The system consists of *N* formal neurons, each of which can be described by Ising variables $S_i(t), (i = 1,2,....N)$. Neurons then are bipolar, $S_i \in \{-1,1\}$, obeying the dynamics $S_i \to \mathrm{sgn}(h_i)$, where the

field, $h_i = \sum_j J_{ij}^{(2)} S_j + J_i^{(1)}$, i and j running over all neurons N, $J_{ij}^{(2)}$ is the synaptic or connectio strength from neuron j to neuron i, and $-J_i^{(1)}$ is the threshold of neuron i.

Restricting the connections to be symmetric and zero-diagonal, $J_{ij}^{(2)} = J_{ji}^{(2)}$, $J_{ii}^{(2)} = 0$, allows one to write a Lyapunov or energy function,

$$E = -\frac{1}{2}\sum_i \sum_j J_{ij}^{(2)} S_i S_j - \sum_i J_i^{(1)} S_i \tag{1}$$

which decreases monotonically with the dynamics.

The two-connection model can be generalized to include higher order connections. This modifies the "field" into

$$h_i = ... + \sum_j \sum_k J_{ijk}^{(3)} S_j S_k + \sum_j J_{ij}^{(2)} S_j + J_i^{(1)} \tag{2}$$

where "….." denotes still higher orders, and an energy function can be written as follows:

$$E = ... - \frac{1}{3}\sum_i \sum_j \sum_k J_{ijk}^{(3)} S_i S_j S_k - \frac{1}{2}\sum_i \sum_j J_{ij}^{(2)} S_i S_j - \sum_i J_i^{(1)} S_i \tag{3}$$

provided that $J_{ijk}^{(3)} = J_{[ijk]}^{(3)}$ for *i, j, k* distinct, with […] denoting permutations in cyclic order, and $J_{ijk}^{(3)} = 0$ for any *i, j, k* equal, and that similar symmetry requirements are satisfied for higher order connections. The updating rule maintains

$$S_i(t+1) = \mathrm{sgn}[h_i(t)] \tag{4}$$

In logic programming, a set of Horn clauses which are logic clauses of the form $A \leftarrow B_1, B_2, ..., B_n$ where the arrow may be read "if" and the commas "and", is given and the aim is to find the set(s) of interpretation (i.e., truth values for the atoms in the clauses which satisfy the clauses (which yields all the clauses true). In other words, we want to find 'models' corresponding to the given logic program.

In principle logic programming can be seen as a problem in combinatorial optimization, which may therefore be carried out on a Hopfield neural network. This is done by using the neurons to store the truth values of the atoms and writing a cost function which is minimized when all the clauses are satisfied.

As an example, consider the following logic program,

$A \leftarrow B, C.$.

$D \leftarrow B.$

$C \leftarrow .$

whose three clauses translate respectively as $A \vee \neg B \vee \neg C$, $D \vee \neg B$ and C. The underlying task of the program is to look for interpretations of the atoms, in this case *A, B, C* and *D* which make up the model for the given logic program. This can be seen as a combinatorial optimization problem where the "inconsistency",

$$E_P = \tfrac{1}{2}(1 - S_A)\tfrac{1}{2}(1 + S_B)\tfrac{1}{2}(1 + S_C) + \tfrac{1}{2}(1 - S_D)\tfrac{1}{2}(1 + S_B) \qquad + \tfrac{1}{2}(1 - S_C) \tag{5}$$

Where S_A, etc. represent the truth values (*true* as 1) of *A*, etc., is chosen as the cost function to be minimized, as was done by Wan Abdullah. We can observe that the minimum value for E_P is 0, and has otherwise value proportional to the number of unsatisfied clauses. The cost function (5), when programmed onto a third order neural network yields synaptic strengths as given in Table 1. We address this method of doing logic programming in neural networks as *Wan Abdullah's method*.

3. Hebbian Learning of Logical Clauses

The Hebbian learning rule for a two-neuron synaptic connection can be written as

$$\Delta J_{ij}^{(2)} = \lambda_2 S_i S_j \tag{6}$$

where λ_2 is a learning rate. For connections of other orders *n*, between *n* neurons $\{S_i, S_j, ..., S_m\}$, we can generalize this to

$$\Delta J_{ij....m}^{(n)} = \lambda_n S_i S_j ....S_m \tag{7}$$

This gives the changes in synaptic strengths depending on the activities of the neurons. In an environment where selective events occur, Hebbian learning will reflect the occurrences of the events. So, if the frequency of the events is dictated by some underlying logical rule, logic should be entrenched in the synaptic weights.

Wan Abdullah (1991, 1993) has shown that Hebbian learning as above corresponds to hardwiring the neural network with synaptic strengths obtained using Wan Abdullah's method, provided that the following is true:

$$\lambda_n = \frac{1}{(n-1)!} \tag{8}$$

We do not provide a detailed analysis regarding Hebbian learning of logical clauses in this paper, but instead refer the interested reader to Wan Abdullah's papers.

4. Comparing Connection Strengths Obtained By Hebbian Learning With Those By Wan Abdullah's Method

In the previous section, we have elaborated how synaptic weights for neurons can be equivalently calculated either by using Hebbian learning or by Wan Abdullah's method. Theoretically, information (synaptic strengths) produced by both methods are similar. However, due to interference effects and redundancies, synaptic strengths could be different [Sathasivam (2006)], but the set of solutions for both cases should remain the same. Due to this, we cannot use direct comparison of obtained synaptic strengths. Instead, we carry out computer simulation of artificially generated logic programs and compare final states of the resulting neural networks.

To obtain the logic-programmed Hopfield network based on Wan Abdullah's method, the following algorithm is carried out:

i) Given a logic program, translate all the clauses in the logic program into basic Boolean algebraic form.

ii) Identify a neuron to each ground neuron.

iii) Initialize all connections strengths to zero.

iv) Derive a cost function that is associated with the negation of the conjuction of all the clauses, such that $\frac{1}{2}(1+S_x)$ represents the logical value of a neuron *X*, where S_x is the neuron corresponding to logical atom *X*. The value of S_x is defined in such a way that it carries the values of 1 if *X* is true and -1 if *X* is false. Negation (*X* does not occur) is represented by $\frac{1}{2}(1-S_x)$; a conjunction logical connective is represented by multiplication whereas a disjunction connective is represented by addition.

v) Obtain the values of connection strengths by comparing the cost function with the energy.

vi)Let the neural network programmed with these connection strengths evolve until minimum energy is reached. Check whether the solution obtained is a global solution (the interpretation obtained is a model for the given logic program).

We run the relaxation for 1000 trials and 100 combinations of neurons so as to reduce statistical error. The selected tolerance value is 0.001. All these values are obtained by try and error technique, where we tried several values as tolerance values, and selected the value which gives better performance than other values. To compare the information obtain in the synaptic strength, we make comparison between the stable states (states in which no neuron changes its value anymore) obtained by Wan Abdullah's method with stable states obtained by Hebbian learning. The way we calculated the percentage of solutions reaching the global solutions is by comparing the energy for the stable states obtained by using Hebbian learning and Wan Abdullah's method. If the corresponding energy for both learning is same, then we conclude that the stable states for both learning are the same. This indicates, the model (set of interpretations) obtained for both learning are similar. In all this, we assume that the global solutions for both networks are the same due to both methods considering the same knowledge base (clauses).

5. Results and Discussion

Figures 1 - 6 illustrate the graphs for global minima ratio (ratio= (Number of global solutions)/ (Number of solutions=number of runs)) and Hamming distances from computer simulation that we have carried out. From the graphs obtained, we observed that the ratio of global solutions is consistently 1 for all the cases, although we increased the network complexity by increasing the number of neurons (NN) and number of literals per clause (NC1, NC2, NC3). Due to we are getting similar results for all the trials, to avoid graphs overlapping, we only presented the result obtained for the number of neurons (NN) = 40. Besides that, error bar for some of the cases could not be plotted because the size of the point is bigger than the error bar. This indicates that the statistical error for the corresponding point is so small. So, we couldn't plot the error bar.

Most of the neurons which are not involved in the clauses generated will be in the global states. The random generated program clause relaxed to the final states, which seem also to be stable states, in less than five runs. Furthermore, the

network never gets stuck in any suboptimal solutions. This indicates good solutions (global states) can be found in linear time or less with less complexity.

Since all the solutions we obtained are global solution, so the distance between the stable states and the attractors are zero. Supporting this, we obtained zero values for Hamming distance. This indicates the stable states for both learning are the same. Therefore they are no different in the energy value. So, models for both learning are proved to be similar. Although the way of calculating synaptic weights are different, since the calculations revolve around the same knowledge base (clauses), the set of interpretations will be similar. This implies that, Hebbian learning could extract the underlying logical rules in a given set of events and provide good solutions as well as Wan Abdullah's method. The computer simulation results support this hypothesis.

6. Conclusion

In this paper, we had evaluated experimentally the logical equivalent between these two types of learning (Wan Abdullah's method and Hebbian learning) for the same respective clauses (same underlying logical rules) using computer simulation. The results support Wan Abdullah's earlier proposed theory.

References

Geszti, T. (1990). *Physical Models of Neural Networks.* Singapore: World Scientific Publication.

Haykin, S. (1994). *Neural Network: A Comprehensive Foundation*. New York: Macmillan.

Hopfield, J. J. (1982). Neural Networks and Physical Systems with Emergent Collective Computational abilities. *Proc. Natl. Acad. Sci. USA,* 79, 2554-2558.

Little, W. A. (1974). The existence of persistent states in the brain. *Math. Biosci*., 19, 101-120.

Pinkas, G. (1991). Energy minimization and the satisfiability of propositional calculus. *Neural Computation,* 3, 282-291.

Sathasivam, S. (2006). Logic Mining in Neural Networks. PhD Thesis. University of Malaya, Malaysia.

Wan Abdullah, W. A. T. (1991). Neural Network logic. In O. Benhar et al. (Eds.), *Neural Networks: From Biology to High Energy Physics*. Pisa: ETS Editrice. pp. 135-142.

Wan Abdullah, W. A. T. (1992). Logic programming on a neural network. *Int. J. Intelligent Sys*., 7, 513-519.

Wan Abdullah, W. A. T. (1993). The logic of neural networks. *Phys. Lett.*,176A, 202-206.

Table 1. Synaptic strengths for $A \leftarrow B, C.$ & $D \leftarrow B$ & $C \leftarrow$ using Wan Abdullah's method

Synaptic Strengths	Clause			Total
	$A \leftarrow B, C.$	$D \leftarrow B.$	$C \leftarrow .$	
$J^{(3)}_{[ABC]}$	1/16	0	0	1/16
$J^{(3)}_{[ABD]}$	0	0	0	0
$J^{(3)}_{[ACD]}$	0	0	0	0
$J^{(3)}_{[BCD]}$	0	0	0	0
$J^{(2)}_{[AB]}$	1/8	0	0	1/8
$J^{(2)}_{[AC]}$	1/8	0	0	1/8
$J^{(2)}_{[AD]}$	0	0	0	0
$J^{(2)}_{[BC]}$	-1/8	0	0	-1/8
$J^{(2)}_{[BD]}$	0	1/4	0	¼
$J^{(2)}_{[CD]}$	0	0	0	0
$J^{(1)}_{[A]}$	1/8	0	0	1/8
$J^{(1)}_{[B]}$	-1/8	-¼	0	-3/8
$J^{(1)}_{[C]}$	-1/8	0	1/2	3/8
$J^{(1)}_{[D]}$	0	1/4	0	¼

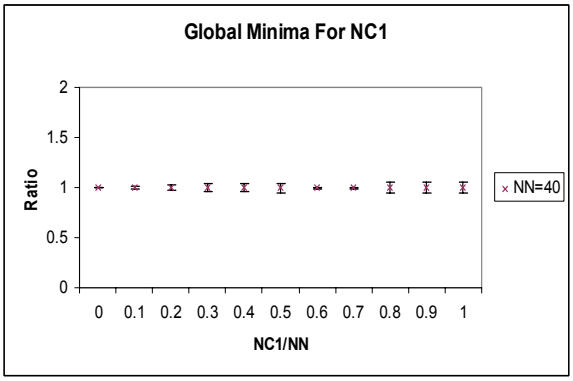

Figure 1. Global Minima Ratio for NC1

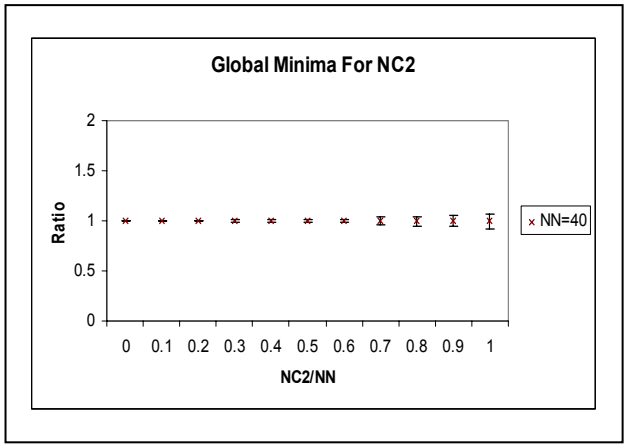

Figure 2. Global Minima Ratio for NC2

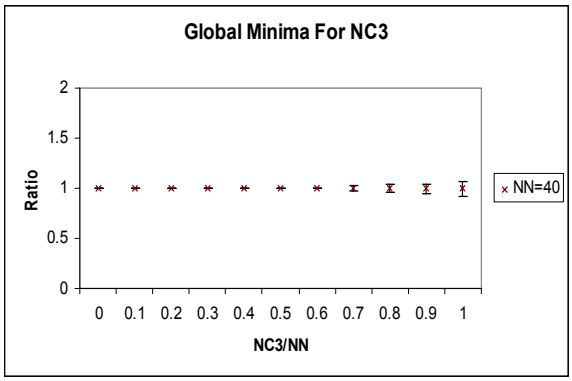

Figure 3. Global Minima Ratio for NC3

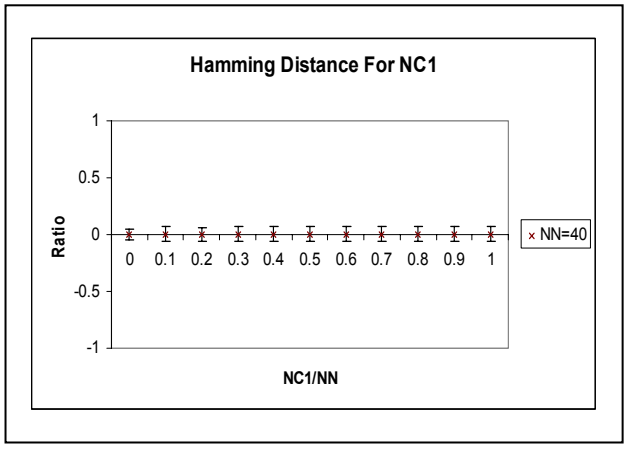

Figure 4. Hamming Distance for NC1

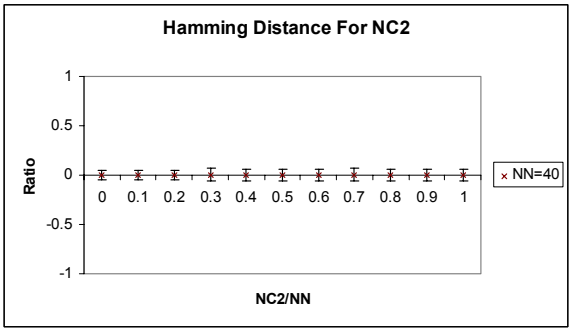

Figure 5. Hamming Distance for NC2

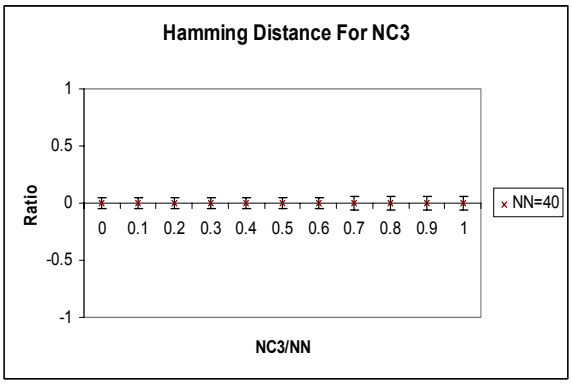

Figure 6. Hamming Distance for NC3

Modern Applied Science

www.ccsenet.org/journal.html

Vol. 2, No. 3

May 2008

Alteration of Iron Metabolism of Elite Female Distance Runners in Intensity Training

Bayar Tsinggel

Physical Education Department, Inner Mongolia Agricultural University

Hohhot 010018, China

E-mail: bayar@126.com

Bao Dagula

Physical Education Department, Inner Mongolia Nationality College

Hohhot 010051, China

Abstract

The hemoglobin (Hb), serum Iron (SI), serum ferritin, serum transferrin (Tr), serum transferrin receptor (sTfR) concentration, Erythrocyte hemoglobin distribution width(RDW) and erythropoietin(EPO) in adults are suggested to provide a sensitive measure of iron depletion and the serum ferritin (Ferr) concentration is able to indicate the entire range of iron status, from iron deficiency to iron overload. However, little is known about those indexes in elite female distant runners. The objective of this study was to determine the above indexes in intensity training of 8 elite female distant runners two months ahead of national competition. Result showed that Hb concentration decreased in second sampling point and then recovered; SI concentration firstly decreased then increased, but it was not significant; Tr concentration, RDW and EPO level increased in second sampling point then fell to baseline; there was no significant difference in Ferr and sTfR concentration. It can be concluded that due to intensity training, iron metabolism in the initial stage of training was disturbed and then modulated in following training phase.

Keywords: Hemoglobin, Transferrin, Transferrin receptor, Iron metabolism, Erythropoietin

1. Introduction

The concentration of hemoglobin is of great significance for intensity training, and for the specialized quality of endurance athletes. The concentration of athletes' hemoglobin is influenced by nutrition, sport load and rest during training and competition. The iron metabolism influences the synthesis of hemoglobin; athletes need more iron than the ordinary person, and iron requirement changes with the training time, intensity and environmental factors (Feng, 2003, P.56-64). Much training will accelerate the iron metabolism and influence the iron balance of body. It is easy for athletes to get sport anemia, accordingly, athletes' competitive ability will be influenced. The main reason for sport anemia is the low synthesis of hemoglobin because of iron deficiency. In this paper, we studied the indexes relating to iron metabolism of elite female distance runners, with the purpose of finding out the changing rule of these indexes and providing evidence for the evaluation and training control of athletes.

2. Materials and methods

2.1 Research object

Study on the indexes of eight female middle-distance runners in intensity training two months before competition. Sampling was carried out in the morning of adjusting day, and athletes were not in menses. The age of athlete is 23.5±2.3 year, the stature is 166.2±5.8 cm, the weight is 54.8±8.9 kg, the training life is 6.7±1.8 year, and percentage body fat is 15.2±5.5%.

2.2 Methods

2.2.1 Training plan

Training cycle was one week, specifically, large intensity training on Monday, mixed aerobic training on Tuesday and Wednesday, aerobic training on Thursday, large intensity training on Friday and aerobic training on Saturday and Sunday. Large intensity training would be agilely arranged in the aspects of distance and rest; the plan would be changed according to the situation of athletes.

2.2.2 Sampling and preservation

Blood sample was taken every two weeks, totally four times. At 7:00-7:30, athletes were hollow, 1mL whole blood was taken with EDTA, and 4mL whole blood was taken with general vacuum tube, the blood with EDTA was used in blood count right away, the other tube of blood will be placed for 30 minutes, two tubes of blood were centrifuged at 3000 rpm for 20 minutes, the serum was isolated and stored at -20 centigrade for the following experiment.

2.2.3 The test of indexes

Blood counting instrument (Sysmex KX-2IN, Japan) was used to test blood routine; reagent kit for determining serum iron from Beijing Zhongsheng Biotech Engineering Corporation was used, wavelength was 540nm, temperature was 37 centigrade, and reaction was automatically finished with AG II System biochemical analyzer (Landmark Scientific Inc. Greensboro, North Carolina USA); method of radioimmunoassay was used to test the serum iron, antigen was labeled with $^{[125]}$I and the antigen that would be tested can competitively interact with specific antibody, which is the principle of serum iron test. Serum ferritin RIA kit was provided by Beijing North Institute of Biological Technology, reaction was done at 37 centigrade for 1 hour, the coefficient of variation within a single assay and between assays were 6.0% and 12% respectively. The impulse number of compound was counted on SN-6958 gamma counter (Shanghai Institute of A-energy). ELISA (Enzyme Linked Inmunosorbent Assay, ELISA) was used to detect the concentration of serum transferrin (Tr), serum transferrin receptor (sTfR). The antigen or antibody was solidified and labeled by enzyme, when the substrate of enzyme was added, the substrate would be catalyzed by enzyme as colored product, and the amount of product would have direct relationship with the target. The serum transferrin kit was provided by Bethyl Company (Bethyl Laboratory, Inc), the coefficient of variation within a single assay was less than 7%, and the coefficient of variation between assays was less than 10%. Serum transferrin receptor kit was provided by R&D Company (R&d Systems, Inc), the coefficient of variation within a single assay was less than 5%, and the coefficient of variation between assays was less than 12%. RT-6000 enzyme-labeled instrument (Rayto Life and Analytical Sciences Co., Ltd. USA) and RT-3000 well wash were used, OD value was got according to the manufacturer's protocols and automatically printed; Chemiluminescent Method was used to determine the erythropoietin, kit was provided by Tianjin Data Processing Center (DPC), Immulite 1000 (DPC, Tianjin Co., Ltd.) was used, the coefficient of variation within a single assay was less than 5%, and the coefficient of variation between assays was less than 9%.

2.2.4 Data analysis

K-S method was used to determine if various indexes of serum fit the normal distribution, if so, single element repeated measurement variance analysis was used to make a 1×4 treatment. Mauchly's test of sphericity was done firstly, if the hypothesis is right, univariate variance analysis will be used to analyze the result, on the contrary, univariate variance analysis was used to correct the result. If the data don't fit the normal distribution, Friedman test was used to compare the difference between assays. Data were represented as average ± standard value, significance level $P<0.05$, great significance level $P<0.01$.

3. Results

3.1 Content variation of red blood cell, hemoglobin, pressure and volume of blood cell, Erythrocyte hemoglobin distribution width (RDW), serum iron and serum ferritin.

As shown in table 1 that, the red blood cell, pressure and volume of blood cell, serum iron and serum ferritin didn't change much, the content of hemoglobin decreased 20 days after training ($P<0.05$), and when 40 days and 60 days after training, the content of hemoglobin increased compared with that 20 days after training ($P<0.05$), but changed little compared with the situation before training ($P>0.05$). RDW 20 days after training was higher than that before training ($P<0.05$), and RDW 40 days and 60 days after training was much lower than that 20 days after training($P<0.05$).

3.2 The variation of athletes' serum transferrin

Repeated measurements variance analysis revealed that the content of serum transferrin 20 days after training is much higher than that before training ($P<0.05$) as shown in Figure 1.

3.3 The variation of athletes' serum transferrin receptor content

Serum transferrin receptor didn't change much in the training as shown in Figure 2.

3.4 The variation of athletes' erythropoietin

Friedman variance analysis showed that the content of erythropoietin 40 days and 60 days after training were higher than that 20 days after training ($P<0.05$), but it didn't change much compared with that before training ($P>0.05$) as shown in Figure 3.

4. Results and discussion

The red blood cell and pressure and volume of blood cell didn't change during the training. The amount of hemoglobin 20 days after training decreased compared with the amount before training ($P<0.05$), the amount of hemoglobin 40 days

and 60 days after training increased compared with the amount 20 days after training ($P<0.05$), but there was no significant difference when compared with the situation before training ($P>0.05$). It is proved that intensity training will lead to the increase of free radicals and the change of antioxidant enzymes activity, also, serum ferritin and hemoglobin concentration will decrease, red blood cell will be more fragile, hence, training will lead to more red blood cell hemolysis, and accordingly cause the loss of iron (Cao, 2004, P.1049-1052; Cao, 2004, P477-483; Cao, 2003, P331-335). Iron is one of the necessary micronutrient, and is the component of hemoglobin, myoglobin and cytochrome, which are enzymes that contain iron and are responsible for oxygen transportation and exchange as well as tissue respiration. During sport, metabolism is accelerated, and synthesis and decomposing activity will be more active, accordingly iron metabolism will be strengthened, so it is easy for athletes to lack iron after sports, the synthesis of some compounds that contain heme iron will be affected, and it is difficult for athlete to get back. Hence, athletes who take part in large intensity training for a long period time get iron deficiency anemia easily. In this study, serum iron and ferritin didn't change greatly, but showed a trend of decrease.

Erythrocyte hemoglobin distribution width 20 days after training is higher than that before training ($P<0.05$), but Erythrocyte hemoglobin distribution widths 40 days and 60 days after training are lower than that 20 days after training ($P<0.05$). Erythrocyte hemoglobin distribution width reflects the red blood cell volume, and it is usually used to diagnose early iron deficiency anemia, while iron deficiency anemia is the most common anemia of athlete. When body lacks iron and hemoglobin is normal, erythrocyte hemoglobin distribution width will be aberrant. In the training, red blood cell will be renewed fast; when the number of reticulocyte increases, erythrocyte hemoglobin distribution width will be increased (Feng, 2003, P.56-64). In addition, the break and dissolution of red blood cell should be taken into consideration, athlete should eat some nutriments, such as antioxidant, phosphatide to protect blood cell membrane, and to reduce and prevent haemolysis.

Transferrin is a globulin that has two iron ions and transfers iron in the blood, the amount of this protein can regulate the absorption of iron (Feng, 2003, P.56-64). When the iron is absorbed by body, transferrin will transport the iron to specific tissue and red blood cells, cells will make the iron as functional iron, transferrin will transport the iron to marrow, liver or spleen and make it as reserve. When the body takes in little iron or iron metabolism is accelerated, transferrin will transport the reserved iron to the cells that need iron, although there is a little transferrin, it reflects the situation of functional iron and reserved iron, and reflects the distribution of iron in the body (Cao, 2003, P. 331-335). In this study, the athletes' transferrin 20 days after training was much higher than that before training ($P<0.05$), it means that in the training, the amount of functional iron decreased, which led to the increase of transferrin. The amount of hemoglobin 40 days and 60 days after training was lower than that 20 days after training ($P<0.05$), maybe the functional iron in the blood increased after training because of the improvement of movement ability.

Serum transferrin receptor (sTfR) is a glycoprotein; it is mainly produced by marrow and reticulocyte. sTfR concentration has correlation with the proliferation of marrow red blood cell, and has negative correlation with serum iron. It is reported recently that EPO and sTfR both can reflect the hematopoietic situation, sTfR can reflect the hematopoietic activity of marrow, if both EPO and sTfR are detected, the situation of iron metabolism can be reflected, accordingly, effective training plan can be made (Abellan, et al., 2007, P. 9-15; Sharp, et al., 2002, P. 1248-57). In addition, serum transferrin receptor can reflect the situation of iron metabolism, the amount of serum transferrin receptor will increase when body lacks iron, and the red blood cell lacks iron, or when body is in the state of iron deficiency anaemia. But at different stages, the increase degrees of serum transferrin receptor are different; it means that serum transferrin receptor is a specific index to check the situation of iron (Virtanen, et al., 1999, P. 256-60). Being different from the above situation, the amount of serum transferrin receptor didn't change much in the training.

Erythropoietin (EPO) is a kind of glycoprotein hormone, its molecular weight is 34 kD, EPO in the blood is composed of 165 amino acid, and is greatly glycosylated by sialic acid. Natural EPO can be classified into two kinds according to the content of carbohydrate, α type contains 34% carbohydrate, β type contains 26% carbohydrate. Two types of carbohydrate are the same in the aspects of biological characteristic, antigen and clinic effect. It is traditionally suggested EPO can act on bone marrow hematopoietic stem cells, and accelerate the proliferation, differentiation of erythroid progenitor cell. In some physical ability dependent sports, such as track and field, EPO can regulate the oxygen supply, and human body has high demand on the oxygen carrying ability of red blood cell. EPO can quickly active the expression of proto-oncogene, *c-myc*, and maintain the life of the cell. Some experiments showed that EPO can not directly accelerate the replication of chromosome and mitosis, so EPO play important roles in anti-apoptosis, which can make red blood cell survive and differentiate into mature red blood cell (Kirito, et al., 2002, P.51-4; Kirito, et al., 1998, P.462-71). It has been proved that the production of EPO has correlation with oxygen supply, but the specific mechanism is still unclear. When the body lacks oxygen, the pressure around renal interstitial cells will decrease, which will influence the state of cytoplasm and finally lead to the increase of EPO expression. In this study, EPO level shows difference between individuals, so we analyzed the data with the method of Friedman variance analysis, it is indicated that the EPO 20 days after training was a little higher than that before training, but it was not significant, this accorded with the situation that in the beginning of training, the body lacked oxygen and the amount of hemoglobin decreased, so

the EPO level increased. With the progress of training, EPO level decreased compared with that 20 days after training, may be this was the adaptation of body to training.

5. Conclusion

In the training, the hemoglobin of elite female middle-distance runners firstly decreased then increased; serum iron firstly decreased then increased, but it is not significant; serum ferritin didn't change apparently; serum transferrin firstly increased then decreased; serum transferrin receptor didn't change much in the training; the Erythrocyte hemoglobin distribution width firstly increased then decreased; EPO firstly increased then decreased in the training.

References

Abellan R, Ventura R, Pichini S, et al. (2007). Effect of physical fitness and endurance exercise on indirect biomarkers of recombinant erythropoietin misuse [J]. *Int J Sports Med*. 28(1): 9-15.

Cao, Jianmin. Jin, Li. Zhao, Jiexiu. Zheng, Hongrong and Tian, Ye. (2004). Effects of nutrition supplement on erythrocyte zinc protoprophyrin, transferrin receptor in rats of sports anemia. [J]. *Journal of Beijing Sport University*. 27 (4): 477-483.

Cao, Jianmin. Tian, Ye. Zhao, Jiexiu and Jin, Li. (2003). Exercise and iron metabolism. [J]. *Journal of Beijing Sport University*. 26 (3): 331-335.

Cao, Jianmin. Zhao, Jiexiu. Jin, Li. Zheng, Hongrong and Tian, Ye. (2004). Effects of nutrition supplement on erythrocyte indexes, serum iron, ferritin and transferrin in rats of sports anemia. [J]. *Journal of Beijing Sport University*. 27 (8): 1049-1052.

Feng, Lianshi. Feng, Meiyun and Feng, Weiquan. (2003). *The functional siagnosis methods in elite athlete and problems*. [M] Beijing. People's Sports Publishing House. 56-64.

Kirito K, Nagashima T, Ozawa K, et al. (2002). Constitutive activation of Stat1 and Stat3 in primary erythroleukemia cells [J]. *Int J Hematol.* 75 (1): 51-4.

Kirito K, Uchida M, Takatoku M, et al. (1998). A novel function of Stat1 and Stat3 proteins in erythropoietin-induced erythroid differentiation of a human leukemia cell line [J]. *Blood*. 92 (2): 462-71.

Sharpe K, Hopkins W, Emslie KR, et al. (2002). Development of reference ranges in elite athletes for markers of altered erythropoiesis [J]. *Haematologica*. 87(12): 1248-57.

Virtanen MA, Viinikka LU, Virtanen MK, et al. (1999). Higher concentrations of serum transferrin receptor in children than in adults [J]. *Am J Clin Nutr*, 69 (2): 256-60.

Table 1. Content variation of red blood cell, hemoglobin, pressure and volume of blood cell, Erythrocyte hemoglobin distribution width (RDW), serum iron and serum ferritin

	Before training	20days after training	40days after training	60days after training
Red blood cell ($\times 10^{12}$/L)	4.52±0.36	4.35±0.47	4.21±0.21	4.21±0.48
Hemoglobin (g/dL)	12.74±1.24	11.43±0.79*	13.16±1.34#	12.84±1.34#
Pressure and volume of blood cell (%)	39.34±4.22	35.10±2.66	39.05±4.35	37.44±3.79
RDW (%)	13.16±0.87	14.75±0.46*	12.64±0.34#	12.66±0.30#
serum iron (ug/dL)	63.62±20.75	54.70±18.29	56.99±22.59	57.19±21.92
serum ferritin (ng/mL)	87.41±46.86	44.49±37.52	61.35±22.61	67.61±33.70

*: P<0.05 **: P<0.01 compared with the situation before training

#: P<0.05 ##: P<0.01 compared with the situation 2 weeks after training

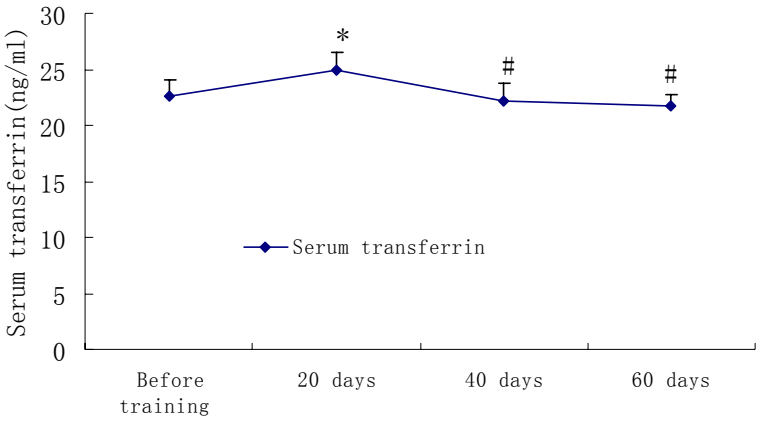

Figure 1. The variation of serum transferrin content of athletes

*: P<0.05 **: P<0.01 compared with the situation before training

#: P<0.05 ##: P<0.01 compared with the situation 20 days after training

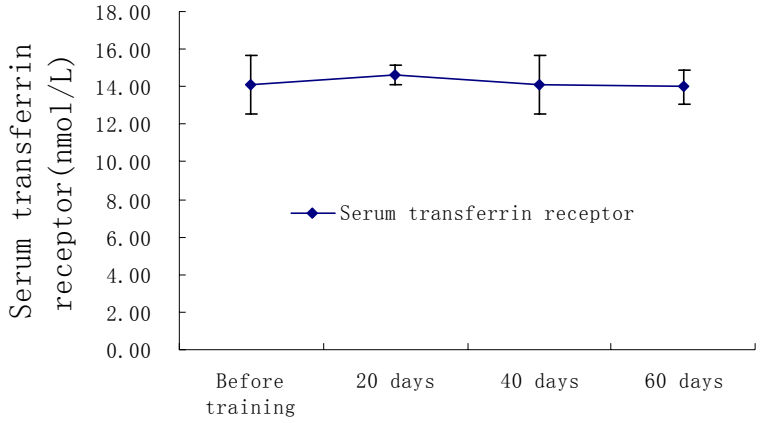

Figure 2. The variation of serum transferrin receptor content of athletes

*: P<0.05 **: P<0.01 compared with the situation before training

#: P<0.05 ##: P<0.01 compared with the situation in the training

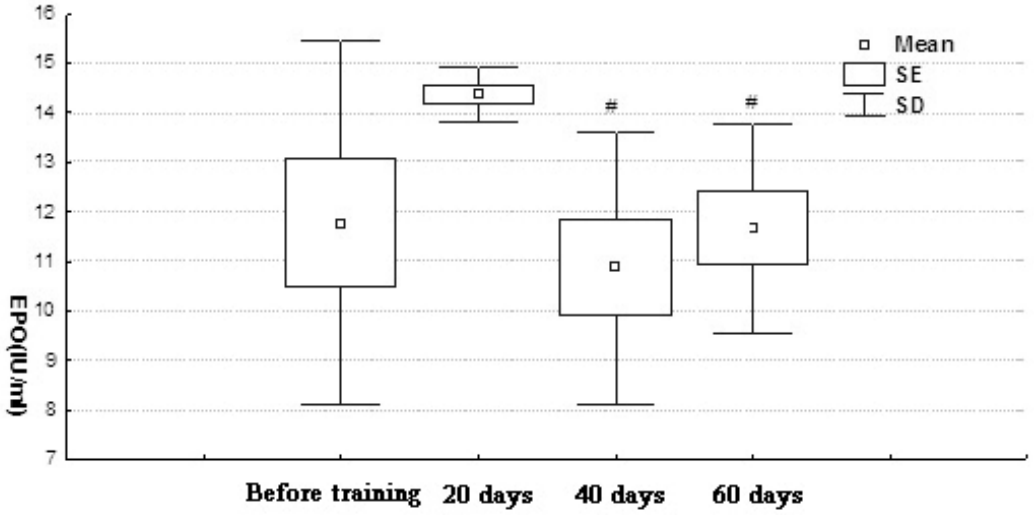

Figure 3. The variation of EPO content of athletes

#: P<0.05 ##: P<0.01 compared with the situation before training

Modern Applied Science

www.ccsenet.org/journal.html

Vol. 2, No. 3

May 2008

InAs/GaAs Quantum Dots Grown By Metal Organic Chemical Vapor Deposition at Different Temperatures

Rosnita Muhammad, Zulkafli Othaman, Lim Kheng Boo

Physics Department, Faculty of Science

University Teknologi Malaysia

81310 UTM Skudai, Johor, Malaysia

E-mail: rosnita@dfiz2.fs.utm.my

Yusuf Wahab

Ibnu Sina Institute for Fundamental Science Studies

University Teknologi Malaysia

81310 UTM Skudai, Johor, Malaysia

Abstract

InAs/GaAs quantum dots (QDs) were grown by low pressure Metal Organic Chemical Vapor Deposition in Stranski-Krastanov growth mode. The influence of growth temperature on the QD density was investigated. Atomic Force Microscopy (AFM) was used to study the growth behaviour of the QD structure. It was identified that the growth temperature plays major role in determining the growth and distribution of InAs QDs due to the temperature-dependent dislocation propagation from the GaAs substrate. A high InAs on GaAs QD density 6.4 x 1010 cm-2 was obtained and this proposes a potential superiority of nanodevice operation.

Keywords: MOCVD, Structural, InAs, Quantum Dot, Atomic force microscopy

1. Introduction

Low dimensional semiconductor structures have reached great interest due to their modified electronic and optical properties. Quantum dot structures, which provide electron confinement in three dimensions, can be grown in-situ, without using lithography, by the so-called "self-assembly" effect or Stranski-Krastanov (S-K) growth mode. In this growth mode at a certain critical thickness, an initially two-dimensional (2D) epitaxial layer under compressive strain relaxes into self organized three-dimensional (3D) coherent islands (dots), and a remaining thinner 2D wetting layer [1]. By forming 3D islands the strain can relax in three dimensions and the total energy of the system is reduced.

Self-assembled growth of InAs/GaAs QDs using S-K growth mode has advanced rapidly by MBE, exhibiting low threshold current densities, reasonable differential efficiencies and output powers for telecommunications [2-4]. However, growth by Metal Organic Chemical Vapor Deposition (MOCVD) has proved more challenging with relatively few reports of MOCVD grown InAs/GaAs QD [5-8]. This is due to an increase role of growth kinetics which can lead to island coalescence and defect formation. This is especially true for the InAs/GaAs system where the lattice mismatch is high and the nucleation process is rapid. In this paper, we will discuss the influence of the growth temperature ranging from 500 to 600 ^{o}C for the InAs/GaAs system fabricated on *n*-type GaAs wafer. The critical issue is to avoid formation of larger islands which are particularly susceptible to dislocation formation in MOCVD growth, yet still achieve the high QD densities necessary for device applications.

2. Experiment

All samples in this work were grown in a vertical low pressure NanoEpi MOCVD reactor with trimethylindium (TMIn), trimethylgallium (TMGa) and Arsine (AsH_3) as precursors and H_2 as carrier gas. The reactor pressure for all the growth was set at 76 Torr. The V/III ratio of the source flow flux was set at 14 and 5 for the GaAs and InAs layers respectively [9]. GaAs wafer used for all growth were epi-ready semi-insulating and oriented in the (001) ± 0.1^{o} direction with 0.4mm thick.

The GaAs wafer were cut to quarter sizes and placed in the vertical reactor. After initial process for soft and hard baking of susceptor, a GaAs buffer layer were grown at 750 ^{o}C to remove any dust or particles. This is then followed by another GaAs buffer layer grown at 550 ^{o}C to stabilize active region between layers and dots. The growth was then

interrupted for 2 sec before series of InAs QDs grown at temperatures between 500 to 600 ^{o}C. The sample was then allowed to cool to room temperature. Figure 1 shows the typical MOCVD flow process for the InAs/GaAs QD structures with 2 sec interrupt.

3. Results and discussions

AFM was used to investigate the QD morphology and to correlate formation trends with changes in growth conditions. InAs/GaAs structures were grown at different temperatures, ranging from 500 to 600 ^{o}C. Increase in temperature provides increase in surface adatom energy. Therefore QD nucleation and formation begins and surface materials migrate towards the existing sites. The extent of adatom surface diffusion during and just after nucleation determines the QD density and uniformity [10]. The kinetics that determine the density and QD size are not fully understood, but the two features are interrelated and strongly temperature dependent.

At low temperatures ($T < 550^{o}C$), high-density QDs are formed due to shorter diffusion wavelengths. The existing surface material distributes over a large number of QDs forming smaller QDs. At higher temperatures, a greater migration distance leads to a lower QD density of large QDs. Figures 2(a) – (e) show the AFM images of InAs QD ensembles grown on a GaAs buffer layer at 500 to 600 ^{o}C. Figures 2(a), 2(b), 2(c), 2(d) and 2(e) correspond to growth temperatures of 500, 525, 550, 575 and 600 ^{o}C respectively. We see that InAs QDs on GaAs form only for the temperature 525, 550 and 575 ^{o}C. Outside of this range, QD formation does not occur due to lack of surface mobility at $T \leq 500$ ^{o}C and indium evaporation at $T \geq 600$ ^{o}C [5]. At temperatures below 500 ^{o}C the InAs QDs still does not occur and we assume that this is due to epilayer material under compression. As for the sample at 600 ^{o}C, the cracking efficiencies begin to drop off significantly and incompletely dissociated metal-organic molecules [11].

In ordinary S-K self-assembled InAs/GaAs QD growth, a few monolayers (ML) of InAs thin layer with a large lattice mismatch is grown on a GaAs buffer. It is reported that the lattice constants of InAs (0.605 nm) and GaAs (0.565 nm) can result in 7% lattice mismatch [12]. This 7% lattice mismatch is good enough to induce S-K growth mode of QDs with a maximum height up to 120 nm, if the mismatched strain is properly relaxed. Growth of QDs can be stopped by stopping the flow of TMIn source while keeping the substrate temperature constant and AsH_3 flowing for post-growth interruption. During the post-growth interruption, coherent three-dimensional islands or QDs are formed by self-assembly, accompanied by a thin wetting layer, to release the strain energy accumulated by the large lattice mismatch between the InAs and GaAs buffer layer. In our case, the interruption for forming InAs QDs was set at 2 sec.

From AFM images, we can see the QD density of InAs QDs decreased from 6.4×10^{10} cm^{-2} at 525 ^{o}C to $0.5 \times 10^{10} cm^{-2}$ at 575 ^{o}C. The QDs start to form uniformly when the temperature reach 550 ^{o}C. The diameter of the QD increases with increasing temperature from 80.6nm at 500 ^{o}C to 129.8 nm at 525 ^{o}C and 149.7 nm at 550 ^{o}C. For the temperatures greater than 550 ^{o}C the size of InAs QDs decreases and this phenomena occurred because the layer of the samples start cracking with In evaporated at $T > 550^{o}C$. The energy of the epilayer system also exceed the ripening process and towards equilibrium, and these phenomena agreed with Ostwald ripening and stable dot-arrays [13,14]. The resulting QD diameter and InAs QD densities data are plotted as a function of growth temperature in Figure 3 and 4.

4. Conclusion

In summary, we have investigated the structural properties of InAs quantum dots grown on GaAs buffer layer at varying temperatures ranging from 500 – 600 ^{o}C using a vertical MOCVD reactor. We find that the QD formation is affected by changes in surface atom mobility relative to the temperature dependence. In this work, we achieve InAs QD densities of $6.4 \times 10^{10} cm^{-2}$ and average dot diameter 149.7nm at optimum temperatures 550 ^{o}C. In future, the fluctuations in size and shape of nanometer scale islands formed in the S-K growth mode have to be further reduced in order to produce QDs with superior electronic performance at room temperature.

Acknowledgements

The authors acknowledge the Ministry of Science, Technology and Environment Malaysia for the financial support through IRPA funding 09-02-06-0056-SR0013/06-01 and also to the Ibnu Sina Institute for Fundamental Science for the laboratory facilities especially the Metal Organic Chemical Vapor Deposition System.

References

J. Liang & Z. Suo, (2001). *Applied Physics Letters*, Vol 79, No 20, pp 3251-3253.

L. Sfaxi et. al., (2006). *Journal of Crystal Growth*, 293, pp 330-334.

D. Leonard, K. Pond, P.M. Petroff, (2004). *Physics Review B*, 50, 11687.

T. R. Ramachandran et. al, (1997). *Applied Physics Letter*, Vol 70, pp 640.

El-Emawy et. al., (2003). *Journal of Applied Physics*, 93, 3529-3534.

Xiaohong Tang et al., (2006). *Nanotechnology*, 17, 295-299.

Terence Yeoh et. al., (2002). *IEEE Quantum Electronics*, 8, No 4, 833-837.

Periyasami et al., (2002). *Applied Surface Science*, 191, pp. 196-204.

R. Muhammad, Z. Othaman, S. Sakrani, (2007). *Reg. Annual Fundamental Sci. Seminar 07*, Ibnu Sina Institute, 28-29 May 2007.

A. Passaseo et. al., (2001). *Applied Physics Letter*, 78, p 1382.

Kallista Sears et al., (2004). *Proceedings of the Conference on Optoelectronic & Microelectronic Materials and Devices*, Australian National University, Dec 2004.

L.J.Salen, L.J.V. Ijzendoorn & M.J.A. de Voigt, (2000). *Phys Review*, 61, pp 8270.

W. Seifert e. al., (1997). *Brazilian Journal of Physics*, Vol 27/A, no 4, 1997.

V. A. Shchukin et. al., (1995). *Physics Review Letter*, Vol 75, p 2968.

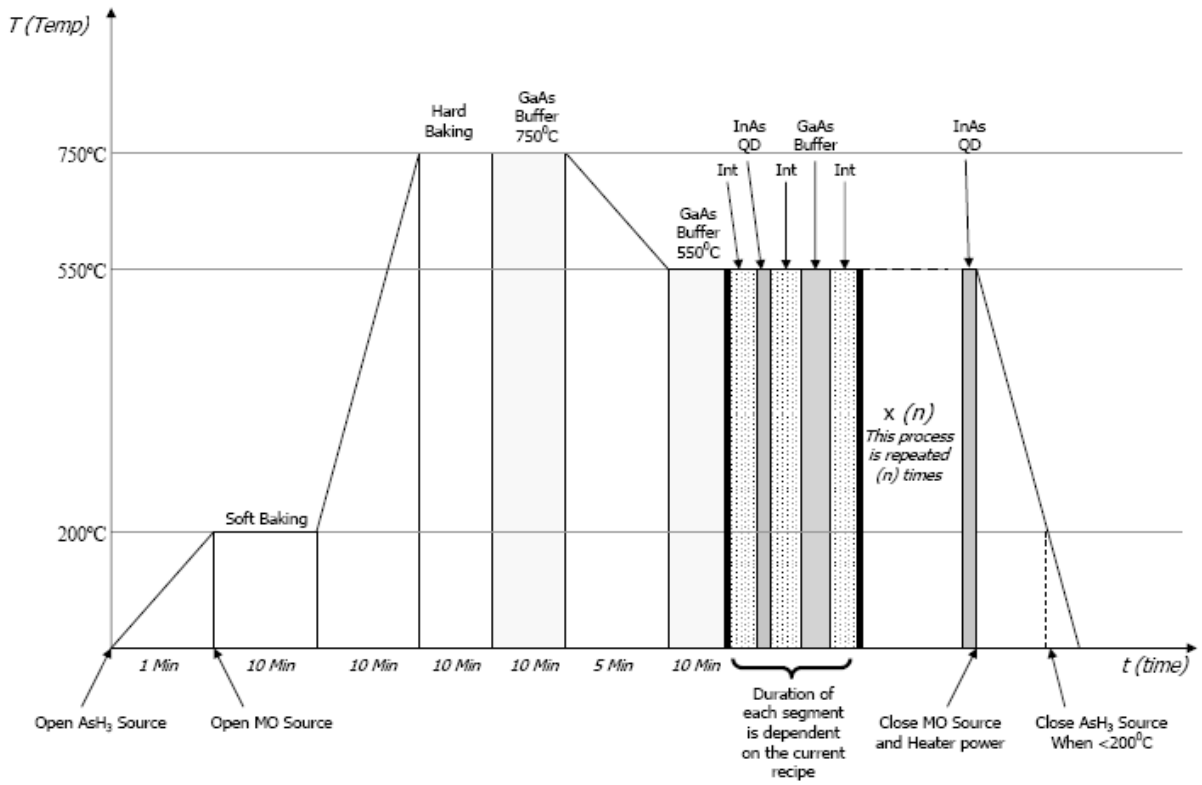

Figure 1. Typical MOCVD Flow Process

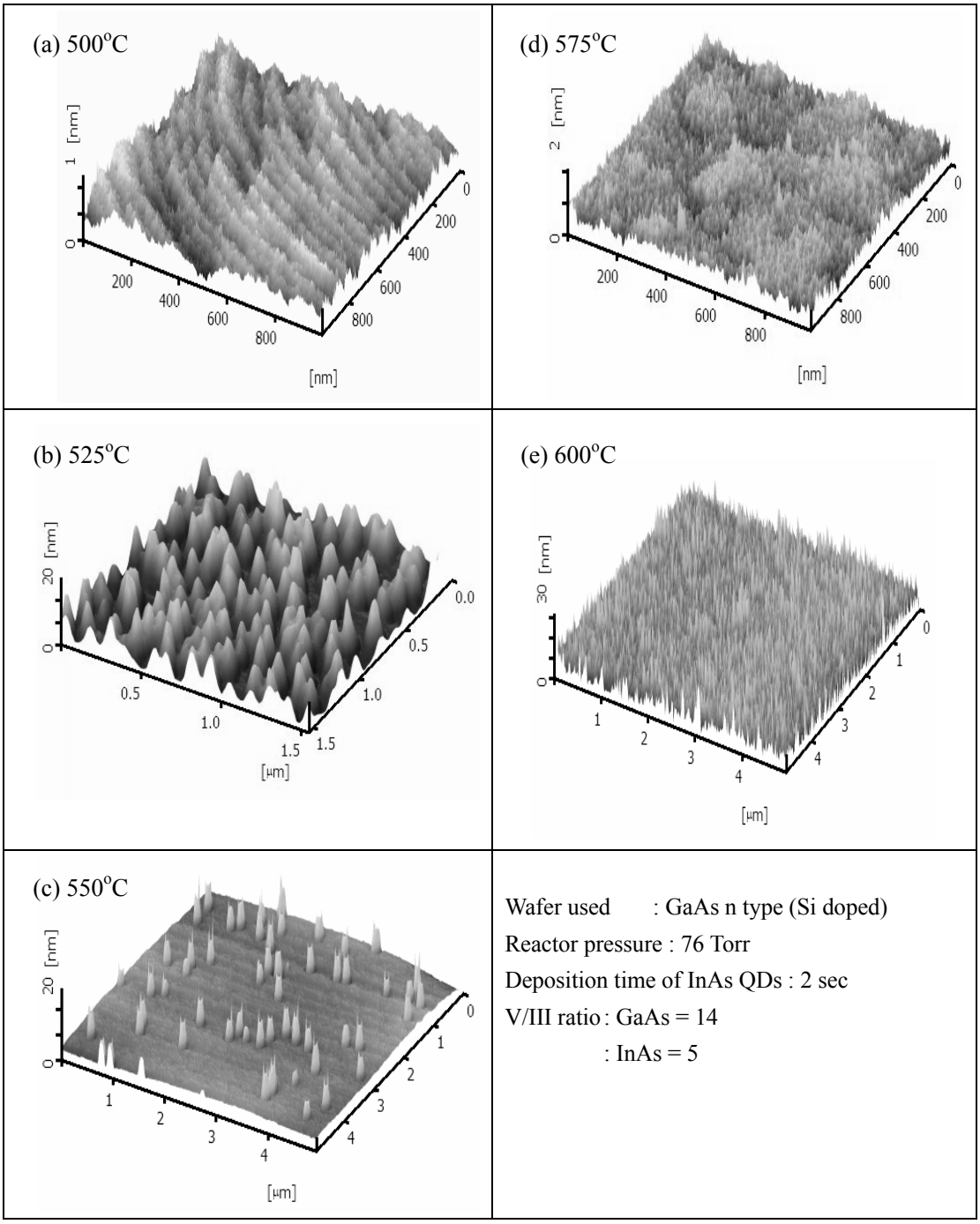

Figure 2. Atomic Force Microscopy 3D images of InAs QDs grown on GaAs buffer layer at (a) 500°C, (b) 525°C, (c) 550°C, (d) 575°C and (e) 600°C

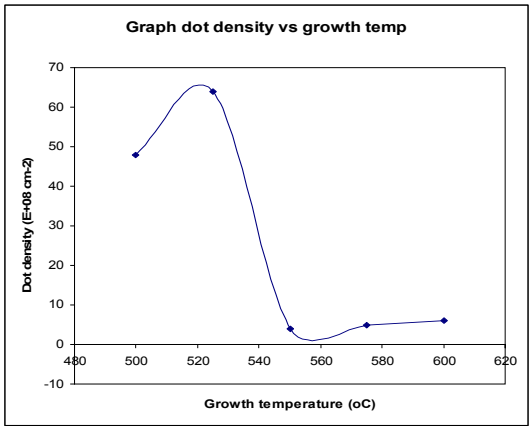

Figure 3. Data plots from AFM measurements of QD density as a function of temperature.

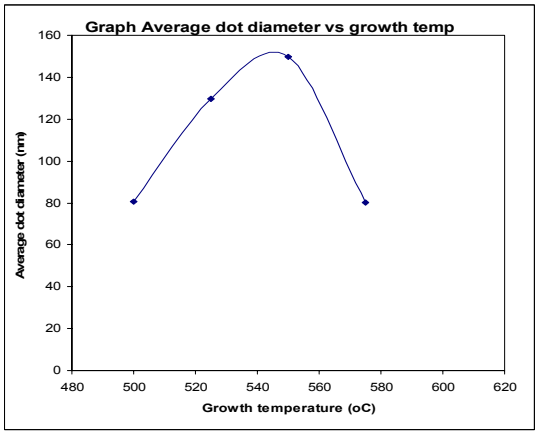

Figure 4. Graph average InAs QD diameter on GaAs buffer layer

Modern Applied Science

www.ccsenet.org/journal.html

Vol. 2, No. 3

May 2008

The Design of the Drive Control Chip for the Solar LED Lighting System

Bonian Mao, Pingjuan Niu & Chunhong Huang

School of Information and Communication Engineering, Tianjin Polytechnic University

Tianjin 300160, China

E-mail: bnmaook@126.com

Abstract

Combining with the application characteristic of solar energy system and the drive characteristic of high-power lighting LED, in this article, we develop a sort of new drive control chip of solar LED lighting system, which not only can be drove by the invariable current of 350mA, but also can realize functions including the regulation of charger and discharge, preventing reverse charge, preventing over charge, preventing over discharge, and preventing reverse connection of the storage battery in the photovoltaic system.

Keywords: Solar energy, High-power LED, Controller

1. Introduction

Light-emitting diode (LED) is a sort of semiconductor emitting apparatus which can translate the electric energy into the visible light and possess advantages such as saving energy, environmental protection, long life and free maintenance. The solar LED lighting is the combination which utilizes the solar battery to offer of electrical source and uses LED as the lamp-house, and the solar battery is directly translate the light energy into the DC electrical energy, and the subassembly of the solar battery can be assembled at will through the series-wound or shunt-wound fashion to obtain the voltage actually needed. These characteristics are just matched with LED and can not be achieved by traditional power supply system (Chen, 2006). If the solar battery is combined with LED, the AC and DC will be translated directly and need not any reverse equipment, so the solar LED lighting system will obtain high energy utilization ratio, which possesses characteristics of safe, environment protection, and zero energy consumption, and is real green lighting system.

In the solar LED lighting system, the drive control circuit is the most important part, which is the key to differ with usual light system, which design is directly relative with the function and reliability of the system, and decides the operation of the system. At present, most solar control circuits are composed by analog electronic circuit, and because of its reliable and mature technology, so its application is very broad. However, this sort of controller is made by independent components which possess characteristics including numerous quantities, low integration degree, large volume and serious power consumption, and the constant voltage signal of output controlled by it is not fit for the drive use for high-power LED.

Therefore, it is necessary to integrate independent components on one piece of silicon wafer, and the solar LED drive control chip and its application circuit which possesses perfect design functions and simple structure can drive high-power LED through the constant current and have the function of usual solar controller. It can not only fulfill the actual requirement of the solar LED lighting system, but also enhance the reliability, reduce power consumption and decrease the volume. Accordingly, it establishes stable base for the popularization and application of the solar LED lighting technology.

2. System composing and function requirement

In the solar LED lighting system, the solar panel is necessary, which is the apparatus translating solar energy into the electrical energy. Because of the covering of clouds, the output of solar energy on the ground is intermittent and can not be forecasted, so some energy system which usually is the storage battery must be founded in the system. To prolong the use life of the storage battery and fully utilize the solar energy, the most important apparatus in the solar LED system are the drive control circuit and the lighting lamp-house LED lamp because of the characteristic of LED. Above four parts compose the solar LED lighting system which is seen in Figure 1. Because this system adopts the DC load (according the characteristic curve of LED, the constant current source is generally used), so the reverse regulation equipment which translates DC into AC doesn't need in the general solar system. The work principle of the system includes that at day, the solar panels stores the electrical energy obtained from solar radiation in the storage battery, and at night, the storage battery supplies powers to the lighting LED lamps and lanterns, illumines the lamp-house, roads or squares. The drive control circuit is the "brain" of the whole system which controls the solar battery, the storage battery and LED lamp to operate conformably.

The functions of the drive control chip of the solar LED lighting system and the application circuit mainly include following aspects.

(1) It can export the constant current of 350mA±5% to the high-power LED, and the current can be regulated by the external resistors Rxt, and the current doesn't change with the change of the voltage or the environmental temperature of the storage battery.

(2) It can turn on the LED lamp at dark and turn off the LED lamp and charge to the storage battery automatically at day. The symbol voltage when the LED lamp turns on is 1.5V.

(3) It can offer the storage battery functions of charge and discharge regulation, preventing reverse charge, preventing over charge, preventing over discharge and preventing reverse connection. The symbol voltage when the storage battery ends discharge and the symbol voltage when the storage battery ends charge are all 3.3V.

(4) It can offer the protection of preventing reverse connection for the solar battery.

3. Circuit structure and work principle

The LED constant current drive part of the chip adopts the mode of linear series-wound control which has good constant current precision, low ripple current, high reliability without any electromagnetic interference. The charge and discharge control part of the solar LED lighting system adopts the single path and bypass charge and discharge controller frame (Zhao, 2004), takes the voltage comparator composed by operational amplified circuits as the control circuit, and sets up the control state of the system through the regulation of the potentiometer. The chip principle structure and the application circuit are respectively seen in Figure 2 and Figure 3.

The chip power is offered by the storage battery which exports 12V DC voltage that is reduced to 5V through the voltage regulator Z1, and the whole circuit is composed by following modules, one high-power NMOS pipe MSG which is connected by 755 NMOS pipes with the ratio of width and length of 10μm/1μm and can offer the drive current of 350mA, one sensor NMOS pipe M5 with the ratio of width and length of 10μm/1μm which uses grid and source together with high-power MSG, one reference voltage source BG which can produce constant voltages 3.3V and 1.5V that can not change with changes of voltage and temperature of the electrical source, one error operation amplifier YF, three buffers HC which are used to isolate the influence of the latter class and increase the output drive ability, LED switch circuit KG which can control charge and discharge of the solar LED system, and various protective circuits. Those apparatus which adopt exterior connection include sampling resistance Rxt, potentiometer Rwskg, Rwbgc and Rwbgf, protective Schottky diode SBD1 and SBD2, protective rectifier diode D1, high-power NMOS switch pipe M0, fuse pipe FUSE1, shunt capacitance C1 and protective capacitance C2, voltage regulator Z1 and resistance R1.

The work principle of the whole circuit includes two parts.

(1) The work principle of LED constant drive part.

The reference voltage source BG produces two reference voltages, 3.3V and 1.5V, where, the reference voltage of 1.5V is exported from the buffer HC and enters into the reverse port of the error operation amplifier WCYF which output controls the grid voltage of the power NMOS pipe MSG and sensor NMOS pipe M5 and makes it fix at 1.8V, and accordingly the corresponding drive current is obtained. The sensor current produces sampling voltage on the sampling resistance Rxt, and the difference between the reference voltage of 3.3V and this sampling voltage is took as the feedback voltage and brought to the in-phase input port of WCYF, and compare with the voltage of reverse input port, i.e. 1.5V produced by BG, and adjust the output voltage and the sensor current I_{set} of the sensor M5, and make the whole closed loop feedback system in dynamic balance to stabilize the drive current of the power pipe MSG (Shen, 2006).

That is to say, when the sensor current I_{set} increases, the voltage drop on the resistance Rxt will increase, the voltage on the in-phase input of the WCYF will decrease, and the voltage on the reverse input is constant and controlled by the reference voltage source BG of 1.5V, so the output V_{out} of WCYF will decrease and induce the decrease of I_{set}, contrarily, when the sensor current I_{set} decreases, the voltage drop on the resistance Rxt will decrease, so the voltage on the in-phase input of the WCYF will increase, so the output V_{out} of WCYF will increase and induce the increase of I_{set}, which is the principle that the sampling sensor current I_{set} is in the dynamic balance. And the power MOS pipe MSG and the sensor MOS pipe M5 together use the grid and the source and work in the saturation area, so the drive current of the power MOS pipe MSG can be stabilized at 350mA.

(2) The work principle of solar LED system charge and discharge control part.

In Figure 3, C1 and C2 can decrease the ripple current and voltage, and stabilize the input voltage of the system. Because the solar system is different, so both the symbol voltage point to end discharge of the storage battery V_1 and the symbol voltage point to cut off charge V_2 are different. But they can be regulated to 3.3V through potentiometers Rwbgc and Rwbgf and matched with comparable level which operates and amplifies in the interior of the chip. Analogously, the symbol voltage point to turn on LED in different lighting system can be regulated to 1.5V through potentiometer.

The NMOS pipe M1 in Figure 2 is the discharge switch of the storage battery and the load LED switch. When the port voltage of solar panels V_{solar} is smaller than the symbol voltage to turn on LED, i.e. V_{vskg}<1.5V, the voltage will make M1 connect through the automatic disposal of the interior LED switch module KG and exporting high level to automatically turn on LED lamp. When the voltage of the storage battery is smaller than the end voltage of discharge, i.e. V_{vbgf}<3.3V, this voltage exports low level and turns off M1 through the disposal of module KG to implement "over discharge protection".

When the storage battery charges fully, the port voltage of the storage battery is larger than the symbol voltage V_2, i.e. V_{vbgc}>3.3V, this voltage exports high level and connects the switch M0 through the reverse comparing of the interior operational and amplified YF, and at the same time, the Schottky diode SBD1 closes, so the output circuit of the solar panels directly discharges through M0 by bypass and doesn't charge to the storage battery, to avoid over charge for the storage battery and implement the function of "over charge protection".

The Schottky diode SBD1 is the "preventing reverse charge diode", and when the output voltage of the solar battery phalanx is larger than the voltage of the storage voltage, SBD1 can be connected, contrarily SBD1 closes, which can ensure the reverse charge to the solar battery phalanx can not occur at night or overcast and rainy day, and "prevent reverse charge".

Rectifier diode D1 is the "accumulator preventing reverse connection diode", and when the polarity of the storage battery is reverse, D1 connects, which makes the storage battery discharge through the short of D1 and produces large current to melt FUSE 1 quickly and "prevent the reverse connection of the storage battery". The Schottky diode SBD1 is the "solar preventing reverse connection diode", and when the polarity of the solar battery is reverse, SBD2 closes to "prevent reverse connection of the solar battery".

4. Integrated circuit combined simulation and testing

The simulation result of the charge and discharge control part of the solar LED lighting system is seen in Figure 4. From the figure, the charge and discharge part can fulfill the function requirement of the solar controller. Next, we simulate the LED constant current drive part. For the LED load, we select three 1W high-power white light LED made by US CREE Company, and the simulation is implemented under conditions including the temperature of 27℃, $V_{skg} \leq 1.5$, $V_{bgf} \geq 3.3V$ and $V_{battery}$=12V. From Figure 5, we can see that when the LED load is three LEDs, the voltage drop range of LED is 9-12V, and the output current of the circuit is 350.75mA, the current precision is ±0.85%. From Figure 6, we can see that when the environmental temperature ascends from -40℃ to 125℃, the current through LED descends from 352.5mA to 346.2mA, decreases 1.79%, which indicates that the chip also has good constant current characteristics when the environmental temperature changes. From Figure 7, we can see that when the output voltage of the storage battery $V_{battery}$ fluctuates in 11V to 14V, the output current of the circuit ascends from 346.3mA to 353.5mA, increases 2.07%, which indicates that the output current of the chip can not be influenced by the storage voltage $V_{battery}$. Figure 8 shows the relationship between the sampling resistance Rxt and the output current I_F, and from Figure 8, we can see that when the sampling resistance Rxt changes in 3.64KΩ~5KΩ, the output current of LED has similar linear relationship with the sampling resistance, and has non-linear relationship in other ranges.

The design of the chip adopts the technology of 0.35μm 2P4M Dual Gate Mixed Mode CMOS offered by Singapore CHARTER, and the total area of the final chip is 1.0mm^2. Figure 9 is the micrograph of the chip, and the testing result of 30 sampling photos shows that the chip can automatically turn on and turn off the LED lamp, implement the charge and discharge regulation of the storage battery and functions of preventing reverse charge, preventing over charge, preventing over discharge, and preventing reverse connection of the storage battery, and the drive current of LED is distributed in 345mA~366mA and most of them is 356mA, which can fully fulfill the use requirement of solar LED lighting system.

5. Conclusions

This article introduces the design and the realization of solar LED lighting system drive control chip based on the technology of 0.35μm CMOS, and the chip can drive LED through constant current of 350mA, and can actualize functions including the regulation of charger and discharge, preventing reverse charge, preventing over charge, preventing over discharge, and preventing reverse connection of the storage battery in the photovoltaic system.

References

Chenwei. (2006). *Research of Household Photovoltaic Architecture Integrated Generating System and Solar-powered Semiconductor Lighting Engineering.* Doctoral Degree Dissertation of University of Science & Technology of China.

Shenhui. (1993). *Design of High-power Lighting LED Constant Current Drive Chip.* Master Degree Dissertation of Zhejing University.

Zhao, Xiuchun, Zhangxi & Li, Peifang. (2004). A New-style Controller for Photovoltaic Lighting System. *Energy Engineering.* No.5.

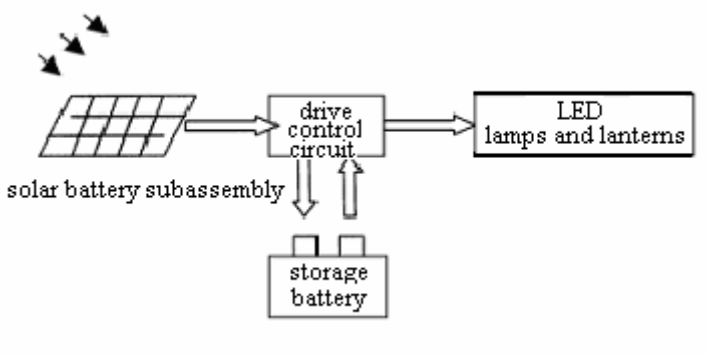

Figure 1. Solar LED Lighting System

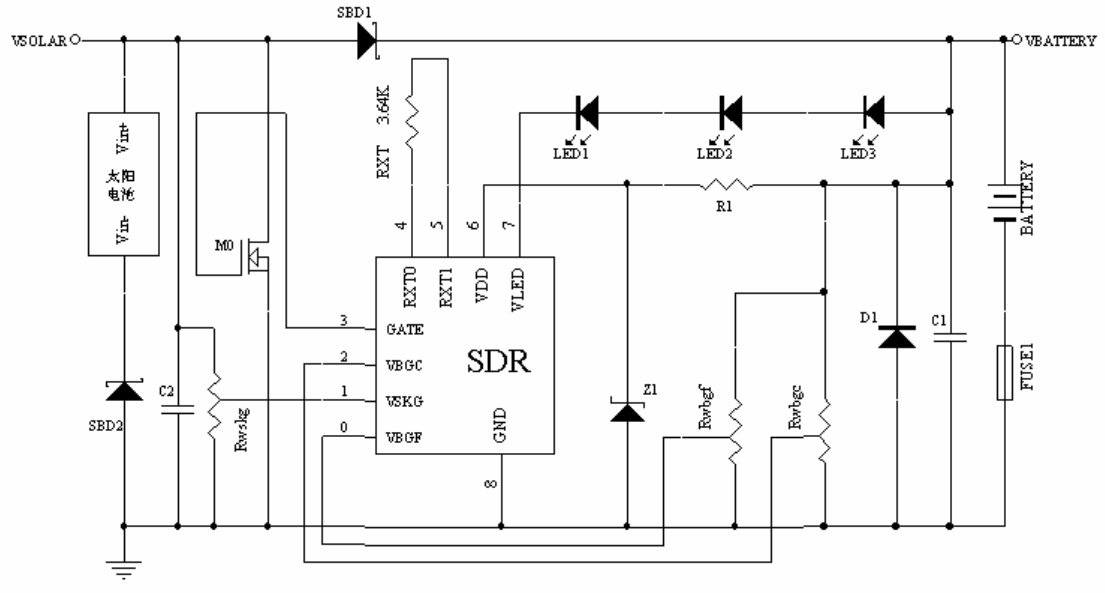

Figure 2. Structure of Chip Principle

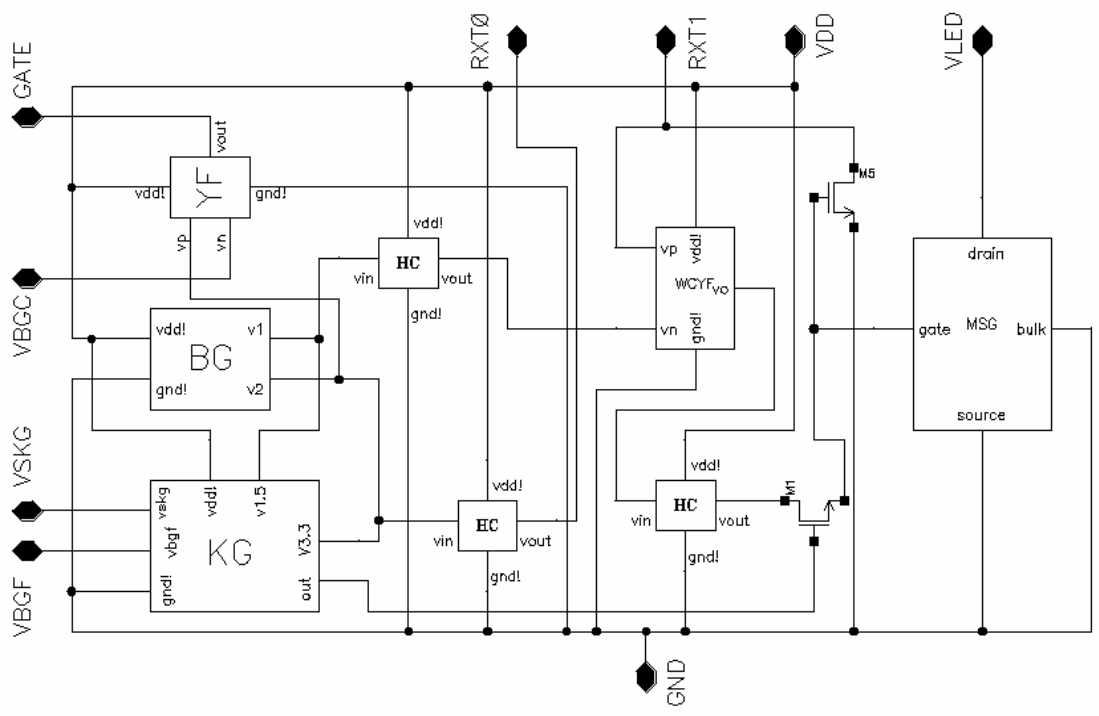

Figure 3. Circuit Diagram of Chip Application

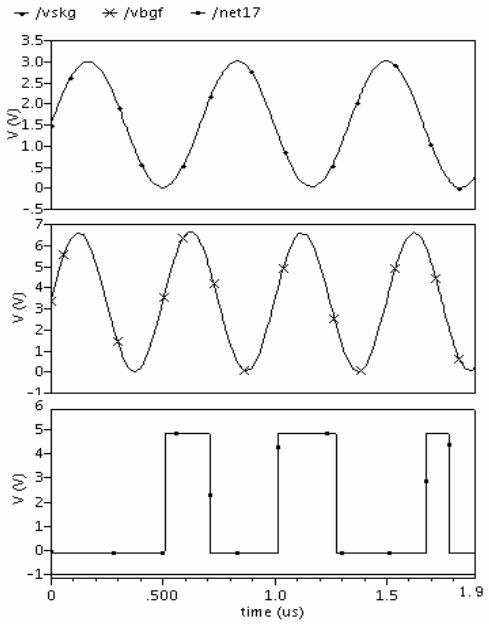

Figure 4. Simulation Waveform of LED Switch

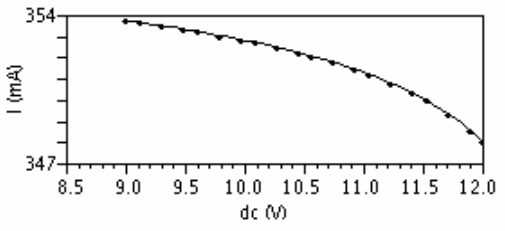

Figure 5. Waveform of LED Output Current

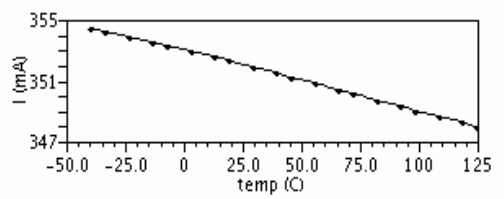

Figure 6. Change Tendency of Output Current When Environmental Temperature Changes

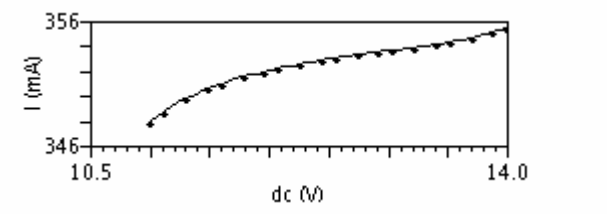

Figure 7. Change Tendency of Output Current When the Voltage of Storage Battery Changes

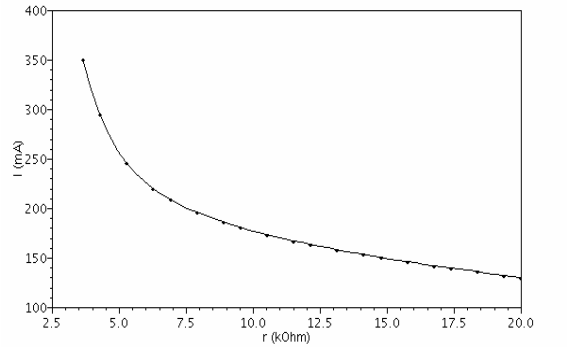

Figure 8. Relationship between the Sampling Resistance Rxt and Output Current

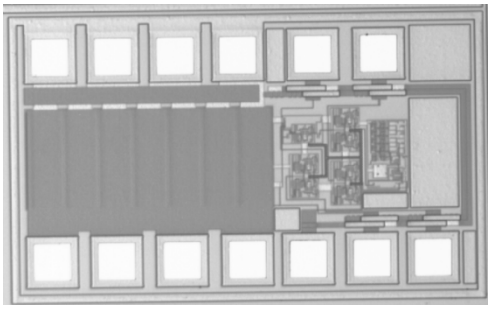

Figure 9. Drive Control Chip

Modern Applied Science

www.ccsenet.org/journal.html

Vol. 2, No. 3

May 2008

Market Research on the *Ephedra* Resource in Xinjiang and its Development Trend

Yundong Liu

College of Life Science, Shihezi University

Shihezi, Xinjiang 832003, China

Tel: 86-993-205-7216 E-mail: liuyundongmail@163.com

Shaoming Wang

College of Life Science, Shihezi University

Shihezi, Xinjiang 832003, China

Tel: 86-993-205-7216 E-mail: westwild@shzu.edu.cn

Abstract

Basing on referring to the literature about the usage of *ephedra* resource in Xinjiang, using the methods of personal investigation, telephone interview and E-mail, market research on the *ephedra* resource in Xinjiang was carried out in relevant governmental department, enterprises, scientific research institute, *ephedra* planter and those who reap *ephedra*. The formation and development of *ephedra* resource market in Xinjiang and the products were analyzed. In accordance with the status quo and future of *ephedra* market in Xinjiang, countermeasures were put forward to make full use of *ephedra* resource in the aspects of enterprise production, combination of traditional Chinese medicine and ecological environment protection.

Keywords: *Ephedra* resource, Xinjiang, Market consumption, Ephedrine

1. Introduction

Ephedra, which belongs to Gymnospermae, Ephedraceae, is an ancient genus (Liu, 2000). There are about 67 species, 40 of which are found in old continent, and 27 of which are found in new continent (14 are in North America, 13 are in South America). There are 15 species in China, two varietas and one forma, and there are 10 species, one forma in Xinjiang, which account for 66% of the total *ephedra* resources in China (Shen, 1995). Chinese Pharmacopoeia (2005 edition) adopted 3 species: *E.sinica* Stapf., *E.intermedia* Schrenk et Mey. and *E.equisetina* Bunge (State Pharmacopeia Committee of China, 2005).

Ephedra is used as an important traditional Chinese medicine since its medicinal value was found. In Shennong's Classic of Materia Medica, *Ephedra* was used in ventilating lung, diaphoresis, pungent warm and relieving rheumatic pains. *Ephedra* is a precious medicinal plant in China, it was recorded in all the medical books in the past dynasties (The Editorial Committee of The Plant Index of Xinjiang, 1994), and it is the only raw material to extract ephedrine. The ephedrine, naphtha, flavone and amylose of *ephedra* can be used as anti-asthmatics, and can raise pressure, shrink blood vessel and lower temperature. In 1885, a Japanese named Shanli extracted ephedrine from *Ephedra* sinica Stapf, after that, *ephedra* is mainly used to extract ephedrine. *Ephedra* is not only a medicinal plant, but also a middling grazing in winter and spring because it has large roots, can endure dry, cold and leanness, also, it is a good windbreak and sand-fixer (Jiang and Sun, 2001).

In recent years, the values of *ephedra* are gradually found, and *ephedra* is greatly consumed in market. The exploitation of *ephedra* resources accelerated the economic development, but *ephedra* is a rare natural resource, over exploitation of *ephedra*, overgrazing and opening up wasteland led to the shrinking of *ephedra* distribution, reduction of output and quality decline. Accordingly, the *ephedra* market changes greatly, stockbreeding is affected to a certain extent, and the vulnerable desert ecological environment will get worse and worse (Zha, et al., 2002). This paper studied the market of medicinal *ephedra* in Xinjiang and analyzed its development trend, with the purpose of providing reference for the scientific management, protection and sustainable utilization of medicinal *ephedra* in Xinjiang, and for solving the contradiction between the sustainable utilization of natural resources and environmental protection.

2. The formation and development of *ephedra* market in Xinjiang

2.1 The geographical condition in Xinjiang and ephedra distribution

Xinjiang is located in the northwest of China, it covers over 1.66 million square kilometers. Xinjiang is about 1/6 of the total area of Chinese land, and is the largest province of China. Xinjiang is located in the inner side of Asia, its landform is complex, the climate in Xinjiang is typical continental climate because it is away from the ocean, and is influenced by the closed landform and atmospheric circulation factors. Xinjiang is located at the connective site of several large geographical units, such as Altai, Tianshan Mountain, Pamirs, Kunlun Mountain, Aerjin Mountain and North Tibet Altiplano. Also, it is located at the connection site of European-Asian forest subregion, European-Asian grassland, central Asia desert, the desert subregion in the central Asia and the Himalayan plant subregion (Institute of Botany, CAS and Team of Xinjiang Comprehensive Scientific Survey, CAS, 1978). Owing to the complex and versatile natural environment, *ephedra* resources in Xinjiang are abundant, there are multiple species and the output is of large potential, *ephedra* spread over champaign, hills, Tulufan Basin that is 154 meters above the sea level, and the valley of mountain that is 4000 meters above the sea level (Liu, 1991).

2.2 The utilization of ephedra resources in Xinjiang and the formation of ephedra market

The pollens of *ephedra* were present in various stratums in the Cretaceous period, and in Oligocene period, it spread over all the stratums. The form of *ephedra* didn't change much since then, so it is an ancient plant (Yang, 2002). *Ephedra* spreads widely in Xinjiang, before it was used in industry to extract ephedrine, nobody paid attention to the plant, it was rarely used as a resource but used as fuel, some were used as pasture in spring and autumn, only a little was used as traditional Chinese medicine, hence, at that time, the amount of *ephedra* used in medicine is stable.

In 1930s, Chinese scholars firstly extracted a pure biotin from *ephedra*, i.e. ephedrine. It is indicated that ephedrine has two optical isomers, the levorotatory one is the well known ephedrine, and the dextrorotatory one is pseudo-ephedrine. The discovery greatly affected the international pharmacy world, after that, ephedrine was taken as a kind of "adrenomimetics" and was recorded by pharmacopoeia of European and American countries (Jiang and Sun, 2001).

Since 1950s, ephedrine production in China increased steadily; ephedrine was mainly manufactured as preparation. The rapid growth of international demand on ephedrine led to the great increase of ephedrine production in China. In 1960s, Xinjiang Pharmaceutical Factory was the first one to produce ephedrine, and in 1990s, there were 8 enterprises that produced ephedrine, the annual output was 200-250 tons, which accounted for 60% of the national output of ephedrine. The wild *ephedra*, the raw material, was not destroyed from 1960s to 1980s. The third statistical investigation into the Chinese traditional medicine resources in 1980s showed that the *ephedra* resources in Xinjiang was 540 thousand tons, Xinjiang Heshuo Ephedrine Products Co. Ltd, which was the largest company, can produce 180 tons of ephedrine annually, others can produce 10 tons to 80 tons. In late 1970s, the price of exported ephedrine was 110 thousand Yuan per ton, after ephedrine was found to play a role in losing weight, the supply of ephedrine in international market became short, and the price rushed to 550 thousand Yuan per ton, which is five times of the price in 1970s (Jia, 1997), Investigation showed that the highest price of ephedrine was over 60 thousand Yuan per ton. Enterprises' planned demand on *ephedra* exceeded the largest *ephedra* output in Xinjiang, most enterprises fell short of *ephedra* resource, so they raised the price to get enough raw material. Most *ephedra* diggers know little about the characteristic of *ephedra*, they dig *ephedra* regardless of season and manner, and some even uproot the ephedrine in order to be faster than others and to hold *ephedra* resources. The area, amount and the quality of *ephedra* are decreasing, and the vegetation and ecological environment of the desert area are destroyed. Once the *ephedra* is destroyed, it will be difficult to be restored. China has put forward several regulations to protect *ephedra* resources, such as Regulations on the Prohibition of the Collection and Selling of Hairy Grass and Unregulated Collection of Liquorice Roots and Chinese *Ephedra* (No.13 (2000) of State Council) (Liu, 2004; He, 2002). Table 1 and table 2 shows the enterprises that produce ephedrine and the enterprises that export ephedrine and it analogues in Xinjiang respectively.

Since 1990s, *ephedra* is cultivated by human in some districts of Xinjiang, such as Mulei, Hutubi, Ataile, Wenquan and Shuodu, sometimes total cultivated *ephedra* is up to 2000 hektares.

3. Changes in *ephedra* resource market in Xinjiang and analysis of the ephedrine export

Ephedrine from Xinjiang is for both domestic market and international market, and all of the ephedrine analogues (Ephedrine extract powder, pseudo-ephedrine) are exported. The products of ephedrine producing enterprises in China are crude extracts; they have low-level technology and small added value. In Martindale, the Complete Drug Reference, at least 360 kinds of preparations that contain ephedrine are recorded. In China, over 90 kinds of medicine contain ephedrine, such as Compound Pseudo-ephedrine Hydrochloride Tablets, Composite Terfenadine Tablets. In China, products from different enterprises are similar to one another, and there is great dependence on foreign market. The United States, the largest customer of Chinese ephedrine, greatly reduced the amount of ephedrine from China, artificial ephedrine is growing up, and the technology is improving day by day, so the demand of international market on ephedrine will grow steadily, the great demand on ephedrine caused by "food for losing weight" in 1990s will never

come up.

Since 2000, the demand of international market on ephedrine is always about 2000 tons, the ephedrine from Xinjiang accounts for 1/4 of the total natural ephedrine in international market. The Food and Drug Administration (FDA) of the United States demanded that ephedrine would be forbidden to be added in food for losing weight from April, 2004. In 2004, China became the third largest country that produce and export ephedrine, following Germany and Indian. Chifeng Pharmacy Group of Inner Mongolia and Kangyu Pharmacy Group of Zhejiang have become the largest domestic ephedrine producing enterprises. Ephedrine export in Xinjiang almost came to a halt in 2003. The export situation of pseudo-ephedrine in recent years would indicate the dynamic variation of *ephedra* product in Xinjiang as shown in figure 1, it can be seen that there was great annual variation in the export of pseudo-ephedrine, the largest amount was 134 thousand kg in 2001, and the smallest amount was 11.075 thousand kg in 2006, generally, the amount of exported ephedrine is decreasing, and it depends on international market to a great extent.

4. The development trend of *ephedra* market in Xinjiang and countermeasure

Artificial synthesized ephedrine is of good quality and costs less than extracted natural ephedrine, in addition, the output of synthesized ephedrine is stable. The international demand on ephedrine decreased greatly, FDA of the United States decided to eliminate ephedrine from the list of "dietary supplement". Ephedrine, morphine and heroin have similar effect, they are raw materials for both medicine and drugs, ephedrine can be manufactured as the famous "ice drug" (Methamphetamine), ecstasy, and so on. So ephedrine is one of the rigidly controlled raw materials for medicine by International Organization against Drug Abuse, Chinese government has established several measures to control the ephedrine product, enterprises are facing up to great challenges in the inspection for environment protection, and they should manage the enterprise scientifically and improve the quality of employees.

The challenges mentioned above demand reform in the enterprises that produce ephedrine. Market competition and governmental guidance will be introduced to cultivate one or two standardized enterprises that will have scientific management, apply high-new technology, produce high-quality product, and improve the added value of product, so the enterprise can base itself upon Xinjiang and meet the need of domestic and international market. The advantage of resource and brand should be brought into play thoroughly, so as to ensure the market share of Xinjiang's ephedrine in domestic and international natural ephedrine product market.

Over digging led to the sharp decrease of wild *ephedra* in Xinjiang, and led to the deterioration of the vulnerable ecological environment and desertification of farmland soil. The wild *ephedra* resource suffered the greatest destroy since 1900. Governmental departments (Department of Animal Husbandry, Department of Forestry, Drug Supervision and Management Department, Department of Agriculture) of Xinjiang Uygur Autonomous Region and Xinjiang Production and Construction Corps should make a thorough investigation into the wild *ephedra* resources, and divide the *ephedra* area into different kinds, including area that is forbidden to be exploited, area that can be exploited by turns, and areas that should be protected. In that way, the destroyed wild *ephedra* will be restored, other vegetation will also be restored and the ecological environment will be protected.

The cultivation of *ephedra* had become a mature technology since 1990s; government will continuously support enterprises to establish their own raw material base, so as to ensure the stable and sufficient raw material supply.

In a word, after the formation, development and rational regression of Xinjiang ephedra market, *ephedra* producing enterprises, *ephedra* cultivating enterprise and individual as well as the government will be more rational in *ephedra* management. *Ephedra* in Xinjiang will mainly be used as raw materials and traditional Chinese medicine, and be used to protect ecological environment. The amount of *ephedra* that is used as raw material for ephedrine producing enterprise will be greatly reduced, so the *ephedra* resources will have an opportunity to be restored.

Acknowledgement

We would like to thank Urumchi Customs People's republic of China; Xinjiang Urumchi Municipality Food and Drug Administration; Xinjiang Foreign Economy Trade; Department of Animal Husbandry of Xinjiang Uygur Autonomous Region; Xinjiang Institute of Ecology and Geography, Chinese Academy of Sciences and Xinjiang International Industry Co. Ltd.

References

He, Baoyen. Si, Jianning and Zhang, Yongqing. (2002). Present Situation of *Ephedra* Resources and Their Exploiting Countermeasures. *World Science and Technology-Modernization of Traditional Chinese Medicine*. 4 (4): 63-68.

Institute of Botany, Chinese Academy of Sciences and Team of Xinjiang Comprehensive Scientific Survey, Chinese Academy of Sciences. (1978). *The Vegetation and its Utilization in Xinjiang*. [M]. Beijing: Science Press.

Jia, Xiaoguang and Sulaiman Halike. (1997). Utilization and protection of Chinese ephedra resources. International workshop about the energy consumption mode and the influence on environment [A]. 397-398.

Jiang, Hailou and Sun, Shuangyin. (2001). *Precious Vegetation Herba Ephedrae*. Inner Mongolia:The Publishing House of Science Technology. 1-19.

Liu, Guojun. (2000). *Ephedra* [M]. Beijing: China Press of Traditional Chinese Medicine.

Liu, Guojun. (1991). Study on the conditions for *ephedra* in Xinjiang. *Abstracts of fiftieth anniversary meeting of Botanical Society of Xinjiang*. Beijing: Science press. 325-328.

Liu, Lei. Liu, Jianjun, Huang, Shaohua and Wang, Jun. (2004). Protection and Utilization of Ephedra resources in Xinjiang. *Arid Environmental Monitoring*. [J]. (18) 3: 146.

Shen, Guanmian. (1995). Distribution and evolution of the genus *ephedra* in china, *Acta Botanica Yunnanica*, [J] 17 (l):15-20.

State Pharmacopeia Committee of China. (2005). *Chinese Pharmacopeia*. [S]. Beijing: Chemical Industry Press. 233.

The Editorial Committee of The Plant Index of Xinjiang. (1994). *The Plant Index of Xinjiang*. Volum 1. [M] Urumchi: Xinjiang Science, Technology and Sanitation Publishing House. (K). 87-88

Yang, Yong. (2002). Classification of Ephedraceae in China and differentiation of Ephedraceae. (D). *Doctor Dissertations of Institute of Botany, Chinese Academy of Sciences*. 92-121.

Zha, Lihang. Su, Zhiguo and Zhang, Guozheng. (2002). Application and research on *ephedra* resource. *Chinese Bulletin of Botany.* [J] 19 (4): 396-405.

Table 1. Enterprises that produce ephedrine and other ephedrine analogues in Xinjiang (2007)

Enterprises	Main products
Xinjiang Pharmaceutical Factory	Ephedrine, Pseudo-ephedrine, Ephedrine extract powder
Xinjiang Tuokexun County Tianshan Mountain Joint Ephedrine Factory	Ephedrine, Pseudo-ephedrine
Xinjiang Heshuo Ephedrine Products Co.Ltd	Ephedrine, Pseudo-ephedrine, Ephedrine extract powder
Xinjiang Hamigequan Pharmaceutical Co., Ltd.	Ephedrine, Pseudo-ephedrine
Xinjiang Tuofeng Pharmaceutical Co., Ltd.	Ephedrine, Pseudo-ephedrine
Xinjiang Wenquan County Ephedrine Factory	Ephedrine, Pseudo-ephedrine, Ephedrine extract powder
Xinjiang Kuche County Joint Ephedrine Factory	Ephedrine, Pseudo-ephedrine
Xinjiang Ashan Pharmaceutical Co., Ltd.	Ephedrine, Pseudo-ephedrine, Ephedrine extract powder

Table 2. Enterprises that export ephedrine and other ephedrine analogues in Xinjiang (2007)

Enterprises that export ephedrine	Enterprise that export ephedrine analogues
Xinjiang Medicines and Health Products Import & Export Corp.	Xinjiang Medicines and Health Products Import & Export Corp.
Xinjiang Machinery, Chemicals, Metals & Minerals, Light Industry Product Import. & Export. Corp.	Xinjiang Machinery, Chemicals, Metals & Minerals, Light Industry Product Import. & Export. Corp.
Xinjiang (Production and Construction Corps) Nongken Foreign Economic & Trade Industry Development Corp.	Xinjiang (Production and Construction Corps) Nongken Foreign Economic & Trade Industry Development Corp.
Xinjiang Heshuo Ephedrine Products Co.Ltd	
Xinjiang Pharmaceutical Factory	
Xinjiang Wenquan County Ephedrine Factory	

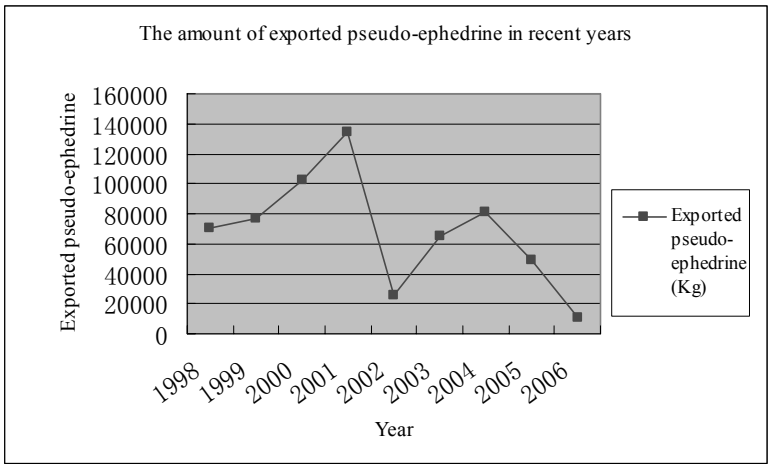

Figure 1. The annual amount of exported pseudo-ephedrine in recent years

Modern Applied Science

www.ccsenet.org/journal.html

Vol. 2, No. 3

May 2008

The Measure of Exogamous Marriage through Disagreement Scaling

Chua Chee Ming

School of Mathematical Sciences, Universiti Kebangsaaan Malaysia

43600 UKM Bangi, Selangor, Malaysia

Tel: 60-012-637-6723 E-mail:cheeming.chua@gmail.com

Ahmad Mahir Razali

School of Mathematical Sciences, Universiti Kebangsaaan Malaysia

43600 UKM Bangi, Selangor, Malaysia

Tel: 60-3-8921-5788 E-mail: mahir@ukm.my

Abstract

In this paper we used the weighted kappa through disagreement scaling proposed by Cohen (1968) to measure the exogamous marriage. It is the interest of sociologist to investigate the trend of exogamous or mixed marriage between different ethnic groups, as the upward trend of mixed marriage can be view as degree of assimilation of particular ethnic groups. We are able to measure the strength of exogamous marriage directly. We found that the upward trend of mixed marriage among Americans of different ethnicity tend to increase from 1980 to 2000. We also used the estimated large sample variance of weighted kappa given by Fleiss *et al*. (1969) to build the Wald confidence interval and hence testing the null hypothesis of nonexistence of exogamous marriage.

Keywords: Weighted kappa, Exogamous marriage, Assimilation, Disagreement scaling

1. Introduction

In American society with multiethnic immigrants, the issue of exogamous marriage has been widely studied. The kappa statistics (Cohen, 1960) were introduced to measure the agreement between two raters for nominal scales. Strauss (1977) has applied the kappa statistics by Cohen to study the endogamous marriage, followed by Rust and Seed (1985) and further developed by Ahmad Mahir (1993). This issue refers to the intersection of race and class.

Lessard (2001) has used the definition given by Chang (1999) who stated that "Intermarriage refers to marriage between members of different groups, identified by one or more socially important dimensions of differentiation". In this paper, we studied the intermarriage data which have been arranged in the form of a square two-ways contingency table. This arrangement was originally introduced by Ahmad Mahir (1991) as shown in table 1. The ethnic groups for both men and women are given by E_1, E_2 ,.., E_k.The diagonal cells refers to the endogamy marriage that is the marriage between the brides and grooms of the same ethnic groups, whereas off diagonal cells give the couples of exogamous marriage that is the marriage between the brides and grooms of different ethnic groups. The main objectives of this paper are using the weighted kappa to measure marriage the strength of the exogamous marriage and to study the trend of the exogamous marriage.

For simplicity, we assigned the weight zero and one to the diagonal and off diagonal cells respectively. Then, weighted kappa was calculated followed by the construction of the 95% confidence interval with the estimated variance given by Fleiss *et al*. (1969).

We extracted the five percent of the 1980, 1990 and 1990 U.S. censuses, made available through the Integrated Public Use Microdata Sample (IPUMS, 2003). By using cross tabulation procedure of SPSS software, we obtained two-ways table shown in table 2, 3 and 4.

2. Theories and the calculation

Cohen (1968) proposed a basic formula for weighted kappa which is given by

$$\kappa_w = 1 - (q_o / q_e) \tag{2.1}$$

where

$$q_o = \sum_{i=1}^{k}\sum_{j=1}^{k} w_{ij} p_{oij} \quad (2.2)$$

and

$$q_e = \sum_{i=1}^{k}\sum_{j=1}^{k} w_{ij} p_{eij} \quad (2.3)$$

Let p_{oij} be the observed proportion of marriage placed in the (*i,j*) cells and p_{eij} be the expected proportion in the (*i,j*) cells. The investigator chose the disagreement weighted scale as follow:

$$w_{ij} = \begin{cases} 0 & if\ i = j \\ 1 & otherwise \end{cases} \quad (2.4)$$

Assume that we have x_{ij} which is the number of observation in the (*i,j*) cell with a total of *n* observations. Let x_{i+} and x_{+j} refer to the total sum of the *i*th row and *j*th column respectively. The estimates of p_{oij} and p_{eij} are given by

$$\hat{p}_{0ij} = x_{ij} / n \quad (2.5)$$

and assuming that the column and the row variables are independent.

$$\hat{p}_{eij} = x_{i+} x_{j+} / n \quad (2.6)$$

By substituted Eq. (2.2) to Eq. (2.6) into Eq. (2.1), we obtained the estimated weighted kappa as below.

$$\hat{\kappa}_w = 1 - (n\sum_{i=1}^{k}\sum_{j=1}^{k} w_{ij} x_{ij} / \sum_{i=1}^{k}\sum_{j=1}^{k} w_{ij} x_{i+} x_{+j}) \quad (2.7)$$

Fleiss *et al.* (1969) has derived the formula for estimated large sample variance of $\hat{\kappa}_w$, useful in setting up confidence interval for comparing two independent values of $\hat{\kappa}_w$. This estimated large sample variance is

$$\hat{\text{var}}(\hat{\kappa}_w) = \{\sum_{i=1}^{k}\sum_{j=1}^{k} p_{ij}[w_{ij}(1-q_e) - (\bar{w}_{i+} + \bar{w}_{+j})(1-q_o)]^2 - (q_o q_e - 2q_e + q_o)^2\} / (n(1-q_e)^4) \quad (2.8)$$

with weighted average of the weights in the *i*th row, $\bar{w}_{i+} = \sum_{j=1}^{k} w_{ij} p_{+j}$ and $\bar{w}_{+j} = \sum_{i=1}^{k} w_{ij} p_{i+}$

a weighted average of the weights in the *j*th column.

We introduced the overall exogamy measure as lambda, λ where the estimate is given by

$$\hat{\lambda} = 1 - \hat{\kappa}_w \quad (2.9)$$

We can show that the variance of $\hat{\lambda}$ is approximately equals to the variance of $\hat{\kappa}_w$ since 1 is a constant. We have

$$\text{var}(\hat{\lambda}) = \hat{\text{var}}(1 - \hat{\kappa}_w) \approx \hat{\text{var}}(\hat{\kappa}_w) \quad (2.10)$$

3. Result and Finding

We computed the strength of exogamy estimate $\hat{\lambda}$ and $\hat{\text{var}}(\hat{\lambda})$ using marriage data sets given in table 2, 3, and 4. The 95 % confidence limit also been constructed to test the hypothesis $\hat{\lambda} = 0$. The results are shown in the table 5.

According to Cohen (1968) both measures are chance corrected proportion. Weighted kappa is a special case of kappa. The value of weighted kappa κ_w is smaller than the κ as it gives weight to the disagreement cells. Normally the value of weighted kappa falls the in the range (0,1), so we can deduce overall exogamy measure is $0 < \hat{\lambda} < 1$. If $\hat{\lambda} = 1$, it said to be perfect exogamy. Where as $\hat{\lambda} = 0$ implied that exogamy does not happen.

By comparing data set 1, 2 and 3 we can conclude that the exogamous marriage in the U.S society has increased over the past two decades as the value of $\hat{\lambda}$ has increased from 0.0967 to 0.1764. The increase of $\hat{\lambda}$ for year 1980 to 1990

is 0.0335 compare to the year 1990 to 2000 is 0.0462. From Figure 1 indicate the upward exogamous marriage trend of American society.

For testing the null hypothesis $\hat{\lambda} = 0$, we can reject the null hypothesis for the two decades that we chosen.

References

Ahmad Mahir R. 1991. Statistical Issues in Interracial Marriages. PhD.Thesis. Medical University of South Carolina.

Bishop Y.M.M.,Feinberg S.E. & Holland P.W. 1975. *Discrete Multivariate Analysis: Theory and Practice.* Cambridge: MIT Press.

Chang Y.C. 1999. Models for Intergroup Association: An Examination of Intermarriage in the United

States, 1980-1990. Department of Sociology, University of South Carolina.

Cohen J.1960. A coefficient of agreement for nominal scales. *Psychological Measurement* 20: 37-46.

Cohen J. 1968. Weighted kappa: Nominal scale agreement with provision for scaled disagreement or partial credits. *Psychological Bulletin* 70: 213-220.

Fleiss J. L., Cohen J. & Everitt B.S. 1969: Large sample standard errors of kappa. *Psychological Bulletin* 72: 323-327.

IPUMS. 2003. *IPUMS User's Guide*. Minneapolis, MN: Minnesota Population Center. [Online] Available: http://www.ipums.org/usa/doc.html

Lessard C. 2001.*Ethnic Exogamy in Canada in 1996: With a special focus on Toronto and Vancouver*.SRA 569. Ottawa : Strategic Research and Analysis, Department of Canadian Heritage.

Rust P. F. & Seed P.1985. Equality Endogamy: Statistical Approaches. *Social Science Research* 14:57-59.

Strauss D.J. 1977. Measuring endogamy. *Social Science Research* 6:225-245.

Table 1. Data Format

		Women								**Total**
		$\mathbf{E}_1$	$\mathbf{E}_2$	.	.	$\mathbf{E}_j$	.	.	$\mathbf{E}_k$	
Men	$\mathbf{E}_1$	x_{11}	x_{12}	.	.	x_{1j}	.	.	x_{1k}	x_{1+}
	$\mathbf{E}_2$	x_{21}	x_{22}	.	.	x_{2j}	.	.	x_{2k}	x_{2+}
	.	.	.	.	.	.	.	.	.	.
	.	.	.	.	.	.	.	.	.	.
	$\mathbf{E}_i$	x_{i1}	x_{i2}	.	.	.	.	.	x_{ik}	x_{i+}
	.	.	.	.	.	.	.	.	.	.
	.	.	.	.	.	.	.	.	.	.
	$\mathbf{E}_k$	x_{k1}	x_{k2}	.	.	.	.	.	x_{kk}	x_{k+}
Total		x_{+1}	x_{+2}	.	.	x_{+j}	.	.	x_{+k}	n

Source : Ahmad Mahir(1991)

Table 2. Data set 1 of marriage by race of U.S. Women 1980 census

		Women							
		White	Black/ Negro	American Indian /Alaska Native	Chinese	Japanese	Other Asian / Pacific Islander	Other races	Total
Men	White	2 228 918	1 639	6 485	1 106	3 266	6 534	1603	2 249 551
	Black/Negro	5 193	171 500	271	53	181	608	166	177 972
	American Indian /Alaska Native	6 355	148	5 993	8	19	79	55	12 657
	Chinese	654	21	9	7 635	223	186	16	8 744
	Japanese	891	23	7	152	5 984	235	17	7 309
	Other Asian or Pacific Islander	2 982	111	66	152	261	16 809	61	20 442
	Other races	1 906	120	59	21	28	75	4131	6 340
	Total	2 246 899	173 562	12 890	9 127	9 962	24 526	6049	2 483 015

Source: 5 % Sample of 1980 U.S.Census IPUMS

Table 3. Data set 2 of marriage by race of U.S. Women 1990 census

		Women							
		White	Black/ Negro	American Indian /Alaska Native	Chinese	Japanese	Other Asian / Pacific Islander	Other races	Total
Men	White	2 355 248	2 541	9 361	2117	4 058	10 083	8 372	2 391 780
	Black/Negro	6 990	150 587	409	72	188	854	870	159 970
	American Indian /Alaska Native	8 973	220	7 769	15	46	147	275	17 445
	Chinese	1 056	36	8	14 994	324	461	79	16 958
	Japanese	1 382	13	23	260	6 707	355	96	8 836
	Other Asian or Pacific Islander	3 977	158	110	308	382	34501	439	3 9875
	Other races	9 753	516	469	65	77	498	61 674	7 3052
	Total	2 387 379	154 071	18 149	17 831	11 782	46 899	71 805	2 707 916

Source: 5 % Sample of 1990 U.S.Census IPUMS

Table 4. Data set 3 of marriage by race of U.S. Women 2000 census

		Women							
		White	Black/ Negro	America Indian /Alaska Native	Chinese	Japanese	Other Asian / Pacific Islander	Other races	Total
Men	White	2 348 792	4 433	9 453	3212	3999	13 266	33 909	2 417 064
	Black/Negro	11 471	165 134	412	77	180	1 190	3 929	182 393
	American Indian /Alaska Native	8 820	214	9 429	16	19	131	1 153	19 782
	Chinese	1 238	26	5	22 448	277	750	265	25 009
	Japanese	1 360	22	16	292	5642	440	301	8 073
	Other Asian or Pacific Islander	4 887	198	98	572	377	58 005	1 695	65 832
	Other races	31 795	2 115	1 410	350	459	2 176	121 530	159 835
	Total	2 408 363	1 72 142	20 823	26 967	10953	75 958	162 782	2 877 988

Source: 5 % Sample of 2000 U.S.Census IPUMS

Table 5 .Parameters estimate, standard errors and 95% confident limit for $\hat{\lambda}$

Data Set	Weighted Kappa, $\hat{\kappa}_w$	Exogamy estimate $\hat{\lambda} = 1 - \hat{\kappa}_w$	Standard Errors ($\hat{\lambda}$)	95% Confidence Limit $\hat{\lambda}$
1	0.9033	0.0967	0.000777	(0.0952, 0.0982)
2	0.8698	0.1302	0.0008381	(0.1286, 0.1318)
3	0.8236	0.1764	0.0009779	(0.1745, 0.1783)

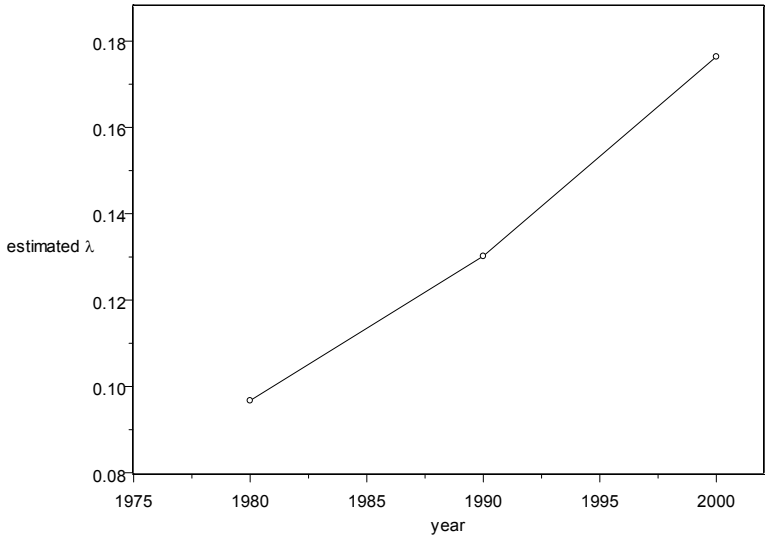

Figure 1. The trend of exogamous marriage in United States for the year 1980, 1990 and 2000 census.

Modern Applied Science

www.ccsenet.org/journal.html

Vol. 2, No. 3

May 2008

Enzymatic Process for The Wool Fabric Anti-felting Finishing

Li Dong & Lei Xu
Textile College, Tianjin Polytechnic University
Tianjin 300160, China
E-mail: dongli0515@yahoo.cn E-mail: suelee_1983@163.com

Abstract
Recently washable wool is strongly requested in order to avoid dry cleaning with chlorinated solvents such as perchlomethyiene. In this paper, a new enzymatic process direction is described for obtaining machine washable wool with acceptable quality. The principle of enzymatic process is introduced. To get a good result, proper pre-treatment process and proper enzyme is discussed. The conclusion gives advice to improve the quality of enzymatic wool fabrics.
Keywords: Enzyme, Wool, Fabric, Anti-felting finishing, Pre-treatment

Introduction

Wool is a natural protein fiber with good wearing properties[1,2], but have some short-cuts either -- Wool textiles in the wet state are sensitive to felt and shrink when applying mechanical action as in the case of washing.This can be explained by the scaled fiber structure. On the fiber surface, the friction of the wool fiber in the scale direction is therefore lower than the friction against the scale direction, a phenomenon which is called the differential frictional effect[3]. The anti-felting treatment is to get the scales partly removed, or the edges from the overlapping scales smoothed.After the treatment, fabric felting tendency is reduced, which make the wool costumes washable.

For this purpose, three anti-felting processes are commercially practiced[4-8]: subtractive (oxidation, reduction), additive (synthetic resin layer) and a combined process (e.g. chlorine/ hercosett process). However, these processes are the same in using strong oxidants, thus cause the contamination of wastewater and change the natural wool character to a more synthetic handle. The necessity to use more environmental friendly processes leads to the replacement of conventional chemical treatments by enzymatic ones.

Enzyme is a biocatalyst, it can act stably in a certain mild temperature. Compare with chemical treatments in anti-felting, enzymes have lot advantages[9,10]:

Water saving. Conventional treatments need repeated rinsing to ensure no chemical residues on the fabric. In most enzymatic treatments, because it is non-toxic, rinsing often take one time, this can save plenty water and cut the production's cost.

Low temperature. Enzyme often acts in mild temperature below 70℃, only few enzyme is active on above 70℃, while chenmical process often need a tenmerature higher than 100℃. So enzyme method can save money in heat energy spent.

Circulation use. Enzyme acts as a biocatalyst, it can't get consumed in the treatment, moreover, it can be used in circulation. Small mount enzymes can treat blocks of fabrics in one batch.

Devices protection. Enzyme treatment act in a neutral-ph (usually 8~10), thus have little corrosion on devices.The course is mild too, there is neither any evaporative emission nor any irritant gas generated in enzymatic process.

Enzyme has been researched for decades, but in wool anti-felting treatment, there are some essencial processes as latter discussed.

1. Pre-treatment

As Fig.1 shows, the structure of wool scales arrays like roof tiles. In fact, one scale contains the epicuticle and the inner layer, the epicuticle has many cross-linked amide bonds on surface, many adipoids also in good arrangement, which made epicuticle chemical stable and water proof. Current enzymatic processes have less weight loss rate, they are difficult to control and are not sufficiently predictable. Such treatment can easily cause excessive damage to the fiber cuticle or enhance the inhomogeneous along fiber. Under the epicuticle is full of proteins formed by Cysteines, this is the part to be removed. So it is essencial to use some oxidants as pretreatment, after being oxidized, the proteins in the scales can be hydrolyzed homogeneously, this will bring a good anti-felting effect.

Usually, some oxidizes such as chlorite salts, hypophosphites, dichloro isocyanates, potassium permanganate and persulfuric acids can act well in the pretreatment. But on considering the pollution they cause, especially chlorite salts, so hydrogen peroxide were used as a replacement. In Fig.2 we can find, after the pretreatment by sodium hypochlorite solution and hydrogen peroxide solution, scales are roughened. But at the same concentration, more upwarpped part of the scale were dissolved in the former. In the fabric, sodium hypochlorite pretreatment(Fig.2.b) can cause 5.7% weight loss and 19.7% in strength loss, which is obviously higher than the hydrogen peroxide one(Fig.2.c: 3.8% in weight loss,

12.6% in strength loss). To reduce the strength loss, pretreatment should taken in saturated aqueous salts solutions, this can conserve a strength loss to 7.2% and 4.9% in Fig.2.b&c's treatment.

Judging from many reaearch reports[11], a feasible pretreatment process is: wool plan knitted fabrics immersed into a ammonia sulfate saturated solution containing 2~8w.t.% hydrogen peroxide, 0.5%owf wetting agents and above 1%owf catalysts. The bath ratio is 1:30, treating time is mainly decided by the concentration of the hydrogen peroxide but less than 15min. After the treatment, fabrics should get washed by plenty water to get further enzyme treatment.

2. Enzymatic treatment

In early days, enzymes only come from common animals and plants, wool treatment enzymes are rather few, the pawpaw proteinase, trypsinase and pepsase are mostly used. Due to the quick development of microbial technology, new enzyme specis come out frequently. For wool fabric anti-felting treatment, proper enzymes can be divided into three groups.

2.1 Animal origined enzymes

Porcine trypsin is the mostly used, because it can be easily extracted from animal visceras. Porcine trypsin's active PH is 7.6~9.5. It's dosage is about 1.5~3owf%[12].

2.2 Plant origined enzymes

Papain is an endolytic cysteine protease which is isolated from papaya latex. The papain has strong biological activity of about 3,000,000 u/g and good water-solubility. It can incorporate any of a wide variety of enzymes and increase the rate of biological changes such as the ripening of fruit. Hence it can help stimulate keratin protein synthesis and repair. It's active PH is 8~10, and the dosage is about 2~5owf%[7,12].

2.3 Synthetic enzymes or enzymes for industrial use

Nowadays, with the rapid bio-technic progress, more synthetic enzymes are desighed for wool treatment, they are cheap in price. In china, a Synthetic enzyme is desighed for wool products called woolase, it is active in PH 8.5~9, 45℃[13]. But enzymes from bacteria have a bright future --- enzyme production is 'green', the residues of the production are good fertilizers; moreover, after the selection and purification, the enzyme have better activity to wool scales. Currently, there have some enzymes act significantly to wool. e.g. Savinase active in PH8~9,45~55℃, Esperase in PH8.5~9, 45℃[14,15].

From Tab.1 we can find, animal and plant origined enzymes are less active than the refined enzymes as savinase etc. But the specificity of the refined enzyme are not so good because it caused only 43~55% strength retain. Comparing this three propeties, esperase is better than the other two refined enzymes. To get a better result, new enzymes with goal to hydrolysis wool scales need to be developed by advanced enzyme refining technique.

3. Conclusion and Prospect

Enzymes in wool anti-felting is a most promising area in order to achieve high-grade, comfortable and washable effects. To sum up the applations of enzymes in wool industry, the developing trend were obtained.

(1) With the environmental consideration, enzymes consumption in wool industries will have a rapid increase. This will call for a simple, low cost technique in enzyme production.

(2) The stability and the specificity of enzymes need to be enhanced. Enzyme is a special protein, its activity can easily be affected by temperature and other chemical reagents. The wool mill should find a proper process to keep enzymatic fabrics quality stability. As previous mentioned, new enzymes should be developed in order to improve the anti-felting effect with less strength loss.

(3) Compound of various enzymes to improve enzyme efficiency. There were questions on enzyme compatibility need future studies to discover.

Acknowledgement

The authors wish to thank Liu J.Z & Zhou Q of Tianjin Polytechnic Univ's Textile Test Center for their kindly help.

References

Pielesz Anna. (2006). Studies of wool keratin by EPR spectroscopy. *Journal of Applied Polymer Science.*102.1459-1465.

Fan, Jie, &Yu, Weidong. (2007). A Critical Review on Separation Methods of Micro-configuration of Wool Fiber and the Possibility of Application of This Anisotropic Material. *Materials Review*. 9. 98- 102.

Yao, Mu & Zhou, Jinfang. (1990). Textile materials(2nd ed.). Beijing:Sino-textile Press, (Chapter 2).

Tonin, Claudio Innocenti, Riccardo. (2007). Process optimization and industrial scale-up of chitosan based anti-felting treatments of wool. *Journal of Natural Fibers*. 4. 77-90.

Shen, Jinsong, Rushforth Mike & Cavaco-Paulo Artur. (2007). Development and industrialisation of enzymatic shrink-resist process based on modified proteases for wool machine washability. *Enzyme and Microbial Technology*. 40. 1656-1661.

Chen, Qihong H, Au K F, Yuen C W M. (2004). An analysis of the felting shrinkage of plain knitted wool fabrics. *Textile Research Journal*. 74. 399-404.

Li, Xia, Gao, Weidong & Lu, Yuzheng. (2006). The Actuality and Prospect of Shrink-proof Finishing of Wool Textiles. China Textile Leader. 9. 64-67.

Wang, Xin & Guo, Lamei. (2006). Effectiveness of NaClO and $KMnO_4$ in anti-felting treatments for wool fabric. Progress in Textile Science&Techology.18.33-35.
Cui, Shuling & Zhang Xuejing. (2006). Application of proteinase as a modifying agent for wool fiber. *Wool Textile Journal*. 35. 17-19.
Li, Shuhua, Gu, Xiaomei & Qiu, Hongjuan. (2007). Application of Bioenzyme Technology to Dyeing and Finishing and Its Prospect. *Textile Dyeing and Finishing Journal.* 29. 13-17.
Lenting H.B.M. Schroeder M & Guebitz GM. (2006). New enzyme-based process direction to pre- vent wool shrinking without substantial tensile strength loss. *Biotechnology Letters*. 28. 711-716.
Zhang, Qian. (2006). The environment firendly finishing for wool fabrics anti-felting. *Wool Textile Journal*. 34. 53-57.
Zhang, Qian, Zhang, Jianfei & He Jiayi. (2007). Shrinkproofing treatment of wool woven fabric using protease. *Journal of Textile Research.* 12. 76-80.
Novo-enzyme Ltd. www.novozymes.com.(September,2007).
Smith Edward, M Green, Laura E. (2003). Savinase is a bactericidal enzyme (multiple letters). *Applied and Environmental Microbiology*. 69. 719-721.

Table1. Performances of wool plan knitted fabrics treated by different enzymes(55℃, PH8.5 for 15min, after the H_2O_2 pretreatment)

	Savinase	Esperase	Woolase	Papain	Porcine trypsin
Felting shrinkage(%)	0.83	4.32	0.95	2.49	3.83
Strength retain(%)	43.00	54.70	74.10	75.80	75.10
Weight loss(%)	12.27	4.56	6.59	6.83	5.81

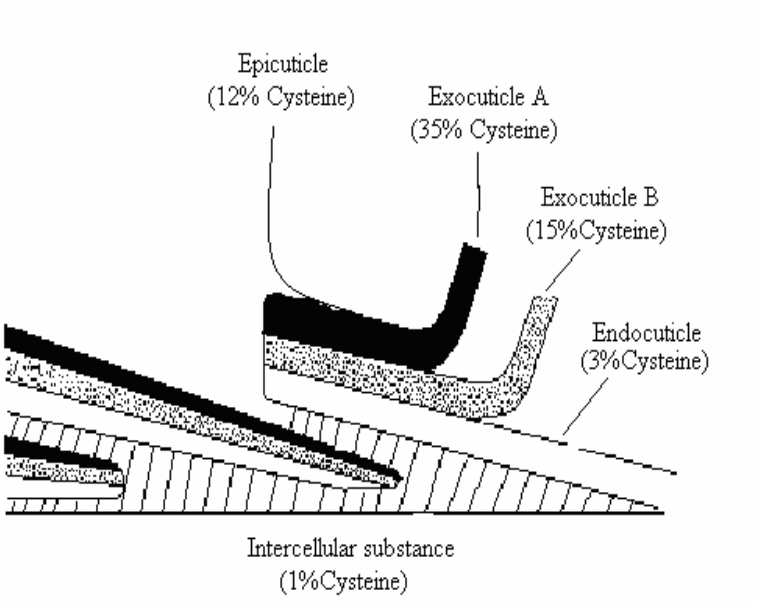

Figure 1. The structure of wool fiber scales and their Cysteine content

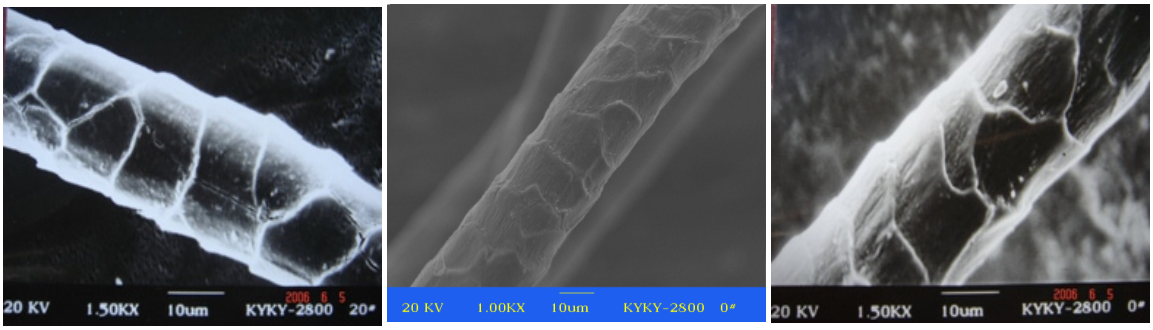

a b c

Figure 2. SEM graphs of rough wool fiber(a) and wool fiber treated with (b)3w.t.% hydrogen peroxide solution, PH=10, 10min and (c) 3w.t.% hydrogen peroxide solution, PH=10 for 10min.

Modern Applied Science

www.ccsenet.org/journal.html

Vol. 2, No. 3

May 2008

An Input-output Analysis of Sources of Growth and Key Sectors in Malaysia

Rohana bt Kamaruddin

Faculty of Business Management

Universiti Teknologi MARA, Malaysia

Tel: 60-3-5544-4935 E-mail: rohana070@salam.uitm.edu.my / rohana77@hotmail.com

Zakariah Abdul Rashid

Faculty of Economics and Management

Universiti Putra Malaysia, Malaysia

Tel: 60-3-8946-7702 E-mail: zakariah@econ.upm.edu.my

Kamaruzaman Jusoff

Faculty of Forestry

Universiti Putra Malaysia

Serdang 43400 Selangor, Malaysia

Tel: 60-3-8946-7176 E-mail: kamaruz@putra.upm.edu.my

Abstract

The paper examines the sources of growth and key sectors of Malaysia's economy over 1978-2000 using a decomposition method and Rasmussen degree of dispersion within the input-output (IO) framework. The model uses three comparable IO tables for 1978, 1991 and 2000 as the main data sources and accounts for output changes from a demand side perspective. The chosen structural decomposition analysis (SDA) based on the comparison between two IO tables, allows us to decompose each sector's and industry's output growth. It decomposes output growth of each sector to domestic demand expansion, export demand expansion, import substitution of final goods, import substitution of intermediate goods, and changes in IO coefficients. The analysis by sub periods, 1978-1991 and 1991-2000 show that there was a switch in the role of domestic-demand and export-demand expansion. The constituent factors that contribute positively to change in the period, 1978-1991 are mostly domestic demand expansion (63.35%) and export demand expansion (33.33%). However in the second sub period, 1991-2000, export demand expansion increased by 12.43% and domestic demand expansion decreased to 48.11%. Taking the whole 1978-2000, domestic demand expansion appears to have been the major source of output growth, contributing about 82%, followed by export demand expansion 62%. Combining the source of growth and key sector through backward linkages, the study revealed that most of the sectors induced its supplying production strongly for domestic market.

Keywords: Structural change, Input-output, Decomposition, Domestic demand expansion, Export demand expansion, Linkages

1. Introduction

The Malaysian economy has experienced rapid economic growth during the past few decades. Malaysia's GDP grew at an average rate of 5.1 percent in the 1960's and 7.8 percent in the 1970s. In the 1980's, the Malaysian economy continued to grow, albeit at a lower average rate of 0.05 percent due to the global recession in 1985 – 1986. With the recovery of the world economy, the Malaysian economy picked up rather rapidly from 1991 to 1995 at an average rate of 9.5 percent per annum. The Malaysian GDP expanded at the average rate of 8.7 percent per annum during the period 1996 – 1997 before registering a negative growth rate of 7.4 percent in 1998 due to the East Asian financial crisis. Efforts by the government to resuscitate the economy starting from the mid 1998 succeeded in generating an average growth rate of 4.75 percent during the period from 1999 – 2002. The experience of the rapid economic growth has been accompanied by low consumer price index, low unemployment and rising per capita income.

A basic development fact is that countries experienced a structural transformation as they develop. This unprecedented rapid economic growth has been accompanied by a marked structural transformation of the Malaysian economy. While the agriculture sector's share in GDP declined from 22.3 percent in 1980 to 8.7 percent in 2002, the contribution of the industrial sector grew from 38.5 percent in 1980 to 44.5 percent in 2002. Most of this surge came from an expanding manufacturing sector, with its contribution to the GDP increasing by 50 percent over two decades from 18.5 percent in 1980 to 29.9 percent in 2002.

The manufacturing sector led in contributing to the buoyant growth of the economy with expansion of output in most industries, brought about by the strong demand in both the domestic and export market.

2. Methodology

2.1 Structural decomposition analysis

This study deals with the composition structural change of relevant economic sectors or industries, within the general approach developed by Chenery (1960) and extended by Syrquin (1988) and Syrquin and Chenery (1989). A considerable number of recent applications of the method exist in the literature (e.g., Dewhurst, 1994; Liu and Sal, 1999). According to Rose and Miernyk (1989), structural decomposition analysis can be defined as a method of distinguishing major changes within an economy by means of comparative static changes in key sets of parameters. Its origins date back to the work of Leontief (1941) on the structure of the United States economy. Structural decomposition analysis (SDA) is a comparative static method to assess the structural changes in an economy using input-output data. Based on the idea that the change over time on some variable is decomposed into the changes in its determinants, it is widely used as a tool to quantify the underlying sources of change.

The I-O model is widely used in the study of economic structural changes for several reasons. First, an I-O table provides a comprehensive and consistent statistical account of an economy by taking into account the most important economic transactions (or direct input coefficients), which generally cannot be obtained from a national statistical book in most countries, especially in developing ones. Second, an I-O table explicitly accounts for the interdependence of different economic activities by incorporating the size and composition of the various industries' mutual input demands (measured by interdependent coefficients or the Leontief inverse), which enable us to incorporate both direct and indirect industrial interrelations into the analysis. Third, as the comparison takes two or more snapshots of the economy at different moments to analyze the changes over a period of time, it exploits most of the advantages of the IO framework and avoids the static nature of the method. Finally, the fourth, within the IO framework, it is possible to decompose the structure changes into different components, such as final demand, import substitution, export expansion, and technological change (Liu and Saal, 1999).

2.2 Analytical framework

The methodology used in this study is based on the contribution of Albala-Bertrand (1999), where the changes in output can be decomposed to final demand expansion (FDE), export demand expansion (EDE), import substitution of final goods (ISF), import substitution of intermediate goods (ISW) and changes in technical coefficients (IOCs). Let us assume that we have available IO accounting matrices for a given economy for at least two years, i.e. a base year 0 and a comparison year 1. An IO accounting framework shows how the gross output of each industry is distributed among the corresponding demands.

$$X = W_i + F + E - M \tag{1}$$

Where X, W, F, E and M are respectively vectors of gross output, matrix of intermediated demand, matrix of domestic final demand, matrix of foreign demand, and matrix of intermediate and final imports.

Let a_{ij} represent the unit-input requirement of the jth industry for the output of the ith industry in terms of standard technical coefficients; $a_{ij} = W_{ij}/ X_j$. Therefore, this generates an n x n matrix A of coefficients or, rearranging, we have

$$AX = W \tag{2}$$

Substituting equation (2) into equation (1), we obtain

$$X = AX + F + E - M \tag{3}$$

Let us assume that, at the level of each industry, imports are demanded for intermediate inputs and for final use in fixed proportions $\hat{M}^{W}$ and $\hat{M}^{F}$ respectively. Then, we have

$$M = \hat{M}^{W} AX + \hat{M}^{F} F \tag{4}$$

where the symbol $\wedge$ indicates a diagonal matrix. Then, substituting equation (4) into equation (3), we have

$$X = (I - \hat{M}^{W})AX + (I - \hat{M}^{F}) + E \tag{5}$$

Let $\hat{U^W} = (I - \hat{M^w})$ and $\hat{U^F} = (I - \hat{M^F})$. Notice that these two matrices give the ratios of domestic-to-total-intermediate demands and domestic-to-total-final demands respectively. As such, they are indicators of import substitution. Using these expressions, equation (5) becomes

$$X = \hat{U}AX + \hat{U^F} + E \tag{6}$$

Therefore, solving for X, we obtain the IO model

$$X = (I - \hat{U}A)^{-1}(\overset{F}{U^F} + E) \tag{7}$$

Notice that the first term on the right-hand side is the Leontief inverse for domestic intermediates only, and represents coefficients or weights, while the second term contains both domestic and foreign final demands, and represents volumes. In order to use less notation, let $D^{-1} = (I - \hat{U^W}A)^{-1}$ and let $G = (\hat{U^F} + E)$. Then the IO system becomes

$$X = D^{-1}G \tag{8}$$

2.2.1 Decomposition of output change

The decomposition of output change, i.e. absolute growth and the growth rate, between two periods amounts to calculating the first difference of equation (8). We have

$$\Delta X = \Delta(D^{-1}G) = D_0^{-1}\Delta G + \Delta D^{-1}G_0 + \Delta D^{-1}\Delta G \tag{9}$$

Using either the Paasche and Laspeyres index weighting respectively by taking the first or the second term on the right-hand side can absorb the third term., i.e.

$$\Delta X = D_1^{-1}\Delta G + \Delta D^{-1}G_0 \tag{10}$$

$$\Delta X = D_0^{-1}\Delta G + \Delta D^{-1}G_1 \tag{11}$$

The numerical results from the two alternative weightings are not normally equivalent and can be very different if the interaction term is large. A simpler method that distributes the interactive term proportionally in the other two terms is to take the simple arithmetical average of the Paasche and Laspeyres weighting results.

$$D_0^{-1}\Delta G = D_0^{-1}(\hat{U_0^F}\Delta F + \Delta E + \Delta\hat{U^F}F_I) \tag{12}$$

and

$$\Delta D^{-1}G_1 = D_0^{-1}(\Delta\hat{U}W_1 i + \hat{U_0^w}\Delta AX_1 \tag{13}$$

Therefore, letting $B_0 = D_0^{-1}$, to carry less notation, the total decomposition for the absolute growth or variation in gross output will be

$$\Delta X = B_0\overset{F}{\hat{U}_0}\Delta F + B_0\Delta E + B_0\Delta\hat{U^F}F_1 + B_0\Delta\hat{U^W}W_1 i + B_0\hat{U}\Delta AX_1 \tag{14}$$

The decomposition for the gross output growth rate can be obtained by dividing equation (14) element-wise by X_0. Each of the five terms on the right-hand side of equation (14), in variation or growth terms, represents a direct and indirect contribution to the total demand for the gross output of the economy. The terms have the following standard meanings:

$B_0\overset{F}{\hat{U}_0}\Delta F$ contribution of domestic demand expansion (FDE);

$B_0\Delta E$ contribution of export demand (EDE);

$B_0\Delta\hat{U}F_1$ contribution of import substitution of final goods (ISF);

$B_0\Delta\hat{U^F}F_1$ contribution of import substitution of intermediate goods(ISW);

$B_0\overset{W}{\hat{U}_0}\Delta AX_1$ contribution of changes in IO coefficients (IOCs).

2.1.1 Decomposition of output share changes

The share change for the ith industry is simply the difference between the gross output shares of the terminal year (S_{i1}) minus that of the base year (S_{i0}), i.e.

$$\Delta Si = S_{it} - S_{t0} = X_{i1}/X_{t1} - X_{i0}/X_{t0} \tag{15}$$

where i = 1,..., n and t denotes the total. Let us first define

$X_{i1} = X_{i0}(1 + g_i)^n$, $X_{t1} = X_{t0}(1 + g_a)^n$ (16)

where g_i and g_a denote the gross output compounded growth rate for the ith industry and the economy's average gross output growth rate respectively. Replacing X_{i0} with

$X_{to}/(1 + g_a)$ in equation (15) and manipulating yields

$\Delta Si = [X_{t1} - (1 + g_a] / X_{t1}$ (17)

Alternatively, letting $\delta X_i = [X_{i1} - (1 + g_a)X_{i0}]$ leads to

$\Delta Si = \delta X_i / X_{t1}$ (18)

The numerator δX_i contains the difference between the actual value of X_i in the terminal year and the value of X_i that would have occurred had it grown at the economy's average growth rate over the period. Therefore, the equation represents the deviation of each industry's gross output from balanced growth, normalized by the actual value of the gross output in the terminal year. This allows us to derive the decomposition formula in a closely analogous way to equation (11).

In matrix form, the case of Laspeyres weighting yields

$$\delta X = D_0^{-1}\delta G + \Delta D^{-1} G_1 \tag{19}$$

By using the Laspeyres derivation. Therefore, applying the same solving procedure as before, and replacing D_0^{-1} with B_o, we obtain

$$\delta X = B_0 \hat{U}_0^{F}\, \delta F + B_0 \delta E + B_0 \Delta \hat{U}^{F} F_1 + B_0 \Delta \hat{U}^{W} W_1 i + B_0 \hat{U}_0^{w} \Delta A X_1 \tag{20}$$

Notice that the last three terms on the right-hand side are the same as before. Dividing equation (20) by X_{t1}, we are back to equation (18), but in matrix form. The meanings of the terms are analogous to those for equation (14), but refer to the absolute value of the share change (δX) and the relative share change ($\delta X/X$ i1), rather than the absolute growth (ΔX) and the growth rate ($\hat{X}^{-1}\Delta X$).

2.2.2 Linkages Analysis in Terms of Production

The expansion of manufacturing industry not only generates demand for its input, but also induces the expansion of industries, which use the commodities produced as inputs. The connection with supplier industries is called backward linkage while with that of purchasing industries is forward linkage. Together, both these linkages can be termed as technological linkages (Mohd Shahwahid, 1992). The backward linkages or input provision or derived demand is defined as an activity, which employs significant amount of intermediate inputs from other activities for production. The output utilization or forward linkages on the other hand, is defined as an activity that caters for final demand but also induces attempts to utilize its outputs as inputs in other new activities (Hirschman, 1958 & Linnemann, 1987)

In the case of backward linkage effect, Rasmussen (1956) defined the power of dispersion (or measure of dispersion), which "describes the relative extent to which an increase in final demand for the products of industry j is dispersed throughout the system of industries". The power o dispersion of sector j is composed of unweighted sum of elements of column j divided by the number of sectors and standardized by the average of all elements of the inverse matrix (Linnemann, 1987).

The direct and indirect backward linkage index (or measures of dispersion) becomes,

$$P_j = \frac{\frac{1}{n}\sum_{i-1}^{n} r_{ij}}{\frac{1}{n^2}\sum_{i=1}^{n}\sum_{j=1}^{n} r_{ij}} \tag{21}$$

The numerator of the ratio P_j denotes the average increase in output of a sector induced by a unit increase of the final demand for products of sector j. In making international comparisons of sectoral linkages patterns, the average degree of sectoral interdependence for the whole economy when final demands increase by unity, must be considered, hence, standardizing P_j by the average r_{ij} in the denominator (Bulmer-Thomas, 1982; Linnemann, 1987).

The value of the power of dispersion for an imaginary sector that equals exactly the average value of backward linkages in an economy is 1. Consequently, if P_j is greater than 1, it implies that sector j

has the above-average backward linkage effects, whereas if P_j is less than 1, it can be stated that the sector j is operating in relative isolation from other sectors (Linnemann,1987).

A dispersion measure for forward linkages, P_j (equation 22), is based on the sum of row elements, r_{ij} , and is denoted by Rasmussen (1956) as the sensitivity of dispersion (Linnemann, 1987). Hirschman (1958) interpreted as high P_i (greater than 1) as the particular sector I has to increase its output more than other sectors for each unit increase in final demand.

$$P_i = \frac{\frac{1}{n}\sum_{j=1}^{n} r_{ij}}{\frac{1}{n^2}\sum_{i=1}^{n}\sum_{j=1}^{n} r_{ij}} \tag{22}$$

High forward linkages occur when a sector's output is or could be used by many others as an input; by expanding capacity in such a sector, "inducement" are provided to using industries which now have an incentives to expand output to take advantage of the increased availability of inputs (Bulmer-Thomas, 1982).

The numerator in equation (22) refers to the ith row sum of Leontif inverse, which in turn measures the total impact on the sector, i when the final demand for all sectors increased by unity. If the impact is large, it suggests that increased investment in sector would induced output increases in all using sectors, as users take advantage of the increased availability of inputs. Basically, the indices in equation (21) and (22) are based on the method of averaging.

2.3 Data

Basically, the present study uses secondary data from Malaysia's input-output tables published by the Department of Statistics. The following three tables represent two period of Malaysia Plan, half term of OPP1 (1978-1990) and OPP2 (1991 –2000), including the latest one.

1. Input-Output Table, 1978 (Malaysia, Department of Statistics 1982)
2. Input-Output Table, 1991 (Malaysia, Department of Statistics 2000)
3. Input-Output Table, 2000 (Malaysia, Department of Statistics 2005)

In order to reveal the real changes in the variables, the nominal 1991 and 2000 input-output tables have been transformed into 1978 constant prices, making all the tables comparable. We use the producer price indices and import indices provided by the Department of Statistics.

3. Results and discussion

3.1 Extent and constituents of change

Table 1 compares the extent of structural shift in the two sub periods, if any, by determining the major sources of growth and the sectors contributing to the growth. At this level of aggregation, structural change was more significant in the 1991-2000 than in 1978 – 1991 periods(Note 1). There was a significant fall in the share of the agriculture and a significant increase in that of the service sector over the whole 1978-2000 periods. Also, the most notable improvement in the share of the manufacturing sector was achieved in the period, 1991-2000.

[Table 1]

A comparison of the two subperiods shows that there was a switch in the role of domestic demand expansion, export demand expansion, imports substitution of final goods and technology. The constituent factors that contribute positively changes in the period, 1978-1991 are mostly domestic demand expansion (63.35%), export demand expansion (33.30%) and technical change (18.18%). However in the second sub period 1991-2000, export demand expansion increased by 12.43 % and domestic demand expansion decreased to 48.11 %. The import substitution of final goods contributed positively to the economy by 9.73 % compare to –10.76 % in 1978 to 1991 period. However the technical change has decreased from 18.18 % in 1978-1991 to 9.26 % in 1991-2000. In both sub periods, import substitution of intermediate goods contributes negatively to the economy. Taking the whole 1978-2000 period, domestic demand expansion appears to have been the major source of output growth, contributing about 82 %, followed by export demand expansion (62%). Generally, the result of the analysis shows that as output grew during the whole period was driven by domestic demand expansion and technological change was less significant. In the first sub period, the greater part of output growth came from the service and the manufacturing (light and heavy industries) sectors, which together contributed about 90 % of the economy's output growth, while the agriculture contributed less than 7%. The second sub period saw a clear shift in sectoral contribution to output growth, with the heavy industries being the major contributing source of output growth, about 67 % and services about 37%. The contribution of light industry declined to about 10% and mining sectors have increase about 5%.

The aggregated results hide the heterogeneous nature of the structural change, so the rest of the section presented a more disaggregated view, and concentrates mostly on the two sub periods; 1991-2000 (OPP2) and 1978-1991 (OPP1). Table 2 present the growth rates for each of the two periods respectively. The aggregated results hide the heterogeneous nature of the structural change, so the rest of the section presented a more disaggregated view, and concentrates mostly on the two sub periods; 1991-2000 (OPP2) and 1978-1991 (OPP1). Tables 2 and Table 3 present the growth rates and

share change for each of the two periods respectively. The first column of Table 5 ($\Delta X/ X_{t1}$) is the growth rate in gross output, expressed in percentage points for each sector, while the first column of Table 6 is the share change of gross output. The other five columns (FDE, EDE, ISF, ISW and IOC) show the way in which growth rates (Table 2) and share variations (Table 3) are disaggregated in terms of demand sources. These sources should sum to the values in the first column. The last column (S_{1978} or S_{2000}) expresses the share of each sector in the total output, in the initial year.

[Table 2]

[Table 3]

3.1.1 Sub period: 1978-1991

Domestic demand expansion and export demand expansion had a relatively strong effect on the economy's gross output growth rate (Table 2), particularly in the heavy industry, light industry, agriculture, services and mining. The industries that were most driven by the domestic and export expansion is electrical machinery, non-electrical machinery and industrial chemical. However the share of domestic and export expansion to the gross output decreased in the overall heavy industries but increased in the sub sectors of electrical machinery and industrial chemical. In the light industries, most of the sub sectors showed positive gross output growth rates. During the period there is evidence of the effects of technological change on output growth occurring in agriculture, light industry, heavy industry and services.

3.1.1.1 Agriculture and mining sectors.

This sector was domestic-oriented, as domestic expansion contributed about 1065 percent to total sectoral output. Export expansion contributed about 623 percent technical change 827 percent. The sector contributed about 2173 percent to the total output growth of the economy.

Within the broad agriculture sector, mainly; other agriculture, rubber, oil palm, livestock, forestry and fishing subsectors have positive growth rate and positive change in gross output share in the domestic and export expansion. Import substitution of final and intermediate output shows a negative contribution to both growth rate (-208.77 and –132.33) (Table 2) and output share (-64.41 and –38.31) (Table3) which indicates that in the agriculture sector, Malaysia still relies on imported commodities to generate growth in this sector. The period saw the effects of technical change on output growth occurring both in growth rate (827 percent) and share changes (134 percent) which indicate there are linkages in this sector.

Domestic demand expansion contributed about 51 percent to this sector's output growth. In terms of growth rate, mining was found to contribute considerably about 227.16 percent in domestic demand expansion and 186.06 in export expansion. However in terms of change in gross output, the share was lower at 30.68 in domestic demand expansion and 35.08 in export demand expansion. Overall the sector only contributed about 351 percent to total output growth of the economy with a negative technical change.

3.1.1.2 Manufacturing sector.

3.1.1.2.1 Light and heavy industry sectors

Like the agriculture sector, the light industry sector was found to be domestic-oriented during the first sub period. Export expansion accounted about 4904 percent, and the export demand expansion about for 3396 percent of the light industry sectoral output growth. Within the sector there were twelve domestic-driven sub sectors, namely diary product, vegetable fruit, grain mill, baker confectionary, other foods, animal feed, beverages, tobacco, textiles, wearing, sawmills, furniture fixture and paper printing; and two export-driven sub sectors, namely oils and fats and furniture fixture.

This sector was found to be domestic-oriented in the sub period. Domestic demand expansion contributed about 12242 percent to its output growth while the industry itself contributed considerably about 18189 percent to the overall output growth of the economy. Two sub sectors were export-driven and are industrial chemical and electrical machinery. Twelve were domestic-driven sub sectors; namely paints & lacquers, other chemical product, petroleum & coal product, rubber product, plastic product, glass product, cement, non-metallic, basic metal, other metal and non electrical machinery. Overall, the heavy industry shows a positive growth rate during the sub periods, however its share declines in the sub sectors namely, paints & lacquers, petroleum & coal product, rubber product, glass product, non metallic, non-electrical machinery and other manufacture products for export and demand expansion. However, the import substitution for intermediate goods and final demand gain in gross output share as the export and domestic demand decline.

3.1.1.3 Services sector

The sector was found to be domestically driven, as domestic demand expansion contributed about 979 percent to the sector's output growth. The service sector contributed 921 percent to the overall output growth of the economy. This study did not show the disaggregate sector of services, however its share of contribution to economy was high (42 percent).

3.1.2 Second sub period: 1991-2000

Like the first sub period, the second sub period witnessed output growth dominated by the effects of domestic demand expansion, which contributed about 48 percent to the overall growth of the economy. Export demand expansion, on the other hand, contributed 46 percent, 2 percent less than the domestic demand. The second sub period witnessed a fall in the effects of technical change on output growth, from 18 percent in the first sub period to 9 percent in the second sub period (Table 4).

[Table 4]

3.1.2.1 Agriculture and mining sectors

As in the first sub period, domestic expansion was also the major source of growth in the agriculture sector during the second sub period, contributing about 234 percent of its growth, while export expansion 85 percent and 70 percent was driven by import substitution of final goods and 217 percent due to the technical change in the sectoral output. The gross output growth rate was positive for all the sub sectors except for oil palm sector, which has a negative rate for, export expansion, domestic and import substitution for final and intermediate goods. However, the change in gross output share was negative for domestic demand expansion and positive for export demand expansion and import substitution in intermediate goods in the sub sector forestry, which implies that most of timber is being exported and are the substitute for intermediate goods.

Unlike in the first sub period, the mining sector becomes export-oriented in the second sub period. Export expansion contributed 284 percent, while import substitution for final goods accounted for 43 percent of the output growth. There was negative effect of technological change on mining output growth. The sector contributed about 378 percent, an increase of about 28 percent from the first sub period.

3.1.2.2 Manufacturing sector

3.1.2.2.1 Light and heavy industry sectors

Unlike the first sub period, the light industry saw a decline in contribution of the domestic demand expansion from 4904 percent in 1978-1991 to 1687 percent in 1991-2000 and export demand expansion from of 1760 percent to output growth. Import substitution of final goods, which contributed negative growth to output in first sub period, has a positive contribution of 353 percent in the second sub period. The sector contribution declined to almost one quarter to the overall output growth compare with the first sub period. In terms of gross output growth rate most of sub sectors contribute positively in the domestic and export expansion to the economy, except oils and fat. However share of sub sectors, dairy product, vegetable fruit, oil and fats, baker confectionary, textiles, wearing, sawmills in gross output declined.

The sector's contribution to overall output growth increased to 67 percent, which took up the share lost by the light industry sector. Export expansion contributed substantially to the gross output growth accounting for 3324 percent, import substitution for final goods 543 percent and domestic demand expansion 2855 percent. Thirteen sub sectors, namely, industrial chemical, paints and lacquers, other chemical product, rubber product, processed rubber, plastic product, glass product, non metallic, basic metal, other metal, non electrical, electrical machinery, other transport and other manufacturing product were found to be export-oriented. The petroleum and coal product, cement and non-metallic were driven by domestic demand expansion. All the sub sectors are driven by import substitution for final goods.

3.1.2.3 Service sector

Like the first sub period, the services sector is still dominated by domestic demand expansion but its contribution declined to 43 percent. However the sector contributed about 350 percent to the overall output growth of the economy, a decline compared to the first sub period.

To sum up, all the major sectors of heavy industries were export oriented during the period 1991-2000, the gross output growth rate was 8128 percent, which is four times higher than light industry. So we can conclude that the Malaysia economy become heavy oriented industrialization during the Second OPP.

3.1.3 Overall Period: 1978-2000

In the overall period, the whole economy appeared to be influenced by domestic demand expansion and export demand expansion. About 82 percent of the economy's overall growth was due to domestic driven, and 61 percent due to export-driven accounted, while technical change and import substitution had negative contribution at –21.72 percent and –18.6 percent respectively. (Table 4)

[Table 4]

- Agriculture sector. The sector was found to be domestic –oriented during the whole period. Domestic demand expansion contributed considerably to the sectoral growth (2471 percent), while export expansion contributed

1152 percent and technical change had contribution of –692 percent. Gross output growth rates for all the sub sectors, namely; other agriculture, livestock, forestry, fishing show a positive growth but rubber plantation, and oil palm show a decline in growth to the economy. The growth rate of domestic and export expansion is positive but its share in gross output declines for all the sub sectors. There is gain in share for import substitution for intermediate and final goods.

- Mining Sector. From the output growth rate the sector was found to be slightly higher in its export expansion (1333 percent) than its domestic expansion (1299 percent) but the output share decreased to –3 percent for domestic and –2.84 percent for export expansion. The import substitution for intermediate output share increased to 10.17 percent. The sector contributed about 8.5 percent to the overall output growth of the economy.
- Manufacturing sector- Light and heavy industry sectors: The sector was found to be driven by domestic demand expansion for the overall period. About 19860 percent of sectoral growth was due to domestic demand expansion, while export expansion accounted for 16272 percent. The sector contributed about 28263 percent to the overall growth of the economy. In the gross output growth rate all the sub sectors in the light industry experienced a positive growth rate for export and domestic expansion, but in terms of gross output share, the share of sub sectors, namely; vegetable fruit, oils and fats, baker confectionery, other foods, animal feed, furniture fixture and paper printing showed a decline. As in the second sub period, this sector was export-oriented driven during the overall period, which contributed about 61 percent to the sector's growth. The sector contributed 61 percent to the overall growth of the economy. All the sub sectors showed a positive growth rate in the export and domestic side, and only a few sub sectors made gain in their output share, namely, rubber product, plastic product and electrical machinery. There were fourteen sub sectors that had negative output share in domestic and export expansion but gain in share of import substitution of intermediate and final goods. These include; industrial chemical, paints and lacquers, other chemical product, petroleum and coal product, processed rubber, glass product, cement, non metallic, basic metal, other metal, non electrical machinery, motor vehicles, other transport and other manufacture products.
- Serv*ices sector.* This sector was domestically driven during the overall period. About expansion, while the sector's contribution to the overall growth of the economy was about 20 percent. In sum, agriculture, light industry and services were found to be domestic oriented in the 1978-2000, while the mining and heavy industry were export-oriented with a very slight increase. The heavy industry sector was found to be the leading sector in terms of contribution to the overall growth of the economy during the overall period.

3.2 Analysis of linkages effect

The results of both backward and forward linkages in terms of output are presented in Appendix 3. After estimation of the linkages, the next step was to rank the sectors. A ranking was done to both backward and forward linkages. Ranking provides a basis for assigning priorities to different sectors in the economy, from the viewpoint of development strategy. Thus, the procedure allowed the sectors to be ranked in the descending order of priority in terms of their potential linkage generation.

A key sector is defined as a sector in which both strong backward and forward linkages are greater than unity. In fact, both backward and forward linkages are two different sides of the same coin, namely a forward linkage of one sector being regarded as a backward linkage of another. But in practice, it is important to know which sector is a catalyst for developing linkages. In this regard, backward linkage likely to be more important since it represents the demand of inputs from other sectors necessitated by productive activity of one sector. Table 3 presents the result of backward linkages in order to determine the key sectors in the Malaysian economy. The key sectors that show a high backward linkage in the year 1978,1991 and 2000 are from the livestock (agriculture), two sectors from light industry (grain mill and rubber product) and one sector from heavy industry (basic metal product).

For the year 1978, 19 sectors show high backward linkages, with the light industry dominating the importance on the supply side production (10 sectors) and follow by heavy industry (8 sectors) and one sector from agriculture. In the year 1991, 18 sectors contributed as key sectors in the economy, with 9 sectors from heavy industry, 8 sectors from light industry and one from agriculture. However, the result of key sector in 2000 show that the contribution from agriculture come from 4 sectors; namely others agriculture, rubber plantation, oil palm and livestock with a higher backward linkages, 7 sectors from the heavy industry and 4 sectors from the light industry.

From the result above, we can conclude that the evolution of intersectoral linkages at different stages of industrialization is important because the nature and extent of intersectoral linkages affect not only the overall growth rate, but also determine the structural balance and international competitiveness of the economy. Hence, in the next analysis, Table 4 presents the link between the sources of growth and the key sectors for the year 2000, in order to look at the relationship.

4. Conclusion and recommendation

The study found that the Malaysian economy had undergone a number of structural changes, caused mainly by the re-orientation of industrialization strategies as well as by variations in the composition of domestic demand. In the period 1978-1991, input-output technique was able to capture the 13 years scenario of the country direction during the second half of OPP1. During this period 1978-1991, the result of the analysis indicates that domestic -demand expansion was the dominant source of growth in the economy especially in the mining and service sectors. However if the comparison would be made between domestic expansion and export expansion in agriculture, light industry and heavy industry, domestic demand expansion is still dominating in all these sectors. In the second OPP2, 1991-2000, the growth in mining and heavy industry were due mainly to export expansion. Surprisingly, the light industry experienced a negative growth during this sub period, while agriculture and services showed a declining growth trend. The decline in the light industry probably due to the Malaysia economic recession in 1987, and government policy focus in heavy industry. During the overall period 1978-2000, the export expansion also appeared to be the dominant source of growth for heavy industry and mining, slightly higher in percentage than the domestic demand expansion. However, the other major sectors of like agriculture, light industry and services appeared to be dominated by domestic demand expansion. It can be concluded that the causes of structural changes in Malaysian economy, using input-output decomposition analysis technique is driven by shifts in final demand – mainly by consumption, trade and changes in the inter-industry relations arising from good linkages.

The changes in manufacturing export structure reflect that the Malaysian government's success in providing conducive settings at the macro level for an export-led industrial reorientation. These environments are shaped by such factors as human capital formation; export promotion measures, market friendly policies, political stability, good macro management and lastly the welfare of the population in general. As Malaysia economic success lies in the performance of the manufacturing sector, the realization of "Vision 2020" depends on the extent to which sector remains strong and can contribute to the economic growth. Lastly, the study has combined the source of growth and key sector through backward linkages; the study revealed that most of the key sectors induced its supplying production strongly for domestic demand expansion and export demand expansion; however leakages still exist in the economy.

References

Albala-Betrand, J. (1999). *Structural Change in Chile: 1960-199*: Economic System Research, Vol. 11, No. 3: 301-319

Bulmer-Thomas, V. (1982). *Input-Output Analysis in Developing Countries: Sources, Methods and Application.* John Wiley & Sons Ltd, USA. 297p

Chenery, H. B., (1960). *Patterns of Industrial Growth*, American Economic Review, Vol. 50. No. 3, pp. 624 – 54

Dewhurst, J.H. (1994). Decomposition of Changes in Input-Output Tables: Economic System Research, 5 (1): 41-53

Hirschman, A.O. (1958). *The Strategy of Economic Development*. Yale University Press, New Haven, 217p.

Leontief, Wassily W. (1941). *The Structure of American Economy. 1919 –1929: An Empirical Application of Equilibrium Analysis.* Ist ed. Cambridge, Mass.: Harvard University Press

Linnemann, H. (1987). *Export-Oriented Industrialization in Developing Countries. Council of Asian Manpower Studies, Manila.* Singapore University Press.

Liu and Saal (1999). *An Input Output Analysis of Structural Change in Apartheid Era South Africa: 1975-1993.* Aston University. Birmingham. UK.

Malaysia, Department of Statistics. (1982). *Input-Output Table*, 1991. Kuala Lumpur.

Malaysia, Department of Statistics. (2000). *Input-Output Table* 2000. Kuala Lumpur.

Malaysia Standard Industrial Classification (2005), Department of Statistics, Kuala Lumpur

Mohd. Shahwahid Othman. (1992). *Economic Impact of Malaysian Timber Exports*. Journal of Tropical Science. 5 (1): 51-67

Syrquin, M. (1988). *Patterns of Structural Change.* In Chenery, H. & T.N. Srinivasan (eds) Handbook of Development Economics. Vol.1. Elvisier Science Publishers, 1988.

Syrquin, M. and Chenery, H. (1989). *Three Decades of Industrialization.* The World Bank Economic Review, Vol. 3, No. 2, pp. 145 – 181

Note 1.

This statement comes from the application of an index of structural change (ISC) to the annualized (40-industry aggregation) share changes of each period. Indices of this nature are summary measures of variability, such as standard

deviation. We use the formula. ISC = $\sum_t$ | S_{t1}-S_{t0} |/ n = $\sum_t$ |Δ S_i|/n, where S_i = is the share; i = 1,….n (industries); n is the number of industries, and || denotes absolute value. The values of ISC are δ (78-91)= 6.30, δ (91-2000) = 9.41, δ (1978-2000)= 3.75.

Table 1. Sources of industrial growth in the Malaysian Economy in the sub periods of 1978-1991, 1991-2000, and Overall Period 1978-2000

Sector	Domestic Demand Expansion	Export Demand Expansion	Import Substitution Final Goods	Import Substitution Intermediate Goods	Technological Change	Total
1978-1991						
Agriculture	55.51	34.77	-10.69	-6.21	26.62	100
	3.78	2.37	-0.73	-0.42	1.81	6.81
Mining	64.76	53.04	-12.05	-5.56	-0.19	100
	2.18	1.79	-0.41	-0.19	-0.01	3.37
Light Industry	29.12	22.27	-5.35	-1.94	55.91	100
	7.32	5.60	-1.35	-0.49	14.05	25.13
Heavy Industry	60.70	48.98	-9.76	-3.05	3.12	100
	20.99	16.94	-3.37	-1.05	1.08	34.58
Services	96.59	21.97	-16.28	-6.41	4.13	100
	29.08	6.62	-4.90	-1.93	1.24	30.11
Total	63.35	33.30	-10.76	-4.08	18.18	100
1991-2000						
Agriculture	67.87	25.44	20.97	-59.46	45.18	100
	1.14	0.43	0.35	-1.00	0.76	1.68
Mining	63.36	75.12	11.39	-19.18	-30.68	100
	3.00	3.55	0.54	-0.91	-1.45	4.73
Light Industry	-35.04	-31.77	-7.56	8.56	165.81	100
	3.58	3.25	0.77	-0.88	-16.96	-10.23
Heavy Industry	36.67	45.41	6.66	-5.61	16.87	100
	24.58	30.44	4.46	-3.76	11.31	67.04
Services	42.97	21.91	9.80	-17.09	42.42	100
	15.80	8.06	3.60	-6.29	15.60	36.78
Total	48.11	45.73	9.73	-12.83	9.26	100
1978-2000						
Agriculture	150.00	73.03	-3.63	-79.46	-39.95	100
	2.81	1.37	-0.07	-1.49	-0.75	1.87
Mining	61.18	62.80	-1.35	-17.01	-5.62	100
	4.15	4.26	-0.09	-1.15	-0.38	6.79
Light Industry	82.71	64.17	-1.88	-23.23	-21.77	100
	8.19	6.36	-0.19	-2.30	-2.16	9.91

Heavy Industry	60.66	61.41	-1.30	-8.32	-12.44	100
	37.04	37.50	-0.80	-5.08	-7.60	61.06
Services	143.99	54.54	-3.20	-42.15	-53.18	100
	29.33	11.11	-0.65	-8.59	-10.83	20.37
Total	81.53	60.59	-1.79	-18.61	-21.72	100

Note: Entries in bold indicate contribution as percentage of total output growth.

Table 2. Gross output growth rate (%)

		Δ1978-1991							
		ΔX/ X78	FDE	EDE	ISF	ISW	IOC	S78	ΔX/X91
I	**Agriculture (1-6)**	**2173.95**	**1065.15**	**622.59**	**-208.77**	**-132.33**	**827.30**	**12.57**	**363.96**
1	Others Agriculture	268.60	200.83	59.14	-38.40	-16.09	63.12	2.59	103.66
2	Rubber Plantation	70.61	44.38	19.25	-13.95	-22.66	43.59	1.93	118.41
3	Oil Palm	741.51	39.02	49.04	-12.90	-24.14	690.49	1.27	-62.15
4	Livestock	290.48	258.65	76.39	-46.86	-24.16	26.45	1.47	60.99
5	Forestry	664.06	358.42	393.45	-61.52	-30.58	4.28	2.82	16.69
6	Fishing	138.69	163.85	25.32	-35.15	-14.70	-0.63	2.48	126.36
II	**Mining**								
7	Petrol Mining	350.79	227.16	186.06	-42.28	-19.51	-0.65	6.24	378.84
III	**Light Industry**	**8796.57**	**4904.62**	**3396.00**	**-858.08**	**-266.16**	**1620.19**	**17.78**	**2070.99**
8	Dairy Product	206.29	235.69	47.61	-45.50	-10.06	-21.45	1.19	132.23
9	Vegetable Fruit	464.68	303.03	234.86	-56.16	-6.05	-11.01	0.61	256.86
10	Oil & Fats	1921.73	110.83	116.66	-26.43	-17.82	1738.49	5.42	-2227.62
11	Grain Mill	52.11	56.61	22.70	-19.37	-9.78	1.95	1.45	146.61
12	Baker Conf	566.87	472.62	188.90	-80.26	-4.70	-9.68	0.64	158.26
13	Other Foods	190.20	154.24	89.34	-32.98	-12.65	-7.76	0.99	427.65
14	Animal Feed	104.03	85.05	45.96	-18.14	-66.27	57.42	0.50	-26.72
15	Beverages	329.05	363.62	41.06	-64.36	-9.37	-1.89	0.46	201.06
16	Tobacco	242.67	267.70	12.98	-51.21	-3.78	16.99	0.79	254.22
17	Textiles	559.79	385.55	355.25	-65.67	-14.51	-100.83	1.57	268.82
18	Wearing	1774.64	999.70	932.03	-156.44	-9.67	9.02	0.59	288.87
19	Sawmills	704.07	421.68	427.95	-71.34	-15.60	-58.61	2.53	294.93
20	Furniture Fixture	1205.35	654.56	667.88	-106.74	-8.26	-2.10	0.21	1515.88
21	Paper Printing	475.09	393.75	212.81	-63.49	-77.62	9.64	0.84	379.94
IV	Heavy Industry	18189.98	12242.51	7886.63	-1922.95	-881.30	865.09	21.35	8128.94
22	Industrial Chemical	2956.79	1503.27	1586.75	-222.74	-76.82	166.33	0.64	390.20
23	Paints. Etc	343.98	553.53	116.97	-85.96	-53.62	-186.95	0.16	416.92
24	Other Chem. Product	505.09	384.21	228.47	-66.36	-19.23	-21.99	0.62	696.92
25	Petrol Product	243.97	265.67	138.97	-46.43	-31.67	-82.58	2.49	1050.63
26	Processed Rubber	65.54	59.43	35.75	-20.97	-2.48	-6.20	3.88	-2.81

27	Rubber Product	1146.84	785.52	565.85	-123.74	-24.45	-56.33	0.81	194.43
28	Plastic Product	1484.78	941.90	551.29	-144.68	-102.23	238.49	0.44	302.88
29	Glass Product	818.89	571.64	375.21	-90.47	-72.29	34.81	0.34	399.75
30	Cement	538.98	371.98	136.19	-59.47	-140.25	230.54	0.33	-26.59
31	Non Metallic	435.47	408.65	158.23	-65.64	-84.86	19.09	0.27	221.03
32	Basic Metal	146.30	128.54	38.10	-29.64	-23.15	32.45	4.33	310.53
33	Other Metal	534.86	450.25	208.90	-72.68	-31.00	-20.61	0.69	774.50
34	Non Electrical Mach.	1433.98	1530.50	140.85	-229.80	-68.33	60.74	0.90	1739.35
35	Elect .Mach	4074.00	1918.05	2399.85	-288.66	-35.74	80.51	3.07	760.92
36	Motor Vehicles	766.34	736.43	45.10	-118.63	-24.64	128.07	1.50	134.62
37	Other Transport	912.99	648.25	113.86	-104.50	-70.87	326.25	0.41	93.68
38	Other Mfg Product	1781.18	984.70	1046.30	-152.59	-19.69	-77.54	0.49	671.97
V	Services	921.49	979.57	133.16	-163.84	-43.52	16.11	42.06	350.63
39	Construction	453.87	555.18	9.32	-91.94	-8.82	-9.87	7.96	101.46
40	Others Services	467.62	424.40	123.84	-71.91	-34.70	25.98	34.10	249.17

Table 2. continued

		Δ1991-2000						Δ1978-2000					
		EDE	ISF	ISW	IOC	S 1991	ΔX/X78	FDE	EDE	ISF	ISW	IOC	S78
I	**Agriculture (1-6)**	**85.44**	**70.15**	**-243.65**	**217.55**	**7.44**	**1491.33**	**2471.46**	**1152.23**	**-60.06**	**-1379.68**	**-692.63**	**12.57**
1	Others Agriculture	31.24	13.79	-27.97	47.23	1.39	289.71	394.65	197.02	-9.68	-155.26	-137.03	2.59
2	Rubber Plantation	26.72	9.62	-38.82	91.28	0.72	-89.21	133.68	81.37	-3.91	-137.47	-162.87	1.93
3	Oil Palm	-13.57	-3.40	-57.28	31.54	0.36	-93.24	133.52	141.84	-3.87	-283.39	-81.32	1.27
4	Livestock	12.01	16.98	-34.29	3.16	1.06	433.55	642.70	153.25	-14.92	-230.64	-116.84	1.47
5	Forestry	10.46	11.15	-38.66	9.88	2.61	590.38	565.59	475.27	-13.33	-340.65	-96.49	2.82
6	Fishing	18.58	22.02	-46.62	34.45	1.30	360.13	601.32	103.49	-14.34	-232.26	-98.08	2.48
II	**Mining**												
7	Petrol Mining	284.59	43.13	-72.68	-116.25	3.56	**2123.75**	**1299.34**	**1333.71**	**-28.74**	**-361.15**	**-119.42**	6.24
III	**Light Industry**	**1636.01**	**353.59**	**-421.76**	**-1184.08**	**11.82**	**28263.53**	**19860.85**	16272.69	-440.08	-3815.07	-3614.86	**17.78**
8	Dairy Product	18.76	14.50	-30.88	95.13	0.65	229.84	439.50	147.76	-10.93	-175.40	-171.10	1.19
9	Vegetable Fruit	126.41	19.58	-13.90	55.31	0.42	1339.77	715.68	863.90	-16.88	-96.91	-126.03	0.61
10	Oil & Fats	-33.67	-8.31	26.47	-2177.70	2.54	86.60	364.00	334.94	-9.19	-255.06	-348.10	5.42
11	Grain Mill	28.48	15.05	-43.37	100.11	0.38	-19.57	159.82	74.01	-5.00	-109.59	-138.81	1.45
12	Baker Conf	55.96	20.12	-11.45	26.19	0.59	1342.64	996.04	558.01	-22.73	-104.29	-84.38	0.64
13	Other	79.24	33.86	-61.94	201.34	0.41	504.92	785.70	344.50	-18.11	-248.15	-359.02	0.99

	Foods												
14	Animal Feed	5.64	8.90	-70.10	-13.32	0.38	-191.35	360.80	82.62	-8.45	-506.79	-119.54	0.50
15	Beverages	36.73	22.80	-22.37	73.86	0.36	769.35	958.65	251.09	-21.92	-168.85	-249.62	0.46
16	Tobacco	139.26	25.40	-3.82	-11.96	0.49	1349.80	793.12	609.73	-18.53	-19.52	-15.00	0.79
17	Textiles	80.31	24.45	-30.59	88.80	1.08	1794.40	1161.80	867.34	-25.92	-226.08	17.28	1.57
18	Wearing	106.29	28.98	-10.07	34.65	1.08	4718.65	2945.14	2304.69	-63.78	-175.60	-291.81	0.59
19	Sawmills	135.17	25.56	-24.28	44.94	2.09	2371.01	1308.11	1289.39	-29.07	-197.73	0.31	2.53
20	Furniture	761.72	92.21	-30.37	123.73	0.26	12984.25	6573.49	7457.22	-140.21	-350.99	-555.27	12.1
	Fixture												
21	Paper Printing	95.70	30.49	-95.07	174.85	1.08	983.21	2298.99	1087.49	-49.38	-1180.11	-1173.77	0.84
IV	Heavy	3324.10	543.7	-883.98	2290.03	30.02	92043.13	60183.39	58781.71	-1289.96	-11345.90	-14286.11	21.35
	Industry												
22	Industrial Chemical	141.78	22.21	-49.29	180.17	1.96	4972.19	4042.30	4790.70	-85.95	-1451.03	-2323.82	0.64
23	Paints. Etc	209.69	31.04	-58.86	65.00	0.17	4046.05	2503.01	2030.70	-53.59	-592.63	158.56	0.16
24	Other Chem. Product	271.72	39.46	-66.52	240.10	0.52	2524.91	1933.84	1927.22	-42.31	-525.29	-768.55	0.62
25	Petrol Product	265.33	64.98	-140.53	460.05	1.45	1892.01	2348.16	1342.64	-50.62	-828.16	-920.00	2.49
26	Processed Rubber	20.26	10.62	-1.75	-35.08	0.92	180.14	72.75	77.61	-3.34	-6.24	39.36	3.88
27	Rubber Product	96.57	18.92	-16.31	29.27	1.20	2918.24	1682.48	1629.71	-36.93	-261.51	-95.50	0.81
28	Plastic Product	182.61	32.17	-27.10	-59.36	1.20	7181.10	4588.07	3737.93	-97.88	-659.90	-387.13	0.44
29	Glass Product	129.22	23.40	-67.79	195.65	0.57	1561.52	2233.61	1879.02	-48.19	-1051.89	-1451.03	0.34
30	Cement	21.23	8.51	-47.30	-43.63	0.71	309.28	952.36	433.74	-20.89	-865.83	-190.10	0.33
31	Non Metallic	32.20	11.38	-88.89	220.40	0.40	-923.87	1043.23	525.56	-22.93	-1210.13	-1259.60	0.27
32	Basic Metal	142.29	22.91	-53.33	88.18	2.22	824.50	673.77	648.43	-15.80	-240.70	-241.19	4.33
33	Other Metal	157.32	27.13	-146.41	603.67	0.60	-882.88	1412.87	1082.93	-30.87	-1219.18	-2128.63	0.69
34	Non Electrical Mach.	922.41	103.11	-20.84	78.78	2.87	39186.72	19332.97	21628.23	-408.40	-597.13	-768.95	0.90
35	Elect .Mach	360.69	50.56	-17.84	85.52	10.99	19399.52	10194.28	11488.18	-216.38	-568.25	-1498.31	3.07
36	Motor Vehicles	27.01	17.31	-20.03	55.04	2.52	674.35	1389.28	286.09	-31.05	-274.66	-695.31	1.50
37	Other Transport	71.17	16.40	-32.97	-24.02	0.87	364.49	1241.08	677.95	-27.72	-518.81	-1008.00	0.41
38	Other Mfg Product	272.59	43.64	-28.24	150.31	0.84	7814.85	4539.33	4595.09	-97.11	-474.55	-747.91	0.49
V	Services	68.84	42.99	-51.41	114.65	47.16	2638.06	722.98	-58.82	-549.19	-620.18	2132.85	42.06
39	Construction	11.97	21.05	-6.39	-0.77	8.57	1249.79	113.11	-28.03	-74.89	0.32	1260.29	7.96

40	Others Services	56.87	21.95	-45.02	115.42	38.60	1388.28	609.87	-30.78	-474.30	-620.50	872.56	34.10

Note: ΔX/X gross output growth rate; FDE-final demand expansion; EDE-export demand expansion; ISF - import substitution of final goods; ISW- import substitution of intermediate goods;IOC-IO coefficient change; S-gross output share.

Table 3. Change in gross output shares (percentage points)

		δ(1978-1991)									
		δ X/ X_{1991}	FDE	EDE	ISF	ISW	IOC	S 1978	δ X/ X2000	FDE	EDE
I	**Agriculture (1-6)**	**366.94**	**247.67**	**87.15**	**-64.41**	**-38.31**	**134.83**	**12.57**	**674.94**	**-2487.46**	**2572.79**
1	Others Agriculture	54.87	38.20	14.20	-11.02	-4.62	18.11	2.59	131.32	108.02	-4.03
2	Rubber Primary Product	78.35	39.34	36.44	-5.14	-8.35	16.06	1.93	133.22	95.55	-31.17
3	Oil Palm	104.95	13.22	7.77	-1.66	-3.10	88.72	1.27	99.12	29.21	-18.49
4	Livestock	40.83	58.89	1.43	-20.50	-10.57	11.57	1.47	107.37	145.35	-21.76
5	Forestry	31.71	21.52	23.86	-9.58	-4.76	0.67	2.82	132.52	-2931.27	2647.63
6	Fishing	56.22	76.50	3.45	-16.53	-6.91	-0.30	2.48	71.38	65.68	0.62
II	**Mining**										
7	Petrol Mining	51.48	30.68	35.08	-9.67	-4.46	-0.15	6.24	47.58	225.04	61.59
III	**Light Industry (8-21)**	**635.66**	**819.84**	**205.14**	**-261.08**	**-24.40**	**-103.85**	**17.78**	**1182.28**	**560.88**	**27.99**
8	Dairy Product	53.96	94.22	4.43	-26.40	-5.84	-12.45	1.19	112.21	75.57	-2.27
9	Vegetable Fruit	42.02	31.54	23.63	-10.09	-1.09	-1.98	0.61	101.27	80.34	-10.89
10	Oil & Fats	62.79	4.67	4.58	-0.84	-0.56	54.95	5.42	80.07	1.96	-0.49
11	Grain Mill	111.46	128.75	4.80	-15.73	-7.94	1.58	1.45	114.25	74.01	0.79
12	Baker Confectionary	31.99	55.75	7.25	-26.30	-1.54	-3.17	0.64	106.19	91.32	-4.14
13	Other Foods	69.94	98.30	6.23	-21.37	-8.20	-5.03	0.99	50.79	22.27	0.68
14	Animal Feed	38.15	54.81	1.17	-11.99	-43.80	37.95	0.50	119.64	-134.11	34.08
15	Beverages	37.53	59.78	4.68	-22.92	-3.34	-0.67	0.46	87.60	55.28	6.34
16	Tobacco	46.94	59.62	0.07	-17.17	-1.27	5.70	0.79	97.16	61.67	31.89
17	Textiles	42.82	223.01	105.09	-103.50	-22.87	-158.92	1.57	79.00	59.03	-13.01
18	Wearing	16.03	30.69	13.53	-28.07	-1.73	1.62	0.59	79.02	77.39	-23.18
19	Sawmills	35.52	33.04	34.98	-15.93	-3.48	-13.09	2.53	81.23	73.79	-15.61
20	Furniture Fixture	23.55	41.46	10.16	-25.59	-1.98	-0.50	0.21	24.56	4.55	14.88
21	Paper Printing	22.97	-95.79	-15.45	64.81	79.23	-9.84	0.84	49.28	17.81	8.93
IV	**Heavy Industry (22-38)**	**484.49**	**-5009.34**		**-662.15**	**3626.19**	**2858.85**	**-329.06**	**21.35**	**1448.93**	**1634.52**	**-729.33**
22	Industrial Chemical	9.58	225.31		159.18	-626.80	-216.17	468.06	0.64	70.97	33.10	0.69
23	Paints. Etc	27.58	-10.41		-1.85	10.49	6.54	22.81	0.16	62.69	21.57	33.48
24	Other Chemical Product	34.93	64.36		15.49	-27.71	-8.03	-9.18	0.62	42.83	11.87	13.25
25	Petrol Product	50.41	-344.04		-89.39	139.82	95.36	248.66	2.49	23.95	4.39	4.98
26	Processed Rubber	123.43	60.28		73.34	-7.20	-0.85	-2.13	3.88	270.19	1479.14	-972.25
27	Rubber Product	19.67	-549.41		-200.69	465.73	92.02	212.02	0.81	112.70	95.67	-3.10

28 Plastic Product	10.70	8.37	2.91	-9.87	-6.98	16.27	0.44	77.51	51.40	50.84
29 Glass Product	17.41	-4455.69	-609.74	3593.83	2871.70	-1382.69	0.34	59.42	18.07	13.98
30 Cement	13.73	8.73	1.70	-6.37	-15.02	24.69	0.33	164.35	-392.32	-14.76
31 Non Metallic	20.01	-79.98	-12.02	55.95	72.33	-16.27	0.27	68.00	22.95	2.18
32 Basic Metal	57.23	29.32	31.71	-5.54	-4.32	6.06	4.33	87.20	39.20	27.85
33 Other Metal	33.71	179.98	59.98	-120.60	-51.45	-34.20	0.69	35.08	6.90	2.19
34 Non Electrical Machinery	9.15	-19.10	-8.23	35.32	10.50	-9.34	0.90	23.38	2.67	17.58
35 Electrical Machinery	8.20	16.71	16.14	-29.17	-3.61	8.14	3.07	46.37	16.53	17.58
36 Motor Vehicles	17.52	18.88	0.29	-12.88	-2.67	13.90	1.50	117.22	80.89	8.20
37 Other Transport	13.96	6.97	0.16	-4.73	-3.21	14.76	0.41	137.71	123.82	56.60
38 Other Manufacture Product	17.27	-169.62	-101.12	175.92	22.70	89.39	0.49	49.37	18.69	11.37
V Services (39-40)	**53.24**	**130.13**	**3.00**	**-68.06**	**-15.94**	**4.10**	**42.06**	**192.09**	**139.70**	**14.12**
39 Construction	27.29	79.23	0.67	-43.72	-4.19	-4.69	7.96	114.96	100.62	5.79
40 Others Services	25.95	50.90	2.33	-24.34	-11.74	8.79	34.10	77.13	39.07	8.33

Table 3 continued

δ(1991-2000)				δ(1978-2000)						
ISF	ISW	IOC	S 1991	δ X/ X2000	FDE	EDE	ISF	ISW	IOC	S1978
-200.05	**956.98**	**-167.32**	**7.44**	140.62	-109.19	-152.95	11.03	275.21	116.53	12.57
11.41	-23.14	39.07	1.39	24.93	-16.24	-4.83	1.48	23.65	20.88	2.59
10.67	-43.06	101.23	0.72	36.11	-12.14	5.05	0.56	19.52	23.13	1.93
10.31	173.75	-95.67	0.36	35.99	-10.95	-2.06	0.51	37.68	10.81	1.27
19.46	-39.30	3.63	1.06	15.16	-9.08	-6.28	1.26	19.43	9.84	1.47
-263.27	912.81	-233.38	2.61	14.54	-51.41	-143.31	6.19	158.24	44.82	2.82
11.37	-24.08	17.80	1.30	13.88	-9.36	-1.53	1.03	16.69	7.05	2.48
70.72	-119.17	-190.60	3.56	8.47	-3.03	-2.84	0.81	10.17	3.36	6.24
78.33	**84.64**	**430.44**	**11.82**	**196.09**	**-0.14**	**77.05**	**-6.30**	**47.92**	**77.56**	**17.78**
7.17	-15.26	47.01	0.65	20.95	-14.80	-4.94	1.24	19.97	19.48	1.19
10.21	-7.25	28.86	0.42	14.72	33.00	38.02	-3.96	-22.75	-29.59	0.61
0.30	-0.96	79.26	2.54	17.40	-4.49	-1.38	0.35	9.69	13.23	5.42
8.27	-23.83	55.01	0.38	44.06	-52.27	-8.00	2.06	45.12	57.15	1.45
10.98	-6.25	14.29	0.59	11.75	15.78	20.46	-2.63	-12.08	-9.77	0.64
5.44	-9.95	32.36	0.41	12.29	-3.56	-2.46	0.53	7.26	10.51	0.99
-26.25	206.66	39.26	0.38	15.79	-2.00	-1.36	0.26	15.29	3.61	0.50
7.97	-7.82	25.83	0.36	11.37	-5.62	-1.41	0.92	7.05	10.43	0.46

9.52	-1.43	-4.48	0.49	15.78	21.99	1.99	-2.86	-3.01	-2.32	0.79	
9.76	-12.21	35.43	1.08	11.70	6.74	18.92	-1.54	-13.44	1.03	1.57	
13.42	-4.66	16.05	1.08	4.38	1.21	7.87	-0.56	-1.55	-2.58	0.59	
12.75	-12.11	22.42	2.09	9.98	5.07	14.61	-1.24	-8.47	0.01	2.53	
2.55	-0.84	3.42	0.26	2.00	-1.05	-4.89	1.06	2.66	4.21	0.21	
6.23	-19.43	35.74	1.08	3.92	-0.14	-0.38	0.09	2.18	2.16	0.84	
137.09	**138.12**	**268.52**	**30.02**	**199.81**	**176.90**	**-97.34**	**-2.24**	**36.28**	**86.22**	**21.35**	
5.39	-11.97	43.77	1.96	2.35	-0.07	-1.63	0.09	1.52	2.44	0.64	
6.38	-12.09	13.35	0.17	5.98	-1.31	-2.09	1.03	11.41	-3.05	0.16	
3.28	-5.53	19.96	0.52	5.17	-0.64	-1.07	0.22	2.71	3.96	0.62	
2.46	-5.33	17.45	1.45	4.18	-0.24	-0.32	0.13	2.18	2.42	2.49	
95.94	-15.82	-316.82	0.92	115.38	184.81	-108.62	-4.39	-8.22	51.79	3.88	
11.95	-10.30	18.48	1.20	7.67	3.46	15.87	-1.09	-7.74	-2.83	0.81	
14.65	-12.34	-27.04	1.20	2.87	-0.54	-2.92	0.54	3.65	2.14	0.44	
4.23	-12.27	35.41	0.57	3.58	-0.15	-0.63	0.08	1.80	2.48	0.34	
-58.96	327.91	302.47	0.71	7.81	-0.58	-1.12	0.18	7.65	1.68	0.33	
3.41	-26.67	66.13	0.40	4.71	-0.16	-0.31	0.05	2.51	2.62	0.27	
7.99	-18.60	30.76	2.22	17.27	-5.07	2.26	0.64	9.71	9.73	4.33	
1.46	-7.85	32.39	0.60	4.09	-0.11	-0.25	0.04	1.61	2.81	0.69	
2.00	-0.40	1.53	2.87	0.74	-0.05	-0.05	0.19	0.28	0.36	0.90	
5.24	-1.85	8.86	10.99	1.32	1.08	18.91	-1.77	-4.65	-12.26	3.07	
9.31	-10.77	29.60	2.52	7.11	-1.21	-0.38	0.27	2.39	6.04	1.50	
17.26	-34.69	-25.28	0.87	6.65	-0.62	-0.56	0.14	2.62	5.08	0.41	
5.09	-3.29	17.52	0.84	2.95	-1.70	-14.42	1.40	6.86	10.81	0.49	
20.03	**-18.43**	**36.68**	**47.16**	**17.78**	**35.86**	**1.42**	**-7.49**	**-16.95**	**4.94**	**42.06**	
12.97	-3.94	-0.47	8.57	10.85	36.80	2.36	-7.73	-20.66	0.09	7.96	
7.07	-14.49	37.15	38.60	6.93	-0.94	-0.94	0.24	3.71	4.85	34.10	

Note: X/X gross output share change; FDE-final demand expansion; EDE-export demand expansion; ISF - import substitution of final goods; ISW- import substitution of intermediate goods;IOC-IO coefficient change; S-gross output share.

Modern Applied Science

www.ccsenet.org/journal.html

Vol. 2, No. 3

May 2008

P-completely Regular Semigroup

Xiujuan Pan

Department of Mathematics, Tianjin Polytechnic University

Tianjin 300160, China

E-mail: pxj10628@126.com

Abstract

In order to prove a completely regular semigroup with the strong semilattice structure is P-completely regular semigroup. Using the strong semilatice structure and the property of congruence. The sufficient condition of which a completely regular semigroup is P-completely regular semigroup is have the strong semilattice structure, and The subclass NBG of the completely regular semigroup is P-completely regular semigroup.

Keywords: Completely regular semigroup, The strong semilattice, Homomorphisms

1. Preliminaries

Definition 1.1. A semigroup S is a semilattice Y of semigroup $S_\alpha\ (\alpha \in Y\}$ if there exists an epimorphism φ of S onto the semilattice Y with $\alpha\varphi^{-1} = S_\alpha\ (\alpha \in Y\}$. We write $S = [Y; S_\alpha]$.

Definition 1.2. Let $S = [Y; S_\alpha]$ be a semilattice of semigroups. If for every $\alpha \in Y$ every congruence on S_α can be extended to a congruence on S,then S is said to be a P-semigroup.

Definition 1.3. A semigroup S is called completely regular, if for every $a \in S$, there exists an element $x \in S$ such that $a = axa$ and $ax = xa$.

In [1], we have known that completely regular semigroup $S = [Y; S_\alpha]$ is a semilattice of completely simple semigroups S_α. In fact, every S_α is a D-class of S. If every congruence on D-class of S can be extended to a congruence on S, then S is said to be a P-completely regular semigroup.

Definition 1.4. Let $S = [Y; S_\alpha]$ be a semilattice of semigroup. For each pair $\alpha, \beta \in Y$ such that $\alpha \geq \beta$, let $\varphi_{\alpha,\beta} : S_\alpha \to S_\beta$ be a homomorphism such that

(i) $\varphi_{\alpha,a} = 1_{S_\alpha}$,

(ii) $\varphi_{\varepsilon,\beta}\varphi_{\beta,\gamma} = \varphi_{\alpha,\gamma}$ *if* $\alpha \geq \beta \geq \gamma$

on $S = \cup_{\alpha \in Y} S_\alpha$ define a multiplication by

$ab = (a\varphi_{\alpha,\alpha\beta})(b\varphi_{\beta,\alpha\beta})$ $(a \in \alpha, b \in \beta)$

with this multiplication S is a strong semilattice Y of semigroup S_α to be denoted by $S = [Y; S_\alpha, \varphi_{\alpha,\beta}]$.

In this paper, we mainly give some views on a open problem“ characterize all the P − completely regular semigroups ”, and find the sufficient condition that a completely regular semigroup is the P-completely regular semigroup.

We shall use the same notations and terminology to [1]. In this paper, we are interested in the symbols:

CR	of completely regular semigroups,
NB	of normal bands,
$Con\,(S)$	of all congruences on S,
NBG	of normal cryptogroups,
$ONBG$	of normal orthogroups,
$Clifford$	of clifford semigroups.

2. The Main Result

Let $S=[Y;S_\alpha,\varphi_{\alpha,\beta}]$ be a strong semilattice of semigroups. If $\rho_\alpha \in Con(S_\alpha)$, then for every $\beta \in Y$ we can define a new relation $\rho_\alpha^* = \cup_{\beta\in Y}\rho_\alpha^*|_{S_\beta}$ as follows:

$$\rho_\alpha^*|_{S_\beta}=\begin{cases}\rho_\alpha & \beta=\alpha\\ \{(a\varphi_{\alpha,\beta},b\varphi_{\alpha,\beta})\in S_\beta\times S_\beta \mid (a,b)\in\rho_\alpha\}\cup 1_{S_\beta} & \beta<\alpha\\ \{(u,v)\in S_\beta\times S_\beta \mid (u\varphi_{\beta,\alpha},v\varphi_{\beta,\alpha})\in\rho_\alpha\} & \beta>\alpha\end{cases} \quad (1^*)$$

Theorem 2.1. Let $S=[Y;S_\alpha,\varphi_{\alpha,\beta}]$ be a strong semilattice of semigroups, if $\rho_\alpha\in Con(S_\alpha)$, then $\rho_\alpha^*|_{S_\beta}\in Con(S_\beta)$.

Proof. We need prove from two parts as follows:

(1) Assume $\beta>\alpha, u,v\in S_\beta$ and $(u,v)\in\rho_\alpha^*|_{S_\beta}$, then by the definition

of ρ_α^* we have $(u\varphi_{\beta,\alpha},v\varphi_{\beta,\alpha})=\rho_\alpha^*|_{S_\beta}=\rho_\alpha^*$.For any $c\in S_\beta, c\varphi_{\phi,\alpha}\in S_\alpha$,since $\rho_\alpha\in Con(S_\alpha)$,this imply that

$(u\varphi_{\beta,\alpha})(c\varphi_{\beta,\alpha})\rho_\alpha(v\varphi_{\beta,\alpha})(c\varphi_{\beta,\alpha})\Rightarrow(uc)\varphi_{\beta,\alpha}\rho_\alpha(vc)\varphi_{\beta,\alpha}\Rightarrow(uc,vc)\in\rho_\alpha^*|_{S_\beta}$.

Similarly,we can show that $(cu,cv)\in\rho_\alpha^*|_{S_\beta}$.Thus $\rho_\alpha^*|_{S_\beta}\in Con(S_\beta)$.

(2) Assume $\beta<\alpha, m,n,u,v\in S_\beta$,and $(m,n),(u,v)\in\rho_\alpha^*|_{S_\beta}$.Form the definition of ρ_α^*,there exist $a,b,c,d\in S_\alpha$,so that $b\varphi_{\alpha,\beta}=v, d\varphi_{\alpha,\beta}=n$,and $(a,b)\in\rho_\alpha^*$, $(c,d)\in\rho_\alpha^*$.Since $\rho_\alpha\in Con(S_\alpha)$,we have $(ac,bd)\in\rho_\alpha$,

$\Rightarrow((ac)\varphi_{\alpha,\beta},(bd)\varphi_{\alpha,\beta})\in\rho_\alpha^*|_{S_\beta}$

$\Rightarrow(a\varphi_{\alpha,\beta})(c\varphi_{\alpha,\beta})\rho_\alpha^*|_{S_\beta}(b\varphi_{\alpha,\beta})(d\varphi_{\alpha,\beta})$

$\Rightarrow(um,vn)\in\rho_\alpha^*|_{S_\beta}$.

Thus $\rho_\alpha^*|_{S_\beta}\in Con(S_\beta)$.From (1) and (2),we conclude that $\rho_\alpha^*|_{S_\beta}\in Con(S_\beta)$ for any $\beta\in Y$.

We have immediately the following corollary and it's proofs are omitted.

Corollary 2.2. Let $S=[Y;S_\alpha,\varphi_{\alpha,\beta}]$ be a strong semilattice of semigroups, and $a,b\in S_\beta$.If $(a,b)\in\rho_\alpha^*$, then $(a\varphi_{\beta,\gamma},b\varphi_{\beta,\gamma},)\in\rho_\alpha$ for any $\gamma\le\beta$.

Theorem 2.3. If $S=[Y;S_\alpha,\varphi_{\alpha,\beta}]$ be a strong semilattice of semigroups,then S is a P-semigroup.

Proof. We need prove for every $a\in Y$ every congruence on S_α can be extended to a congruence on S, that is to say, we only need prove $\rho_\alpha^*\in Con(S)$. Let $(a,b)\in\rho_\alpha^*$. By the definition of ρ_α^* as (1□), we know a is in the same subsemigroup of S with b.Assume that $a,b\in S_\beta$, then for any $c\in S$, let $c\in S_\gamma$, by Definition1.4.,we have

$ac=(a\varphi_{\beta,\beta\gamma})(c\varphi_{\beta,\beta\gamma})$, $bc=(b\varphi_{\beta,\beta\gamma})(c\varphi_{\beta,\beta\gamma})$.

Since $(a,b)\in\rho_\alpha^*|_{S_\beta}$, thus

$\Rightarrow(a\varphi_{\beta,\beta\gamma},b\varphi_{\beta,\beta\gamma})\in\rho_\alpha^*|_{S_{\beta\gamma}}\in Con(S_{\beta\gamma})$

$\Rightarrow(a\varphi_{\beta,\beta\gamma})(c\varphi_{\gamma,\beta\gamma})\rho_\alpha^*|_{S_{\beta\gamma}}(b\varphi_{\beta,\beta\gamma})(c\varphi_{\gamma,\beta\gamma})$

$\Rightarrow(ac,bc)\in\rho_\alpha^*|_{S_{\beta\gamma}}$

$\Rightarrow(ac,bc)\in\rho_\alpha^*$.

Similarly, we may show that $(ac,bc)\in\rho_\alpha^*$. This show that $\rho_\alpha^*\in Con(S)$. By arbitrariness of α, we get S is P-semigroup.

From Theorem2.3. we know the sufficient condition of which a semigroup is the P-semigroup. If $S\in CR$, then we have immediately the following corollary.

Corollary 2.4. Let $S\in CR$. If $S=[Y;S_\alpha,\varphi_{\alpha,\beta}]\in NBG$,then S is P- completely regular semigroup.

From Corollary2.4.,it is obvious that all the subclass of NBG, i.e. NB , $ONBG$, $Clifford$, is P -

completely regular semigroup.

References

M Petrich & N R Reilly. (1999). *Completely Requlars Semigroups*. New York: Wiley.

Howie, J.M. (1995). *Fundamentals of Semigroup Theory*, Oxford Science Publications, Oxford.

Pastijn, F., *Idempotent distributive semirings II*, Semigroup Forum 26 (1983), 151–166.

X.Z. Zhao, Guo Y.Q. & Shum K.P. (2001). *D-subvarieties of the variety of idempotent semi- rings*. Algebra Colloq 9, pp 15-28.

Modern Applied Science

www.ccsenet.org/journal.html

Vol. 2, No. 3

May 2008

The Reliability Analysis of N-Unit Series Repairable System With One Replaceable Repair Facility and a Repairman Doing Other Work

Xianyun Meng

Department of Science, Yanshan University

Qinhuangdao 066004, China

Yanqin Guan (Corresponding author)

Department of Science, Yanshan University

Qinhuangdao 066004, China

E-mail: guanyanqin123@163.com

Jianying Yang

Department of Science, Yanshan University

Qinhuangdao 066004,China

Taotao Wang

Department of Science, Yanshan University

Qinhuangdao 066004, China

Supported by the Foundation for the natural science of He Bei province of China (A2005000301)

Supported by the Plan Projects of Hebei Education Office (No.2007323).

Abstract

A model of N-unit series repairable systems with a repairman doing other work is studied and the impact on the system reliability because of a replaceable facility is also considered. It is assumed that the life of each unit, the life of the facility are exponentially distributed, the repair time of the unit, the replace time of the facility and the work time of the repairman outside the system are all generally distributed. By using approach of supplementary variables and method of generalized Markov progress, some important reliability indicates of the system and the facility are obtained.

Keywords: Reliability, Vector Markov process, Laplace-transform

1. Introduction

In reliability analysis of repairable systems, it is usually assumed that the repairman has two states, either repairing the failed unit or idle. However, in actual practice, in order to increase system income, the administrator of system often will consider that the repairman should service for customer of outside system without affecting the system at the same time. The question is that, the system allows the repairman to service for customer of outside system, will how affect the reliability of indicators. If it is permitted, how to restrict the repairman's service for customers, will increase the system's total receipts without affecting the system. Theoretically, repairable system with replaceable repair facilities and repairman doing other work are in class of more general repairable systems. Liu and Tang studied an N-unit series repairable system with a repairman doing other work, more reliability indices of the system are obtained by using the Laplace-transform technique. In practical applications, it is necessary to consider the effect that caused by replacing the repair facility. In view of the reference (Liu and Tang), we consider the reliability analysis of N-unit series repairable system with one replaceable system with one replaceable repair facility and a repairman doing other work. It is assumed that the life of each unit, the life of the facility are exponentially distributed, the repair time of the unit, the replace time of the facility and the work time of the repairman outside the system are all generally distributed. By using approach of supplementary variables and method of generalized Markov progress, some important reliability indicates of the system and the facility are obtained.

2. The description of system

(1) The system consists of N-dissimilar-unit operate in a series configuration with a single repair facility. The lifetime X_i of the units has an exponential distribution $F_i(t) = 1 - e^{-\lambda_i t}, t \geq 0$. The repair time Y_i of failed unit has an arbitrary distribution $G_i(t)$ with mean $\mu_i (0 \leq \mu_i < \infty), (i = 1,2,\cdots,n)$ At time t=0, all the units are new, and all are in working state while the repairman is idle. If a unit is waiting for the repairman or being repaired, the other unit won't fail any more and the system is down;

(2) The service time H for customer of the repairman has an arbitrary distribution $H(t)$ with mean $d(0 \leq d \leq \infty)$;

(3) The time interval from the repairman idle to the customer arrival and the time interval from the first customer arrival to the second customer arrival have an exponential distribution $F(t) = 1 - e^{-ct}, t \geq 0$; The repairman is idle only when the system is in working state and there is no customer arrival. And the customer may arrival only when the system is in working state. If the repairman is busying with a customer and the other customer is waiting for the repairman or the system has failed units, another customer won't arrive any more. If a unit failed when a customer is waiting for the repairman, the customer will leave the system, and the failed unit is waiting for the repairman until the repairman completing the repair of the earlier customer.

(4) The lifetime U of the repair facility has an exponential distribution $U(t) = 1 - e^{-\alpha t}$ $(0 \leq \alpha < \infty, t \geq 0)$. The replacement time V of the repair facility has an arbitrary distribution $V(t)$ with mean $\beta (0 \leq \beta < \infty)$. It is assumed that the repair facility neither fails nor deteriorates in its idle periods. When the repair facility fails, it is replaced by a new one and the failed unit must wait for repair. When the replacement of the failed repair facility is completed, the new repair facility continues to repair the failed unit. The repair time for the failed unit cumulative repair time for failed unit exceeds Y_i;

(5) All the random variables are mutually independent. After being repaired, the failed unit is as good as new.

3. The equations of the system

Let $N(t)$ be the state of the system at time t, we have:

State 0 : the system works and the repairman idles;

State 1i : repairing the failure unit i;

State 2i : unit i has not been completed the repair and replacement of the repair facility;

State 3 : the system works and repairman services for customer;

State 4i : the failure unit i is waiting to be repaired and the repairman services for customer;

State 5: the system works ,the repairman services for customer and the other customers is waiting for service.

The introduction of supplementary variables:

Where $N(t) = 3, 4i, 5, i = 1,2,\cdots,n;$ let $X(t)$ be the hours that the customer has spent on the service for customer at time $t, 0 \leq X(t) < \infty$.

Where $N(t) = 1i, i = 1,2,\cdots,n;$ let $Y_i(t)$ be the hours that the failure unit has been repaired at time $t, 0 \leq Y_i(t) < \infty$.

Where $N(t) = 2i, i = 1,2,\cdots,n;$ let $Z(t)$ be the hours that the repair facility has been replaced at time $t, 0 \leq Z(t) < \infty$.

Then $\{N(t), X(t), Y_i(t), Z(t), t \geq 0, i = 1,2,\cdots,n\}$ constitute a vector Markov process.

The state probability of the system at time t is defined by

$P_0(t) = P\{N(t) = 0\}$,

$P_{1i}(t,y)dy = P\{N(t) = 1i, y \leq Y_i(t) < y + dy\}$, $\quad i = 1,2,\cdots,n;$

$P_{2i}(t,y,w)dydw = P\{N(t) = 2i, Y_i(t) = y, w \leq Z(t) < w + dw\}$, $\quad i = 1,2,\cdots,n;$

$P_3(t,x)dx = P\{N(t) = 3, x \leq X(t) < x + dx\}$,

$P_{4i}(t,x)dx = P\{N(t) = 4i, x \leq X(t) < x + dx\}$, $\quad i = 1,2,\cdots,n;$

$P_5(t,x) = P\{N(t) = 5, x \leq X(t) < x + dx\}$.

Where $\lambda = \lambda_1 + \lambda_2 + \cdots + \lambda_n$, we can obtain the following differential equations for the system from a probability analysis:

$$[\frac{d}{dt}+\lambda+c]P_0(t)=\int_0^\infty d(x)P_3(t,x)dx+\sum_{i=1}^{n}\int_0^\infty \mu_i(y)P_{1i}(t,y)dy, \quad (1)$$

$$\left[\frac{\partial}{\partial t}+\frac{\partial}{\partial y}+\mu_i(y)+\alpha\right]P_{1i}(t,y)=\int_0^\infty \beta(w)P_{2i}(t,y,w)dw, \qquad i=1,2,\cdots,n; \quad (2)$$

$$\left[\frac{\partial}{\partial t}+\frac{\partial}{\partial w}+\beta(w)\right]P_{2i}(t,y,w)=0, \qquad i=1,2,\cdots,n; \quad (3)$$

$$\left[\frac{\partial}{\partial t}+\frac{\partial}{\partial x}+d(x)+c+\lambda\right]P_3(t,x)=0, \quad (4)$$

$$\left[\frac{\partial}{\partial t}+\frac{\partial}{\partial x}+d(x)\right]P_{4i}(t,x)=\lambda_i P_3(t,x)+\lambda_i P_5(t,x), \qquad i=1,2,\cdots,n; \quad (5)$$

$$\left[\frac{\partial}{\partial t}+\frac{\partial}{\partial x}+d(x)+\lambda\right]P_5(t,x)=cP_3(t,x) \quad (6)$$

The boundary conditions are:

$$P_{1i}(t,0)=\lambda_i P_0(t)+\int_0^\infty d(x)P_{4i}(t,x)dx, \qquad i=1,2,\cdots,n;$$

$$P_{2i}(t,y,0)=\alpha P_{1i}(t,y), \qquad i=1,2,\cdots,n;$$

$$P_3(t,0)=cP_0(t)+\int_0^\infty d(x)P_5(t,x)dx$$

$$P_{4i}(t,0)=0 \qquad i=1,2,\cdots,n; \qquad P_5(t,0)=0$$

The initial conditions are: $P_0(0)=1,$ the others are 0.

4. The solutions of the equations

Remarks: This paper adopts the following notation:

$D^*(s)$ denotes the L transform of $D(t)$, and $\hat{D}(s)$ denotes the LS transform of $D(t)$, that is $D^*(s)=\int_0^\infty D(t)e^{-st}dt, \hat{D}(s)=\int_0^\infty e^{-st}dD(t)$, $\bar{D}(t)=1-D(t)$. Taking Laplace transforms on both sides of the above differential equations and using the boundary and initial conditions, we can obtain:

$$P_{1i}^*(s,y)=P_{1i}^*(s,0)e^{-\left[s+\alpha-\alpha\hat{H}(s)\right]y}\bar{G}_i(y), \qquad i=1,2,\cdots,n;$$

$$P_{2i}^*(s,y,w)=P_{2i}^*(s,y,0)e^{-sw}\bar{H}(w)=\alpha P_{1i}^*(s,y)e^{-sw}\bar{H}(w), \qquad i=1,2,\cdots,n;$$

$$P_3^*(s,x)=P_3^*(s,0)e^{-(s+c+\lambda)x}\bar{H}(x),$$

$$P_{4i}^*(s,x)=\frac{\lambda_i}{\lambda}P_3^*(s,0)e^{-sx}\left(1-e^{-\lambda x}\right)\bar{H}(x), \qquad i=1,2,\cdots,n;$$

$$P_5^*(s,x)=P_3^*(s,0)e^{-(s+\lambda)x}\left(1-e^{-cx}\right)\bar{H}(x),$$

$$P_{1i}^*(s,0)=\lambda_i P_0^*(s)\cdot A_1, \qquad i=1,2,\cdots,n;$$

$$P_3^*(s,0)=\frac{cP_0^*(s)}{1-\hat{H}(s+\lambda)+\hat{H}(s+\lambda+c)},$$

$$P_0^*(s)=\frac{1}{s+\lambda+c-A_3-\sum_{i=1}^{n}\lambda_i\hat{G}\left(s+\alpha-\alpha\hat{H}(s)\right)\cdot A_1}$$

where

$$A_1=1+\frac{c}{\lambda}\cdot\frac{\hat{H}(s)-\hat{H}(s+\lambda)}{1-\hat{H}(s+\lambda)+\hat{H}(s+\lambda+c)} \qquad A_2=\sum_{i=1}^{n}\frac{\lambda_i\left[1-\hat{G}_i\left(s+\alpha-\alpha\hat{H}(s)\right)\right]}{s+\alpha-\alpha\hat{H}(s)}$$

$$A_3=\frac{c\hat{H}(s+\lambda+c)}{1-\hat{H}(s+\lambda)+\hat{H}(s+\lambda+c)} \qquad A_4=1+\frac{c}{\lambda}\cdot\frac{1-\hat{H}(\lambda)}{1-\hat{H}(\lambda)+\hat{H}(\lambda+c)}$$

$$A_5 = \frac{c}{d} \cdot \frac{1}{1-\hat{H}(\lambda)+\hat{H}(\lambda+c)}$$

5. System reliability

Theorem 1: The system's point availability $A(t)$, The Laplace transform of $A(t)$ is given by

$$A^*(s) = P_0^*(s)\left[1+\frac{c}{s+\lambda}\cdot\frac{1-\hat{H}(s+\lambda)}{1-\hat{H}(s+\lambda)+\hat{H}(s+\lambda+c)}\right] \tag{7}$$

And the steady state availability of system is

$$\begin{aligned} A &= \lim_{t\to\infty} A(t) = \lim_{s\to 0} sA^*(s) \\ &= \frac{A_4}{1+A_5+\sum_{i=1}^{n}\frac{\lambda_i}{\mu_i}\left(1+\frac{\alpha}{h}\right)A_4} \end{aligned} \tag{8}$$

The rate of occurrence of failure (ROCOF) $W_f(t)$, and the Laplace transform of the ROCOF $W_f(t)$ is

$$W_f^*(t) = \lambda A^*(s) \tag{9}$$

And the steady-state ROCOF of the system is given by

$$W_f = \lambda A \tag{10}$$

Theorem 2: The time rate of the repairman services for customer at time t is $D(t)$, and the Laplace transform of $D(t)$ is given by

$$D^*(s) = \frac{c\hat{H}(s)P_0^*(s)}{1-\hat{H}(s+\lambda)+\hat{H}(s+\lambda+c)} \tag{11}$$

The mean number of the repairman services for customer of system in the steady-state in [0,t] is given by

$$N = \frac{\frac{c}{1-\hat{H}(\lambda)+\hat{H}(\lambda+c)}}{1+A_5+\sum_{i=1}^{n}\frac{\lambda_i}{\mu_i}\left(1+\frac{\alpha}{h}\right)\cdot A_4} \tag{12}$$

Theorem 3: The replacement time probability of the repair facility at time t is $\varphi(t)$, and the Laplace transform of $\varphi(t)$ is given by

$$\varphi^*(s) = \frac{\alpha\hat{H}(s)\cdot A_1\cdot A_2}{s+\lambda+c-A_3-\sum_{i=1}^{n}\lambda_i\hat{G}_i\left(s+\alpha-\alpha\hat{H}(s)\right)\cdot A_1} \tag{13}$$

In steady-state, the result is:

$$\lim_{t\to\infty}\varphi(t) = \lim_{s\to 0^+} s\varphi^*(s) = \frac{\frac{\alpha}{h}\cdot A_4\cdot\sum_{i=1}^{n}\frac{\lambda_i}{\mu_i}}{1+A_5+\sum_{i=1}^{n}\frac{\lambda_i}{\mu_i}\left(1+\frac{\alpha}{h}\right)\cdot A_4} \tag{14}$$

Theorem 4: The repair facility's point replacement rate is $M_f(t)$, and the Laplace transform of $M_f(t)$ is given by

$$M_f^*(s) = \frac{\alpha\cdot A_1\cdot A_2}{s+\lambda+c-A_3-\sum_{i=1}^{n}\lambda_i\hat{G}_i\left(s+\alpha-\alpha\hat{H}(s)\right)\cdot A_1} \tag{15}$$

and in steady-state, the result is:

$$M_f = \lim_{t\to\infty} M_f(t) = \lim_{s\to 0^+} sM_f^*(s) = \frac{\alpha\cdot A_4\cdot\sum_{i=1}^{n}\frac{\lambda_i}{\mu_i}}{1+A_5+\sum_{i=1}^{n}\frac{\lambda_i}{\mu_i}\left(1+\frac{\alpha}{h}\right)\cdot A_4} \tag{16}$$

6. The analysis of system benefit

Assuming that the system average revenue per unit time for the x_1, each unit fault caused a loss for the average x_2, the replacement of equipment once caused the average loss for x_3, repairman services for one customer bring a system of the average income of x_4, assuming that the system in a steady state, the average time units total receipts:

$$Y = Ax_1 - W_f x_2 - M_f x_3 + Nx_4$$

$$= \frac{\left(x_1 - \lambda x_2 - \alpha x_3 \sum_{i=1}^{n} \frac{\lambda_i}{\mu_i}\right) \cdot A_4 + \frac{cx_4}{1 - \hat{H}(\lambda) + \hat{H}(\lambda + c)}}{1 + A_5 + \sum_{i=1}^{n} \frac{\lambda_i}{\mu_i}\left(1 + \frac{\alpha}{h}\right) \cdot A_4} \tag{17}$$

References

Liu, R.B, Tang, Y.H. & Luo, C.Y (2005). An N-unit series repairable system with a repairman doing other work. *Science of Hen Long Jiang University*. 22 (4): 493-496.

Cao, J.H. & Wu, Y.H. (1989). Reliability analysis of a two-unit cold standby system with a replaceable repair facility. *Microelectronics & Reliability*.29 (2):145-150.

Zhou, J.L. (1994). Reliability analysis of a two-unit paralled repairable system with a repairable facility. *J. of Eng. Math*.11 (4): 73-80.

Cao, J.H. & Cheng. K. (1986). Introduction to Reliability Mathematics. Beijing: Academic Press.

Tang, Y. H. (1996). Some new reliability problems and results for one unit repairable system. *Microelectronics & Reliability*. 34 (4): 465-468.

Widder, D.V. (1946). The Laplace Transform. Princeton University Press.

Liu, R.B. & Tang, Y.H. (2007). A new kind of N-unit series repairable systems and its reliability analysis. *Mathematica Applicate*. 20 (1): 164-170.

Liu, R.B. & Tang, Y.H. (2006). Two-different-units paralleled repairable system with a replaceable facility and repair delay. Apple Math.J Chinese Univ. Ser. A. 21(2): 127-140.

Tang, Y.H. & Yu, G. J. (2005). Two-unit same paralleled repairable system with a replaceable facility and delay repair. *Chinese Journal of Engineering Mathematics*. 22(1): 1-8.

Modern Applied Science

www.ccsenet.org/journal.html

Vol. 2, No. 3

May 2008

Estimation for Product Life Expectancy Paramaters under Interval Censored Samples

Kaiwen Guo

Department of Maths, Tianjin Polytechnic University

Tianjin 300160, China

Tel: 86-022-2459-0532 E-mail: guokaiwen04@126.com

Abstract

From basic consept for reliability theory, we computed the moment and maximum likehood estimation for product life expectancy paramaters by means of interval censor data. This is a feasible and efficient estimator for life parameters

Keywords: Exponential distribution, Reliability function, Interval censored data, Moment estimation, Maximum likehood estimation

1. Introduction

In survival analysis and reliable research, often because of the restriction of objective conditions,

the time lapse could not be accurately observed values, which they can only be observed by their interval. Generally this kind of data is called interval censored data . In 1972 Hole and Walburg had the research and the application in the medicine clinical test domain to the interval censored data . In 1991 Keiding and walburg gave the definition of the interval censored data theoretically. When the survival variable turns to the product life, the products to maintain their performance time are an imporant quality indicator, such reliability and product life are linked each other. When the censored variable turns to a time variable, we assume that this variable be a continuous random variable, the probability density function have un-known parameters which need to be estimated. In this paper, by means of interval censored data, we gave the monment estimation and maximum likehood estimation.

2. Suppose that survival variable and the interruption variable all obey the single parameter exponential distribution

Let X be a survival variable, which is a continuous random variable, the probability density function of X is $f(x)$, the distribution function of X is $F(x)$. Suppose that survival variable obeys the single parameter exponential distribution, $f(x) = e^{-x/\theta}/\theta \quad (x \geq 0)$, $f(x) = 0 \quad (x < 0)$. Let Y be a survival variable, which is a continuous random variable, the probability density function of Y is $g(y)$, the distribution function of Y is $G(y)$. Suppose that survival variable obeys the single parameter exponential distribution, $g(y) = e^{-y/\theta_0}/\theta_0 \quad (y \geq 0), g(y) = 0 \quad (y < 0)$. Assume X and Y be mutually independent, $\theta > \theta_0$ means that the average life span of censored variables not less than that of test objects . Let $(x_1, x_2, ..., x_n)$ be a simple sample which comes from the overall X, $(y_1, y_2, ..., y_n)$ be a simple sample which comes from the overall Y. When we observe them actually, we can obtain the sample (Y_i, δ_i), where $\delta_i = 1 \quad (X_i \leq Y_i)$ or $\delta_i = 0 \quad (X_i > Y_i) \quad (i = 1,2,...,n)$. Now we consider the monment estimation of interal $X_i \leq Y_i$, the mathematical expectation of them

$$EZ = \iint xyf(x)g(y)dxdy = \int_0^\infty \int_x^\infty xy\, e^{-x/\theta}/\theta\; e^{-y/\theta_0}/\theta_0\, dxdy$$

$$= \int_0^\infty e^{-(\theta+\theta_0)x/\theta\theta_0}\, x/\theta\, dx = \theta_0/(\theta+\theta_0)$$

Let $EZ = \bar{\delta}$, where $\bar{\delta} = \sum_i \delta_i / n$, we have $\bar{\delta} = \theta_0/(\theta+\theta_0)$, then $\bar{\theta} = (1-\bar{\delta})\theta_0/\bar{\delta}$

3. Suppose that survival variable obeys the single parameter exponential distribution and the interruption variable obeys the even distribution

Let X be a survival variable, which is a continuous random variable, the probability density function of X is $f(x)$, the distribution function of X is $F(x)$. Suppose that survival variable obeys the single parameter exponential distribution, $f(x) = e^{-x/\theta}/\theta \quad (x \geq 0)$, $f(x) = 0 \quad (x < 0)$. Let Y be a survival variable, which is a continuous random variable, the probability density function of Y is $g(y)$, the distribution function of Y is $G(y)$. Suppose that survival variable obeys the even distribution, $g(y) = 1/\theta_0 \quad (y \in (0, \theta_0))$, $g(y) = 0 \quad (y \notin (0, \theta_0))$. Assume X and Y be mutually independent, $\theta > \theta_0$ means that the average life span of censored variables not less than that of test objects. Let $(x_1, x_2, ..., x_n)$ be a simple sample which comes from the overall X, $(y_1, y_2, ..., y_n)$ be a simple sample which comes from the overall Y. When we observe them actually, we can obtain the sample (Y_i, δ_i), where $\delta_i = 1 \quad (X_i \leq Y_i)$ or $\delta_i = 0 \quad (X_i > Y_i) \quad (i = 1,2,..., n)$. Now we consider the monment estimation of interal $X_i \leq Y_i$, the mathematical expectation of them

$$EZ = \iint xyf(x)g(y)dxdy = \int_0^{\infty}\int_x^{\theta_0} xye^{-x/\theta}/(\theta\theta_0)dxdy$$

$$= \int_0^{\infty} e^{-x/\theta}(\theta_0 - x)xd\,x/(\theta\theta_0) = \theta - \frac{2\theta^2}{\theta_0}$$

Let $EZ = \overline{\delta}$, where $\overline{\delta} = \sum_i \delta_i / n$, we have $2\theta^2 - \theta_0\theta + \theta_0\overline{\delta} = 0$

$\overline{\theta} = (\theta_0 - \sqrt{\theta_0^2 - 8\theta_0\overline{\delta}})/2$ (Charities) then $\overline{\theta} = (\theta_0 + \sqrt{\theta_0^2 - 8\theta_0\overline{\delta}})/2$

4. Suppose that survival variable obeys the single parameter exponential distribution and the censored variable is a time variable

Let X be a survival variable, which is a continuous random variable, the probability density function of X is $f(x)$, the distribution function of X is $F(x)$. Suppose that survival variable obeys the single parameter exponential distribution, $f(x) = e^{-x/\theta}/\theta \quad (x \geq 0)$, $f(x) = 0 \quad (x < 0)$. In the moment $t_0 = 0$ we start to admit experimental n-products. In the moment t_1, t_2, …, t_i, we remove for examination, these n-products in the product life have ended to remove, the remaining time puts the latter to continue testing. In the period of $(0, t_1]$, $(t_1, t_2]$, $(t_2, t_3]$, $...,(t_{i-1}, t_i]$, we assume that the number of products which products lives are lost be respectively $m_1, m_2, ..., m_i$, the number of their remaining products $n - m_1 - m_2 - ... - m_i = c$. These c-experimental products will be lost their life during (t_i, ∞). Let the interval of $(0, t_1]$, $(t_1, t_2]$, $(t_2, t_3]$, $...,(t_{i-1}, t_i]$ be the same, which means $t_j = jt_1 \ (j = 1,2,..., i)$, during the period of $(0, t_1], (t_1, t_2], (t_2, t_3]$, $...,(t_{i-1}, t_i]$, we assume that the probability of $m_1 + m_2 + ... + m_i$ products lives be lost, but c-products lives haven't lost , then we give a reliability function

$$L(\theta) = (\int_{t_i}^{\infty} f(x)dx)^c (\int_0^{t_1} f(x)dx)^{m_1} ... (\int_{t_{i-1}}^{t_i} f(x)dx)^{m_i}$$

Then $$\ln L(\theta) = c\ln\int_{t_i}^{\infty} f(x)dx + m_1 \ln\int_0^{t_1} f(x)dx + ... + m_i \ln\int_{t_{i-1}}^{t_i} f(x)dx$$

Let $(\ln L(\theta))'_\theta = 0$, we have their maximum likehood estimation

$$\overline{\theta} = t_1 \Big/ \ln[1 + (n-c)] \Big/ (ci + \sum_{j=2}^{i}(j-1)m_j)]$$

Let $EX = \overline{X}$, we have the monment estimation $\overline{\theta} = \int_0^{\infty} f(x)dx = \overline{X}$

5. Example

Let the product life obey the single parameter exponential distribution, we extract 12- products to carry on the experiment. When 8-products lives have already finished we stop experiment, the products lives closure time presses

the arranged in order is 2, 10, 18, 36, 60, 180, 720, 2880, we discuss the maximum likehood estimate and the monment estimate solution. From the time order 2, 10, 18, 36, 60, 180, 720 and 2880, we know that 8 time compartments separately belong to $(0,2], (4\times 2, 5\times 2]$, $(8\times 2, 9\times 2]$, $(17\times 2, 18\times 2], ..., (1439\times 2, 1440\times 2]$. Let the time-gap be the same, then $t_i = jt_1$, $t_1 = 2$, $j = 1$, 4, 8, 17, 29, 89, 179 and 1439. Because 8 time compartments products life finished, then $m_1 = m_2 = ... = m_8 = 1$. Sutituting the maximum likehood estimate formula, we have $\overline{\theta} = 460.769$. Sutituting the monment formula we have $\overline{\theta} = 460.769$

6. conclusion

The monment estimate and the maximum likehood estimate to obtain the product life only to be able to small partially to carry on the experiment, the sample which we can take are quite small, but the monment estimate and the maximum likehood estimate to the unknown parameter is a kind of feasible and efficient estimate method.

References

Zheng, Z.K. (2003). A class of estimators of the mean survival time from intervalcensored data with application to linear regression. Manuscript.

Zheng, Zukang, (1992). A class K of estimators of mean lifetimewith applications. the Development of Statistics: Re-cent Contributions from China. Pitman Research Notesin Mathematics. *Longman Scientific and Technical.* 1992 (258). 289-298.

Zheng, zhukang, (2007). Estimation of parameter of a linear regression model under internal censored covariate. *Applied Mathematics.* 2007 (02). 427-432.

Zheng, Zukang, Ma, (1999). Rong & Zhang, Xiufeng, An estimator of survival function under random censorship model, *Applied mathematics*. J. Chinese Univ. Ser.A (Chinese edition).1999 (03). 285-292.

Gomez G., Espinal A. and Stephen W. (2003). Inference for linear regression model with an internal censored covariate. *State in Medicine*. 2003(22). 409-425.

He, Qixiang & Zheng, Ming. (2005). Empirical likehood-based inference in an internal censored covariate Applied. Mathematics. J. Chinese Univ. Ser. B (Chinese edition) 2005 (20) 338-346.

Modern Applied Science
www.ccsenet.org/journal.html
Vol. 2, No. 3
May 2008

The Existences of Positive Solution for Neutral Difference Equations with Muitiply Delay

Xiaozhu Zhong, Ning Li, Ping Yu, Wenxia Zhang & Shasha Zhang
Department of Mathematics
Yanshan University
Qinhuangdao 066004, China
E-mail: lining0229@163.com

Supported by the Foundation for the natural science of Hebei province of China (Z2007431)

Abstract

We prove the existences of positive solution for neutral difference equation with multiply delay.

Keywords: Difference equation, Positive solution, Much retard

1. Introduction

In recent years, Difference equations have beed applied in many areas,such as population dynamics, stability theory, circuit theory, bifurcation analysis, dynamical behavior of delayed network systems and so on. The oscillation or asymptotic behaviour of difference equations was the subject of invesigation by many authors.

In this paper, we are concerned with the following neutral difference equation with positive and negative coefficients.

$$\Delta\left[x(n)-\sum_{l=1}^{w}R_l(n)x(n-r_l)\right]+\sum_{i=1}^{m}P_i(n)x(n-\tau_i)-\sum_{j=1}^{k}Q_j(n)x(n-\sigma_j)=0 \quad (*)$$

We will investigate the existences of positive solution of this equation.

where $m\geq k$; $R_l, P_i, Q_j\in([n_0,\infty],R^+)$; r_l,τ_i,σ_j are non-negative and non-de-creasing about $l,i,j,\tau_i\geq\sigma_i$.

Throughout the paper,we suppose the following assumptions

(1) $H_i(n)=P_i(n+\tau_i-\sigma_i)-Q_i(n)\geq 0$, $n\geq n_0, i=1,2,...m$

(2) $H(n)=\sum_{i=1}^{m}H_i(n)\cdot$

(3) $Q_j(n)\equiv 0, \sigma_j\equiv 0,\ j=k+1,k+2,...m$

When $w=m=k=1$,the equations changed to

$$\Delta\left[x(n)-R(n)x(n-r)\right]+P(n)x(n-\tau)-Q(n)x(n-\sigma)=0 \quad n=0,1,... \qquad (4)$$

Where $\{P(n)\},\{Q(n)\},\{R(n)\}$ are sequence of nonnegative real numbers, τ,σ,r are integers with $0\leq\sigma\leq\tau-1, r>0$.The oscillatory and non-oscillatory solutions of Eq(4) have been investigateed by several authors. The aim of the present is to investigate the behavior of eventually positive solutions of Eq(1)On the bases of the references of [2].

2. Some lemmas

Lemma1 Assume that (1)(2) holds $n\geq n_0$ and $\sum_{l=1}^{w}R_l(n)+\sum_{i=1}^{m}\sum_{u=n}^{n+\tau_i-\sigma_i}P_i(n)\leq 1$.if $x(n)$ is an eventually positive solutions of the following inequality

$$\Delta\left[x(n)-\sum_{l=1}^{w}R_l(n)x(n-r_l)\right]+\sum_{i=1}^{m}P_i(n)x(n-\tau_i)-\sum_{j=1}^{k}Q_j(n)x(n-\sigma_j)\leq 0$$

Setting $$y(n)=x(n)-\sum_{l=1}^{w}R_l(n)x(n-r_l)+\sum_{i=1}^{m}\sum_{u=n}^{n+\tau_i-\sigma_i}P_i(u)x(u-\tau_i)$$

then we eventually have $\Delta y(n)\leq 0,\ y(n)>0$.

Lemma 2 Assume (1) $\{p_n\}$ are sequences of nonnegative real numbers; (2) k and l are integers; (3) $\{q_n\}$ are sequences of nonnegative real numbers and $p_n + lq_n > 0$ $(n \geq N)$, $l > 0$; or $l > 0, q_s \geq 0$ $s \in [n.n+1]$

Setting $b = \max\{k, l\}$ assume the inequality

$$y_n \geq p_n y_{n-k} + \sum_{s=n}^{\infty} q_s \max_{u \in [s-l,s]} y_u \quad n \geq N$$

has an eventually positive solution $\{y_n\}_{N-b}^{\infty}$, then the corresponding difference equation

$$x_n = p_n x_{n-k} + \sum_{s=n}^{\infty} q_s \max_{u \in [s-l,s]} x_u \quad n \geq N$$

has an eventually positive solution $\{x_n\}_{N-b}^{\infty}$

3. Main results and proof

Theorem 1 Assume $\sum_{l=1}^{w} R_l(n) + \sum_{i=1}^{m} \sum_{u=n}^{n+\tau_i-\sigma_i} P_i(u) \equiv 1$, equation(*) has an eventually positive solution if and only if the inequality

$$\Delta\left[x(n) - \sum_{l=1}^{w} R_l(n) x(n-r_l)\right] + \sum_{i=1}^{m} P_i(n) x(n-\tau_i) - \sum_{j=1}^{k} Q_j(n) x(n-\sigma_j) \leq 0 \tag{5}$$

has an eventually positive solution.

Proof: We can see the sufficient condition of the theorem is obvious.we only proof the Necessary condition.

Assume $\{x(n)\}$ is an eventually positive solution of the inequality (5).

define
$$y(n) = x(n) - \sum_{l=1}^{w} R_l(n) x(n-r_l) + \sum_{i=1}^{m} \sum_{u=n}^{n+\tau_i-\sigma_i} P_i(u) x(u-\tau_i) \tag{6}$$

then in view of lemma 1, we have $\Delta y(n) \leq 0$, $y(n) > 0$ .and $\lim_{n\to\infty} y(n) \geq 0$.

setting $y_\infty = \lim_{n\to\infty} y(n)$ in view of (6), we have

$$\begin{aligned}
\Delta y(n) &= \Delta\left(x(n) - \sum_{l=1}^{w} R_l(n) x(n-r_l) + \sum_{i=1}^{m} \sum_{u=n}^{n+\tau_i-\sigma_i} P_i(u) x(u-\tau_i)\right) \\
&\leq \sum_{j=1}^{k} Q_j(n) x(n-\sigma_j) - \sum_{i=1}^{m} P_i(n) x(n-\tau_i) - \sum_{i=1}^{m} P_i(n+\tau_i-\sigma_i) x(n-\sigma_i) + \sum_{i=1}^{m} P_i(n) x(n-\tau_i) \\
&\leq \sum_{j=1}^{k} Q_j(n) x(n-\sigma_j) - \sum_{i=1}^{m} P_i(n+\tau_i-\sigma_i) x(n-\sigma_i) = -\sum_{i=1}^{m} H_i(n) x(n-\sigma_i) \leq 0
\end{aligned} \tag{7}$$

Summing both side of the inequality (7) form n to ∞ and takeing limt on both side of the resulting inequality, we have

$$y_\infty - y(n) \leq -\sum_{s=n}^{\infty} \sum_{i=1}^{m} H_i(s) x(s-\sigma_i)$$

Then we can see that $y(n) \geq \sum_{s=n}^{\infty} \sum_{i=1}^{m} H_i(s) x(s-\sigma_i) + y_\infty \geq \sum_{s=n}^{\infty} \sum_{i=1}^{m} H_i(s) x(s-\sigma_i)$

i.e $x(n) - \sum_{l=1}^{w} R_l(n) x(n-r_l) \geq \sum_{i=1}^{m} \sum_{u=n}^{n+\tau_i-\sigma_i} P_i(u) x(u-\tau_i) + \sum_{s=n}^{\infty} \sum_{i=1}^{m} H_i(s) x(s-\sigma_i)$

Then the corresponding difference equation

$$z(n) = \sum_{l=1}^{w} R_l(n) z(n-r_l) + \sum_{i=1}^{m} \sum_{u=n}^{n+\tau_i-\sigma_i} P_i(u) z(u-\tau_i) + \sum_{s=n}^{\infty} \sum_{i=1}^{m} H_i(s) z(s-\sigma_i)$$

has an eventually positive solution $z(n)$ .obvious $\{z(n)\}$ are positive solutions of (*).

Theorem 2 Assume $\sum_{l=1}^{w} R_l(n) + \sum_{i=1}^{m} \sum_{u=n}^{n+\tau_i-\sigma_i} P_i(u) \equiv 1$ .if $\Delta^2 y(n) + \frac{1}{k} \sum_{i=1}^{m} H_i(n) y(n) = 0$ (8)has an eventually positive solution, the the equation(*) aslo has an eventually positive solution.

Proof: Assume $y(n)$ is an eventually positive solution of (8). then we have

$$\Delta^2 y(n) = -\frac{1}{k} \sum_{i=1}^{m} H_i(n) y(n) \leq 0 \tag{9}$$

Necessarily we have $\Delta y(n) > 0$ .if it is not true, there must be exist n_0 ,if $n \geq n_0$, we have $\Delta y(n) < 0$, then $y(n)$ exist an nonnegative limt.

Setting $\lim_{n\to\infty} y(n) = M > 0$

We have $\Delta^2 y(n) \le -\frac{M}{k}\sum_{i=1}^{m} H_i(n)$ Summing both side of the inequality form n_2 to n twice

we can see that $$y(n+2)-y(n_2+1) \le -\frac{M}{k}\sum_{s_2=n_2}^{n}\sum_{s_1=s_2}^{n}\sum_{i=1}^{m} H_i(n)$$

then $\lim_{n\to\infty} y(n) = -\infty$ which contradicts with $y(n)$ is an eventually positive solution. so $\Delta y(n) > 0$.

we eventually have $y(n) > 0, \Delta y(n) > 0, \Delta^2 y(n) \le 0$ .so $\{y(n)\}$ are sequences of nondecreasing, $\{\Delta y(n)\}$ are sequence of nonincreasing

setting $a(n) = \Delta y(n)$

we have $a(n) > 0, \Delta a(n) \le 0$ $n \ge n_1$

define a sequence $\{x(n)\}$ as follows

$$x(n) = \begin{cases} \dfrac{y(n_1)}{k} (n_1 \le n \le n_1 + L) \\ a(n) + \sum_{l=1}^{w} R_l(n)x(n-r_l) + \sum_{i=1}^{m}\sum_{u=n}^{n+\tau_i-\sigma_i} P_i(u)x(u-\tau_i) \\ (n_1 + L + tk \le n \le n_1 + L + (t+1)k)(t = 0,1,2,\ldots) \end{cases}$$

then we have $x(n) > 0 (n \ge n_1)$

$$a(n) = x(n) - \sum_{l=1}^{w} R_l(n)x(n-r_l) - \sum_{i=1}^{m}\sum_{u=n}^{n+\tau_i-\sigma_i} P_i(u)x(u-\tau_i) \quad n \ge n_1 + L \qquad (10)$$

$$x(n) = \frac{y(n_1)}{k} \le \frac{y(n)}{k} = \frac{1}{k}\sum_{s=n_1}^{n-1} a_s + \frac{1}{k} y(n_1) \quad n_1 \le n \le n_1 + L$$

Therefore
$$\begin{aligned} x(n) &= a(n) + \sum_{l=1}^{w} R_l(n)x(n-r_l) + \sum_{i=1}^{m}\sum_{u=n}^{n+\tau_i-\sigma_i} P_i(u)x(u-\tau_i) \\ &\le a(n) + (\sum_{l=1}^{w} R_l(n) + \sum_{i=1}^{m}\sum_{u=n}^{n+\tau_i-\sigma_i} P_i(u))(\frac{1}{k}\sum_{s=n_1}^{n-k-1} a_s + \frac{1}{k} y(n_1)) \\ &\le \frac{1}{k}\sum_{s=n-k}^{n-1} a(s) + \frac{1}{k}\sum_{s=n_1}^{n-k-1} a(s) + \frac{1}{k} y(n_1) \\ &= \frac{1}{k}\sum_{s=n_1}^{n-1} a(s) + \frac{1}{k} y(n_1) \end{aligned}$$

By induction, we can show that

$$x(n) \le \frac{1}{k}\sum_{s=n_1}^{n-1} a(s) + \frac{1}{k} y(n_1) \quad (n_1 + L + tk \le n \le n_1 + L + (t+1)k)(t = 0,1,2,\ldots)$$

and hence
$$x(n) \le \frac{1}{k}\sum_{s=n_1}^{n-1} a(s) + \frac{1}{k} y(n_1) \qquad n \ge n_1$$

$$x(n-\sigma_i) \le \frac{1}{k}\sum_{s=n_1}^{n-\tau_i-1} a(s) + \frac{1}{k} y(n_1) = \frac{1}{k} y(n-\tau_i) \le \frac{1}{k} y(n) \qquad n \ge n_1 + L$$

Substituting this into (9) we obtain $\Delta a(n) + \sum_{i=1}^{m} H_i(n)x(n-\sigma_i) \le 0 \quad n \ge n_1 + L$

So, it follows form (10) that

$$\begin{aligned} &\Delta\left[x(n) - \sum_{l=1}^{w} R_l(n)x(n-r_l)\right] - \sum_{i=1}^{m} P_i(n+\tau_i-\sigma_i)x(n-\sigma_i) + \sum_{i=1}^{m} P_i(n)x(n-\tau_i) \\ &\quad + \sum_{i=1}^{m} P_i(n+\tau_i-\sigma_i)x(n-\sigma_i) - \sum_{i=1}^{m} Q_i(n)x(n-\sigma_i) \le 0 \end{aligned}$$

i.e $$\Delta\left[x(n) - \sum_{l=1}^{w} R_l(n)x(n-r_l)\right] + \sum_{i=1}^{m} P_i(n)x(n-\tau_i) - \sum_{j=1}^{k} Q_j(n)x(n-\sigma_j) \le 0$$

By theorem 1, Eq(*) has an eventually positive solution.

Lemma 3 Let $\{d(n)\}$ be a sequence of nonnegative real numbers,Assume that, for some integer n^* and sufficiently large n the inequality

$$(n-n^*)\sum_{s=n}^{\infty} d_s \le \frac{1}{4}$$

holds,Then,the following difference equation

$$\Delta^2 y(n) + d_n y(n) = 0$$

has an eventually positive solution.

Now we are ready to give out result :

Theorem 3 Assume $\sum_{l=1}^{w} R_l(n) + \sum_{i=1}^{m} \sum_{u=n}^{n+\tau_i-\sigma_i} P_i(u) \equiv 1$ holds,for some integer n^* and sufficiently large n, the inequality $(n-n^*)\sum_{s=n}^{\infty}\sum_{i=1}^{m} H_i(s) \le \frac{k}{4}$

is satisfied, Then, Eq(*) has an eventually positive positive.

References

Dong, Weilei. (2006). The oscillation for neutral difference equations with multiply delay. *Journal of Hebei Normal University*(Natural Science Edition), 30(2): 136-139.

Tang, Xianhua, & Yu, Jianshe. (2000). Oscillation and nonoscillation of neutral difference equations with positive and negative coefficients. *Computer Math Appl*, 39: 169-181.

Tian, J.C.(2003). Oscillation Criteria for neutral equations with positive and negative coefficients. Bol SocParana Math, 21: 19-30.

Wu, Dong. (2003). Oscillation and nonscillation of neutral difference equations with maxima term. *JOURNAL OF OCEAN UNIVERSITY OF QINGDAO*, 3(6): 975-982.

Zhang, B G, &Wang, H. (1996). The exience of oscillatory and non-oscillatory solutions of neutral difference equations. *Chinese J Math*, 24: 377-393.

Modern Applied Science

www.ccsenet.org/journal.html

Vol. 2, No. 3

May 2008

Study on the Establishment of "People Oriented" Values System in IT Enterprise

Haiqing Shao

College of Business Administration

Shandong University of Finance

Jinan 250014, China

E-mail: shqsing@sina.com

Abstract

If IT enterprise wants to acquire long-term development, it must solve the problem of people first. The establishment of "people oriented" value system is the important content in the cultural construction of IT enterprise. This article will primarily discuss main contents and factors which should be considered in the establishment of "people oriented" value system in IT enterprise.

Keywords: IT enterprise, Enterprise values, Innovation

The essential of enterprise is human career, and if enterprise wants to acquire long-term development, the problem of people must be solved first. The IT enterprise is the collectivity consisted by a group of high quality person with common ideas, so the problem of human dignity in IT enterprise is especially important. If an excellent manager of IT enterprise wants to exert the leading efficiency, he must know humanity well, or else, he cannot lead things to the right direction.

The enterprise culture theory coming into being in 1980s makes the emphasis of management transform from "hard" to "soft", and very emphasize the function of people. The "three P theory" of enterprise means the concept of the people, by the people and for the people. The enterprise culture is the important approach to implement the "people oriented strategy", and the "people oriented" concept is the important content of IT enterprise culture construction.

1. What is the value concept of enterprise?

The value concept is the core and base of enterprise culture, which decides other various aspects of the enterprise culture. The enterprise value view is employees' opinions and judgments to various things and activities in the enterprise, and it is a sort of psychological cogitation on the deep layer. The enterprise value view offers basic direction and action rule for the survival and development of the enterprise. Only one enterprise confirms right value concept, it can uniform the idea of the enterprise, and accordingly effectively agglomerate all employees and make them actively devote themselves to the development of the enterprise.

In various value views influencing the development of enterprise, the function of the enterprise management value view is the most important. The management value view of western enterprise approximately experiences three evolvement stages. The first stage is the maximum profit value view, i.e. all management functions and actions of the enterprise must start from the maximum profit, and that is the only standard to evaluate the enterprise. The second stage is the satisfaction value view. Though enterprise still takes profits as its aim, but in the process of management, it must give attention to employees' and customers' benefits at the same time. Only investors, employees, and customers all fell satisfactory, enterprise can survive and develop. The third stage is the comprehensive benefit value view. Since 1970s, when western enterprise management confirms profit level, it not only considers enterprise owner's and interior employees' benefits, but also considers the uniform of enterprise benefit and social benefit, and it even thought that stockholders' benefits are not more important than benefits of other aspects. So the management value view changes tenderly. However, as viewed from the practice, because the economic benefit is closely linked with the benefits of the whole big system, so modern successful enterprises are those enterprises which possess the comprehensive benefit value view. For example, the management theory (the value view) of Hitachi Company is "honest, exploitation spirit, harmonious", and the value view of Fountain Company is "excellent products, excellent ideas, world Fountain".

2. Main contents included in the "people oriented" value system of IT enterprise

The main contents of "people oriented" value system of IT enterprise should include following several aspects.

2.1 Reform and innovation

With the advent of knowledge economy and the economic globalization, enterprises will face more complex and changeable international competition environment. Especially, those enterprises with high new technology will face more inclement environment, for example, the cycle of technology refresh is shortened increasingly, and the market demand changes quickly and so on. Under this background, enterprises must establish the idea of reform, and answer changes of exterior environment by the flexible means, and they may acquire success.

Innovation can transform enterprises from adapting the change of environment passively to actively facing challenges. Through innovation, enterprises can lead reform before the time, and acquire the predominance of competition, and finally remain invincible in the drastic competition. The management master, Peter F. Drucker had said that "no innovation, enterprise will die". So we can think that if enterprises want to survive and develop, they must implement innovation. An obvious character that knowledge economy knows from agriculture economy and industry economy is innovation. Innovation is the spring of the enterprise energy and the drive force to make enterprises sustainable develop. All successful enterprises in the world depend on innovation to acquire developments. The Microsoft Company continually gets rid of the stale and brings forth the fresh in the "Windows", which makes it become the outstanding manufacture in the industry. Intel Company can lead the computer CMOS chip market because of its continual innovations in the CMOS chip.

To advance the innovation of enterprise, the key is to advocate the innovation consciousness in the enterprise, and accordingly form a sort of cultural atmosphere advocating innovation. To advocate innovation consciousness is to encourage innovation and continually encourage employees to put forward new opinions, create new methods, boldly attempt new things and can not limit their eyes on the existed things. To advocate innovation consciousness also should foster employees' psychological quality without fearing risks and failures, give employees the courage of risk, tolerate and understand employees' failures, and relieve employees' worries of innovation. Only all employees of the enterprise possess the innovation consciousness, the innovation of the enterprise can be really actualized, and the innovation can be huge impetus to drive the development of the enterprise.

2.2 Cooperation and sharing

No matter how a person's ability is strong, but it is limited after all, and it can not grasp all knowledge and skills needed in modern production and management. Especially in high technology enterprises, because of the complexity of the technology, their products and services always need many employees with different knowledge and skill to cooperate. So to advocate cooperative value view in the enterprise is a sort of necessary need. Good atmosphere of cooperation formed between leaders with common employees, between employees with employees is propitious to learn from others' strong points to offset their weakness among employees, form harmonious human relation and strengthen the agglomeration of the enterprise.

Sharing is the base of cooperation. When we advocate the cooperation, we should advocate the concept of sharing. Sharing is the sharing of benefit firstly. Employees in modern enterprises have not been "talking machines" or "exploited tools", and they are human capitals of the enterprise. Especially in high technology enterprises like IT enterprise, "people" has been the most important capital investment, the key resource that can bring profits for the enterprise. So employees should share benefits with enterprises together. Only in virtue of the sharing of benefit, enterprises can effectively encourage employees and acquire the effect of "double-win". In the next place, sharing is the sharing of information. The sharing of information in enterprises can offer good conditions for the cooperation among employees, and create advantaged environment that employees can participate in the decision of enterprise.

2.3 Trust and respect

Most works of IT enterprise are creationary works, and most employees in IT enterprise are knowledge employees with high quality. Based on that characteristic, enterprise should give employees full trust and respect, and create loose cultural environment for employees to fully exert their own talents. In the atmosphere of trust and respect, employees' efforts are respected, employees' productions are recognized, employees' innovations are permitted, and employees' values are actualized. Only that, employees can fully exert their own enthusiasms, and realize self-management and self-restriction, and combine individual object with enterprise object consciously.

In famous Hewlett-Packard Company, we can fully see this sort of trust and respect. One creator of HP, William Hewlett in his book of "The HP Way" had summarized the successful way of HP, "The HP way is to respect individual honesty and faithfulness in the final analysis". In HP, the experiment storeroom which stores electric components and mechanism accessory is completely opened, which not only allow engineers use these accessories at will in work, but encourage them to take these accessories home to use for individual, because the opinion of HP is that "No matter whether they use these accessories is relative with work, only they can learn something from these things". HP is the enterprise which implements the flexible work, the company has no the work and rest time, and doesn't check on work attendance, and employees can begin on duty from six, seven or eight in the morning if only they complete eight hours'

works, thus every employee can adjust his work time according to his own living need.

2.4 Loyalty and responsibility

The employees' high fluidity has been one of the worst things for IT managers. So IT managers try themselves to hold talents and keep the stability of the enterprise. Some encouragement systems such as year salary system, stock right system and so on have certain active functions. But when other enterprises give more favorable work conditions, even more year salaries and more stock rights are hard to avoid failure in the competition of talents. But if we can effectively establish employees' loyalty to the enterprise, this situation may be changed. To advocate employees' loyalties to the enterprise is to encourage employees to take the business of the enterprise as their own businesses, to take the development of the enterprise as their own development, to try themselves for the development of the enterprise, and contribute their lifetime energies. Just with the idea of loyalty, employees can be most willing to try themselves for the development of the enterprise, and the enterprise and employees can be the real community of the fate.

With the premise of loyalty, the responsible concept of line of duty seems be the easy thing. Because knowledge employees' work process is hard to supervise, and their work results are hard to measured, so their responsibilities are hard to confirmed. To advocate the concept of line of duty is to foster employees' good occupational morality and professional dedication, and make employees assume responsibilities consciously in works, and establish good bases for the accomplishment of various works of the enterprise.

3. Factors should be considered in the establishment of "people oriented" value system of IT enterprise

To construct the enterprise culture, IT enterprise should fully consider the characteristics of IT enterprise and the need of exterior environment, and establish the value system which adapts to its own development. So the establishment of "people oriented" value system must comprehensively consider various factors and seriously choose.

3.1 Characteristics of age

The advance of science and technology is leading the deep reform of modern society, which makes this age we are in present bright characteristics differing with ago ages. (1) Knowledge becomes the decisive factor to promote the development of society and economy. In the knowledge economic society, knowledge has replaced other factors and occupied the extrusive position. So the enterprise which possesses the knowledge carrier, talents, can lead the economic development. (2) The information-based degree is fully enhanced. With the development of information technology and network technology, the information-based degree of the whole society is enhanced largely. Through internet, enterprises can conveniently, quickly and broad acquire relative information. The improvement of information-based degree fully changes traditional management mode of the enterprise. Enterprises must implement deep reforms in market competitive strategy, organizing system and other aspects, which can adapt the development of informationization. (3) The course of economic globalization is expedited. The world economy is increasingly breaking the limitation of national boundaries and regions, and its connection in the world is becoming closer and closer. That means the development of the enterprise cannot only be established in the domestic, and it must scan widely to the whole world. The management concept and pattern of the enterprise must take the world culture as their backgrounds and fully exert their advantages in the world stage.

3.2 Characteristics of enterprise

IT enterprise is the classic enterprise with high and new technology, which presents following characteristics. (1) The knowledge content and technology content of products are high. In the composing of product cost, the cost of raw material occupies a little part, but the proportion of affixation composed by knowledge and technology occupies very high. For example, the cost of raw material of semiconductor chip only occupies about 13% of the total cost. (2) The lifecycle of the product is short. The product update of IT enterprise is very quick, only new technology and new products can acquire better profits. (3) The risk faced by the enterprise is large. The first one is the risk of product exploitation. The foreign and domestic practices show that the exploitation of one product needs pay large of manpower, material resources and financial, and the final successful probability is very low. Because IT enterprise must continually push new products, their investments in the product exploitation are certainly large, which makes enterprise firstly face the risk of product exploitation. The second one is the market risk. Even if the product exploitation is successful, enterprise still faces the test from the market. The new product of the enterprise maybe cannot be accepted by the market, or other competitors have arrived first. Under this situation, enterprise also faces large risks from the market. (4) Most employees of the enterprise are knowledge employees with high quality.

3.3 Characteristics of employee

The knowledge employees are the main body to compose employees of IT enterprise. The concept of knowledge employee was put forward by the management master Drucker, and he thought that the knowledge employee were "those employees who grasp and operate symbols and concepts, utilize knowledge or information to work". Today, the knowledge employees generally refer to those employees who utilize their own knowledge and wisdoms to work, and

they have following characteristics. (1) Their independences are very strong. The quality of knowledge employees is high, and they possesses rich knowledge and work abilities, so they would like to accomplish their works independently without supervision and controls. (2) Their desires of self-realization are very strong. Knowledge employees pay more attention to the realization of their own values, and they want to succeed in their works and develop in their careers. Comparing with that, the demand of money has not been the first need in their lives. (3) The work process is hard to control and the work result is hard to measure. Knowledge employees utilize their brains to work, and enterprise cannot supervise them as traditional enterprises supervise the machining process effectively. Knowledge employees' work results can not be measured exactly. (4) The fluidity is strong. For knowledge employees, traditional "iron rice bowl" can not produce attractions. Because the knowledge resource can not be consumed like other one-off natural resources, so knowledge employees worry unemployment less. They always want to flow to the enterprise with higher salary or better work conditions in order to prove their own strengths or actualize their own values.

3.4 Excellent factors in China traditional culture

Facing the new situation with increasing frequent economic and cultural international communications, enterprises need extracting useful experiences from foreign advanced enterprises, and use all helpful thins in foreign culture. But the absorption of foreign cultures can not copy word for word in spite of the situation of China and the actuality of the enterprise. In the process to construct the enterprise value system, enterprises should fully emphasize those excellent factors in Chinese traditional culture. Five thousand years' civilization history brings up abundant and deep traditional culture of China, and there is no lack of many excellent factors such as the unity of universe and human beings, the recognition to human relations, the emphasis to morality and education and the worship to proprieties. If enterprises can utilize these excellent factors in the traditional culture to the construction of enterprise value system, they will more fit for Chinese employees cultural psychologies and strengthen the agglomeration of the enterprise.

References

Chen, Honggang, et al. (2003). *Management and Culture of Software Enterprise (1st Edition).* Beijing: Tsinghua University Press. Feb, 2003.

Chenyan. (2006). *Opening Culture (1st Edition).* Beijing: China Economy Press. Jan, 2003.

Li, Lijun. (2002). Thinking of Internet Enterprise Culture in New economy. *Commercial Research.* No.20.

Su, Qingqing, et at. (2007). Discussion on the Cultivation of Enterprise Innovational Culture and Enterprise Core Competitiveness. *Productivity Research.* No.15.

A journal archived in Library and Archives Canada
A journal indexed in CANADIANA (The National Bibliography)
A journal indexed in AMICUS
A leading journal in applied science research
A journal indexed in Zentralblatt MATH

Modern Applied Science

Bimonthly

Publisher Canadian Center of Science and Education
Address 4915 Bathurst St. Unit # 209-309, Toronto, ON. M2R 1X9
Telephone 1-416-208-4027
Fax 1-416-208-4028
E-mail mas@ccsenet.org
Website www.ccsenet.org
Printer William Printing Inc.
Price CAD.$ 20.00

ISSN 1913-1844